

UNIVERSITY OF WALES
PRIFYSGOL CYMRU
CAERDYDD

Design and synthesis of dUTP nucleotidohydrolase inhibitors for use as anti-parasitic drugs

University
of Wales
Cardiff



Prifysgol
Cymru
Caerdydd

A Thesis submitted to the University of Wales for the Degree of

Doctor of Philosophy

by

Orla Mc Carthy



December 2006

Supervisor: Professor Ian Gilbert

UMI Number: U584139

All rights reserved

INFORMATION TO ALL USERS

The quality of this reproduction is dependent upon the quality of the copy submitted.

In the unlikely event that the author did not send a complete manuscript and there are missing pages, these will be noted. Also, if material had to be removed, a note will indicate the deletion.



UMI U584139

Published by ProQuest LLC 2013. Copyright in the Dissertation held by the Author.
Microform Edition © ProQuest LLC.

All rights reserved. This work is protected against
unauthorized copying under Title 17, United States Code.



ProQuest LLC
789 East Eisenhower Parkway
P.O. Box 1346
Ann Arbor, MI 48106-1346

Dedicated to my family who were always there for me, especially to my mother for her love and support and to the memory of my beloved father.

Abstract

Parasitic protozoa cause many widespread diseases known to man such as malaria, African sleeping sickness, leishmaniasis and Chagas' disease. These diseases are particularly prevalent in the developing world and the need for new, safe and affordable drugs to treat them is urgent. Current drug treatments often result in adverse side effects and the continual emergence of resistance is extensive.

The main function of nucleic acid DNA is to preserve and store genomic information in all living organisms and its integrity must be scrupulously maintained by the cell. The ubiquitous enzyme dUTP nucleotidohydrolase (dUTPase) catalyses the hydrolysis of dUTP to dUMP and can be considered as the first line of defence against incorporation of uracil into DNA. Inhibition of this enzyme results in overincorporation of uracil into DNA, leading to DNA fragmentation and cell death and is therefore lethal.

By taking advantage of structural differences between the human and parasitic forms of dUTPase, selective inhibitors of the enzyme can be designed and synthesised with the aim of being developed into novel anti-parasitic drugs.

Analogue based design was used to target the *Plasmodium falciparum* dUTPase (PfdUTPase). The structures of previously discovered selective inhibitors of the PfdUTPase were modified by insertion of an amide bond. A series of tritylated uracil acetamide derivatives were synthesised and assessed for inhibition of the enzyme and parasite growth *in vitro*. Unfortunately these compounds were not potent inhibitors of the PfdUTPase but do show good *in vitro* activity.

Following the elucidation of the crystal structure of the PfdUTPase, work was focused on the improvement of known selective inhibitors of the enzyme. Structure based design methodologies were used to search for interactions within the active site and to design potentially more potent analogues *in silico*. The biological results are currently being awaited.

Structure based design was also used to design potential lead inhibitors of the *Trypanosoma cruzi* dUTPase (TcdUTPase), for which no previous selective inhibitors were known. A library of uracil amino acid conjugates were synthesised by solid phase methodology. Unfortunately, the compounds did not inhibit the enzyme or parasite growth *in vitro*.

Acknowledgements

First and foremost I would like to thank my supervisor, Ian Gilbert for his valuable knowledge and guidance over the past three years and for giving me the opportunity to work in his group.

I would like to thank the Welsh School of Pharmacy and the European Union for funding this PhD project and the School of Life Sciences, University of Dundee.

Thanks to our partners who collaborated on the dUTPase project: Dr. D. Gonzalez-Pacanowska and her laboratory at the Instituto de Parasitología y Biomedicina, Consejo Superior de Investigaciones Científicas in Granada; Dr. Reto Brun and co-workers at the Swiss Tropical Institute, Basel; Dr. Keith Wilson and his group at the Structural Biology Laboratory of the University of York and Nils Gunnar Johansson at Medivir AB, Stockholm.

A special thanks to the technical staff at the Welsh School of Pharmacy and at the James Black Centre in Dundee, especially to Ron Edwards for his help with the mass spectrometer and Gina Mackay for her NMR and mass spectrometry expertise.

A sincere thanks to the past and current members of the Gilbert group; Federica, Alessandro B., Corinne, Simon, Gian Filippo, Alessandro S., Shahienaz, Ludovic, Shane, Cyrille, Salvatore, Olivier, Jeremie and Valery for all of their advice and support and of course for all the times we enjoyed together inside and outside the lab.

I would like to thank my friends in the Welsh School of Pharmacy, especially the members of the McGuigan, White and Simons groups and also the Marquez, Eggleston, Nikolaev, Brenk, Ferguson and Fairlamb group in the School of Life Sciences, Dundee for making both places such pleasurable places in which to work.

Publications

Part of this thesis has been published in the following journal:

McCarthy, O. K.; Schipani, A.; Musso Buendía, A.; Ruiz-Perez, L. M.; Kaiser, M.; Brun, R.; Gonzalez-Pacanowska, D.; Gilbert, I. H. Design, synthesis and evaluation of novel uracil amino acid conjugates for the inhibition of *Trypanosoma cruzi* dUTPase. *Bioorg. Med. Chem. Lett.* **2006**, *16*, 3809-3812.

The full articles are referred to in Appendix 2.

Contents

1	Background	- 1 -
1.1	Protozoal infections	- 1 -
1.2	The Trypanosomiasis	- 2 -
1.2.1	Human African trypanosomiasis	- 2 -
1.2.2	Chagas' disease	- 6 -
1.3	The Leishmaniasis	- 8 -
1.3.1	Leishmaniasis	- 8 -
1.3.2	Transmission of the parasite	- 10 -
1.3.3	Drug treatment	- 10 -
1.4	Plasmodium	- 12 -
1.4.1	Malaria	- 12 -
1.4.2	Transmission of the parasite	- 13 -
1.4.3	Drug treatment	- 14 -
2	The dUTPase enzyme	- 23 -
2.1	Function of the enzyme	- 23 -
2.2	dUTPase, cell proliferation and thymineless death	- 24 -
2.3	Structure and classification	- 26 -
2.3.1	Trimeric dUTPases	- 26 -
2.3.2	Dimeric dUTPases	- 32 -
2.3.3	Monomeric dUTPases	- 36 -
2.3.4	Comparison of active sites	- 38 -
2.4	dUTPase enzymes as potential chemotherapeutic targets	- 42 -
3	Aims and Objectives	- 45 -
3.1	The trimeric <i>Plasmodium falciparum</i> dUTPase	- 45 -
3.2	The dimeric <i>Trypanosoma cruzi</i> dUTPase	- 46 -
4	Triphenylmethylamino and <i>tert</i>-butyldiphenylsilyloxy uracil acetamide derivatives	- 47 -
4.1	Rational drug design and isosteric replacement	- 47 -

4.2	Triphenylmethoxy and triphenylmethylamino monoalkyl chain derivatives – coupling of primary amines to 1- carboxyuracil.....	- 48 -
4.2.1	Synthesis of 1-carboxymethyluracil	- 49 -
4.2.2	Attempted coupling with 1,2-ethanolamine.....	- 50 -
4.2.3	Synthesis of the triphenylmethoxy derivatives	- 50 -
4.2.4	Synthesis of the triphenylmethylamino derivatives	- 54 -
4.3	Triphenylmethylamino and hydroxy (triphenyl methyl)amino dialkyl chain derivatives – coupling of secondary amines to 1-carboxymethyluracil	- 56 -
4.3.1	Triphenylmethylamino dialkyl chain derivatives	- 57 -
4.3.2	Hydroxy(triphenylmethyl)amino dialkyl chain derivatives.....	- 67 -
4.4	Tritylamino phosphate dialkyl chain derivatives.....	- 69 -
4.4.1	Synthesis of benzyl protected phosphate ester	- 70 -
4.4.2	Deprotection of the benzyl phosphate ester	- 71 -
4.5	Restricted rotation around the amide bond and variable temperature NMR	- 72 -
4.6	Biological results: Trimeric dUTPases and <i>P. falciparum</i> parasites.....	- 75 -
4.6.1	Results and discussion	- 77 -
4.7	Biological results: Dimeric dUTPases and trypanosome parasites.....	- 80 -
4.7.1	Results and discussion	- 81 -
4.8	General discussion	- 81 -
4.9	Conclusions	- 87 -
5	Acyclic uridine analogues.....	- 89 -
5.1	Acyclic uridine analogues	- 89 -
5.2	GRID calculations on <i>P. falciparum</i> dUTPase enzyme.....	- 90 -
5.3	Docking of proposed compounds into PfdUTPase	- 97 -
5.4	Modifications at position 11.....	- 102 -
5.4.1	TBDPS-O derivatives	- 103 -
5.4.2	Triphenylmethylamino derivatives	- 115 -
5.5	Modifications at position 10.....	- 120 -
5.5.1	Orthogonal protection of compound 57	- 121 -
5.5.2	Deprotection of compound 87	- 124 -
5.5.3	Oxidation of alcohol 88.....	- 125 -
5.5.4	Amide coupling	- 126 -

5.6	Single chain derivatives	- 126 -
5.6.1	Synthesis of N-3 - benzoyl uracil.....	- 127 -
5.6.2	Coupling to protected diol 93	- 128 -
5.6.3	Deprotection of compound 94	- 128 -
5.6.4	Oxidation of alcohol 95	- 129 -
5.6.5	Oxidative amidation by a radical mechanism	- 130 -
5.7	Biological results.....	- 131 -
5.8	Discussion	- 132 -
5.9	Conclusion.....	- 133 -
6	Uracil amino acid conjugates as inhibitors of the <i>Trypanosoma Cruzi</i> dUTPase enzyme	- 135 -
6.1	Probing of the <i>T. cruzi</i> active site.....	- 135 -
6.2	Molecular modelling studies.....	- 137 -
6.2.1	FlexX	- 137 -
6.2.2	Results and discussion of docking studies	- 141 -
6.3	Solid phase amino acid uracil acetamide synthesis	- 149 -
6.3.3	Loading of resin	- 150 -
6.3.4	Coupling to amino acids.....	- 152 -
6.3.5	Monitoring of the reactions.....	- 153 -
6.3.6	Cleavage from the resin beads	- 154 -
6.3.7	Results of solid phase synthesis	- 154 -
6.4	Biological results: Dimeric dUTPases and trypanosome parasites.....	- 156 -
6.4.8	Results and discussion	- 157 -
6.5	Conclusion.....	- 158 -
7	Conclusions.....	- 159 -
7.1	Trimeric PfdUTPase inhibitors for use as anti-malarials.....	- 159 -
7.2	Dimeric TcdUTPase inhibitors as trypanocides.....	- 160 -
8	Experimental I.....	- 161 -
8.1	General remarks.....	- 161 -
8.2	General procedures.....	- 163 -
8.3	(1) Synthesis of 1-carboxymethyluracil	- 164 -
8.4	(3) Synthesis of 2-(<i>tert</i> -butyldimethylsilyloxy)-ethylamine	- 165 -
8.5	(4) Synthesis of 2-(<i>tert</i> -butyldiphenylsilyloxy) ethylamine	- 166 -

8.6	(5) Synthesis of 3-(<i>tert</i> -butyldiphenylsilyloxy) –propylamine ... - 167 -
8.7	(6) Synthesis of 4-(<i>tert</i> -butyldiphenylsilyloxy)-butylamine - 168 -
8.8	(8) Synthesis of N-[3-(<i>tert</i> -butyldiphenylsilyloxy)-propyl] uracil acetamide - 169 -
8.9	(9) Synthesis of N-[4-(<i>tert</i> -butyldiphenylsilyloxy)-butyl] uracil acetamide - 170 -
8.10	(10) Synthesis of N-(3-hydroxypropyl) uracil acetamide - 171 -
8.11	(11) Synthesis of N-(4-hydroxybutyl) uracil acetamide - 172 -
8.12	(14) Synthesis of 2-(triphenylmethylamino) ethylamine - 173 -
8.13	(15) Synthesis of 3-(triphenylmethylamino) propylamine - 174 -
8.14	(16) Synthesis of 4-(triphenylmethylamino) butylamine - 174 -
8.15	(17) Synthesis of 1-[N-(2-triphenylmethylaminoethyl)-acetamide] uracil - 175 -
8.16	(18) Synthesis of 1-[N-(3-triphenylmethylaminopropyl)-acetamide] uracil - 176 -
8.17	(19) Synthesis of 1-[N-(3-triphenylmethylaminobutyl)- acetamide] uracil - 177 -
8.18	(20) Synthesis of carbobenzoxyimidazole - 178 -
8.19	(21) Synthesis of N ¹ N ^{1'} -(dicarbobenzyloxy) diethylene triamine - 179 -
8.20	(22) Synthesis of N ¹ N ^{1'} -(dicarbobenzyloxy)di(<i>n</i> -propyl) triamine ... - 180 -
8.21	(23) Synthesis of N ¹ N ^{1'} -dicarbobenzyloxyspermidine - 181 -
8.22	(24) Synthesis of 1-carboxymethyluracil succinimide ester - 182 -
8.23	(25) Synthesis of 1-[N ¹² N ^{12'} -(dicarbobenzyloxy)diaminodi (<i>n</i> - propyl)acetamide] uracil - 183 -
8.24	(26) Synthesis of N-(1-carboxymethyluracil)-N ¹³ N ^{13'} - (dicarbobenzyloxy) spermidine - 184 -
8.25	(27) Synthesis of 1-[N ¹¹ N ^{11'} -(dicarbobenzyloxy)diamino diethyl acetamide] uracil - 185 -
8.26	(28) Synthesis of 1-[diaminodiethylacetamide] uracil - 186 -
8.27	(29) Synthesis of 1-[diaminodi(<i>n</i> -propyl)acetamide] uracil - 187 -
8.28	(30) Synthesis of N-(1-carboxymethyluracil) spermidine - 188 -
8.29	(31), (31b) and (33) Synthesis of 1-[N,N'(triphenylmethyl) diaminodi(<i>n</i> -propyl)acetamide]uracil, 1-[N-(carboxybenzyl)-N- (triphenylmethyl)diaminodi(<i>n</i> -propyl) acetamide] uracil and 1-[N' (triphenylmethyl)diaminodi(<i>n</i> -propyl)acetamide]uracil - 189 -

8.30	Synthesis of 1-[N-di(triphenylmethylaminoethyl) acetamide] uracil (36) and 1-[N-(triphenylmethyloxyethyl)-N-(aminoethyl) acetamide] uracil (35)	- 192 -
8.31	(37) Synthesis of N-(<i>tert</i> -butyldiphenylsilyloxy)ethyl ethylendiamine	- 194 -
8.32	(38) Synthesis of N-(<i>tert</i> -butyldiphenylsilyloxy) ethyl -N-(triphenylmethylamino)ethyl amine	- 195 -
8.33	(39) Synthesis of 1-[N-(<i>tert</i> -butyldiphenylsilyloxy) ethyl- N-(triphenylmethylamino)ethyl-acetamide] uracil	- 196 -
8.34	(40) Synthesis of 1-[N-hydroxyethyl-N-(triphenylmethyl amino) ethyl-acetamide] uracil	- 197 -
8.39	(41) Synthesis of 1-[N-(dibenzylphosphoxy) ethyl-N-(triphenylmethylamino)ethyl acetamide] uracil	- 198 -
8.40	(42) Synthesis of 1-[N-(phosphoxy)ethyl-N-(triphenylmethyl amino) ethyl acetamide] uracil	- 199 -
9	Experimental II.....	- 201 -
9.1	GRID calculations	- 201 -
9.2	FlexX docking	- 201 -
9.3	General procedures	- 202 -
9.4	(58) 1-[2-(carboxy)-4-(<i>tert</i> -butyldiphenylsilyloxy)butyl] uracil or 1-[2-(carboxy)-4-(<i>tert</i> -butyldimethylsilyloxy)butyl] uracil.....	- 202 -
9.5	(59) 1-[2-(acetaldehyde)-4-(<i>tert</i> -butyldimethylsilyloxy) butyl] uracil.....	- 204 -
9.6	(61) 1-[2-(acetamide)-4-(<i>tert</i> -butyldiphenylsilyloxy)butyl] uracil ..	- 206 -
9.7	(62) 1-[2-(methylamido)-4-(<i>tert</i> -butyldiphenylsilyloxy)butyl] uracil.....	- 207 -
9.8	(64) 1-[2-(ethylamido)-4-(<i>tert</i> -butyldiphenylsilyloxy) butyl] uracil.	- 208 -
9.9	(65) 1-[2-(diethylamido)-4-(<i>tert</i> -butyldiphenylsilyloxy) butyl] uracil.....	- 209 -
9.10	(67) 1-[2-(N-Z-piperazinamido)-4-(<i>tert</i> -butyldiphenyl silyloxy) butyl] uracil	- 210 -
9.11	(70) 2-(1-methyluracil)-4-hydroxybutyanal	- 211 -
9.12	(73) 1-[2-(carbobenzoxyethyl)-4-aminobutyl] uracil	- 212 -
9.13	(74) 1-[2-(carbobenzoxyethyl)-4-(triphenylmethyl)amino butyl] uracil.....	- 213 -
9.14	(75) 1-[2-(hydroxymethyl)-4-(triphenylmethyl)aminobutyl] uracil.	- 214 -

9.15	(76) 1-[2-(carboxy)-4-(triphenylmethyl)aminobutyl] uracil	- 215 -
9.16	(79) 1-[2-(acetamide)-4-(triphenylmethyl)aminobutyl] uracil	- 216 -
9.17	(81) Attempted synthesis of 1-[2-(piperazinamido)-4-(triphenylmethyl)aminobutyl] uracil.....	- 217 -
9.18	(85) 1-[2-(hydroxymethyl)-4-(<i>tert</i> -butyldimethylsilyloxy)butyl]-3- (<i>para</i> -methoxyphenyl) uracil	- 219 -
9.19	(87) 1-[2-(dihydropyranloxy)-4-(<i>tert</i> -butyldimethylsilyl oxy)butyl] uracil and (88) 1-[2-(dihydropyranloxy)-4-(<i>tert</i> -butyldiphenylsilyl oxy)butyl] uracil.....	- 220 -
9.20	(89) 1-[2-(dihydropyranloxy)-4-hydroxybutyl] uracil	- 222 -
9.21	(90) 1-[2-(dihydropyranloxy)-4-carboxybutyl] uracil	- 223 -
9.22	(92) 3-benzoyl uracil	- 224 -
9.23	(94) 1-(4-benzoylbutyl)-3- benzoyl uracil	- 225 -
9.24	(95) 1-(4-hydroxybutyl) uracil	- 226 -
9.25	(96) 1-(4-butanal) uracil	- 227 -
10	Experimental III	- 229 -
10.1	Docking of amino acid uracil conjugates	- 229 -
10.2	General solid phase synthesis	- 229 -
10.2.1	Loading of resin procedure	- 230 -
10.2.2	Fmoc deprotection procedure	- 230 -
10.2.3	Ninhydrin test procedure	- 230 -
10.2.4	Coupling procedure.....	- 230 -
10.2.5	Cleavage from the resin.....	- 231 -
10.3	Results of amino acid uracil acetamide conjugate syntheses.....	- 232 -
11	Appendix 1: Biological assays	- 237 -
11.1	Enzyme assays.....	- 238 -
11.2	<i>In vitro</i> assays.....	- 238 -
11.2.1	<i>Trypanosoma brucei</i> (Sleeping sickness)	- 238 -
11.2.2	<i>Trypanosoma cruzi</i> (Chagas' Disease)	- 238 -
11.2.3	<i>Leishmania donovani</i> (Leishmaniasis)	- 239 -
11.2.4	<i>Plasmodium falciparum</i> (Malaria)	- 240 -
12	Appendix 2: Publications	- 241 -

Abbreviations

1-CU	1-Carboxymethyl uracil
4-MPM	4-methoxyphenylmethyl
ACD	Advanced Chemistry Developmant
ACE	Angiotensin converting enzyme
ACN	Acetonitrile
ACT	Artemisinin combination therapy
AdoMetDC	S-adenosylmethionine decarboxylase
AIBN	Azobisisobutyronitrile
AP	Apyrimidic
BAIB	Bis-acetoxyiodobenzene
BBB	Blood brain barrier
BER	Base excision repair
Bn	Benzyl
Boc	<i>tert</i> -Butoxycarbonyl
br	Broad
Bz	Benzoyl
CbZ	Benzyloxycarbonyl
CjdUTPase	<i>Campylobacter jejuni</i> dUTPase
CL	Cutaneous leishmaniasis
CNS	Central nervous system
CPM	Counts per minute
CQ	Chloroquine
d	Doublet
DALY	Disability Adjusted Life Years
DBF	Dibenzofulvene
DCC	Dicyclohexylcarbodiimide
DCM	Dichloromethane
dCTP	Deoxycytidine triphosphate
DCU	Dicyclohexylcarbourea
DDQ	Dichlorodicyanoquinone
DhbtOH	3-hydroxy-3,4-dihydro-4-oxo-1,2,3-benzotriazine
DHFR	Dihydrofolate reductase
DHP	3,4-Dihydro-2 <i>H</i> -pyran
DIPEA	Diisopropylethylamine

DMAP	4-Dimethylaminopyridine
DMF	Dimethylformamide
DMS	Dimethylsulfide
DMSO	Dimethylsulfoxide
DMT-dU	5'-O-(4-4'-dimethoxytrityl)-2'-deoxyuridine
DNA	Deoxyribonucleic acid
dTMP	Deoxythymidine monophosphate
DTT	Dithiolthreitol
dTTP	Deoxythymidine triphosphate
dUDP	Deoxyuridine diphosphate
dUMP	Deoxyuridine monophosphate
dUpNHp	2'-Deoxy-uridine-5'-[(α,β)-imido]diphosphate,
dUTP	Deoxyuridine triphosphate
dUTPase	Deoxyuridine nucleotidohydrolase
EBV	Epstein-Barr virus
EDC	<i>N</i> -ethyl- <i>N'</i> -(3-dimethylaminopropyl)carbodiimide
EDU	<i>N</i> -ethyl- <i>N'</i> -(3-dimethylaminopropyl)carboureia
EIAV	Equine infectious anemia virus
ES	Electrospray
EtOAc	Ethyl acetate
EtOH	Ethanol
FBS	Foetal bovine serum
FePPIX	Ferriprotoporphyrin IX
FIV	Feline immunodeficiency virus
Fmoc	9-Fluorenylmethoxycarbonyl
FUdR	5-Fluorodeoxyuridine
G6PD	Glucose-6-phosphate dehydrogenase
GI	Gastro intestinal
h	hour
HAPT	High affinity pentamidine transporter
HAT	Human African trypanosomiasis
HBA	Hydrogen bond acceptor
HBD	hydrogen bond donor
HEPES	4-(2-hydroxyethyl)-1-piperazinethanesulfonic acid
HOBt	1-Hydroxybenzotriazole
HRMS	High resolution mass spectrometry
HSV	Herpes simplex virus

IC ₅₀	Concentration required for 50% inhibition
IR	Infra red
<i>i</i> -Pr	<i>iso</i> -propyl
<i>J</i>	Coupling constant
K _i	Inhibition constant
LAPT	Low affinity pentamidine transporter
LCR	Low complexity region
LDL	Low density lipoprotein
LRMS	Low resolution mass spectrometry
<i>m</i>	Multiplet
MC	Mucocutaneous
MEM	Minimum essential medium
MeOD	Deuterated methanol
MeOH	Methanol
min	Minutes
MMTV	Mouse mammary tumour virus
MQ	Mefloquine
MS	Mass spectrometry
MW	Microwave
NBS	<i>N</i> -bromosuccinimide
NHS	<i>N</i> -hydroxysuccinimide
NMO	<i>N</i> -methylmorpholine
NMR	Nuclear magnetic resonance
ODC	Ornithine decarboxylase
P2	Purine 2
PABA	<i>para</i> -aminobenzoic acid
Pbf	2,2,4,6,7-pentamethyldihydrobenzofuran-5-sulfonyl
PCC	Pyridinium chlorochromate
PDB	Protein data bank
PDC	Pyridinium dichromate
PfDHFR	<i>Plasmodium falciparum</i> DHFR
PfdUTPase	<i>Plasmodium falciparum</i> dUTPase
PG	Protecting group
<i>q</i>	Quartet
<i>qn</i>	Quintet
R _f	Retention factor
RT	Room temperature

s	Singlet
SAR	Structure activity relationship
SDM	Semidefined minimal medium
SI	Selectivity index
SM	Synthetic minimal
spp	Several species
t	Triplet
TBAF	Tetrabutylammonium flouride
TBAI	Tetrabutylammonium iodide
TBDMS	<i>tert</i> -Butyldimethylsilyl
TBDPS	<i>tert</i> -Butyldiphenylsilyl
TBTU	O-(Benzotriazol-1-yl)-N,N,N',N'-tetramethyluronium tetrafluoroborate
<i>t</i> -Bu	<i>tert</i> -Butyl
TcdUTPase	<i>Typanosoma cruzi</i> dUTPase
TDR	Tropical disease research
TEMPO	2,2,6,6-Tetramethyl-1-piperidinyloxy, free radical
THF	Tetrahydrofuran
THP	Tetrahydropyran
TFA	Trifluoroacetic acid
TLC	Thin layer chromatography
TPAP	Tetrapropylammonium peruthenate
TPS	Triphenylsilyl
Trt	Triphenylmethyl
TS	Thymidilate synthase
UNG	Uracil DNA glycosylase
UTP	Uridine triphosphate
UV	Ultra violet
VL	Visceral leishmaniasis
VMD	Visual Molecular Dynamics
WHO	World Health Organisation

1 Background

This project was concerned with the design and synthesis of anti-protozoal agents for the treatment of neglected tropical diseases. In particular, these compounds were targeted toward the inhibition of the essential enzyme dUTP nucleotidohydrolase. This is as of yet an un-investigated drug target.

1.1 Protozoal infections

Parasites which are transmitted by some means through a vector host to a human host are the causative organisms of many serious and debilitating parasitic diseases. Most of these diseases predominantly affect people living in tropical and sub-tropical regions and constitute a great burden on the developing world.

Disease	Infective organism	Transmission vector	DALYs*	Deaths per annum
African trypanosomiasis	<i>Trypanosoma brucei</i>	Tsetse fly	1,525,000	48,000
Dengue	<i>Flaviviridae</i> viruses	Some mosquitoes	616,000	19,000
Leishmaniasis	<i>Leishmania donovani</i>	Phlebotomine sandflies	2,090,000	51,000
Malaria	<i>Plasmodium</i> spp.	Anopheles mosquito	46,486,000	1,272,000
Schistosomiasis	<i>Schistosoma mansoni</i>	Freshwater snails	1,702,000	15,000
Tuberculosis	<i>Mycobacterium tuberculosis</i>	Airborne	34,736,000	1,566,000
Chagas disease	<i>Trypanosoma cruzi</i>	Triatomine bugs	667,000	14,000
Leprosy	<i>Mycobacterium leprae</i>	Human-to-human	199,000	6,000
Lymphatic filariasis	<i>Wuchereria bancrofti</i> , <i>Brugia timori</i> , <i>Brugia malayi</i>	Some mosquitoes	5,777,000	0
Onchocerciasis	<i>Onchocerca volvulus</i>	Blackflies	484,000	0

Table 1-1: WHO Tropical Disease Research (TDR) list of target diseases. *DALYs - Disability Adjusted Life Years (the number of healthy years of life lost due to premature death and disability)¹ Parasitic protozoal diseases highlighted in grey

Due to the lack of economic incentive, companies are generally unwilling to invest in combating these diseases. Many of the current drug treatments were developed more than 50 years ago and are unsatisfactory due to toxicity, emerging resistance and their parenteral mode of administration or expense. Lack of clinical efficacy is a major issue with many current drug treatments.

¹ World Health Report, 2004. May be accessed at <http://www.who.int/tdr/diseases.default.htm>

The need for new, efficient, cheap and orally bioavailable drugs to treat these diseases is therefore urgent. Of interest to this project are the parasitic protozoal diseases African trypanosomiasis, Chagas' disease, leishmaniasis and malaria, highlighted in grey in Table 1-1.

1.2 The Trypanosomiasis

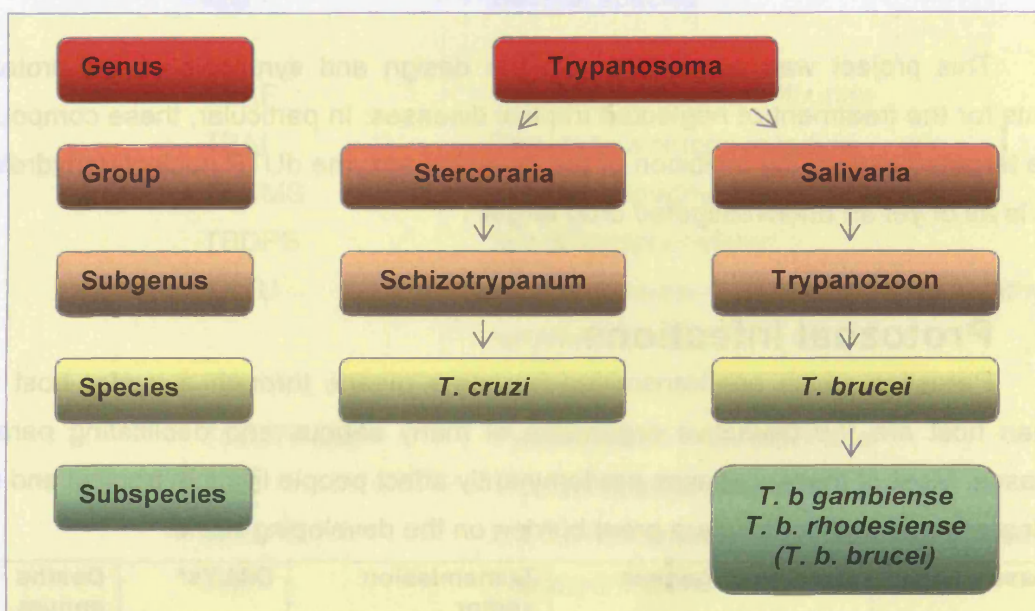


Figure 1-1: Classification of trypanosomes²

The trypanosomiasis are parasitic protozoa that belong to the order kinetoplastida. They are divided into two major groups, the Stercoraria and the Salivaria. (Figure 1-1)

1.2.1 Human African trypanosomiasis

The two subspecies *T. b. gambiense* and *T. b. rhodesiense* are responsible for African trypanosomiasis in humans and belong to the group Salivaria. African sleeping sickness is a severe disease and fatal if left untreated. The disease is prevalent in sub-Saharan Africa (Figure 1-2) and it is estimated that approximately 60 million people are at risk of contraction.³

The disease occurs in two forms. A chronic disease is caused by *T. brucei gambiense* and occurs in West and Central Africa. An acute form is caused by *T. brucei rhodesiense* and occurs in East and Southern Africa. The chronic infection can last for years, whilst the acute disease may only last for weeks.⁴

² James, D. M.; Gilles, H. M. Human Antiparasitic Drugs: Pharmacology and Usage; Wiley and Sons, 1985.

³ <http://who.int/tdr>

⁴ Barrett, M. P.; Burchmore, R. J. S.; Stich, A.; Lazzari, J. O.; Frasch, A. C.; Cazzulo, J. J.; Krishna, S. The trypanosomiasis. *The Lancet* 2003, 362, 1469-1480.

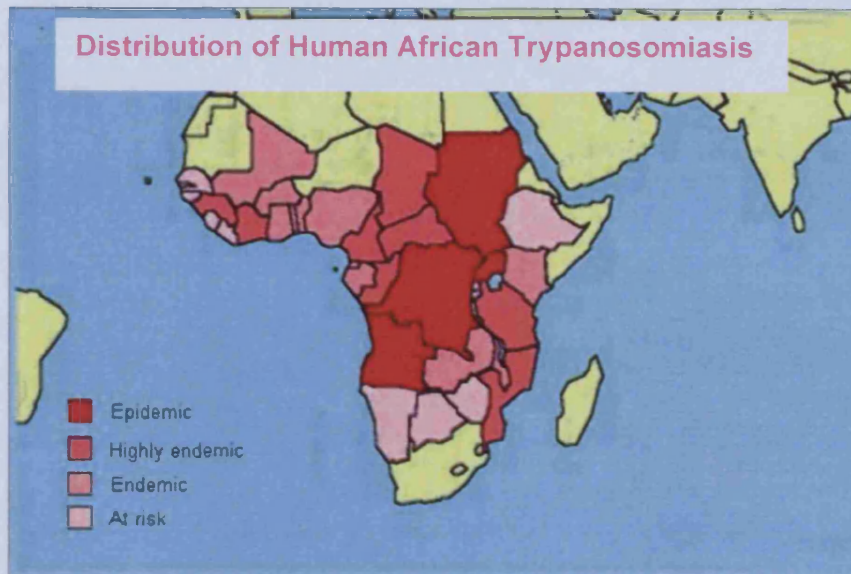


Figure 1-2: Distribution of African trypanosomiasis⁵

1.2.1.1 Symptoms

There are two stages to the disease. During the first stage parasites can be detected in the blood, lymph and tissue, though are sometimes below detection levels. This is the haemolymphatic stage of the disease. Symptoms include general malaise, headache and irregular fevers. In the more acute rhodesiense infection, inflammation of the heart, congestive heart failure and pulmonary oedema can cause fatalities at this early stage.

In the second stage of the disease parasites invade internal organs and the CNS. This stage of the disease is characterised by severe headaches, sleeping disorders, personality changes, various other neurological disorders and endocrine malfunctions. Progressive CNS involvement leads to eventual coma and death. This stage can last for months and years with the gambiense infection but death may occur within a few weeks with the rhodesiense infection.⁴

1.2.1.2 Transmission of the parasite

T. brucei are known as salivaria because they are transmitted in the saliva of the vector, the tsetse fly. The small, infective metacyclic trypomastigotes in the saliva of the tsetse fly are transferred to the bloodstream of the mammalian host. The trypomastigotes in the bloodstream undergo antigenic variation to evade the host immune system. At this stage, they are mostly slender trypomastigotes but change to the stumpy forms, which can then enter the CNS as the disease progresses. Transmission from the host to the vector occurs when the bloodstream forms are ingested by the tsetse as it takes its blood meal. In this case, the parasites differentiate

⁵ <http://www.who.int/emc/diseases/trypano/trypanogeo.html>

1 Background

into procyclic trypomastigotes within the gut of the tsetse and subsequently migrate to the saliva glands of the vector. After reaching the saliva glands, the procyclic trypomastigotes transform into epimastigotes and attach to the epithelial cell wall where they divide before developing into mature, infective, metacyclic trypomastigotes again (Figure 1-3).

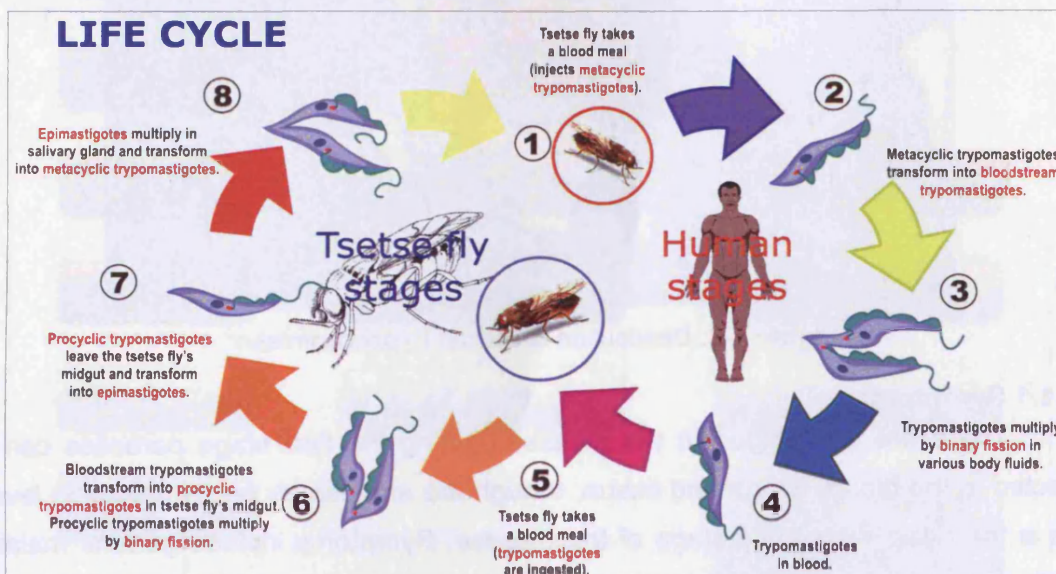


Figure 1-3: Life cycle of *Trypanosoma brucei*⁶

1.2.1.3 Drug treatment

4 drugs are currently registered for the treatment of human African trypanosomiasis.

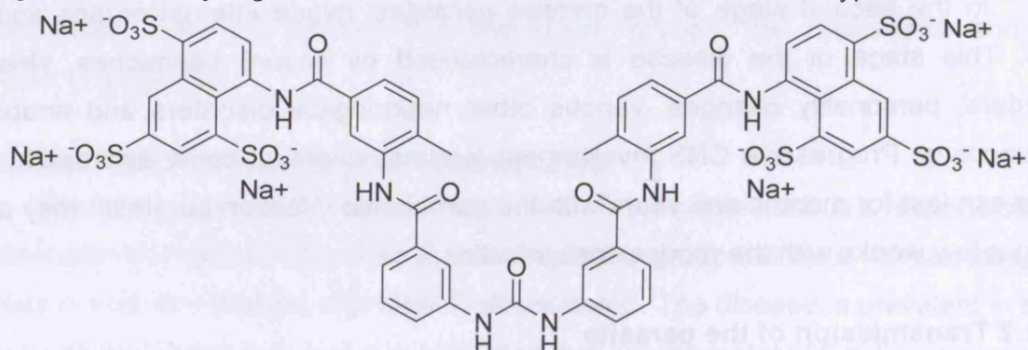


Figure 1-4: Suramin

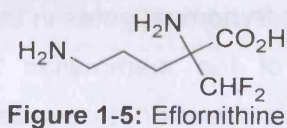


Figure 1-5: Eflornithine

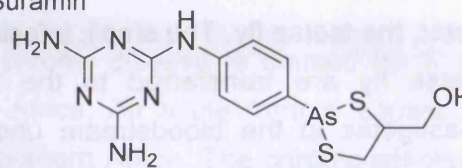


Figure 1-6: Melarsoprol

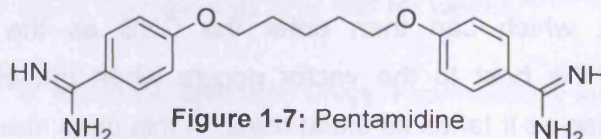


Figure 1-7: Pentamidine

⁶ Baliani, A. Design and Synthesis of New Potential Drugs for the Treatment of Human African Trypanosomiasis. In *Welsh School of Pharmacy*; University of Wales, Cardiff: Cardiff, 2005.

Stage 1	<p>Suramin (1920) (Figure 1-4)</p>	<p>Accumulated in the cell by receptor mediated endocytosis of drug bound to low density lipoprotein (LDL) and maybe other carriers. Suggested mechanisms include: 1) Inhibition of glycolytic enzymes; 2) Inhibition of polyamine biosynthesis; 3) Promiscuous enzyme inhibitor with many targets. Unwanted side effects include nausea, vomiting, shock, dermatitis, anaemia, jaundice, and diarrhoea. Suramin must be injected intravenously and does not cross the BBB (blood brain barrier). It has a long half life due to tight protein binding and also undergoes very little metabolism. Used for initial phase against <i>T. b. rhodesiense</i>.</p>
	<p>Pentamidine (1941) (Figure 1-7)</p>	<p>Actively transported into the cell by the P2 transporter and also by a high affinity and low affinity purine transporter (HAPT1 and LAPT1). It has been shown that the drug binds to negatively charged cellular components such as phospholipids and nucleic acids and that it disrupts the structure of kinetoplast DNA. It also inhibits S-adenosylmethionine decarboxylase (AdoMetDC) <i>in vitro</i>, which is involved in polyamine biosynthesis. It may cause damage to liver and kidneys and also to the pancreas which may cause diabetes. It has poor bioavailability, must be injected intramuscularly and does not penetrate the BBB. Pentamidine is used against <i>T. b. gambiense</i> but is not as effective against <i>T. b. rhodesiense</i>.</p>
Stage 2	<p>Melarsoprol (1949) (Figure 1-6)</p>	<p>A prodrug of melarson oxide, which is taken up by the P2 transporter into the parasitic cell. It has been shown that a stable adduct with trypanothione (MeIT), which is a competitive inhibitor of trypanothione reductase, is formed. It may be that this compound therefore interferes with polyamine metabolism but trivalent arsenicals are promiscuous inhibitors. Melarsoprol causes serious reactive encephalopathy in 5-10% of patients. Vomiting, abdominal colic, peripheral neuropathy, joint pain and blood clotting are other unwanted side effects. Melarsoprol is administered intravenously in a 3.6% w/v solution of propylene glycol. It is used against late stage <i>T. b. rhodesiense</i> and <i>T. b. gambiense</i> infections.</p>
	<p>Eflornithine (1977) (Figure 1-5)</p>	<p>Eflornithine is an irreversible inhibitor of ornithine decarboxylase, an essential enzyme in the biosynthesis of polyamines. Selectivity is probably due to the limited ability of parasites to uptake trace amount of polyamines in response to starvation or differences in turnover rates of human and parasitic ODC. Side effects include anaemia and diarrhoea. Eflornithine however, is costly as it requires infusions of 400mg kg⁻¹ 4 times day⁻¹ for 14 days. <i>T. b. rhodesiense</i> also show poor response.</p>

Table 1-2: Drugs used to treat African trypanosomiasis^{7,8}

⁷ Fairlamb, A. H. Chemotherapy of human African trypanosomiasis: current and future prospects. *Trends Parasitol.* 2003, 19, 488-494.

1.2.2 Chagas' disease

The causative agent for South American trypanosomiasis or Chagas' disease is *Trypanosoma cruzi* which belongs to the Stercoraria group of trypanosomes. It is estimated that approximately 120 million people, i.e. 25% of the inhabitants of Latin America (Figure 1-8) are at risk of contracting the disease.³ In the past decade, transmission control programmes utilising insecticides to kill the transmission vector have been successful in several endemic countries in substantially reducing the incidence of Chagas' disease in Latin America but not eradicating it. Current drug treatment is unsatisfactory and there is, at present no effective treatment for the chronic stage of the disease.

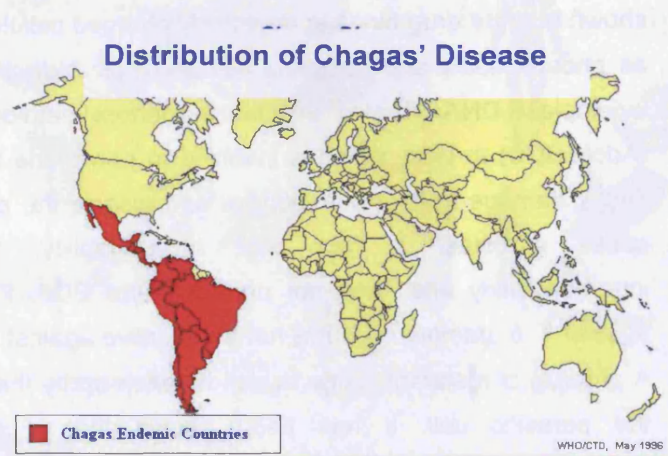


Figure 1-8: Distribution of Chagas' disease⁹

1.2.2.1 Symptoms

The acute stage of the disease manifests itself 6-10 days after infection and can last 1-2 months. Frequently, inflammation at the site of infection leads to oedematous swelling known as chagoma. Romaña's sign is a swelling of the eyelids that occurs after infection at this site and is often used to detect the disease at early stage. The acute phase can pass unnoticed with symptoms typical of general malaise. However, death can ensue at this stage due to inflammation of the heart or brain. Other symptoms include fever, rash, oedema, increased heart rate and autoimmune responses. During this stage parasites are easily detected in the blood and this phase of the disease ends when the host immune system greatly reduces the number of circulating trypomastigotes to an undetectable level.

After the acute phase patients become asymptomatic, this phase is known as the indeterminate form of Chagas' disease. Approximately 70%-85% of people remain

⁸ Fries, D. S.; Fairlamb, A. H. *Burger's Medicinal Chemistry and Drug Discovery*; Wiley and sons, 2003.

⁹ <http://www.who.int/ctd/chagas/geo.htm>.

in this state for the rest of their lives. However, 10%-15% of patients reach the chronic stage of the disease 10-25 years after initial infection when they start to show symptoms of serious organ damage such as digestive and nervous complications, chest pain, palpitations, dizziness and peripheral oedema. Arrhythmia and thromboembolism are frequent and death normally ensues due to heart failure. Congenital infection accounts for stillbirths and early postnatal death.^{2,4}

1.2.2.2 Transmission of the parasite

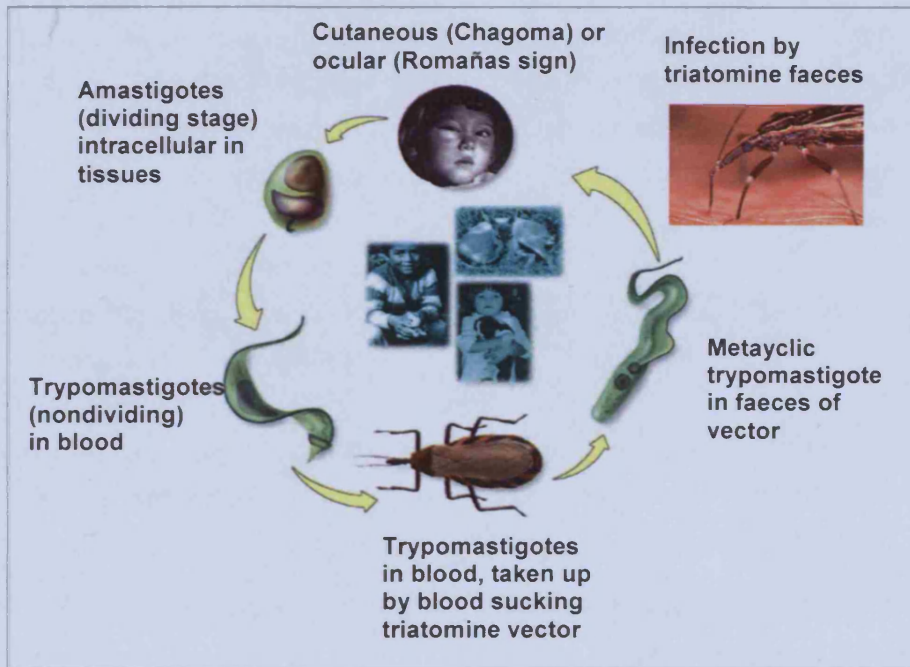


Figure 1-9: Life cycle of *T. cruzi*¹⁰

T. cruzi are transmitted by arthropods belonging to the subfamily Triatomoniidae in the family Reduviidae through the faeces of the vector as they bite the human host.

Trypanosomes taken up by the vector, change into epimastigotes before multiplying and transforming into contaminating metacyclic trypomastigotes. In the human host circulating trypomastigotes enter the tissues where they change into the amastigote form. These divide and some enter other tissues or are released into the blood as circulating trypomastigotes where they may again be taken up by the vector or infect other tissues (Figure 1-9).^{2,4}

1.2.2.3 Drug treatment

Only two drugs are currently in use for the treatment of Chagas' disease. They are nifurtimox and benznidazole. Both drugs occasionally induce serious side effects and neither has high efficacy against chronic Chagas' disease. The trypomastigotes are cleared from the blood but treatment has to be administered over a long period of

¹⁰ <http://www.uta.edu/chagas/html/biolTcru.html>.

1 Background

time to ensure that trypomastigotes released from the tissues are eliminated. Neither drug is sufficiently well tolerated for the long administration needed for a complete cure. Other drugs such as diuretics, ACE inhibitors, β -blockers and antiarrhythmics are used to treat symptomatic complications of the disease.^{2, 4, 8}

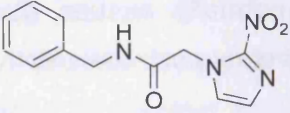
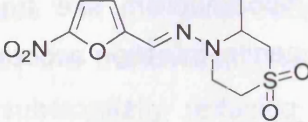
Drug	 Benznidazole (1979)	 Nifurtimox (1964)
Mode of action	Acts via reductive stress that involves covalent modification of macromolecules by nitroreduction intermediates. It does not induce production of superoxide radical anions as does nifurtimox.	Acts via oxidative stress. The nitro group is reduced to give nitroanion radicals which in turn lead to the production of highly toxic reduced oxygen metabolites including superoxide radical anion.
Side effects	Fewer than those of nifurtimox.	Nausea, vomiting, abdominal pain, restlessness, insomnia, seizures, dermatitis, fever, anaphylaxis.
Notes	Drug of choice against Chagas' disease. Given orally at a dose of 5-7mg kg ⁻¹ day ⁻¹ in 2 divided doses for 30-90 days	Given orally at a dose of 8-10mg kg ⁻¹ day ⁻¹ in 4 divided doses for 90-120 days.

Table 1-3: Drugs used to treat American trypanosomiasis^{4, 8, 11, 12}

1.3 The Leishmaniasis

Leishmania are parasitic protozoa that belong to the same order as the trypanosomiasis, that is the kinetoplastida. Together they comprise the family Trypanosomatidae which are often simply called the haemoflagellates. More than 20 different species and subspecies of *Leishmania* are known to be pathogenic to man.²

1.3.1 Leishmaniasis

Leishmaniasis is endemic in 88 countries on four continents. It is estimated that 350 million people are at risk and overall prevalence is 12 million people. Annual incidence is estimated at 1-1.5million cases of cutaneous leishmaniasis and 500,000 cases of visceral leishmaniasis. There are three main forms of the disease, depending on the infective parasite.^{3, 13}

¹¹ Urbina, J. A. Parasitological cure of Chagas disease: Is it possible? Is it relevant? *Mem. Inst. Oswaldo Cruz* **1999**, *94*, 349-355.

¹² Maya, J. D.; Bollo, S.; Nunez-Vergara, L. J.; Squella, J. A.; Repetto, Y.; Morello, A.; Perie, J.; Chauviere, G. Trypanosoma cruzi: effect and mode of action of nitroimidazole and nitrofurans derivatives. *Biochem. Pharmacol.* **2003**, *65*, 999-1006.

¹³ Herwaldt, B. L. Leishmaniasis. *Lancet* **1999**, *354*, 1191-1199.

i) Visceral leishmaniasis (VL) :

(*L. donovani*, *L. infantum*, *L. Chagasi*) (Fig. 1-10) This is caused by infection of the lymphatics after the parasites have multiplied in the macrophages. VL is characterised by irregular bouts of, swelling of the spleen and liver and anaemia. It is the most serious form of the disease and if left untreated has a fatality rate of nearly 100%. Post-kala-azar dermal leishmaniasis (PKDL) is a form of dermal leishmaniasis that occurs as an outcome of visceral leishmaniasis when therapy for VL has been unsuccessful.^{2, 3}



Figure 1-10: Visceral leishmaniasis and its global distribution³

ii) Cutaneous (CL):

(*L. major*, *L. tropica*, *L. aethiopica*, *L. mexicana*, *L. amazonensis*, *L. pifanoi*, *L. guyanensis*, *L. panamensis*, *L. peruviana*) (Fig 1-11, 1-12) This is the most common form of the disease. 1-200 simple skin lesions form. These are self healing but can leave unsightly and debilitating scars. Diffuse cutaneous leishmaniasis (DCL) causes disseminated skin lesions resembling lepromatous leprosy. Treatment is difficult.^{2, 3}

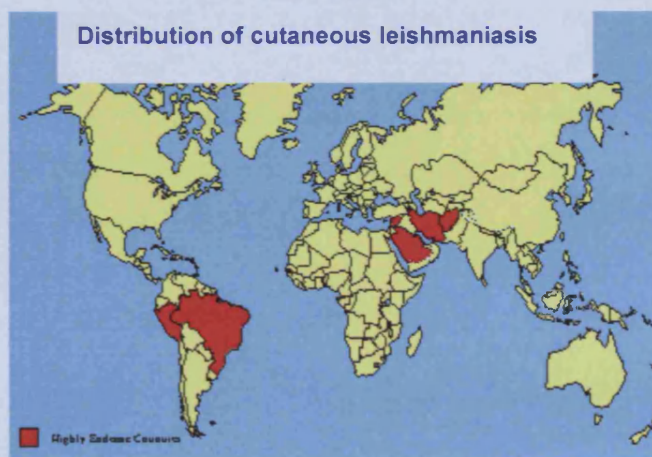


Figure 1-11: Global distribution of cutaneous leishmaniasis³

iii) Mucocutaneous: (MC)

(*L. braziliensis*) This starts with skin ulcers which spread causing massive tissue destruction especially of the nose and mouth (Fig. 1-13). This form of the disease occurs only in South America. It can often have fatal consequences.^{2, 3}



Figure 1-12:
Cutaneous leishmaniasis



Figure 1-13:
Mucocutaneous leishmaniasis

1.3.2 Transmission of the parasite

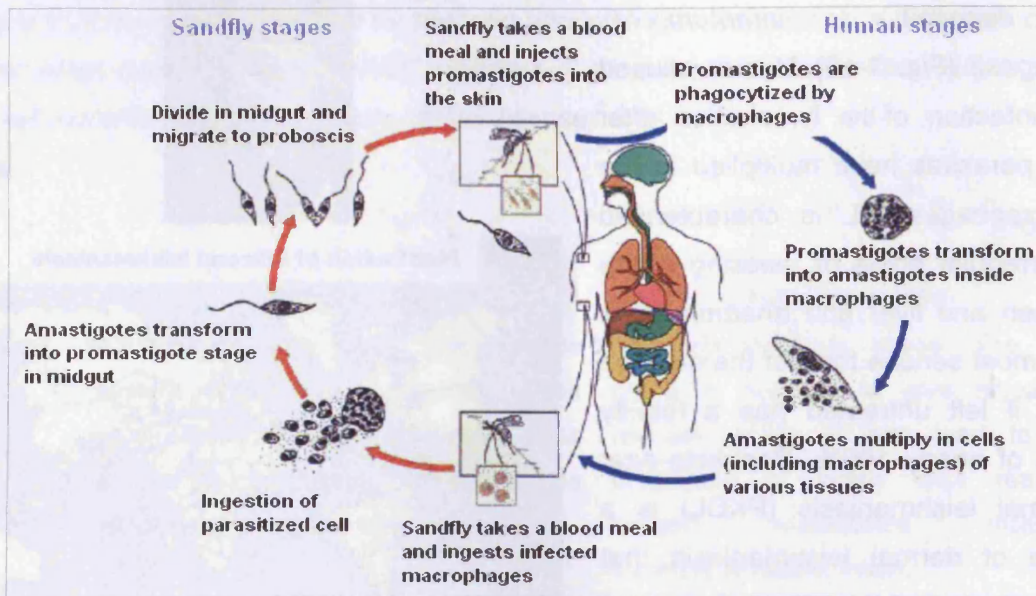


Figure 1-14: Life cycle of *leishmania*¹⁴

The female sandfly is the vector that transmits these parasites. As the vector feeds on the blood of a human, promastigote forms of the parasite enter the host via the insect's proboscis. These are ingested by macrophages in the host, where they metamorphose into the amastigote form. The parasites then multiply by binary fission until the host cell bursts. The amastigotes then infect more macrophages where they multiply or are taken up again by feeding vectors (Fig. 1-14). In visceral leishmaniasis the parasites cause a widespread infection of the lymphatics. In cutaneous leishmaniasis, the lesions remain localised to the skin and skin ulcers develop.³

1.3.3 Drug treatment

Currently 5 drugs are registered for the treatment of Leishmaniasis. (See Figure 1-7 for penatmidine)

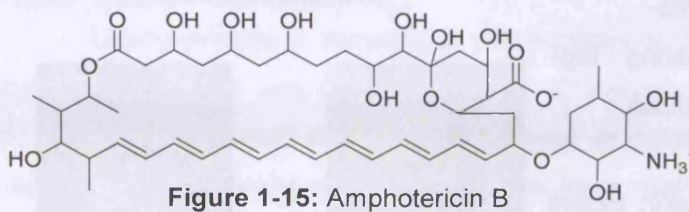


Figure 1-15: Amphotericin B

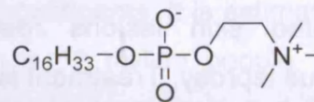


Figure 1-16: Miltefosine

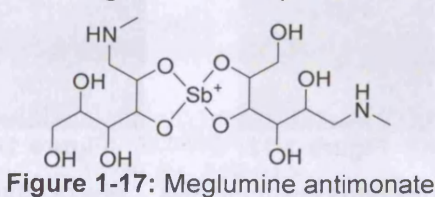


Figure 1-17: Meglumine antimonate

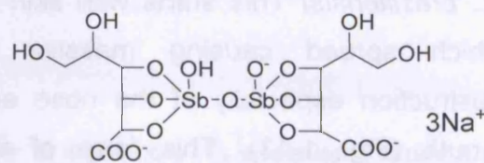


Figure 1-18: Sodium stibogluconate

¹⁴ Hailu, A.; Mudawi Musa, A.; Royce, C.; Wasunna, M. Visceral Leishmaniasis: New Health Tools Are Needed. *PLoS Medicine* **2005**, *2*, e211.

Drug	Pentamidine (Figure 1-7)	Miltefosine (Figure 1-16)	Meglumine antimonite and sodium stibogluconate (Figure 1- 17, 1-18)	Amphotericin B (Figure 1-15)
Used to treat	VL, CL, ML	VL (so far only licensed in India)	VL, CL, ML	VL, ML (deoxycholate complex, Fungizone ®) VL (lipid formulations)
Mode of action	See table 2.	Thought to perturb ether-lipid remodelling in <i>Leishmania</i> by inhibiting key enzymes involved in ether-lipid metabolism including acyl-coA acyl transferases.	Prodrugs requiring reduction from Sb^{5+} to Sb^{3+} which occurs in amastigotes. They are found to inhibit trypanothione reductase and probably inhibit other sulfhydryl containing enzymes.	Complexes with ergosterol in cell membrane of leishmania leading to pore formation, ion leakage and cell death.
Side effects	See table 2.	Gastrointestinal distress. Elevated aspartate aminotransferase and creatine levels.	Fatigue, body aches, electrocardiographic abnormalities, raised aminotransferase levels, pancreatitis	Nephrotoxicity, fever, chills, muscle spasms, vomiting, headache, hypotension, anaphylaxis.
Notes	Considered a back up therapy for pentavalent antimonials and amphotericin B lipid complex.	Was developed as an anti-cancer agent. It is a bioisostere for phosphatidyl-choline where the ester moiety has been changed for an ether. Resistance may become a problem. The drug is teratogenic. Given orally at a dose of 100-150mg day ⁻¹ for 28 days.	Are first line treatments for all types of Leishmaniasis, however, long duration of therapy is required and they are not always effective. Resistance is an issue. They are administered as polymeric mixtures. Both given at 20mg Sb kg ⁻¹ day ⁻¹ intramuscularly or intravenously for 20-28 days.	Lipid complex allows for increased dosing without extra side effects. Effective against antimonial resistant strains. Disadvantages include high cost, need for hospitalisation and long treatment periods. Lipid complex given at a dose of 3mg kg ⁻¹ day ⁻¹ for days 1-5, 14, 21. Deoxycholate given at dose of 0.5-1.0mg kg ⁻¹ day ⁻¹ for 8 weeks.

Table 1-4: Drugs used to treat leishmaniasis^{2, 13, 14}

1.4 Plasmodium

The genus *Plasmodium* are parasitic protozoa that belong to the class Sporozoea.

Four species of the parasite are responsible for malaria in man.

Parasite species (clinical disease form)	Distribution	Percentage of total cases	Survival time of host if left untreated
<i>P. falciparum</i> (falciparum malaria)	Tropical and subtropical, Africa, Nepal and southeast Asia	50	1-4 years
<i>P. vivax</i> (vivax malaria)	Tropical, subtropical, temperate, South America, Asia	42	2-8 years
<i>P. malariae</i> (quartan malaria)	Tropical and subtropical, Africa, Nepal, Southeast Asia	7	4-53 years
<i>P. ovale</i> (ovale malaria)	Tropical Africa and Western Pacific	1	1-5 years

Table 1-5: Species of plasmodium parasitic to man²

1.4.1 Malaria

Malaria is a health problem in more that 90 countries, placing about 40% of the world's population at risk of contracting the disease (Fig. 1-19). It is endemic to tropical and subtropical regions. The economic burden of this disease is also extremely high, accounting for an estimated reduction of 1.3% in economic growth in malaria endemic countries.³ 90% of deaths due to malaria occur in Africa south of the Sahara, mostly among young children.

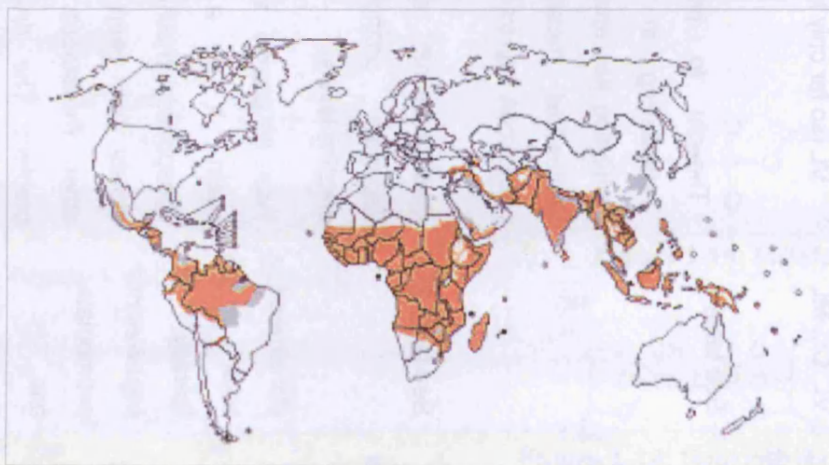


Figure 1-19: Worldwide distribution of malaria¹⁵

¹⁵ http://www.rollbackmalaria.org/cmc_upload/0/000/015/372/RBMInfosheet_1.htm

Plasmodium falciparum is the main cause of severe clinical malaria and death and is also the most common form of the disease complex. For this reason it is often called malignant tertian malaria. The other forms caused by *P. vivax*, *P. malariae*, and *P. ovale* are often termed benign malarias as they are less severe.²

Symptoms of malaria include fever, headache, muscular aches and weakness, vomiting, diarrhea and cough. Cycles of fever, chill and drenching sweats develop. Death may ensue due to infected red blood cells blocking blood vessels supplying the brain (cerebral malaria) or damage to other vital organs.³

The diseases cause periodic fevers, the periodicities of which differ among the infective species and may be indistinguishable in falciparum malaria. They are coincidental with the rupture of mature blood schizonts and the release of merozoites into the circulation. The severities of the symptoms are also clinically distinguishing features among the different disease forms. The four species are morphologically distinguishable at all stages of erythrocytic development.² Relapses with vivax and ovale malaria can occur due to persistence of the latent liver forms and is more common with vivax malaria. Recrudescences due to persistent residual erythrocytic forms can occur with all four species, however they are more common in quartan malaria.^{2,3}



Figure 1-20: Female anopheles vector³



Figure 1-21: A child with malaria³

1.4.2 Transmission of the parasite

Malaria is transmitted through the female *Anopheles* mosquito vector (Fig 1-20). As the vector feeds on the blood of a human, parasite sporozoites enter the host's blood. They are carried to the liver where they enter hepatocytes and undergo exo-erythrocytic schizogony. The hepatocytes eventually rupture and merozoites are released into the bloodstream. These then invade red blood cells where they transform into trophozoites and undergo asexual schizogony again. The schizonts eventually rupture releasing more merozoites into the blood and inducing an attack of fever in the host. Some trophozoites differentiate into gametocytes and are taken up by the vector within which they form a zygote and initiate sporogony (Figure 1-22).¹⁶

¹⁶ Menard, R. Medicine: Knockout malaria vaccine? *Nature* 2005, 433, 113-114.

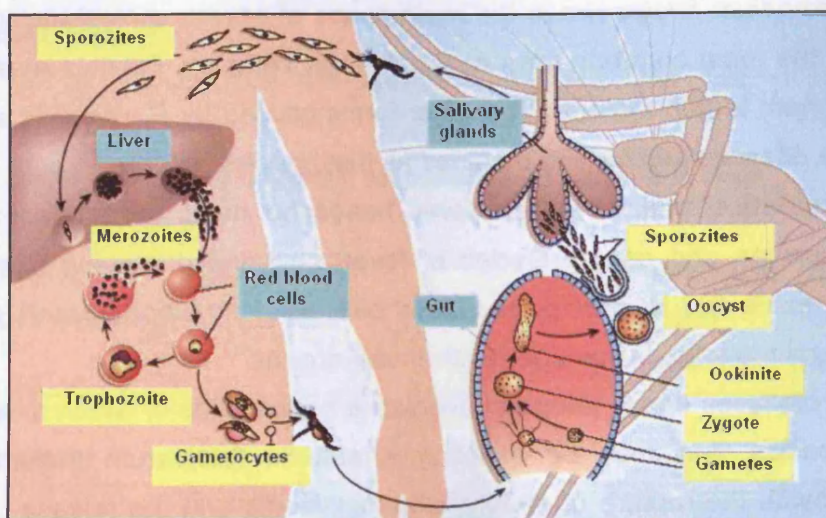


Figure 1-22: Life cycle of plasmodium¹⁶

1.4.3 Drug treatment

Antimalarials can be divided into four arbitrary groups based on close similarities in their antimalarial activity.²

The first group are the **rapidly acting blood schizontocides**. The oldest of this group is quinine; it was one of the first antimalarials ever used and was found as the active component from the bark of the cinchona tree. From quinine, the other 4-aminoquinolines and 4-quinolinemethanols were developed. Chloroquine is one of the most potent and widely used of this class of drugs but resistance to it has developed. Amodiaquine is active against chloroquine resistant strains but some adverse reactions to it have been observed due to *in vivo* activation to a reactive metabolite. Isoquine, which is a regioisomer of amodiaquine that does not form toxic metabolites is currently undergoing preclinical evaluation.¹⁷ Mefloquine and lumefantrine are other commonly used drugs in this category. The site of action of this class of drugs is limited to the stages of the parasite life cycle which are actively involved in haemoglobin degradation. These drugs accumulate in the food vacuole of the trophozoite in the human red blood cell. The postulated mode of action is that as the parasite degrades human haemoglobin into the potentially toxic ferriprotoporphyrin IX (FePPIX, free haem) and the essential globin, the drugs bind to FePPIX, preventing it from being crystallised into the non toxic haemozoin form by the parasite (Figure 1-23).^{18, 19}

¹⁷ O'Neill, P.; Mukhtar, A.; Stocks, P. A.; Randle, L. E.; Hindley, S.; Ward, S. A.; Storr, R. C.; Bickley, J. F.; O'Neill, I. A.; Maggs, J. L.; Hughes, R. H.; Winstanley, P. A.; Bray, P. G.; Park, K. B. Isoquine and Related Amodiaquine Analogues: A New Generation of Improved 4-Aminoquinoline Antimalarials. *J. Med. Chem.* **2003**, *46*, 4933-4945.

¹⁸ Pandey, A. V.; Bisht, H.; Babbarwal, V. K.; Srivastava, J.; Pandey, K. C.; Chauhan, V. S. Mechanism of malarial haem detoxification inhibition by chloroquine. *Biochem. J.* **2001**, *355*, 333-338.

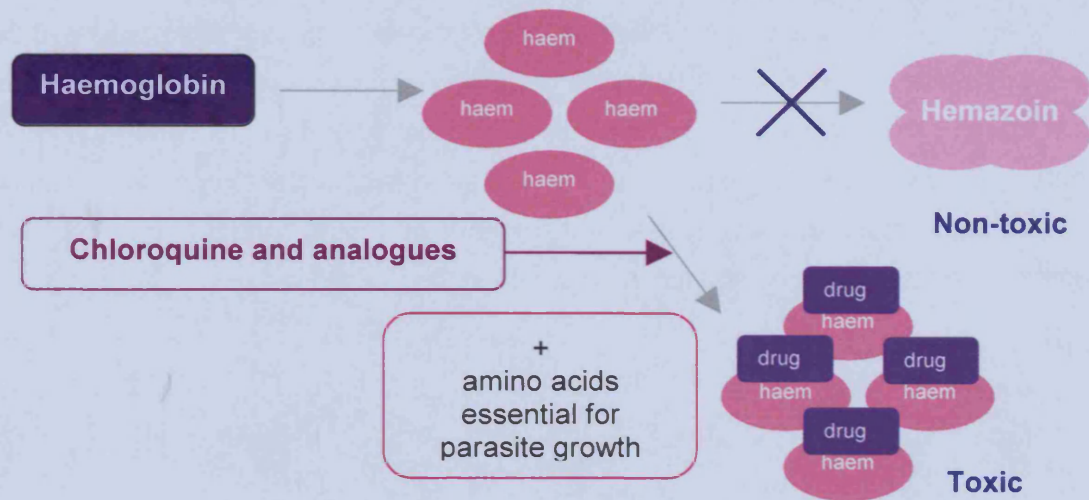


Figure 1-23: Mechanism of action of 4-aminoquinolines and 4-quinolinemethanols

Chloroquine resistance was originally thought to be due to an efflux mechanism²⁰, however, it is now thought that chloroquine resistance is related to diminished uptake of the drug.²¹

Also belonging to the group of blood schizontocides are the sesquiterpene lactones. They emerged from artemisinin (qinghaosu), which was used in China for multidrug resistant *P. falciparum*. The parasites in the erythrocytic cells take up haemoglobin into their food vacuoles to use it as a source of food. The haemoglobin is broken down into FePPIX (free heme) and globin. The free heme bioactivates the endoperoxide bridge of artemisinin to a cytotoxic radical species. It has been proposed that following lipid peroxidation, a variety of reactive oxygen species such as hydroxyl radicals and superoxide radicals are generated. These reactive species cause oxidative damage to cellular proteins resulting in parasite death (Figure 1-24).²²

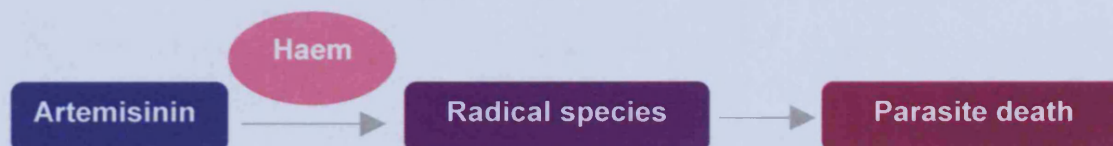


Figure 1-24: Mechanism of action of artemisinin

¹⁹ Sullivan, D. J.; Matile, H., Jr.; Ridley, R. G.; Goldberg, D. E. A Common Mechanism for Blockade of Haem Polymerization by Antimalarial Quinolines. *J. Biol. Chem.* **1998**, *273*, 31103-31107.

²⁰ Krogstad, D. J.; Gluzman, I. Y.; Kyle, D. E.; Oduola, A. M. J.; Martin, S. K.; Milhous, W. K.; Schlesinger, P. H. Efflux of Chloroquine from Plasmodium-Falciparum - Mechanism of Chloroquine Resistance. *Science* **1987**, *238*, 1283-1285.

²¹ Bray, P. G.; Mungthin, M.; Ridley, R. G.; Ward, S. A. Access to hemozoin: The basis of chloroquine resistance. *Mol. Pharmacol.* **1998**, *54*, 170-179.

²² O'Neill, P. M.; Posner, G. H. A Medicinal Chemistry Perspective on Artemisinin and Related Endoperoxides. *J. Med. Chem.* **2004**, *47*, 2945-2964.

1 Background

Although the exact mechanism by which these compounds produce radical species in the cell is debatable, it is known that the endoperoxide bridge is essential for activity. There are a number of synthetic and semi-synthetic endoperoxide analogues (Figure 1-25) under development with the aim of increasing water solubility, resistance to first pass metabolism and ease of synthesis of these compounds. They are chemically stable and active against the parasite in the low nM range.

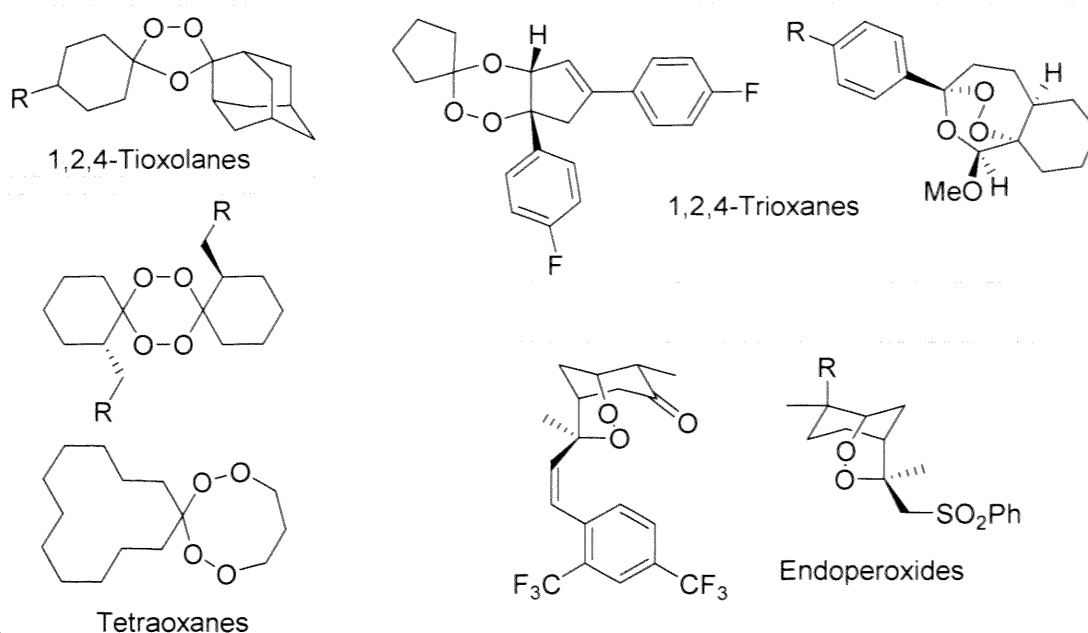


Figure 1-25: Some semi-synthetic and synthetic endoperoxide analogues under development²²

Artemisinin combination therapy (ACT) is a strategy in use for the control of emerging resistance to antimalarials. It involves the combination of artemisinin with another antimalarial agent to treat the disease. It exploits the fact that the artemisinin derivatives cause a rapid reduction in parasite biomass, leaving fewer parasites to be eradicated by the second drug, therefore decreasing the chance of resistance emerging. This strategy is recommended by WHO for control of malaria in Africa.²²

The second group of antimalarials are the antifolates which can be divided into two subclasses; The **antifolate type 1** inhibitors which include sulphonamides and sulphones and the **antifolate type 2** drugs consisting of the biguanidines and 2,4-diaminopyridines. Malaria parasites cannot transport folate, they must synthesise it *de novo*. These drugs act in the folate pathway (Figure 1-26).² Resistance to pyrimethamine and proguanil has occurred through point mutations of the *PfDHFR* gene, the principal mutation being the S108N substitution which reduces the drug's affinity without affecting the enzyme's operation.²³

The basis of selectivity of the **type 1** inhibitors is that this pathway is not present in mammalian cells. The DHFR enzyme, is present in mammalian cells; However, the structure of the human enzyme is very different to that of the plasmodial DHFR and it has a much lower affinity for the drug, therefore selective inhibition is viable.²⁴

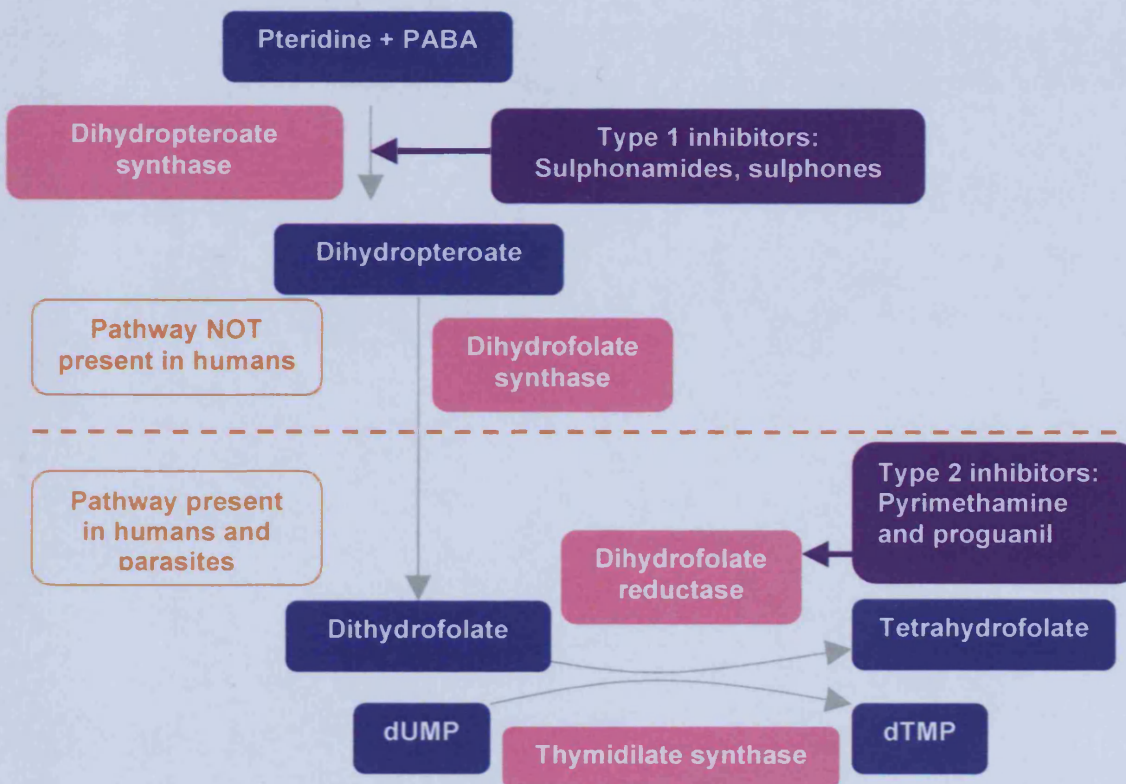


Figure 1-26: Targets of antifolate antimalarials²⁵

²³ Kongsaree, P.; Khongsuk, P.; Leartsakulpanich, U.; Chitnumsub, P.; Tarnchompoo, B.; Walkinshaw, M. D.; Yuthavong, Y. Crystal structure of dihydrofolate reductase from *Plasmodium vivax*: Pyrimethamine displacement linked with mutation-induced resistance. *Proc. Natl. Acad. Sci. U. S. A.* **2005**, *102*, 13046-13051.

²⁴ Yuvaniyama, J.; Chitnumsub, P.; Kamchonwongpaisan, S.; Vanichtanankul, J.; Sirawaraporn, W.; Taylor, P.; Walkinshaw, M. D.; Yuthavong, Y. Insights into antifolate resistance from malarial DHFR-TS structures. *Nat. Struct. Biol.* **2003**, *10*, 357-365.

²⁵ Le Bras, J.; Durand, R. The mechanisms of resistance to antimalarial drugs in *Plasmodium falciparum*. *Fundam. Clin. Pharmacol.* **2003**, *17*, 147-153.

The third group of antimalarials are the **tissue schizontocides**. Currently primaquine is the only drug belonging to this group. It is the only drug effective in clearing persistent liver forms of the parasite responsible for relapses in *P. vivax* and *P. ovale*. Its exact mechanism of action is unknown but it is thought to be an oxidative-reductive agent similar to the 4-aminoquinolines.²⁶

The last group of antimalarials is comprised of other drugs that do not belong to any one of the above groups in particular. Doxycycline, a tetracycline molecule belongs to this group. It can be used in areas of high chloroquine and mefloquine resistance. It acts by binding to the ribosome 30S subunit and therefore inhibiting protein synthesis.²⁶

Some more recently developed antimalarials also do not belong to the three classical groups described above. One such compound is atovaquone which is a hydroxynaphthoquinone. It is a weak inhibitor of dihydroorotate dehydrogenase, an enzyme in the *de novo* pyrimidine biosynthetic pathway in *P. falciparum* and it also acts on the mitochondrial electron transport pathway by mimicking ubiquinone. Its effect on the mitochondrial membrane potential is enhanced by proguanil.²⁹

²⁶ Casteel, D. A. *Burger's Medicinal Chemistry and Drug Discovery*; Sixth ed.; Wiley and sons, **2003**.

²⁷ Britain, B. M. A. a. R. P. S. o. G. *British National Formulary*, **2003**.

²⁸ Edwards, G.; Biagini, G. A. Resisting resistance: dealing with the irrepressible problem of malaria. *Br. J. Clin. Pharmacol.* **2006**, *61*, 690-693.

²⁹ Srivastava, I. K.; Vaidya, A. B. A mechanism for the synergistic antimalarial action of atovaquone and proguanil. *Antimicrob. Agents Chemother.* **1999**, *43*, 1334-1339.

³⁰ Lang, T.; Greenwood, B. The development of Lapdap, an affordable new treatment for malaria. *Lancet Infectious Diseases* **2003**, *3*, 162-168.

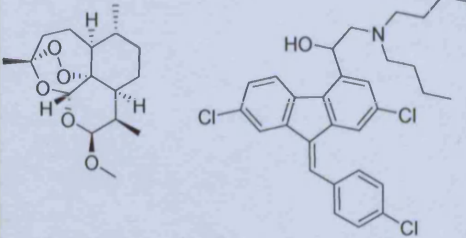
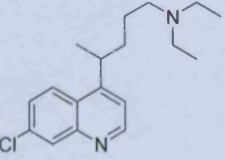
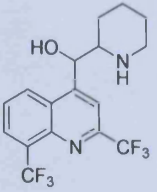
	Drug	Mechanism of action	Side effect	Notes	Refs.
Blood schizonticide	Artemether + lumefantrine (Riamet®) 	Artemether acts by forming radical species that damage cellular components and lumefantrine is a relative of mefloquine which acts by preventing polymerisation of free haem.	Abdominal pain, anorexia, diarrhoea, vomiting, nausea, palpitations, cough, headache, dizziness, sleep disturbances, rash	Used for treatment of acute uncomplicated falciparum malaria. Cost is an issue. Given as an oral tablet. ³¹	22, 26
	Chloroquine 	Prevents polymerisation of toxic free haem to non-toxic haemazoin	GI disturbances, headache, convulsions, visual disturbances, depigmentation, loss of hair, skin reactions, very toxic in overdose	Widespread resistance has occurred. Only used for prophylaxis of malaria in areas where resistance is low. Also used for benign malarial. Sulphate or phosphate salts as oral tablets.	2, 17, 26, 27
	Mefloquine 	Prevents polymerisation of toxic free haem to non-toxic hemazoin	Nausea, vomiting, diarrhoea, abdominal pain, loss of balance, dizziness, headache, sleep disorders, visual disturbances, neuropsychiatric disorders, chest pain, muscle weakness, rash, fatigue, fever	Used for prophylaxis of malaria in areas where high chloroquine resistance is known. Used for falciparum treatment, also if infection is not known or is mixed. Not used for treatment if has been used for prophylaxis. Oral tablets.	2, 26, 27

Table 1-6a: Currently used antimalarials

1 Background

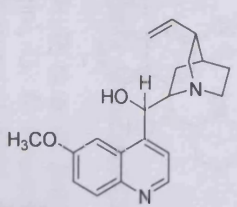
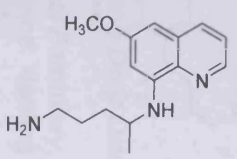
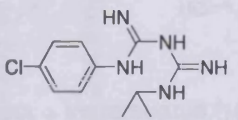
	Drug	Mechanism of action	Side effects	Notes	Refs.
Blood schizonticide	Quinine 	Prevents polymerization of toxic free heme to non-toxic hemozoin.	Cinchonism, headache, hot and flushed skin, nausea, abdominal pain, rashes, visual disturbances, confusion, renal failure, hypoglycaemia, cardiovascular effects, very toxic in overdose	Used for falciparum treatment or if infective agent is not known or is mixed. Not suitable for prophylaxis. Oral tablets of hydrochloride or sulphate salts.	2, 26, 27
	Primaquine 	Acts on mitochondria of parasite cell causing them to swell and inhibiting their activity. Proposed mechanism involves oxidation to a quinone-imine derivative which may mimic ubiquinone.	Nausea, vomiting, anorexia, abdominal pain, less common methaemoglobinaemia in G6PD deficient patients	Used to eliminate liver stages of <i>P. vivax</i> or <i>P. ovale</i> following chloroquine treatment. Given at a dose of 15mg daily for 14 to 21 days.	2, 27
Anti-folate	Proguanil 	Was thought that proguanil was a prodrug of cycloguanil which acts exclusively on <i>P. falciparum</i> DHFR. However proguanil may have other targets.	Mild gastric intolerance, diarrhoea, mouth ulcers, skin reactions.	Hydrochloride salt taken orally is used for prophylaxis of malaria but not suitable alone for treatment. Used in combination with atovaquone (Malorone) for treatment of acute uncomplicated malaria.	2, 26, 27

Table 6b: Currently used antimalarials

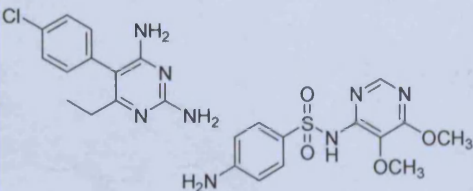
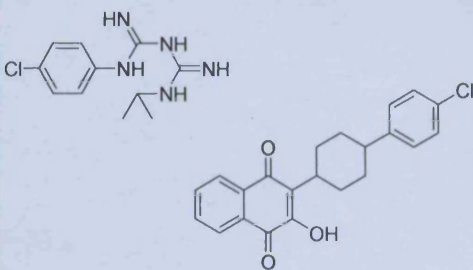
	Drug	Mechanism of action	Side effects	Notes	Refs.
Anti-folates	Pyrimethamine + sulfadoxine (Fansidar®) 	Structurally similar to proguanil, pyrimethamine acts as a DHFR inhibitor. Sulfadoxine is an inhibitor of dihydropterate synthase by competing with the natural substrate PABA.	Depression of blood cell formation and proliferation with high doses, rash, insomnia	Used as treatment for falciparum malaria. Oral tablets of 25mg pyrimethamine and 500mg sulfadoxine. Not recommended for prophylaxis.	2, 25, 26, 27
	Proguanil + atovaquone (Malarone®) 	Proguanil, in this case is known to enhance the effect of atovaquone on mitochondrial membrane potential. Atovaquone acts as described above.	Nausea, vomiting, mouth ulcers, diarrhoea, anorexia, fever, headache, dizziness, rash, insomnia.	Used for treatment of acute uncomplicated falciparum malaria. Also for prophylaxis in areas of high mefloquine or chloroquine resistance. 4 tablets (100mg PG and 250mg atov.) given 4 times daily for 3 days.	25, 26, 27, 29

Table 6c: Currently used antimalarials

1 Background

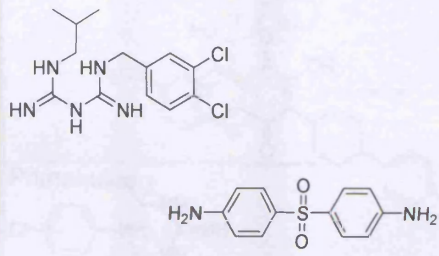
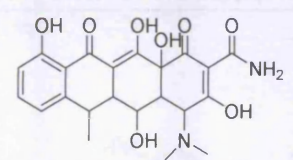
	Drug	Mechanism of action	Side effects	Notes	Refs.
Anti-folate	<p>Clorproguanil + dapsone (Lapdap®)</p>  <p>The image shows two chemical structures. The top structure is Clorproguanil, a pyrimidopyrimidinone derivative with a chlorine atom and a chlorine atom on the benzene ring. The bottom structure is Dapsone, a diphenylsulfone derivative with amino groups on both benzene rings.</p>	Chlorproguanil inhibits DHFR while dapsone is an inhibitor of dihydropteroate synthetase.	Still under post-marketing surveillance but most commonly noted side effect has been anaemia.	Used to treat uncomplicated <i>P. falciparum</i> malaria. Given as oral tablets twice daily for 3 days.	2, 25, 26, 28, 30
Tetracyclines	<p>Doxycycline</p>  <p>The image shows the chemical structure of Doxycycline, a tetracycline antibiotic. It features a tetracyclic core with multiple hydroxyl groups, a methyl group, and a dimethylamino group.</p>	Acts by inhibiting protein synthesis by binding to the 30S ribosome unit.	Nausea, vomiting, diarrhoea, oesophageal irritation, hepatotoxicity, photosensitivity and hypersensitivity, headache, visual disturbances.	Used for prophylaxis in areas of high CQ or MQ resistance. Also used as adjunct to quinine in falciparum treatment. Oral hyclate capsules.	6, 27

Table 6d: Currently used antimalarials

2 The dUTPase enzyme

2.1 Function of the enzyme

Deoxyuridine triphosphate nucleotidohydrolase, also called dUTP pyrophosphatase or dUTPase is an enzyme which catalyses the hydrolysis of dUTP to dUMP in the presence of magnesium ions (Figure 2-1).^{31,32}

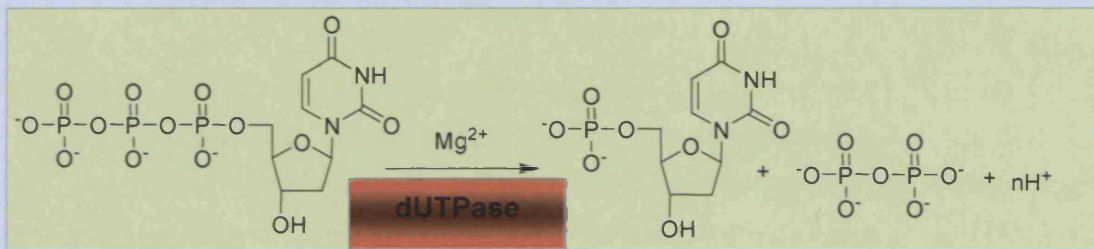


Figure 2-1: dUTPase catalysed hydrolysis of dUTP

The dUTPase catalysed reaction is part of the elaborate network of reactions that control nucleotide metabolism (Figure 2-2).

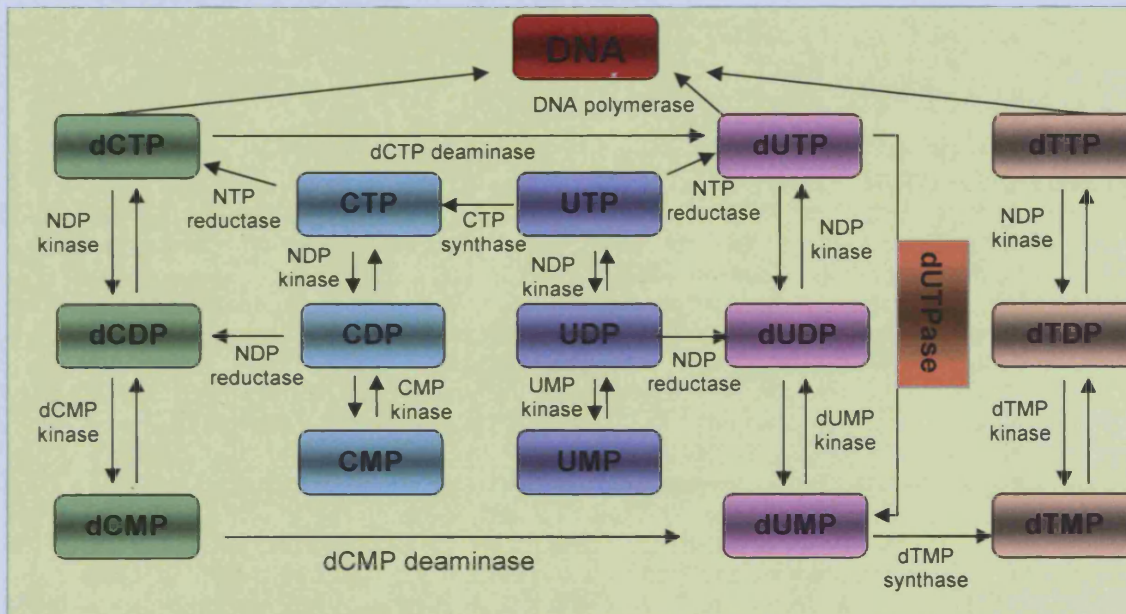


Figure 2-2: De novo synthesis of pyrimidines³³

³¹Bertani, E. L.; Häggmark, A.; Reichard, P. Synthesis of Pyrimidine Deoxyribonucleoside Diphosphates with enzymes from *Escherichia coli*. *J. Mol. Biol.* **1961**, 236, 67-68.

³²Greenberg, G. R.; Somerville, R. L. Deoxyuridylylate Kinase Activity and Deoxyuridinetriphosphatase in *Escherichia coli*. *Proc. Natl. Acad. Sci. U.S.A.* **1962**, 48, 242-247.

The enzyme has two major roles in maintaining the correct free nucleotide balance in the cell.^{33, 34}

1. It provides dUMP, a major cellular source for dTMP which is in turn needed for dTTP formation.
2. It maintains the concentration of dUTP 10^{-5} times lower than that of dTTP thereby minimising mistaken incorporation of dUTP into DNA.

The catalytic reaction is Mg^{2+} dependent^{35, 36, 37} and it has been shown that this is due to the fact that divalent metal ions bind to the triphosphate moiety of the substrate, holding it in the correct orientation and making it more susceptible to nucleophilic attack by an appropriately positioned nucleophile through product stabilisation.^{38, 39, 40, 41}

2.2 dUTPase, cell proliferation and thymineless death

Uracil is not normally a constituent of DNA, however its misincorporation does occur occasionally due to either i) deamination of cytosine or ii) DNA polymerases using dUTP as a substrate in mistake for dTTP. When uracil incorporation occurs, the base excision repair (BER) process is initiated. The enzyme uracil-DNA glycosylase (UNG) catalyses the initial step. UNG specifically removes uracil residues from DNA by cleaving the N-glycosyl bond, releasing uracil and creating an apyrimidinic (AP) site.⁴²

³³ Nyman, P. O. dUTPases: Essential Factors in Preventive DNA Care - Introduction. *Curr. Protein Pept. Sci.* **2001**, *2*, 277-285.

³⁴ Studebaker, A. W.; Ariza, M. E.; Balendiran, G. K.; Williams, M. V. Novel Approaches for Modulating dUTPase and Uracil-DNA Glycosylases: Potential Uses for Cancer and Viral Chemotherapy. *Drug Design Reviews* **2004**, *1*, 1-13.

³⁵ Hoffmann, I.; Widstrom, J.; Zeppezauer, M.; Nyman, P. O. Overproduction and Large-Scale Preparation of Deoxyuridine Triphosphate Nucleotidohydrolase from Escherichia-Coli. *Eur. J. Biochem.* **1987**, *164*, 45-51.

³⁶ Climie, S.; Lutz, T.; Radul, J.; Sumnersmith, M.; Vandenberg, E.; McIntosh, E. Expression of Trimeric Human DUTP Pyrophosphatase in Escherichia-Coli and Purification of the Enzyme. *Protein Expression Purif.* **1994**, *5*, 252-258.

³⁷ Larsson, G.; Nyman, P. O.; Kvassman, J. O. Kinetic characterization of dUTPase from Escherichia coli. *J. Biol. Chem.* **1996**, *271*, 24010-24016.

³⁸ Mustafi, D.; Bekesi, A.; Vertessy, B. G.; Makinen, M. W. Catalytic and structural role of the metal ion in dUTP pyrophosphatase. *Proc. Natl. Acad. Sci. U. S. A.* **2003**, *100*, 5670-5675.

³⁹ Mol, C. D.; Harris, J. M.; McIntosh, E. M.; Trainer, J. A. Human dUTP pyrophosphatase: uracil recognition by β hairpin and active sites formed by three separate subunits. *Structure* **1996**, *4*, 1077-1092.

⁴⁰ Persson, R.; Cedergren-Zeppezauer, E. S.; Wilson, K. S. Homotrimeric dUTPases; Structural solutions for Specific Recognition and Hydrolysis of dUTP. *Curr. Protein Pept. Sci.* **2001**, *2*, 287-300.

⁴¹ Barabas, O.; Pongracz, V.; Kovari, J.; Wilmanns, M.; Vertessy, B. G. Structural insights into the catalytic mechanism of phosphate ester hydrolysis by dUTPase. *J. Biol. Chem.* **2004**, *279*, 42907-42915.

⁴² Krokan, H. E.; Drablos, F.; Slupphaug, G. Uracil in DNA - occurrence, consequences and repair. *Oncogene* **2002**, *21*, 8935-8948.

Under normal dUTP concentrations the AP site would then be filled with the correct base by the action of DNA polymerase.⁴³ In the latter case this would be dTTP. Since DNA polymerases, however, do not discriminate between nucleotide bases well, the insertion of the correct nucleotide depends on its cellular concentration.³⁴ Under elevated concentrations of dUTP the BER can become self-perpetuating where, at the final stage, dUTP is again incorporated by DNA polymerases into DNA.

Inhibition or mutation of the dUTPase enzyme leads to a large increase in the dUTP:dTTP ratio in the cell and extensive incorporation of uracil into DNA. This has been observed in bacteria,⁴⁴ yeast,⁴⁵ and is likely in all cellular systems.⁴⁶ The BER then becomes self-perpetuating and eventually leads to single/double strand breaks,⁴⁷ DNA fragmentation and cell death.^{44, 45}

This phenomenon has also been induced by thymidylate synthase inhibitors such as the anti-cancer agent 5-fluorouracil or dihydrofolate reductase inhibitors such as methotrexate (Figure 2-3) and is termed “thymineless death”. It has been shown in mammalian cell lines that inhibitors of thymidylate synthase and DHFR induce elevated intracellular dUTP:dTTP ratios and promote incorporation of uracil into DNA⁴⁸ and this then induces DNA strand breakage leading to increased cell death.^{49, 50}

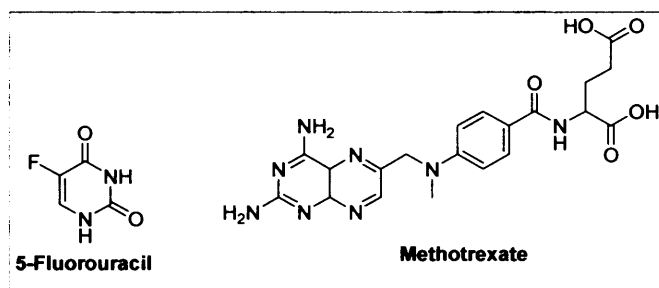


Figure 2-3: 5-Fluorouracil, an inhibitor of TS and methotrexate, an inhibitor of DHFR

⁴³ Augusto-Pinto, L.; Regis da Silva, C. G.; de Oliveira Lopes, D.; Machado-Silva, A.; Machado, C. R. *Escherichia coli* as a model system to study DNA repair genes of eukaryotic organisms. *Genetics and Molecular Research* **2003**, *2*, 77-91.

⁴⁴ El-Hajj, H. H.; Zhang, H.; Weiss, B. Lethality of a dut (deoxyuridine triphosphatase) mutation in *Escherichia Coli*. *J. Bacteriol.* **1988**, *170*, 1069-1075.

⁴⁵ Gadsden, M. H.; McIntosh, E. M.; Game, J. C.; Wilson, P. J.; Haynes, R. H. dUTPase is an essential enzyme in *Saccharomyces cerevisiae*. *EMBO J.* **1993**, *12*, 4425-4431.

⁴⁶ McIntosh, E. M.; Haynes, R. H. dUTP pyrophosphatase as a potential target for chemotherapeutic drug development. *Acta Biochim. Pol.* **1997**, *44*, 159-172.

⁴⁷ Kouzminova, E. A.; Kouzminov, A. Chromosomal fragmentation in dUTPase-deficient mutants of *Escherichia coli* and its recombinational repair. *Mol. Microbiol.* **2004**, *51*, 1279-1295.

⁴⁸ Curtin, N. J.; Harris, A. L.; Aherne, G. W. Mechanism of cell death following thymidylate synthase inhibition, 2'-deoxyuridine-5'-triphosphate accumulation, DNA damage, and growth inhibition following exposure to CB3717 and dipyridamole. *Cancer Res.* **1991**, *51*, 2346-2352.

⁴⁹ Barclay, B. J.; Kunz, B. A.; Little, J. G.; Haynes, R. H. genetic and biochemical consequences of thymidylate stress. *Can. J. Biochem.* **1982**, *60*, 172-194.

⁵⁰ Goulian, M.; Bleile, B.; Teng, B. Y. Methotrexate-induced misincorporation of uracil into DNA. *Proc. Natl. Acad. Sci. U. S. A.* **1980**, *77*, 1956-1960.

In addition, correlations have been made between resistance of certain cancer cell lines to drugs acting on the folate pathway and dUTPase activities within the cells.^{34, 51} It is therefore possible that inhibition of the dUTPase enzyme could act as an alternative or adjunct therapy to the use of TS and DHFR inhibitors as anti-infective or anti-cancer agents.

2.3 Structure and classification

dUTPase is classified into three groups of homologous proteins according to the associative state of their subunits. The three groups are monomeric, homodimeric and homotrimeric (Figure 2-4).

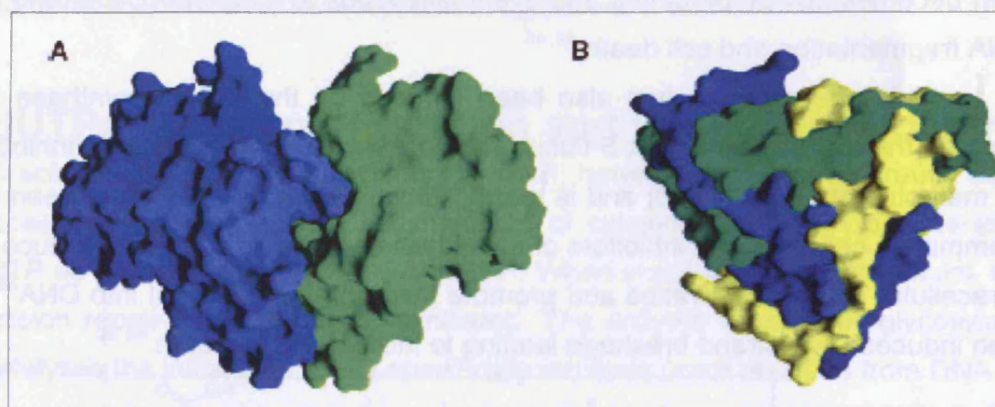


Figure 2-4: Surface representation of A) the dimeric *T. cruzi* dUTPase and B) the trimeric human dUTPase⁵²

2.3.1 Trimeric dUTPases

These are the most well known and best characterised group of dUTPase enzymes. They include the dUTPase enzymes from animals, higher plants, fungi, most bacteria and most viruses.

The crystal structure of that from *E. coli*⁵³ (PDB entries 1DUD, 1DUP), human³⁹ (PDB entries 1Q5U, 1Q5H), FIV⁵⁴ (PDB entries 1EU5, 1DUT), EIAV⁵⁵ (PDB entries

⁵¹ Canman, C. E.; Radany, E. H.; Parsels, L. A.; Davis, M. A.; Lawrence, T. S.; Maybaum, J. Induction of Resistance to Fluorodeoxyuridine Cytotoxicity and DNA-Damage in Human Tumor-Cells by Expression of Escherichia-Coli Deoxyuridinetriphosphatase. *Cancer Res.* **1994**, *54*, 2296-2298.

⁵² Harkiolaki, M.; Dodson, E. J.; Bernier-Villamor, V.; Turkenburg, J. P.; González-Pacanowska, D.; Wilson, K. S. The Crystal Structure of *Trypanosoma cruzi* dUTpase Reveals a Novel dUTP/dUDP Bindind Fold. *Structure* **2004**, *12*, 41-53.

⁵³ Larsson, G.; Svensson, L. A.; Nyman, P. O. Crystal Structure of the *Escherichia coli* dUTPase in Complex with a Substrate Analogue (dUDP). *Nat. Struct. Biol.* **1996**, *3*, 532.

⁵⁴ Prasad, G. S.; Stura, E. A.; McRee, D. E.; Laco, G. S.; Hasekus-Light, C.; Elder, J. H.; Stout, C. D. Crystal structure of dUTP pyrophosphatase from feline immunodeficiency virus. *Protein Sci.* **1996**, *5*, 2429-2437.

⁵⁵ Dauter, Z.; Persson, R.; Rosengren, A. M.; Nyman, P. O.; Wilson, K. S.; Cedergren-Zeppezauer, E. S. Crystal structure of dUTPase from Equine Infectious Anaemia Virus; active site metal binding in a substrate analogue complex. *J. Mol. Biol.* **1999**, *285*, 655-673.

1DUN, 1DUC), *M. tuberculosis*⁵⁶ (PDB entries 1MK7, 1SJM) are known with both liganded and unliganded forms and that of *Plasmodium falciparum* with a novel inhibitor bound has recently been published⁵⁷ (PDB entry 1VYQ).

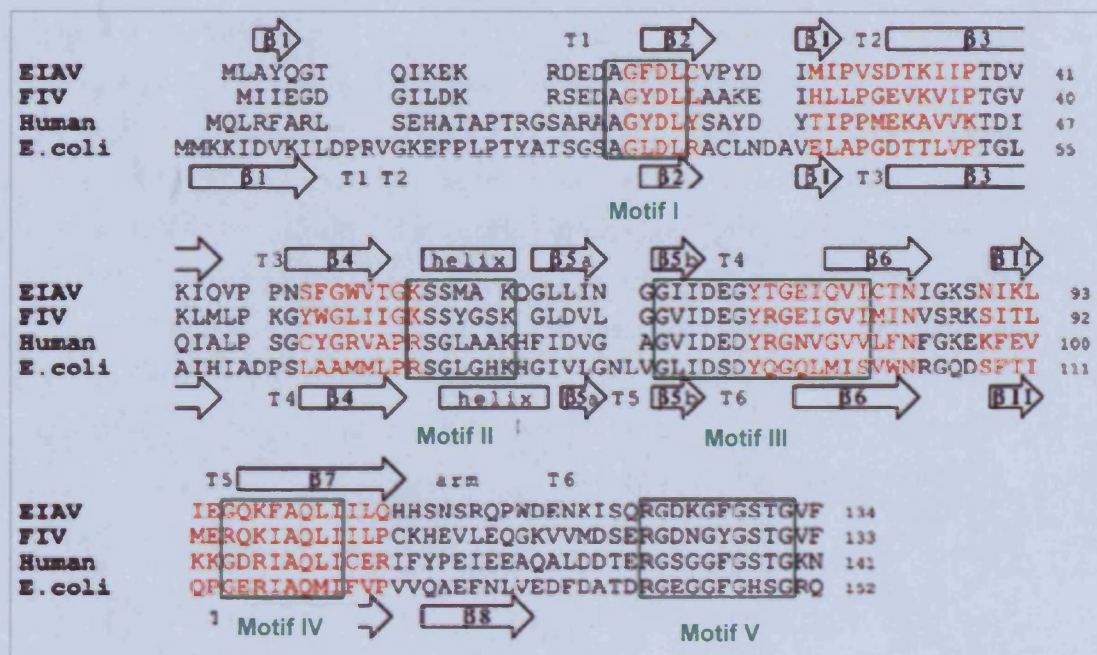


Figure 2-5: Sequence alignment of some of the trimeric dUTPase showing the 5 conserved motifs in green boxes (also see Figure 2-6)⁵⁵

The trimers consist of three identical subunits consisting of approximately 150 amino acids each and composed primarily of β -pleated sheets. There are three active sites per molecule and amino acids from all three subunits contribute to each active site. Sequence comparison studies have shown that the trimeric dUTPases all possess five highly conserved motifs which are positioned in the active site (Figure 2-5).⁵⁸

⁵⁶ Chan, S.; Segelke, B.; Legin, T.; Krupka, H.; Cho, U. S.; Kim, M.; So, M. Y.; Kim, C. Y.; Naranjo, C. M.; Rogers, Y. C.; Park, M. S.; Wald, G. S.; Pashkov, I.; Cascio, D.; Perry, J. L.; Sawaya, M. R. Crystal structure of the Mycobacterium tuberculosis dUTPase: Insights into the catalytic mechanism. *J. Mol. Biol.* **2004**, *341*, 503-517.

⁵⁷ Whittingham, J. L.; Leal, I.; Nguyen, C.; Kasinathan, G.; Bell, E.; Jones, A. F.; Berry, C.; Benito, A.; Turkenburg, J. P.; Dodson, E. J.; Perez, L. M. R.; Wilkinson, A. J.; Johansson, N. G.; Brun, R.; Gilbert, I. H.; Pacanowska, D. G.; Wilson, K. S. dUTPase as a Platform for Antimalarial Drug Design: Structural Basis for the Selectivity of a Class of Nucleoside Inhibitors. *Structure* **2005**, *13*, 329-338.

⁵⁸ McGeoch, D. J. Protein sequences show that 'pseudoproteases' encoded by poxvirus and certain retroviruses belong to the deoxyuridine triphosphatase family. *Nucleic Acids Res.* **1990**, *18*, 4105-4110.

Both nuclear and mitochondrial forms of the human dUTPase have been characterised.^{59, 60} In contrast to the dimeric dUTPases, the trimeric group are extremely exclusive towards dUTP as the substrate (Table 2-1).

The subunit monomers (Figure 2-6) of these enzymes have a β -strand core. Two β -sheets are formed, which combine to form a β -barrel structure, the interior of which is closely packed with hydrophobic residues. The β -strands are connected by loops, some of which are regular β -turns, one of which normally contributes to the active site of the enzyme. There is one α -helical structure on the surface of the enzyme.⁴⁰ Extended loops are found on the surface of the human and *E. coli* enzymes. (Figure 2-6) The outermost C-terminal part of the polypeptide forms a tail that is disordered in unliganded X-ray structures but becomes ordered on ligand binding in the human and FIV enzymes. Here it can be seen this "arm" traverses the face of the trimer and contributes a β -strand to the β -barrel of a neighbouring subunit. A conserved proline residue acts as a hinge for this "arm".³⁹

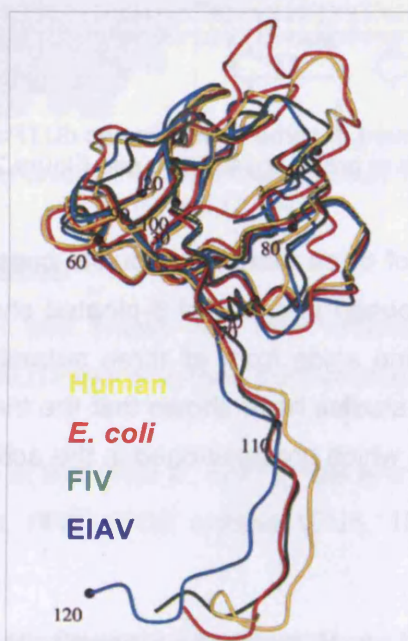


Figure 2-6: Superimposition of the human (yellow), *E. coli* (red), EIAV (blue) and FIV (green) monomeric subunit backbones⁵⁵

⁵⁹ Ladner, R. D.; McNulty, D. E.; Carr, S. A.; Roberts, G. D.; Caradonna, S. J. Characterization of distinct nuclear and mitochondrial forms of human deoxyuridine triphosphate nucleotidohydrolase. *J. Biol. Chem.* **1996**, *271*, 7745-7751.

⁶⁰ Ladner, R. D.; Caradonna, S. J. The human dUTPase gene encodes both nuclear and mitochondrial isoforms - Differential expression of the isoforms and characterization of a cDNA encoding the mitochondrial species. *J. Biol. Chem.* **1997**, *272*, 19072-19080.

The exception to this is the *Plasmodium falciparum* dUTPase (PfdUTPase) where the C-terminal chain is redirected (Figure 2-7), executing a sharp turn and the last β -strand interacts with the first β -strand of the same monomer. This is facilitated by the substitution of a normally bulky side chain by a Gly residue in the PfdUTPase. Therefore many of the intersubunit interactions present in other trimeric dUTPases involving the C-termini of neighbouring subunits are absent in PfdUTPase.⁵⁷

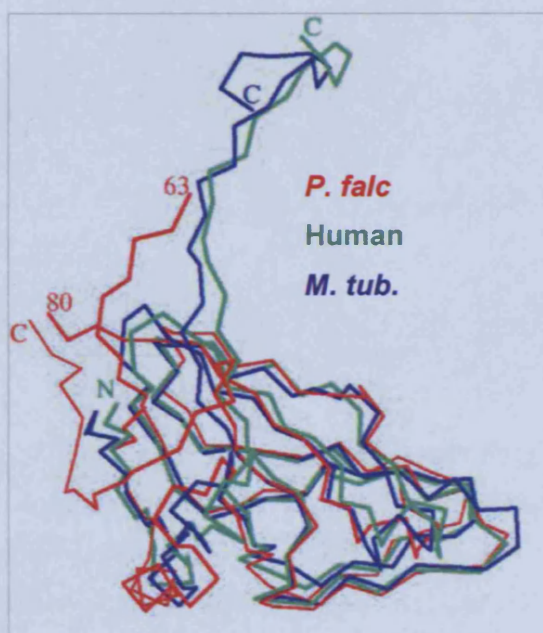


Figure 2-7: Superimposition of monomeric subunits from human (green), *P. falciparum* (red) and *M. tuberculosis* (blue)⁵⁷

The monomers arrange themselves around a three-fold axis to form a homotrimer (Figure 2-8) and interact in three ways (Figure 2-8). Firstly, through “arm” exchange as described above. Secondly, side chain interactions along the three fold axis which vary from purely hydrophobic interactions in the *E. coli* dUTPase to alternating layers of positively and negatively charged residues in the human dUTPase that enhance trimer stability. Thirdly, subunit-subunit interface contacts along the perimeter of the trimer.³⁷ In the FIV dUTPase crystal structure, the presence of an octa-coordinating Mg^{2+} within the axis may also stabilise trimer association.⁵⁴ Aromatic clusters have also been found within the channel of some of the dUTPase enzymes, these again may interact in such a way as to stabilise the homotrimer.³⁹ Thus, while the overall subunit arrangement is highly conserved between the dUTPase enzymes, the specific interactions providing their stabilities vary.

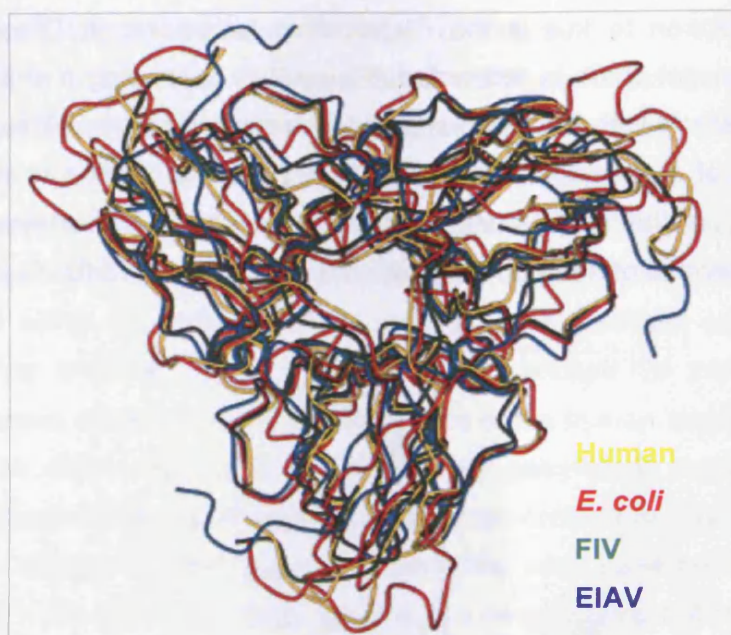


Figure 2-8: Trimeric backbone structure of human (yellow), *E. coli* (red), EIAV (blue) and FIV (green) dUTPases⁵⁵

The PfdUTPase contains large insertions in each monomer known as low complexity regions (LCRs) which are composed of 24 hydrophilic amino acid residues and are absent in the other dUTPases. They form three large loops gathered together at the top of the trimer (Figure 2-9). Their function is not certain but it is known they do not interfere with substrate binding or trimer formation.⁵⁷ However, these LCR regions are known to be typical of *P. falciparum* proteins.⁶¹

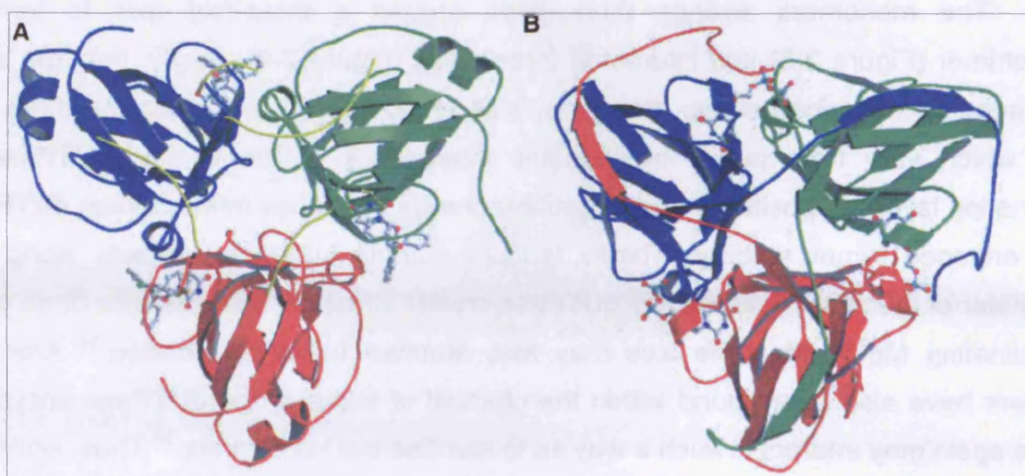


Figure 2-9: A) PfdUTPase, LCRs in yellow. C-termini are folded back B) Human dUTPase⁵⁷

⁶¹ Brocchieri, L. Low-complexity regions in Plasmodium proteins: In search of a function. *Genome Res.* 2001, 11, 195-197.

The mechanism of catalysis was shown from ^{18}O studies to be a nucleophilic attack of water on the α -phosphate (Figure 2-10) which is in contrast to the dimeric enzymes where there is an attack on the β -phosphate.³⁷ The crystal structures of the *E. coli*, wild type and mutant,⁴¹ and *M. tuberculosis*⁵⁶ enzyme complexed with the non-hydrolysable α,β -imino-dUTP inhibitor have also shed light on the mechanism of catalysis which is facilitated by i) the coordination of the Mg^{2+} ion to all three phosphate groups, holding the phosphate chain in an orientation optimal for catalysis and ii) a number of non-covalent bonding interactions between conserved residue side chain and backbone atoms to various water molecules and the triphosphate groups. The residues which are proposed to interact with the catalytic water molecule (W_{cat}) are highly conserved between species (Figure 2-10).

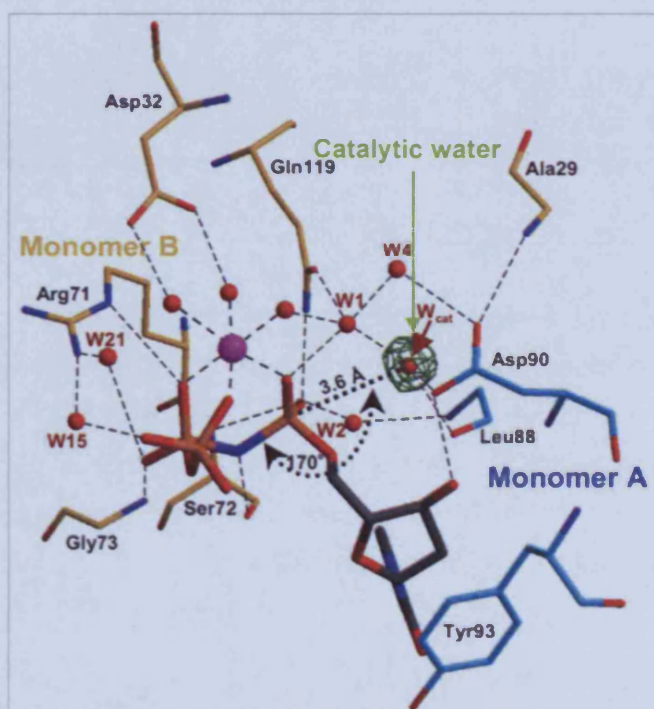


Figure 2-10: Proposed mechanism of phosphate (shown in orange) ester hydrolysis in the trimeric dTUPases⁴¹

2.3.2 Dimeric dUTPases

dUTPase enzymes from trypanosomes,^{62, 63, 64} *Campylobacter jejuni*⁶⁵ and some other bacteria and T4 bacteriophages function as physiological dimers of approximately 62-64kDa. The crystal structures of the *T. cruzi*⁵² (PDB entries 1OGK, 1OGL) and *C. jejuni*⁶⁵ (PDB entry 1W2Y) dUTPases have been solved.

There is no significant sequence similarity, however between this family of dUTPases and the monomeric and trimeric forms. This group of enzymes possess five conserved motifs (Figure 2-11) but they are different to the five conserved motifs that are present in the other families of dUTPases. In fact this group of enzymes is so different that it is suggested that they reached their catalytic potential through very different evolutionary routes.^{52, 63}

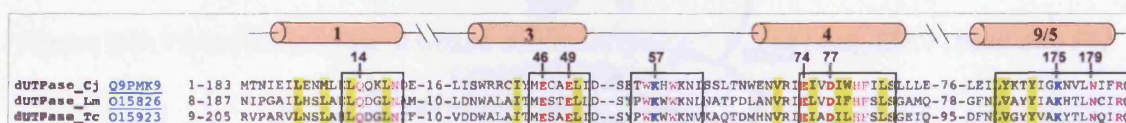


Figure 2-11: Sequence alignment of dUTPase from *C. jejuni*, *L. major* and *T. cruzi* showing the 5 conserved motifs boxed in black⁶⁶

The dimeric dUTPase enzymes show significant specificity toward the uracil base and the deoxyribose sugar as do the trimeric enzymes, they are less specific toward the phosphate moiety. A characteristic difference of the dimeric dUTPases is that they also hydrolyse dUDP, which acts as a weak competitive inhibitor toward the monomeric and trimeric forms. The K_m values are higher than those obtained for dUTP but the specificity constants are similar. (Table 2-1)

⁶² Camacho, A.; Arrebola, R.; PenaDiaz, J.; LuisPerez, L. M.; GonzalezPacanowska, D. Description of a novel eukaryotic deoxyuridine 5'-triphosphate nucleotidohydrolase in *Leishmania major*. *Biochem. J.* **1997**, *325*, 441-447.

⁶³ Camacho, A.; Hidalgo-Zarco, F.; Bernier-Villamor, V.; Ruiz-Perez, L. M.; Gonzalez-Pacanowska, D. Properties of *Leishmania major* dUTP nucleotidohydrolase, a distinct nucleotide-hydrolysing enzyme in kinetoplastids. *Biochem. J.* **2000**, *346*, 163-168.

⁶⁴ Bernier-Villamor, V.; Camacho, A.; Hidalgo-Zarco, F.; Perez, J.; Ruiz-Perez, L. M.; Gonzalez-Pacanowska, D. Characterization of deoxyuridine 5'-triphosphate nucleotidohydrolase from *Trypanosoma cruzi*. *FEBS Lett.* **2002**, *526*, 147-150.

⁶⁵ Moroz, O. V.; Harkiolaki, M.; Galperin, M. Y.; Vagin, A. A.; Gonzalez-Pacanowska, D.; Wilson, K. S. The crystal structure of a complex of *Campylobacter jejuni* dUTPase with substrate analogue sheds light on the mechanism and suggests the "basic module" for dimeric d(C/U)TPases. *J. Mol. Biol.* **2004**, *342*, 1583-1597.

⁶⁶ Moroz, O. V.; Murzin, A. G.; Makarova, K. S.; Koonin, E. V.; Wilson, K. S.; Galperin, M. Y. Dimeric dUTPases, HisE, and MazG belong to a new superfamily of all-alpha NTP pyrophosphohydrolases with potential "house-cleaning" functions. *J. Mol. Biol.* **2005**, *347*, 243-255.

Nucleotide	<i>T. cruzi</i>	<i>L. Major</i>	<i>E. coli</i>	EIAV	HSV-1	MMTV
dUTP: $K_m(k_{cat}/K_m)$	0.53 ($5.2 \cdot 10^6$)	2.11 ($2.3 \cdot 10^7$)	0.2 ($4 \cdot 10^7$)	1.1 ($2 \cdot 10^7$)	0.3 ($2 \cdot 10^7$)	0.8 ($2 \cdot 10^6$)
dTTP: $K_m(k_{cat}/K_m)$	>800 ($2.5 \cdot 10^3$)	1514 ($5.5 \cdot 10^3$)	>20000 (34)	260 (<2000)	400 (1000)	nd (2000)
dCTP: $K_m(k_{cat}/K_m)$	nd	>2500 ($5.0 \cdot 10^3$)	4000 (<100)	3000 (1000)	1000 (2000)	nd
UTP: $K_m(k_{cat}/K_m)$	nd	2500 ($2.0 \cdot 10^3$)	2500 (<100)	nd	1000 (200)	nd
dUDP: $K_m(k_{cat}/K_m)$	6.23 ($1.7 \cdot 10^6$)	62.7 ($1 \cdot 10^6$)	$K_i=15$	$K_i=3.6$	$K_i=17$	nd
dUMP: K_{ip}	18.4	13.05	1500	130	170	nd

Table 2-1: Michaelis-Menten, specificity and inhibition constants of viral, bacterial and trypanomastid dUTPases for different nucleotides. Units for K_m and K_i are μM and for k_{cat}/K_m $\text{M}^{-1} \text{s}^{-1}$.⁶⁷

The crystal structure for the dimeric *T. cruzi* dUTPase (TcdUTPase) enzyme, native and with dUDP bound has been published but Mg^{2+} ions are not present (Figure 2-12 B).⁵² Nevertheless, it elucidated the fact that the enzyme undergoes a very significant conformational change on binding the substrate, which effects almost all of the protein topology (Figure 2.15). The active site is also very open in the unbound form but closes around the substrate in the bound form, effectively burying the ligand within the active site (Figure 2-14). The crystal structure, of *C. jejuni* dUTPase (CjdUTPase), however, revealed the Mg^{2+} binding sites (Figure 2-16) but has only been determined as a closed, substrate-bound form (Figure 2-12).⁶⁵

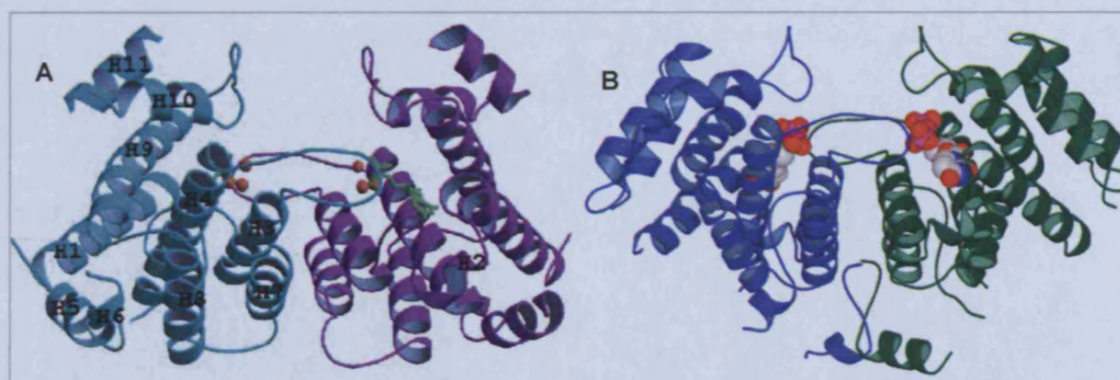


Figure 2-12: Crystal structures of A) The CjdUTPase and B) the TcdUTPase. Both are in the liganded forms.^{52, 65}

⁶⁷ Hidago-Zarco, F.; González-Pacanowska, D. Trypanosomal dUTPases as potential targets for drug design. *Curr. Protein Pept. Sci.* **2001**, *2*, 389-397.

Both structures are very similar with some small differences. The subunits are predominantly helical in structure. CjdUTPase consists of 11 α -helices and 2 β -strands in the complexed form and TcdUTPase is comprised of 12 α -helices in the native conformation (with the formation of two new β -strands on complexation) which are arranged into two distinct domains termed "rigid" and "mobile". The molecular units are homodimers, formed through association of the rigid domains of two subunits, complimented by insertion of the latch of one subunit into the groove of its partner (Figure 2-13).

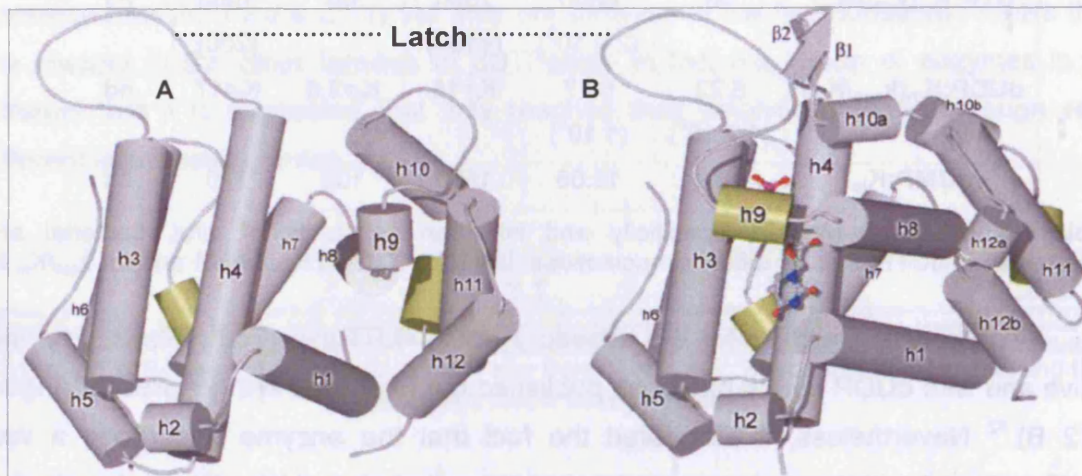


Figure 2-13: A) The native subunit of TcdUTPase with helices represented as rods B) The subunit of TcdUTPase complexed with dUDP⁵²

There are two active sites per dimer, each residing in the groove formed at the interface of the two subunits. Amino acids from both subunits contribute to ligand binding in the active site. When an active site becomes occupied the mobile domain moves to engulf the nucleotide through a series of structural rearrangements that effectively bury the molecule beneath the subunit surface (Figure 2-14).

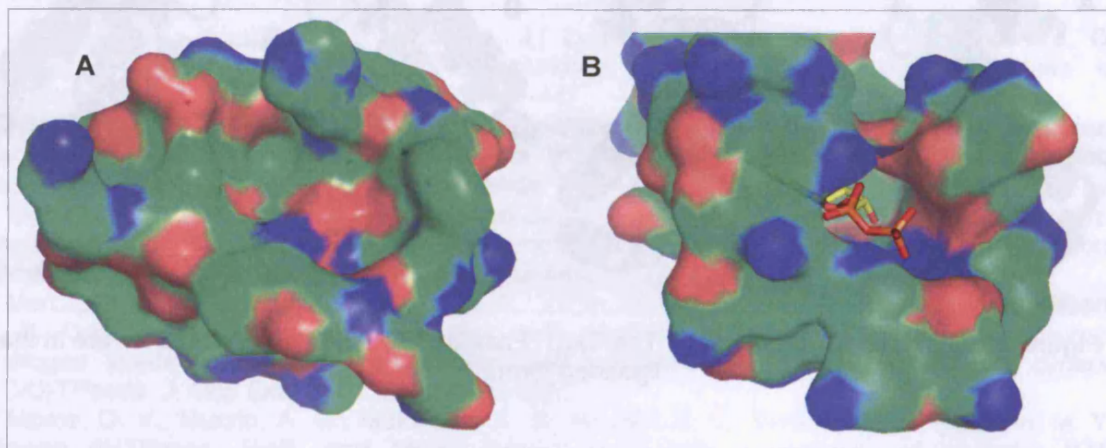


Figure 2-14: Surface representations of the active site of A) the native and B) the complexed TcdUTPase. Generated using VMD 1.8

The “open” or “native” form refers to the ligand free and the “closed” form refers to the ligand bound conformation of the enzyme. The rigid domains retain the native conformation upon nucleotide binding. Figure 2-15 shows the structure of the dimeric TcdUTPase in its native and complexed form where the structural rearrangements which the enzymes undergo can be clearly seen.⁵²

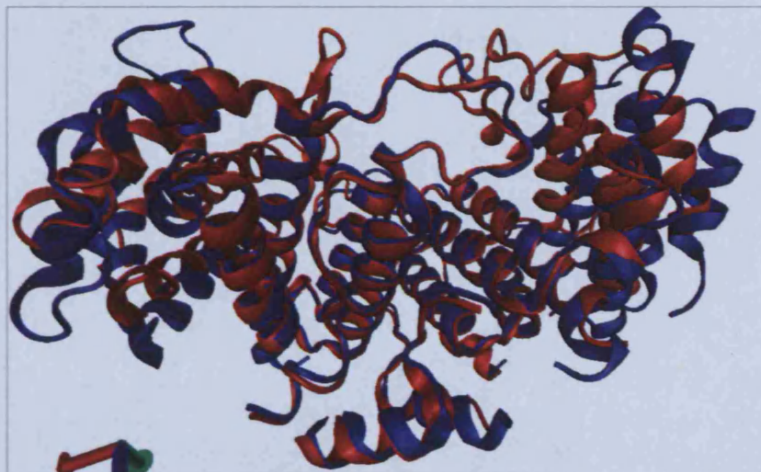


Figure 2-15: Superimposition of the native (blue) and complexed (red) TcdUTPase. Generated using VMD 1.8

Two mechanisms of binding and conformational change can be proposed. One proposal is that the uracil and deoxyribose moieties are initially recognized by helix 1 and helix 4 followed by the recognition and hydrogen bonding of the α and β -phosphates. The second proposal is that the phosphates are recognized first, bringing the rest of the molecule into its docking site where it is recognized in a sequential fashion.⁵²

The crystal structure of the CjdUTPase reveals the presence and positions of three Mg^{2+} ions shown in orange in Figure 2-16 and 2-17.

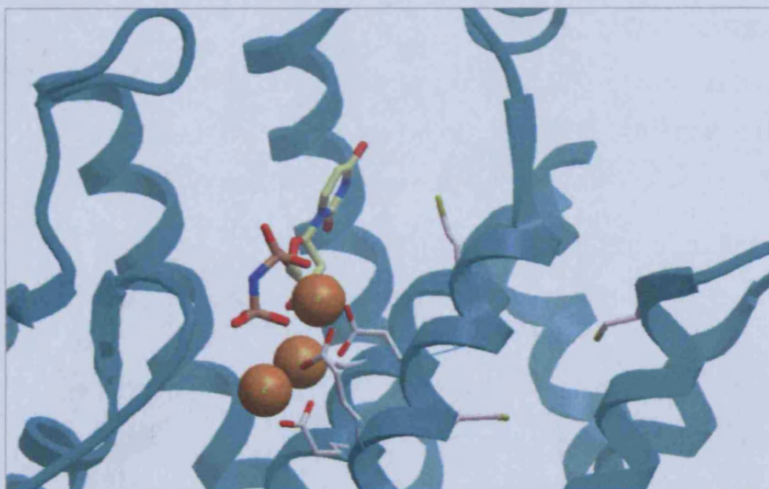


Figure 2-16: Crystal structure of CjdUTPase with ligands dUpNHp and Mg^{2+} ions bound. Generated using MolSoft Browser.

2 The dUTPase Enzyme

The presence of these Mg^{2+} ions can help to propose a mechanism by which the enzyme catalyzes hydrolysis. There are three Mg^{2+} ions per active site. They are hexa-coordinated to three conserved Glu residues, one Asp and many water atoms. Two of the Mg^{2+} ions, coordinate one of the water atoms in such a way that they orientate it in the correct position for direct nucleophilic attack on the β -phosphate (Figure 2-17). At the same time all metal ions increase the nucleofugality of the leaving group.⁶⁵

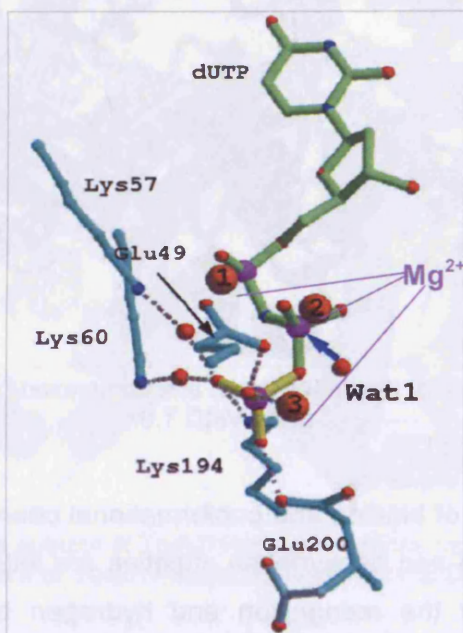


Figure 2-17: Hypothetical γ -phosphate position and proposed catalytic mechanism for dimeric dUTPases. Mg^{2+} shown in orange.⁶⁵

The structures of the active sites differ dramatically to those of the trimeric enzymes and will be discussed in more detail in section 2.3.4.

2.3.3 Monomeric dUTPases

The herpes virus dUTPases are active as monomers.^{68, 69} The crystal structure of the dUTPase from the EBV (Epstein-Barr virus, a γ -herpesvirus) in complex with dUMP and α,β -imino-dUTP has been published (PDB entry 2BSY).⁷⁰

⁶⁸ Williams, M. V. Deoxyuridine Triphosphate Nucleotidohydrolase Induced by Herpes-Simplex Virus Type-1 - Purification and Characterization of Induced Enzyme. *J. Biol. Chem.* **1984**, *259*, 10080-10084.

⁶⁹ Bjornberg, O.; Bergman, A. C.; Rosengren, A. M.; Persson, R.; Lehman, I. R.; Nyman, P. O. DUTPase from Herpes-Simplex Virus Type-1 - Purification from Infected Green Monkey Kidney (Vero) Cells and from an Overproducing Escherichia-Coli Strain. *Protein Expression Purif.* **1993**, *4*, 149-159.

⁷⁰ Tarbouriech, N.; Buisson, M.; Seigneurin, J. M.; Cusack, S.; Burmeister, W. P. The monomeric dUTPase from Epstein-Barr virus mimics trimeric dUTPases. *Structure* **2005**, *13*, 1299-1310.

In terms of evolution, it is thought that the ancestral gene for the monomeric enzymes arose from a gene coding for a trimeric one.⁷¹

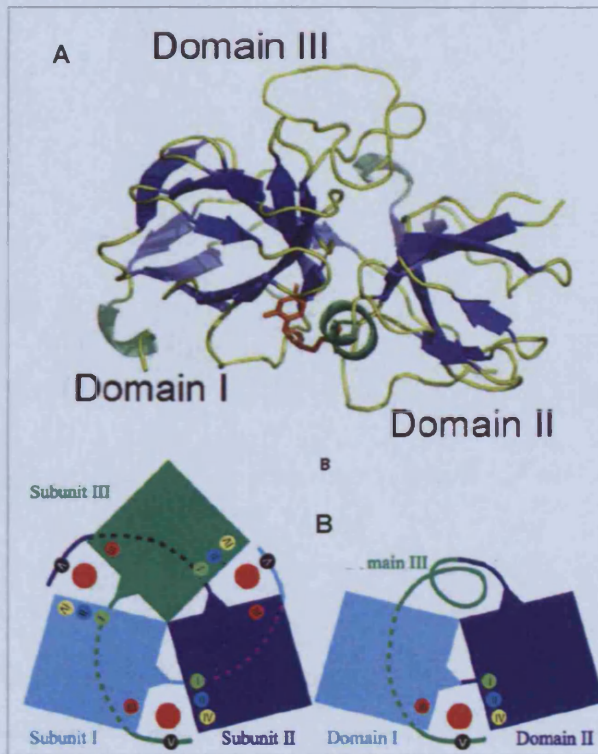


Figure 2-18: A) Crystal structure of the EBV dUTPase complexed with dUMP (PDB entry 2BSY) B) comparison of the trimeric and monomeric dUTPase enzyme folds and localisation of the conserved motifs I-V around the active sites represented by red dots

The monomeric dUTPases contain the same 5 conserved motifs as the trimeric enzymes but in a different order and they are spread out over a single polypeptide chain 249 residues long (twice as long as one subunit from a trimeric enzyme). The EBV dUTPase has shown to be almost an entirely β -strand structure and folds into 3 domains, each of which can be corresponded to a subunit of the trimeric form (Figure 2-18). The monomeric dUTPase has one active site located at the interface of domain I and II. The 5 conserved motifs interact within the active site in some way. One unusual feature of the monomeric dUTPases is a disulfide bridge found between Cys4 and Cys246 which locks motif 5 in such a way as to cover the active site during catalysis.⁷⁰

Kinetic stereospecificity studies have been carried out on HSV-1 versus *E. coli* and EIAV (equine infectious anaemia virus) homotrimeric dUTPases.⁷² The enzymes are highly specific towards dUTP. Other nucleotides such as dTTP, dCTP, UTP and dUTPaS are also hydrolysed but at a much slower rate. dUMP and dUDP act as weak inhibitors of these enzymes.

⁷¹ McGeehan, J. E.; Depledge, N. W.; McGeoch, D. J. Evolution of the dUTPase gene of mammalian and avian herpesviruses. *Curr. Protein Pept. Sci.* **2001**, 2, 325-333.

Substrate	HSV	<i>E. coli</i>	EIAV	Inhibitor	HSV	<i>E. coli</i>	EIAV
dUTP				dUMP			
K_m (μM)	0.3	0.2	1.1	K_i (μM)	170	1500	150
dUTP α S				dUDP			
K_m	0.2	0.9	Nd	K_i	17	15	3.6
dTTP				dU			
K_m	400	>20000	260	K_i	400	1000	1500
dCTP				Uracil			
K_m	1000	4000	3000	K_i	5000	>10000	nd
UTP				dUMP α S			
K_m	1000	2500	Nd	K_i	900	nd	nd

Table 2-2: Catalytic parameters of viral (HSV, EIAV) and bacterial (*E. Coli*) dUTPases towards nucleoside triphosphates and uracil containing compounds⁷²

2.3.4 Comparison of active sites

In dUTPase active sites, specific structural arrangements confer highly selective ligand binding for both dimeric and trimeric forms. However, the way in which they do so differs greatly between the different associative forms.

The five conserved motifs that are seen throughout the dimeric dUTPases all contain residues that play crucial roles in substrate binding and specificity. Figure 2-19 and 2-20 show the interactions of the ligands, dUpNHp and dUDP, with the active sites of the CjdUTPase and TcdUTPase respectively.

For the dimeric enzymes, base pairing mimics bind uracil through selective hydrogen bonding with side chains from conserved motif 1 and motif 3. Motif 3 presides on the latch of the neighbouring subunit. There is an extra Asn hydrogen bonding residue in the CjdUTPase. The hydrogen bonding His58 in CjdUTPase and Trp61 in TcdUTPase from motif 3 are the main residues for discrimination of the enzyme against cytosine as they would repel the NH₂ form cytosine due to its positive charge potential. The bulky Trp39 in CjdUTPase and His83 in TcdUTPase from conserved motif 2 aids in discrimination against thymidine by preventing binding of substrates with substitution on C-5.

The deoxyribose sugar moiety hydrogen bonds to an Asn residue from conserved motif 5 in both proteins and is flanked by two aromatic residues of Phe and His from motif 4.

⁷² Bergman, A. C.; Nyman, P. O.; G., L. Kinetic Properties and Stereospecificity of the Monomeric dUTPase from herpes simplex virus type 1. *FEBS Lett.* **1998**, *441*, 327-330.

The Gly rich site for phosphate binding which is present in the trimeric dUTPases, is absent in the dimeric forms, instead the phosphates form an intricate network of hydrogen bonds with charged residues from Motifs 2, 3, 4 and 5 and also coordinate to Mg^{2+} ions as well as water molecules. In *Cjd*UTPase, the Mg^{2+} ions can be seen to be hexa-coordinate with charged residues from motifs 2, 3, 4 and also water molecules.^{52, 65}

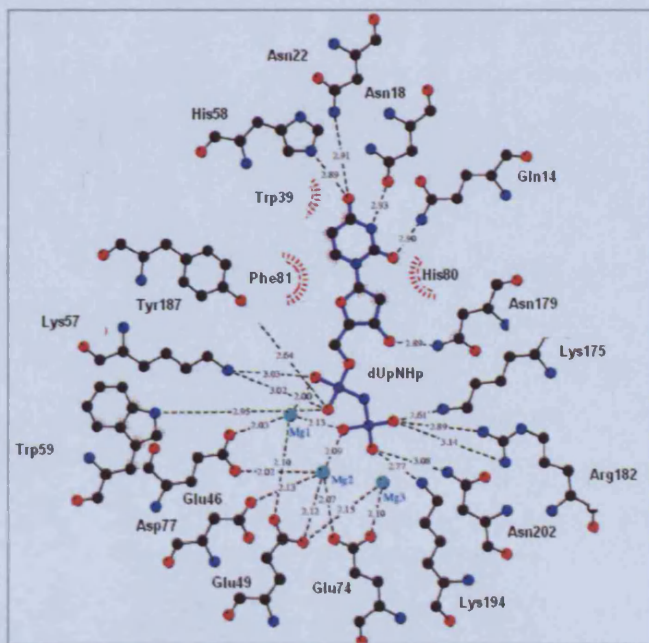


Figure 2-19: A LIGPLOT diagram of the active site of the *C. jejuni* dUTPase complexed with dUDP⁶⁵

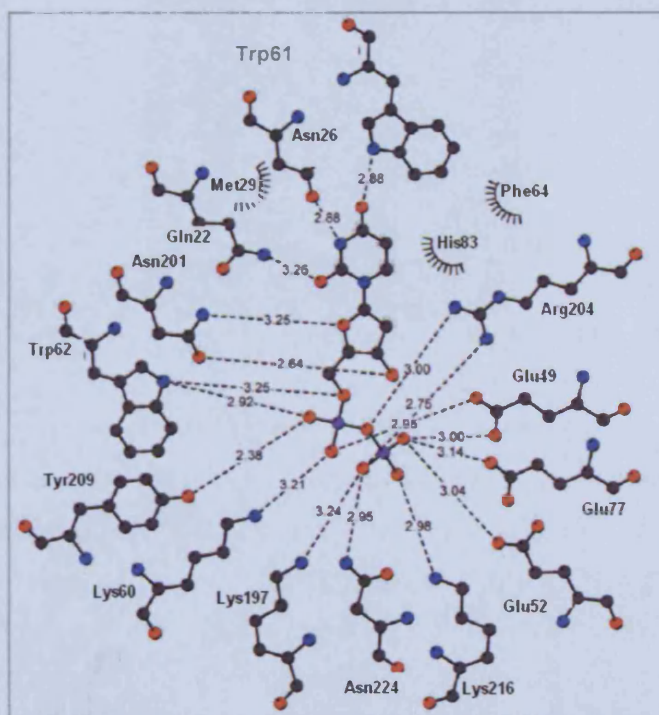


Figure 2-20: A LIGPLOT diagram of the active site of the *T. cruzi* dUTPase in complex with dUpNHP⁵²

The trimeric dUTPases contain three active sites per molecule, each buried in shallow depressions at the subunit interfaces. Within each active site all three subunits are involved in ligand binding. All 5 conserved motifs from each subunit contribute ligand binding residues. Motif 1, 2 and 4 are contributed by one subunit, motif 3 by a second subunit and motif 5 by the third subunit (Figure 2-22, Figure 2-23)..⁴⁰

Motif 3 forms a β -hairpin pocket, of mainly hydrophobic nature which mediates the binding of the uracil and sugar moiety at its open end (Figure 2-21). As with the dimeric enzymes, the uracil base binds to the enzyme in a mode mimicking base pair hydrogen bonding. However, due to the hydrophobic nature of the β -hairpin residues, the uracil base hydrogen bonds to main-chain atoms. This is in contrast to the dimeric enzymes, where hydrogen bonding is mainly to side-chain atoms. O-4 of the uracil base also hydrogen bonds through a conserved water molecule. Specificity towards the uracil over the cytosine base is maintained by the formation of a strong hydrogen bond between a main chain carbonyl atom and N-3 of the base which is a hydrogen bond donor in uracil but not in cytosine. Steric hindrance also excludes thymine from binding in the β -hairpin region, as the β -hairpin is narrow and steric clashes between the 5'-methyl group and the polypeptide would occur.

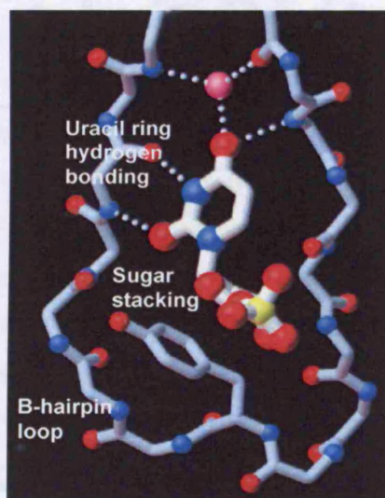


Figure 2-21: The β -hairpin recognition motif for uracil in human dUTPase³⁹

Binding of the deoxyribose moiety occurs at the turn of the β -hairpin which also renders the enzyme specific towards the deoxyribose over ribose. A tyrosine residue (Phe in MMTV) which is highly conserved throughout the enzymes is stacked against the sugar ring and its OH group is hydrogen bonded to the opposite β -hairpin wall which stabilizes its position. This Tyr together with another highly conserved Ile residue, sandwich the sugar moiety and this tight packing sterically precludes ribose binding. An aspartate residue that hydrogen bonds to the 3'-OH is also strictly conserved.⁴⁰

Motif 2 and 4, both from a second subunit contribute to binding interactions to the β and γ phosphate through side chain interaction with basic residues and a conserved Ser. Motif 5 from the flexible arm of a third subunit is Gly rich. On ligand binding, the flexible arm of the third subunit becomes ordered and this Gly rich sequence from motif 5 is essential for catalysis in the trimeric dUTPases. This is in contrast to the dimeric enzymes where the phosphate binding region of the active site consists of many charged and hydrophilic residues.⁵²

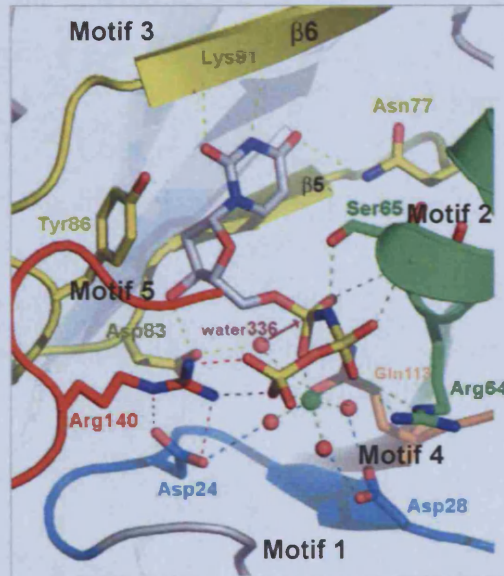


Figure 2-22: Active site of *M. tuberculosis* with α,β -imido dUTP ligand bound. Motif 1(blue), motif 2(green), motif 3(yellow), motif 4(orange), motif 5 (red) are shown.⁵⁶

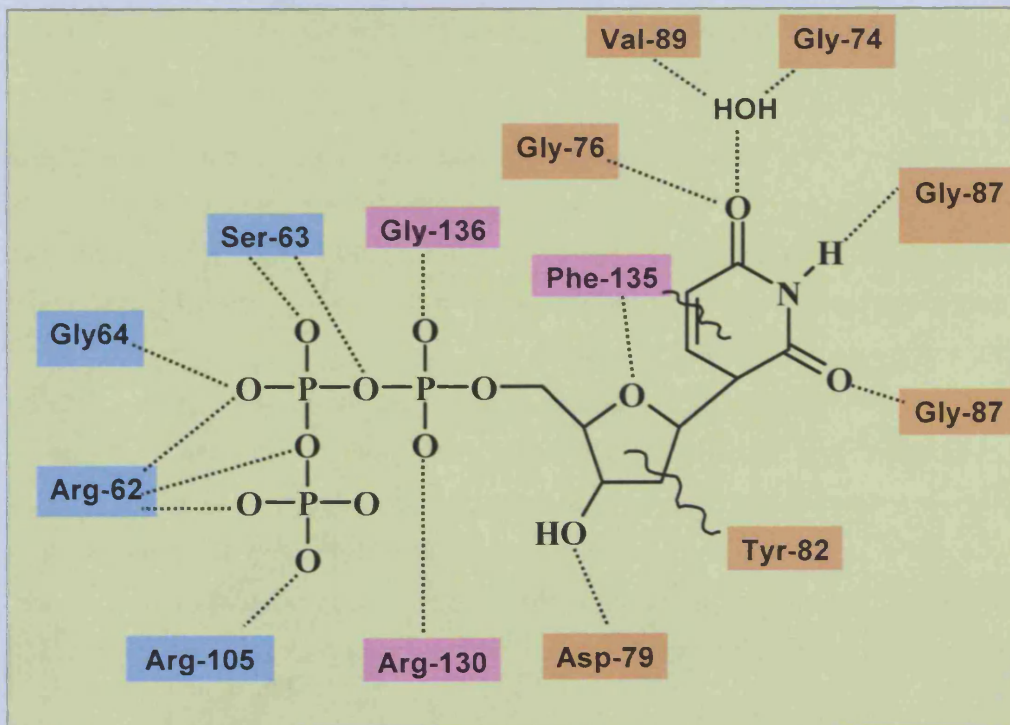


Figure 2-23: Binding in the active site of the human dUTPase enzyme. Different colours represent residues from the different subunits³⁹

2.4 dUTPase enzymes as potential chemotherapeutic targets

It has been shown that the role of dUTPase is essential for cell viability in *Escherichia coli*,⁴⁴ *Saccharomyces cerevisiae*⁴⁵ and *Leishmania major*.⁷³ The fundamental role of the enzyme in mammalian cells is inferred from the observations made to thymineless death induced by certain anti-folates and the preceding reduction in the intracellular dTTP:dUTP. dUTPase is clearly, then a valid target for inhibition by anti-cancer and anti-infective agents.³⁴

The structural differences between the human dUTPase and that of the dimeric dUTPases can be taken advantage of in designing novel anti-parasitic agents.⁶⁷ When the nucleotide ligands from trimeric dUTPase complexes and that of dUDP from the dimeric *T. cruzi* dUTPase are superimposed, it can be seen that the ligands bind with very different conformation with respect to the uracil ring, sugar moiety and especially the phosphate chain (Figure 2-24).



Figure 2-24: Superimposition of ligand models from trimeric (washout) and dimeric (bold) enzyme complexes⁵²

Considering the large differences between the active sites as well as the overall structure of the dimeric and trimeric enzymes, it should be possible to selectively inhibit the dimeric dUTPase enzymes. These inhibitors could then possibly be used as therapeutic agents to treat diseases caused by the trypanomastidae protozoa such as HAT, Chagas' disease and leishmaniasis.

The only known inhibitors of the dimeric dUTPases are dUMP, which causes product inhibition and α,β -imido-dUTP, a non hydrolysable nucleotide analogue.⁷³ Both, however, are unsuitable drug candidates due to their inherent physicochemical properties and poor cell permeability. One of the aims of this project is to utilise available structural data of the dimeric enzymes to design novel inhibitors *in silico* and to test these compounds against the dimeric enzymes and intact parasites.

⁷³ Hidalgo-Zarco, F.; Camacho, A. G.; Bernier-Villamor, V.; Nord, J.; Ruiz-Perez, L. M.; Gonzalez-Pacanowska, D. Kinetic Properties and Inhibition of the Dimeric dUTPase-dUDPase from *Leishmania major*. *Protein Sci.* **2001**, *10*, 1426-1433.

Previously designed and synthesised cyclic and acyclic nucleoside analogues have been shown to be selective inhibitors of the *P. falciparum* dUTPase (PfdUTPase) enzyme over the human dUTPase (Figure 2-25).^{74, 75} The crystal structure of the PfdUTPase complexed with one of these inhibitors has been solved (Figure 2-26), showing subtle differences within the active site of the PfdUTPase that may be exploited to design novel anti-malarial therapeutic compounds.⁵⁷ It was shown that deoxyuridine derivatives with triphenylmethyl (Trt), tert-butyldiphenylsilyl (TBDPS) or triphenylsilyl (TPS) substituents on the 5' position, which have been synthesised in the group, were selective inhibitors of PfdUTPase.⁷⁴ Subsequently, acyclic nucleoside analogues, in which the Trt, TBDPS or TPS groups were positioned at varying distances from the uracil ring, were synthesised. These also proved to be selective inhibitors of the PfdUTPase.⁷⁵

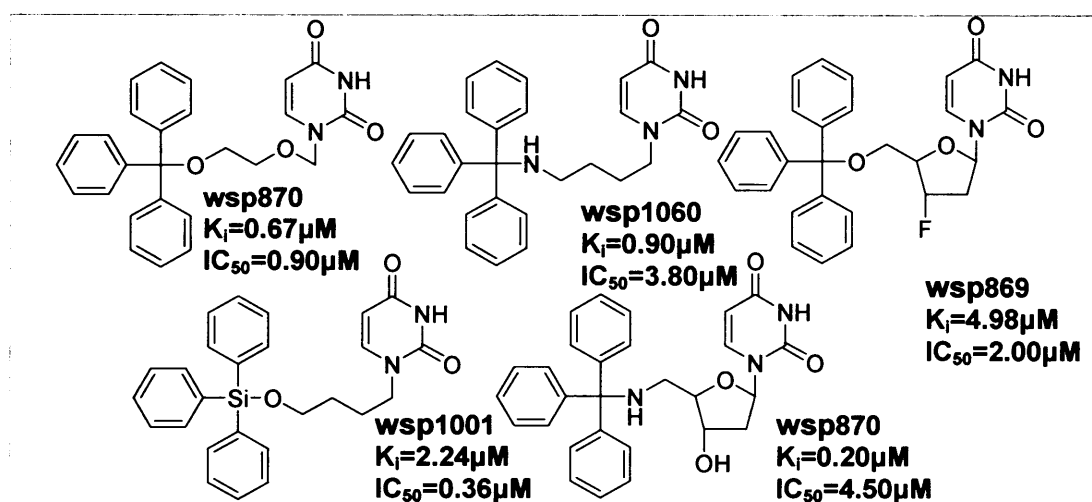


Figure 2-25: Previously synthesized PfdUTPase inhibitors

The selectivity of these compounds is thought to be due to the interactions of the bulky hydrophilic groups with the side chains of residues Phe46 and Ile117 (Figure 2-26) in the PfdUTPase which are substituted by two small, less hydrophobic Val42 and Gly87 in the human dUTPase. These compounds also show good anti-parasitic *in vitro* activity and are therefore successful leads for the design of novel anti-malarial drugs. Another aim of this project was to design and synthesise further Trt or TBDPS uracil nucleoside analogues using structure based and analogue based design with the objective of improving the activity of these compounds.

⁷⁴ Nguyen, C.; Kasinathan, G.; Leal-Cortijo, I.; Musso-Buendia, A.; Kaiser, M.; Brun, R.; Ruiz-Perez, L. M.; Johansson, N. G.; Gonzalez-Pacanowska, D.; Gilbert, I. H. Deoxyuridine triphosphate nucleotidohydrolase as a potential antiparasitic drug target. *J. Med. Chem.* **2005**, *48*, 5942-5954.

⁷⁵ Nguyen, C.; Ruda, G. F.; Schipani, A.; Kasinathan, G.; Leal, I.; Musso-Buendia, A.; Kaiser, M.; Brun, R.; Ruiz-Perez, L. M.; Sahlberg, B. L.; Johansson, N. G.; Gonzalez-Pacanowska, D.; Gilbert, I. H. Acyclic nucleoside analogues as inhibitors of Plasmodium falciparum dUTPase. *J. Med. Chem.* **2006**, *49*, 4183-4195.

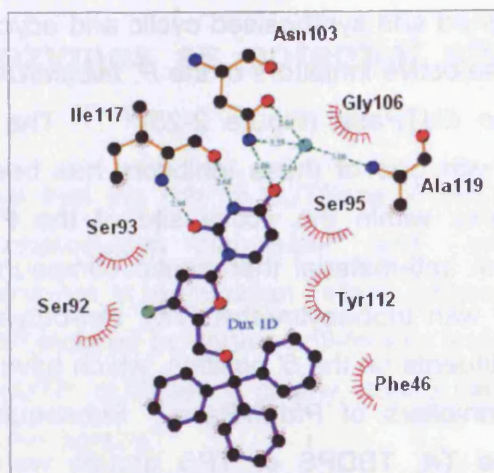


Figure 2-26: A LIGPLOT diagram of the active site of PfdUTPase complexed with 5'-Trt-deoxyuridine inhibitor⁵⁷

Other reported trimeric dUTPase inhibitors include the non-hydrolysable α,β - imido-dUTP⁷⁶ and some mercury (II) compounds,⁷⁷ again, these compounds are unlikely drug candidates due to their chemical and enzymatic instability and poor bioavailability and membrane permeability.

It is known that levels of dUTPase vary between individual cell types. dUTPase levels are usually low in breast, lung and colon cancers whereas neuroblastomas and hematopoietic malignancies have high levels of the enzyme.³⁴ Thus the human dUTPase enzyme could be targeted with anti-cancer dUTPase inhibitors for the former group of cancers. DHFR inhibitors, such as methotrexate and thymidylate synthase inhibitors such as FUdR are already used as to perturb the dUTP:dTTP ratio in cancer cells but resistance has emerged. It is thought that dUTPase over expression could play a role in this resistance.⁵¹ Therefore, dUTPase inhibitors could act as alternatives or adjuvants on DHFR inhibition cancer chemotherapy.

In this project we are particularly interested in targeting parasitic protozoa dUTPases. Whereas kinetoplastida protozoa cannot synthesise purines "de novo", they do possess the enzymatic machinery required for pyrimidine synthesis including dUTPase.⁶⁷ With regard to the plasmodium species, anti-folate drugs are already a successfully used chemotherapy, though resistance is emerging. Given the necessity of this enzyme for cell viability and the differences in sequence and structure from the human enzyme, it seems a good choice of target for anti-parasitic agents.

⁷⁶ Persson, T.; Larsson, G.; Nyman, P. O. Synthesis of 2'-deoxyuridine 5'-(α,β -imido)triphosphate: A substrate analogue and potent inhibitor of dUTPase. *Bioorganic & Medicinal Chemistry* **1996**, *4*, 553-556.

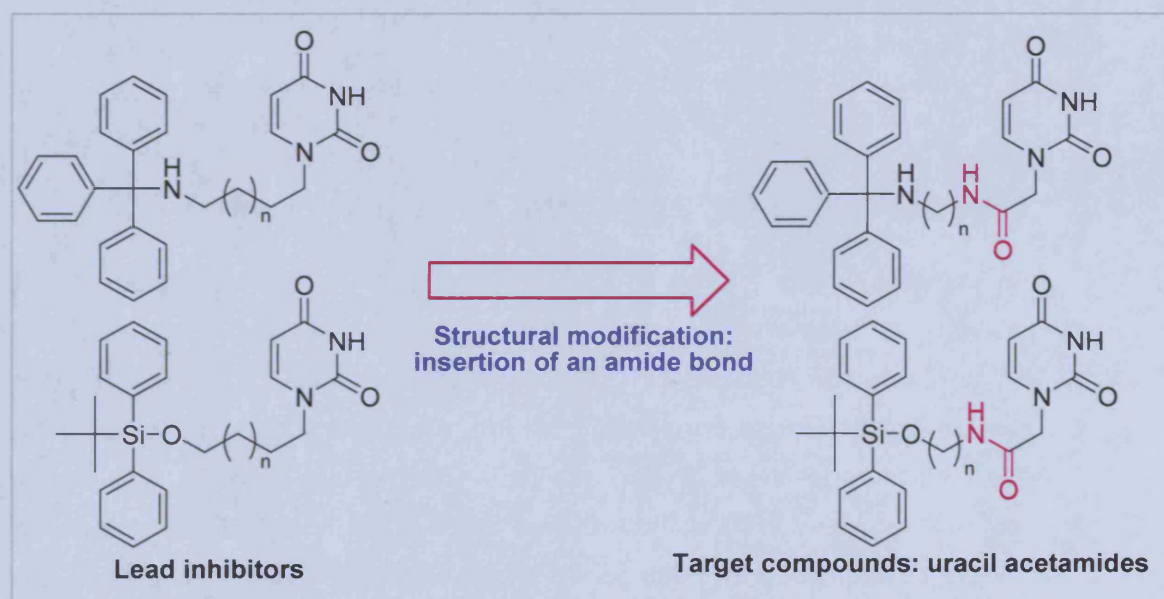
⁷⁷ Williams, M. V. Effects of Mercury (II) Compounds on the Activity of DUTPases from Various Sources. *Mol. Pharmacol.* **1986**, *29*, 288-292.

3 Aims and Objectives

The aim of this project was to design, synthesise and evaluate novel inhibitors of the essential enzyme dUTP nucleotidohydrolase for use as anti-parasitic agents by employing both analogue based and structure based drug design methodologies.

3.1 The trimeric *Plasmodium falciparum* dUTPase

- Analogue based design in which the insertion of an amide bond into previously synthesised selective inhibitors of the PfdUTPase was initially to be carried out, (Scheme 3-1) resulting in the synthesis of uracil acetamide derivatives. The rationale behind this modification is explained in Chapter 4.



Scheme 3-1: Analogue based design and introduction of an amide bond

- Branched chain derivatives (Figure 3-1), as well as single chain derivatives were to be synthesised, allowing for further diversification studies to be carried out, without introducing a chiral centre in to the molecules.

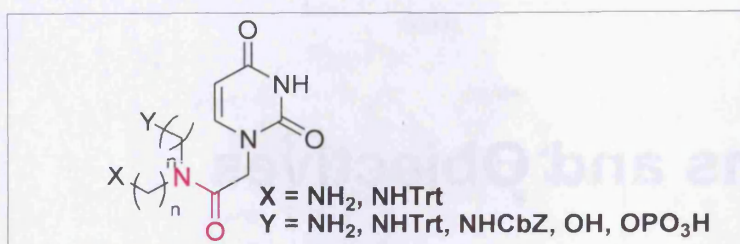


Figure 3-1: Branched chain uracil acetamides

- Following the elucidation of the crystal structure of the PfdUTPase in 2005,⁵⁷ structure based design strategies were then be employed and used in combination with the analogue based design results to attempt to increase the potency of our inhibitors toward the enzyme.

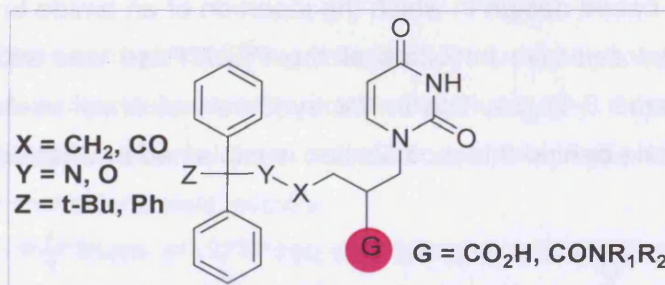


Figure 3-2: Proposed modified compounds from structure based design

3.2 The dimeric *Trypanosoma cruzi* dUTPase

- In contrast to the trimeric PfdUTPase, no selective lead inhibitors of the dimeric enzymes were known. However, the crystal structure of the TcdUTPase was elucidated in 2004 and therefore allowed for structure based design approaches to be utilised from the beginning in order to find potential lead inhibitors for these dimeric enzymes. Docking studies were to be carried out on the closed form of the enzyme, followed by the syntheses of some of the successfully docked compounds, which ultimately was to result in a library of uracil amino acid conjugates (Fig. 3-3) to be evaluated for biological activity.

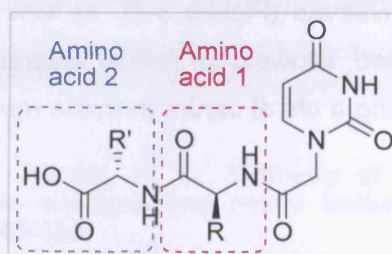


Figure 3-3: Uracil amino acid conjugates for the inhibition of the dimeric dUTPases

4 Triphenylmethylamino and *tert*-butyldiphenylsilyloxy acetamide derivatives uracil

4.1 Rational drug design and isosteric replacement

Classical isosteres can be defined as atoms, ions or molecules in which the peripheral layers of electrons can be considered to be identical. They are often used in rational drug design to determine whether one particular group in a molecule is important in binding to the target receptor. Replacement of one group with an isostere can tell us about the effect of factors such as steric tolerance, electronic distribution and hydrogen bonding in as controlled a manner as possible. Nonclassical bioisosteres, more broadly, do not necessarily have the same number of electrons in their outer shells but they do produce a similar biological effect. They are often used to introduce structural diversity into the molecule of interest or to replace an easily metabolised moiety of the molecule by one which is more metabolically stable.⁷⁸


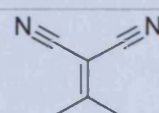
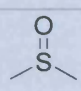
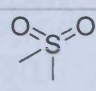
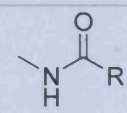
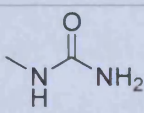
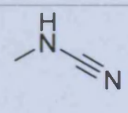
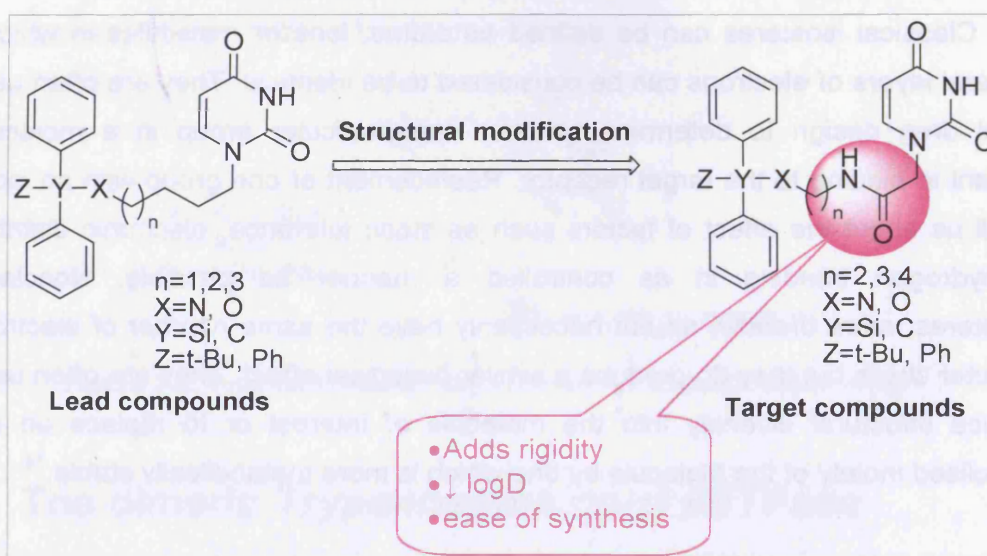
	Group	Isosteres			
Classical isosteres	CH ₃	NH ₂	OH	F	
	CH ₂	NH	O	S	
Nonclassical bioisosteres	Halogen	CF ₃	CN	N(CN) ₂	
					
	OH				

Table 4-1: Examples of classical isosteres and nonclassical bioisosteres

⁷⁸ Silverman, R. B. *The Organic Chemistry of Drug Design and Drug Action*; 2nd ed.; Elsevier Academic Press, 2004.

In this part of the project the aim was to introduce an amide bond into the structures of some of the lead compounds already designed and synthesised in our laboratories. The primary advantage of this modification is that structural diversity can be introduced through the ease in which amide coupling can be carried out. The potential for hydrogen bonding between the amide moiety and the dUTPase active site, as well as the introduction of a certain degree of rigidity into the molecule by the insertion of an amide moiety in place of a short alkyl chain are factors that may lead to a change in how potently and selectively these compounds inhibit the dUTPase enzymes. The logD values would be predicted to decrease and this may also effect the pharmacokinetic properties of these compounds as anti-parasitic agents.

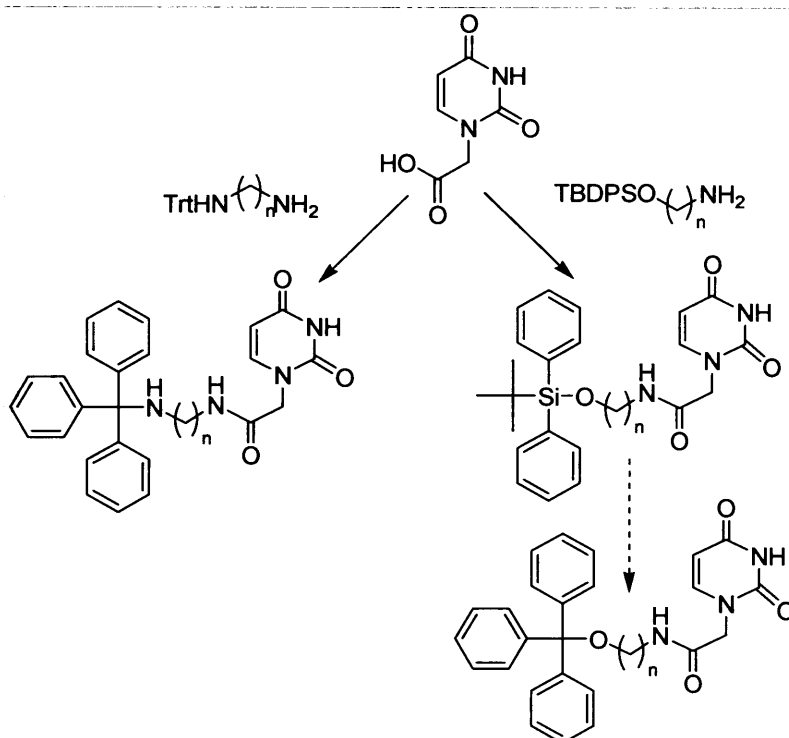


Scheme 4-1: Introduction of an amide bond

4.2 Triphenylmethoxy and triphenylmethylamino monoalkyl chain derivatives – coupling of primary amines to 1-carboxyuracil

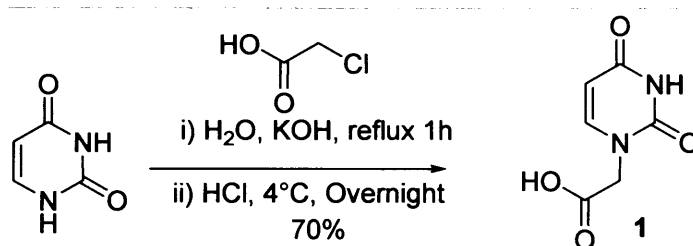
A small series of mono alkyl chain uracil acetamides were synthesised. The overall strategy involved the coupling of 1-carboxymethyluracil with diamino alkanes and amino alcohols of various chain lengths. In the case of the amino alcohols, the hydroxyl group was protected with the *tert*-butyldiphenylsilyl (TBDPS) group to ensure selective coupling to the amine moiety. In the case of the diamines protection was not necessary and selective monotriylation was carried out by adding triphenylmethyl chloride (TrtCl) dropwise at 0°C to a ten fold excess of the diamine.

The overall synthetic strategy is as follows:



Scheme 4-2: Overall synthesis of monoalkyl chain derivatives ($n = 2,3,4$)

4.2.1 Synthesis of 1-carboxymethyluracil



Scheme 4-3: Synthesis of 1-carboxymethyluracil

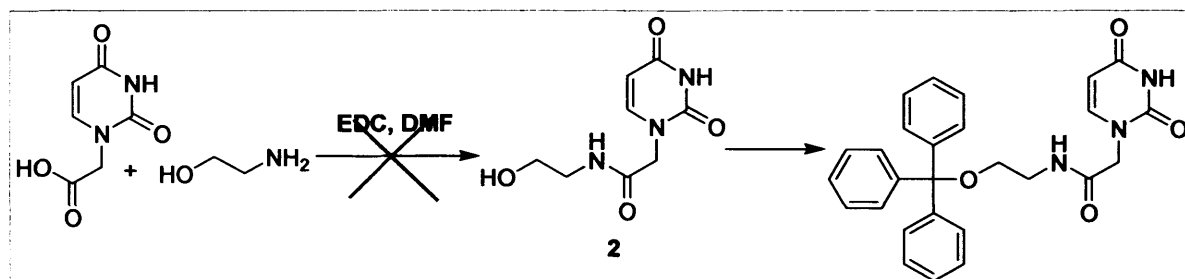
The first step was to prepare 1-carboxymethyluracil (Scheme 4-3), originally synthesised in 1908,⁷⁹ and was carried out according to the procedure of Jacobsen *et al.*⁸⁰ Uracil was reacted with chloroacetic acid in the presence of KOH and the mechanism involved a nucleophilic substitution at the acid chloride by the N-1 of the uracil ring. After acidification, the product was precipitated out as the free acid. The monosubstituted product was the sole product isolated as determined by mass spectrometry and NMR analysis.

⁷⁹ Wheeler, H. L.; Liddle, L. M. Researches on pyrimidines: Synthesis of uracil-3-acetic acid. *J. Am. Chem. Soc.* **1908**, *30*, 1152-1156.

⁸⁰ Jacobsen, J. R.; Cochran, A. G.; Stephans, J. C.; King, D. S.; Schultz, P. G. Mechanistic studies of antibody-catalyzed pyrimidine dimer photocleavage. *J. Am. Chem. Soc.* **1995**, *117*, 5453-5461.

4.2.2 Attempted coupling with 1,2-ethanolamine

Initially, coupling was attempted with the unprotected ethanolamine according to the procedure by Ahn *et al.*⁸¹ This selective amide coupling could be achieved using 1-ethyl-3-(3'-dimethylaminopropyl)carbodiimide (EDC) in dimethylformamide (DMF) conditions and subsequently, direct tritylation could be carried out. The reaction mixture was left stirring overnight and a new spot with a higher R_f than the starting materials could be seen by thin layer chromatography (TLC). However, following aqueous work up and column chromatography on silica gel, no pure product could be isolated. A complex mixture, which by NMR showed the presence of the uracil ring and EDC was isolated from the column. The product could not be seen by mass spectrometry. The reaction was repeated and aqueous work up was avoided as the product was possibly water soluble. Following purification by column chromatography, however, only starting materials were isolated.



Scheme 4-4: Attempted unprotected coupling with ethanolamine

It is possible that the β -oxygen effect in which the hydroxy function β to the amino function deactivates the amine through an inductive effect may be responsible for a decrease in nucleophilicity of the amine. Alternatively, intramolecular hydrogen bonding may be responsible for the deactivation of the amino function. A method by which the hydroxy function was first protected was therefore employed. Due to the hydrophilic nature of these compounds, the use of a lipophilic protecting group was logical as this would aid solubility and purification.

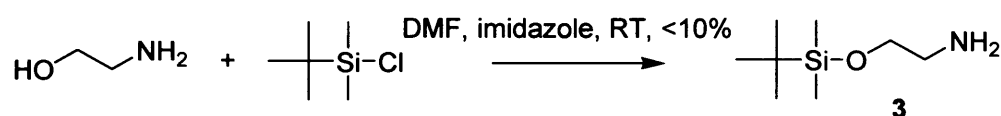
4.2.3 Synthesis of the triphenylmethoxy derivatives

4.2.3.1 Protection with TBDPS

A silyl protecting group was chosen to selectively protect the hydroxyl group over the amino group due to the strong nature of the silicon oxygen bond. Initially, attempts were made to protect with *tert*-butyldimethylsilyl (TBDMS) chloride as this

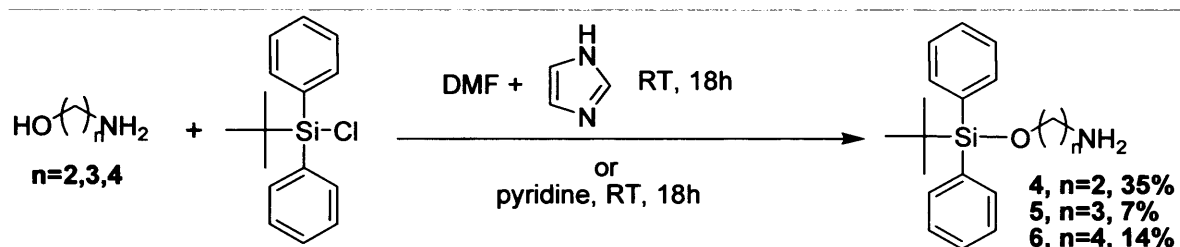
⁸¹ Ahn, D.; Mosimann, M.; Leumann, C. J. Synthesis of cyclopentane amide DNA (cpa-DNA) and its pairing properties. *J. Org. Chem.* 2003, 68, 7693-7699.

moiety is stable under most conditions.⁸² However, the product crystallised on the silica column during purification, resulting in isolation in low yield.



Scheme 4-5: Synthesis of TBDMS protected compound 3

It was thought that increasing the lipophilicity of the protecting group further might improve the purification and isolated yields. The TBDPS group was then chosen as a protecting group. The TBDPS is more stable than TBDMS under acidic conditions but less stable in basic conditions.⁸³



Scheme 4-6: Synthesis of TBDPS protected compounds 4, 5, 6

A mixture of TBDPSCI and imidazole were added to the relevant amino alcohol in DMF and the reaction was left at room temperature overnight (Scheme 4-6). The yields of these reactions however were still quite low after purification. The TBDPS group, though normally resistant to cleavage on silica columns may, in this case have been cleaved under the conditions used. The basic amino moieties of the compounds would also have a high affinity for the slightly acidic silica used and therefore caused much of the product to stick to the column.

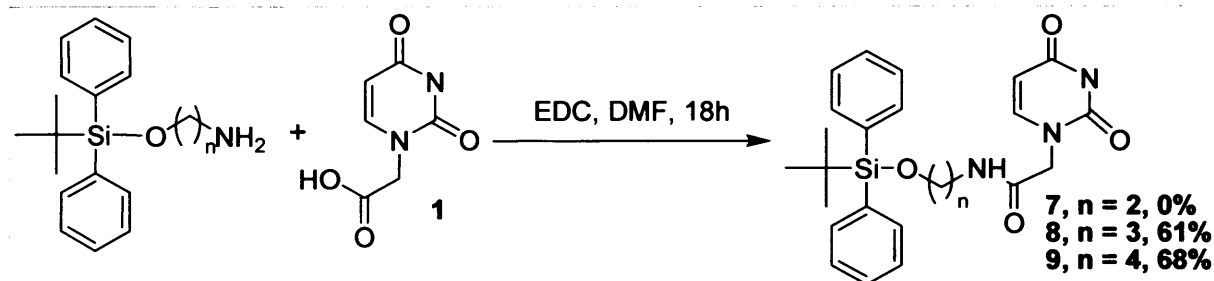
In the case of 4, it was found that the yield of the reaction could be increased slightly to 38% by carrying out the reaction in pyridine. In this case pyridine acts as both solvent and base and therefore the addition of imidazole is not necessary. Traces of imidazole impurity were therefore eliminated, however, column chromatography on silica gel still resulted in a low yield.

⁸² Corey, E. J.; Venkateswarlu, A. Protection of hydroxyl groups as tert-butyldimethylsilyl derivatives. *J. Am. Chem. Soc.* **1972**, *94*, 6190-6191.

⁸³ Hanessian, S.; Lavellee, P. The Preparation and Synthetic Utility of tert-Butyldiphenylsilyl Ethers. *Can. J. Chem.* **1975**, *53*, 2975-2977.

4.2.3.2 **Coupling with 1-carboxymethyluracil**

The next stage was coupling to the 1-carboxymethyluracil **1**. EDC was again used as a coupling reagent as it was thought the by-product produced, 1-ethyl-3-(3'-dimethylaminopropyl)carboureia (EDU) could be simply removed by washing with water. Coupling with the propyl and butyl chains were successful, though initially the yields were low. It was found that by avoiding aqueous work up yields could be increased from 25% to 68%. The EDU could still easily be removed by purification on a silica gel column.



Scheme 4-7: Coupling of the protected amino alcohols to 1-carboxymethyluracil

1-Carboxymethyluracil in DMF was added to the relevant TBDPS-oxyamine in DMF and EDC in a solution of DMF was then added. The reaction was performed under N_2 and left overnight for completion.⁸¹

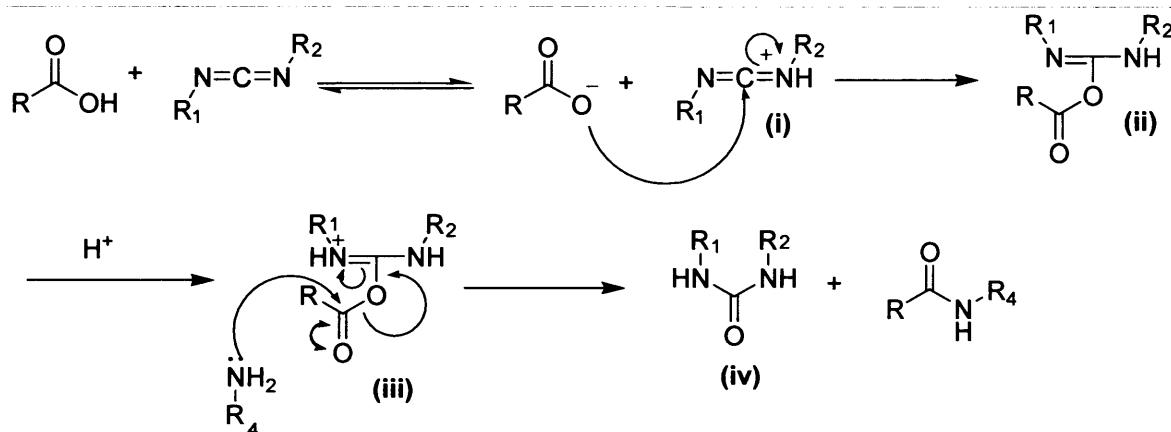
This method was successful for the propyl ($n=3$) and butyl ($n=4$) derivatives. In the case of the ethyl chain derivatives however, no coupling was achieved and only starting material was recovered. The reaction was attempted at higher temperatures and also using dicyclohexylcarbodiimide (DCC) as a coupling reagent but proved fruitless. There may have been too much steric hindrance around the amino function for the reaction to occur due to the presence of the bulky TBDPS group attached to the β -oxygen. With the longer propyl and butyl chains, it is possible for the amino function to extend out further and attack the activated intermediate. The failure of the reaction may also have been due to the inductive effect of the β -oxygen which would result in reducing the nucleophilicity of the amino group rendering it less reactive. This β -oxygen effect is not present in the propyl and butyl derivatives.

EDC is a carbodiimide coupling reagent⁸⁴ and is often used as its product of reaction EDU is water soluble.⁸⁵ The mechanism of carbodiimide mediated amide bond formation is shown in Scheme 4-8.

⁸⁴ Sheehen, J. C.; Hess, G. P. A new method of forming peptide bonds. *J. Am. Chem. Soc.* **1955**, *77*, 1067-1068.

⁸⁵ Sheehen, J. C.; Cruickshank, P. A.; Boshart, G. L. A convenient synthesis of water-soluble carbodiimides. *J. Org. Chem.* **1961**, *26*, 2525-2528.

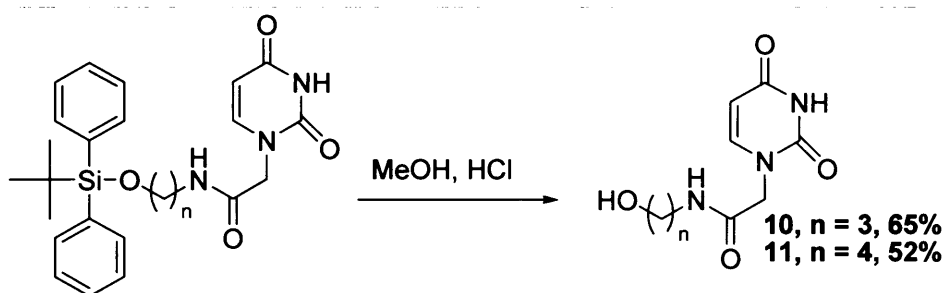
The protonated carbodiimide (i) undergoes nucleophilic attack by the carboxylate, forming the activated O-acylisourea intermediate (ii) which after a reprotonation will form a delocalized carbocation (iii). A nucleophilic addition-elimination reaction by the amine then results in the release of the desired amide and the carbourea (iv).



Scheme 4-8: Mechanism of carbodiimide mediated amide bond formation^{86, 87, 88}

4.2.3.3 Desilylation

The standard utilisation of tetrabutylammonium fluoride (TBAF) to cleave the TBDPS group⁸³ proved difficult as the product could only be isolated in the water layer from the aqueous work up as the TBAF salt. Desilylation was carried out, therefore using the methanolic hydrochloride method which avoided work up and proved to be a clean reaction.⁸⁹ The product could then be recrystallised from ethanol. The mechanism involves protonation of the silyl oxygen and then attack of a water or hydroxide molecule on the silicon to release silanol and the desired alcohol.



Scheme 4-9: Removal of the TBDPS protecting group

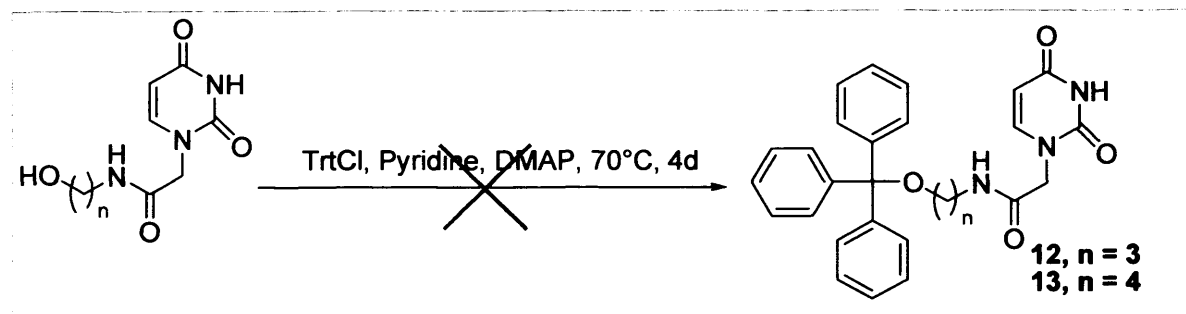
⁸⁶ Rebek, J.; Feitler, D. Improved Method for Study of Reaction Intermediates - Mechanism of Peptide Synthesis Mediated by Carbodiimides. *J. Am. Chem. Soc.* **1973**, *95*, 4052-4053.

⁸⁷ Nakajima, N.; Ikada, Y. Mechanism of Amide Formation by Carbodiimide for Bioconjugation in Aqueous-Media. *Bioconjugate Chemistry* **1995**, *6*, 123-130.

⁸⁸ Marder, O.; Albericio, F. Industrial application of coupling reagents in peptides. *Chimica Oggi - Chemistry Today* **2003**, *21*, 35-40.

⁸⁹ Magaraci, F. Design and synthesis of novel potential 24-methyltransferase inhibitors. In *Welsh School of Pharmacy*; University Wales Cardiff: Cardiff, 2002.

4.2.3.4 Tritylation

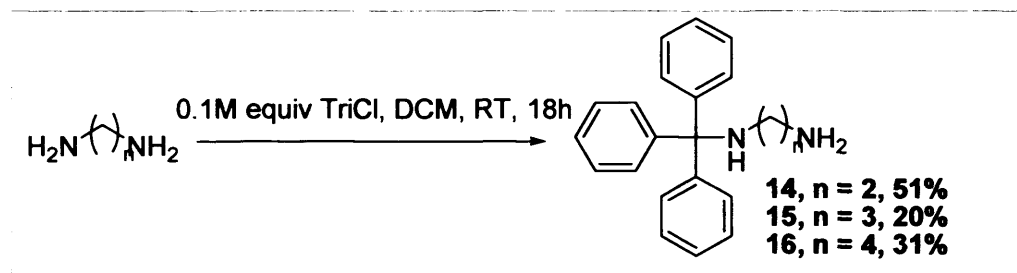


Scheme 4-10: Attempted tritylation 10 and 11

The tritylation of both the propyl and butyl chain derivatives was attempted by dissolving DMAP, TrtCl and the starting material in pyridine. However after one week, a total of 4 eq TrtCl had been added and the mixture was heated 70°C and still no product could be seen by TLC. Only starting material was isolated.

4.2.4 Synthesis of the triphenylmethylamino derivatives

4.2.4.1 Tritylation

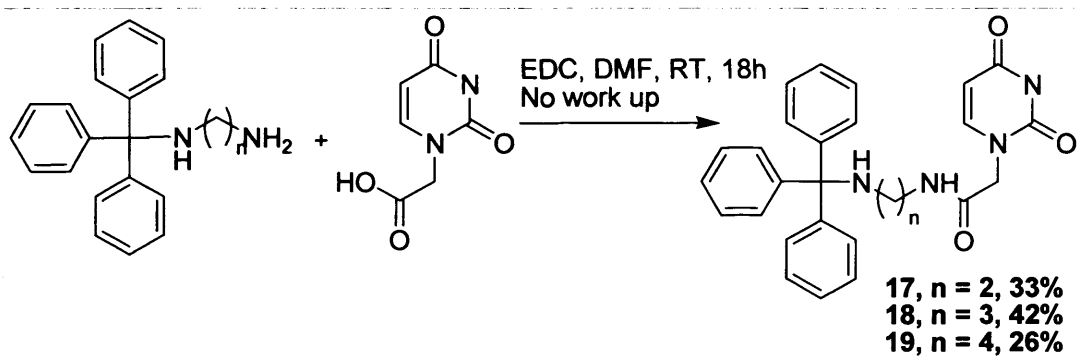


Scheme 4-11: Mono tritylation of diamines

In the case of the diamino alkyl series, the compounds were mono-tritylated selectively by using 0.1M equivalents of TrtCl and adding it dropwise at 0°C .⁹⁰ By mass spectrometry and integration of NMR it was found that only the mono-tritylated compound had been isolated. The second amino moiety was therefore free to react with the 1-carboxymethyluracil.

⁹⁰ Tilley, J. W.; Levitan, P.; Kierstead, R. W.; Cohen, M. Antihypertensive (2-Aminoethyl)Thiourea Derivatives .1. *J. Med. Chem.* **1980**, *23*, 1387-1392.

4.2.4.2 Coupling with 1-carboxymethyluracil



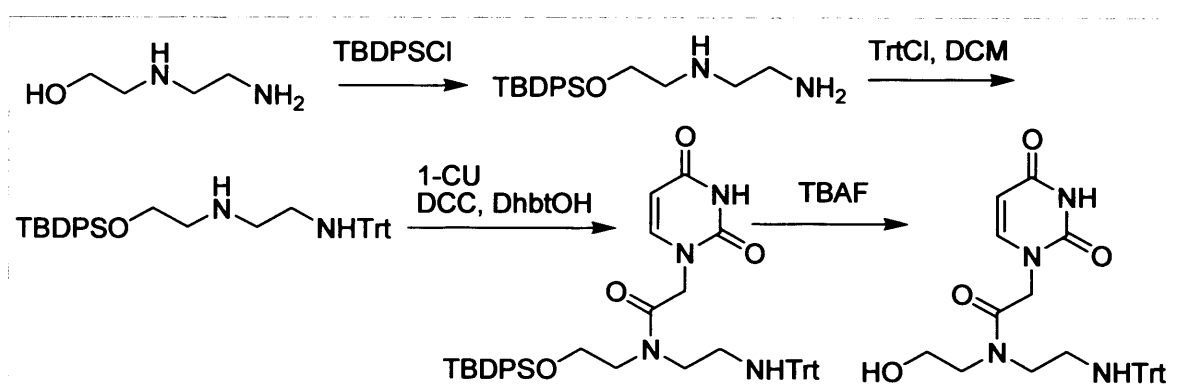
Scheme 4-12: Coupling of mono tritylated diamines to 1-carboxymethyluracil

EDC was again used as the coupling reagent as it could be easily separated from the product. The procedure was the same as that described in 4.2.1.2 and the mechanism of EDC coupling is shown in scheme 4-8. In contrast to the TBDPS derivatives, the reaction was successful with $n=2$. This was probably due to the absence of the β -oxygen effect in the Trt-amino derivatives

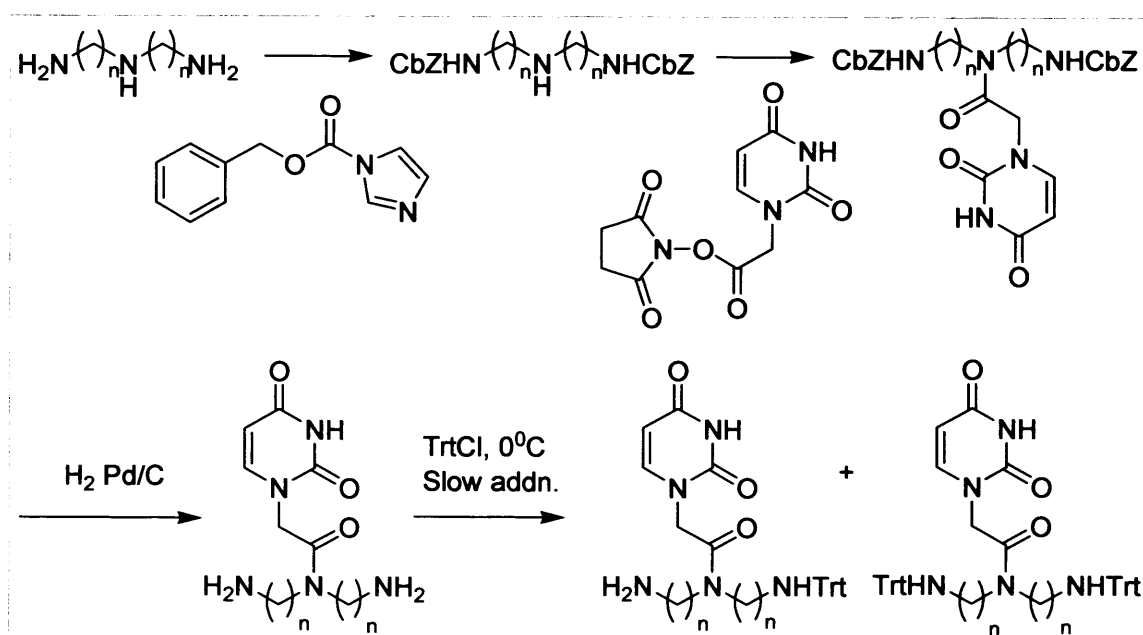
4.3 Triphenylmethylamino and hydroxy (triphenyl methyl)amino dialkyl chain derivatives – coupling of secondary amines to 1-carboxymethyluracil

Subsequent to the synthesis of monoalkyl chain acetamide uracil derivatives, dialkyl chain derivatives were synthesised. The extra “arm” on these molecules could be used to probe for extra interactions as well as steric tolerance within the active site of the enzyme.

The overall synthetic strategies were as follows:



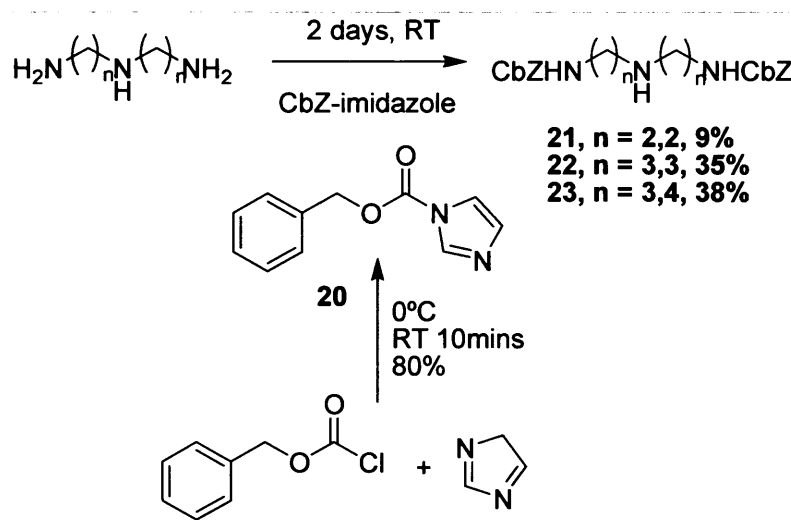
Scheme 4-13: Overall synthetic strategy for hydroxy diamino compounds 1-CU = 1-carboxymethyluracil



Scheme 4-14: Overall synthetic strategy for the triamino compounds

4.3.1 Triphenylmethylamino dialkyl chain derivatives

4.3.1.1 Carbobenzoxy protection of primary amines



Scheme 4-15: Carbobenzoxy protection of primary amines

As coupling of 1-carboxymethyluracil to the secondary amine of these compounds was required, the first step was to selectively protect the terminal, primary amines of the starting triamino compounds. It can be argued that the more nucleophilic secondary amine will react more readily with electrophiles and therefore selective protection may be difficult. However, the primary amines are more reactive for steric reasons and this can be exploited for selective primary amino protection. By using bulky protecting groups it has been found that selective primary amino over secondary amino protection can be achieved.^{91, 92}

Much work has been carried out on developing methods for the selective functionalisation of spermidine and other naturally occurring polyamines. Reagents such as 3-benzyloxycarbonyl-1,3thiazolidine-2-thione,⁹³ and [2-(tert-butoxycarbonyloximino)-2-phenylacetonitrile]⁹⁴ have been used for this purpose.

⁹¹ Sharma, S. K.; Miller, M. J.; Payne, S. M. Spermexatin and spermexatol: new synthetic spermidine-based siderophore analogues. *J. Med. Chem.* **1989**, *32*, 357-367.

⁹² Alummoottil, V.; Scott, J.; Scott, J. R. A simple method for the bis-acylation of the primary amino groups in spermidine and other linear triamines. *Tetrahedron Lett.* **1984**, *25*, 5725-5728.

⁹³ Nagao, Y.; Miyasaka, T.; Hagiwara, Y.; Fujita, E. Total Synthesis of Parabactin, a Spermidine Siderophore. *J. Chem. Soc., Perkin Trans. 1* **1984**, 183-187.

⁹⁴ Bergeron, R. J.; Stolowich, N. J.; Porter, C. W. Reagents for the Selective Secondary N-Acylation of Linear Triamines. *Synthesis-Stuttgart* **1982**, 689-692.

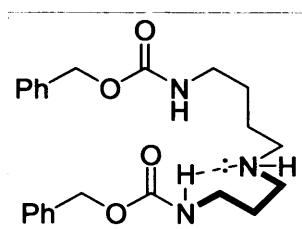
Carbobenzoxy-imidazole (CbZ-imidazole) has also been shown to selectively protect an unhindered primary amine in the presence of hindered primary and secondary amines and this reagent is easily prepared by treatment of CbZ-Cl with imidazole.⁹¹ It was the reagent of choice in this case.

CbZ-imidazole was prepared by reaction of CbZ-Cl with imidazole at 0°C and then at room temperature for 10min. After washing with citric acid to remove the side product of imidazole, the pure product was isolated in good yield.⁹¹

The relevant triamines were reacted with the CbZ-imidazole in the presence of a catalytic amount of dimethylaminopyridine (DMAP).⁹¹ The reaction proved to be more difficult with the shorter chain (n=2) analogues. It was found aqueous work up had to be avoided as the amines could not be recovered from either the organic or aqueous phase. After attempts at recrystallisation from various solvents, it was found that the best method for purification was column chromatography. The eluent had to have a high percentage of MeOH and some NH₃ present to prevent the amines from sticking to the acidic silica in the columns. For n=2,2 the fractions collected were washed further with H₂O. For n=3,3 recrystallisation of the pure product from the fractions collected could be achieved from EtOAc. For n=3,4 the fractions collected were washed with 0.5% w/v HCl to remove imidazole after which the remaining impurities were precipitated out from CHCl₃.

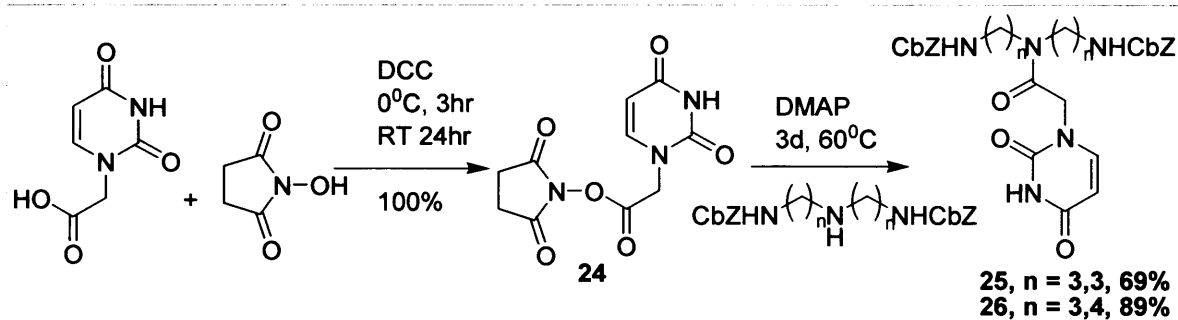
4.3.1.2 Coupling of 1-carboxymethyluracil to secondary amines

It has been proposed that in compounds such as these triamines, especially where n=3,4, intramolecular hydrogen bonding can be responsible for the reduction in nucleophilicity of the secondary amino group.⁹³



Scheme 4-16: Intramolecular hydrogen bonding on triamines⁹³

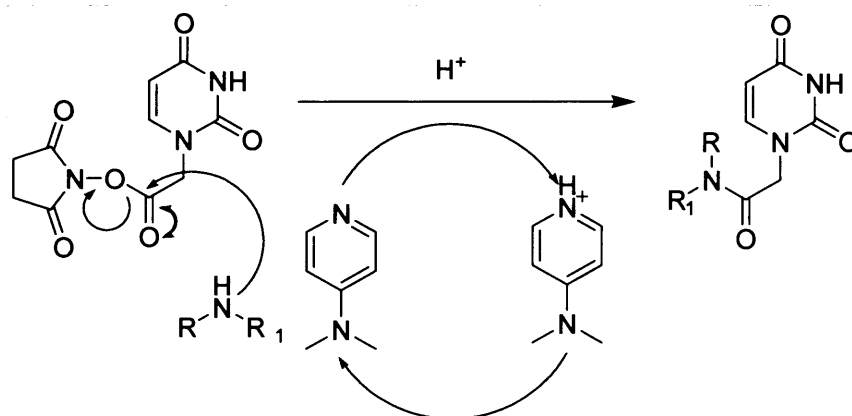
However, use of appropriate coupling reagents can overcome this barrier. For n=3,3 and n=3,4 coupling reactions were successful with the use of the activated succinimidyl ester of 1-carboxymethyluracil in the presence of a catalytic amount of DMAP.⁹¹



Scheme 4-17: Coupling of 1-carboxymethyluracil to secondary amines (n=3,3 or 3,4)

The succinimidyl ester of 1-carboxymethyl uracil was prepared by adding a solution of DCC to a mixture of N-hydroxysuccinimide (NHS) and 1-carboxymethyluracil at 0°C. The succinimidyl ester could be precipitated out from MeOH and was isolated in quantitative yields. The mechanism of carbodiimide ester formation is similar to that shown in Scheme 4-8. The OH group of the NHS acts as the nucleophile which attacks the activated intermediate (iii), releasing the ester and urea by-product.

This activated succinimidyl ester and relevant protected triamine along with a catalytic amount of DMAP were dissolved in DMF under N₂. Reactions were heated to 60°C for 3d. It was found that after work up, no product could be isolated. Therefore aqueous work up was avoided. It was also found that **24** was completely decomposed after 2 months, even at -18°C and should be newly synthesised for the reaction to take place. The pure product (**25** and **26**) was obtained in good yields after recrystallisation from EtOAc. The mechanism is as follows:

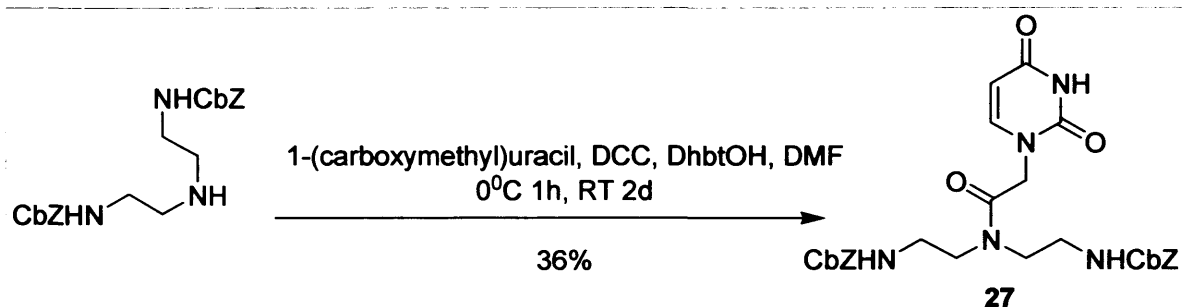


Scheme 4-18: Coupling to activated succinimidyl ester

4 Trityl-amino and TBDPSOxy uracil acetamide derivatives

Where $n=2,2$, however, this coupling procedure resulted in very low yields of still impure product being isolated. This was most likely due to steric hindrance around the amino function due to the shorter alkyl chain lengths to which the Cbz group was attached. An alternative coupling procedure using DCC as a coupling reagent and 3-hydroxy-1,2,3-benzotriazin-4(3H)-one (DhbtOH) as an activating agent was therefore used.⁹⁵

1-carboxymethyluracil and DhbtOH were added to a solution of the protected triamine in DMF under N_2 atmosphere. After cooling to $0^\circ C$, a solution of DCC in DMF was added. The mixture was left stirring at $0^\circ C$ for 1h and then at RT for 2 days after which time a precipitate had formed. The side product, DCU was removed by precipitation from EtOAc. The product was then precipitated out of the remaining solution with diethyl ether.



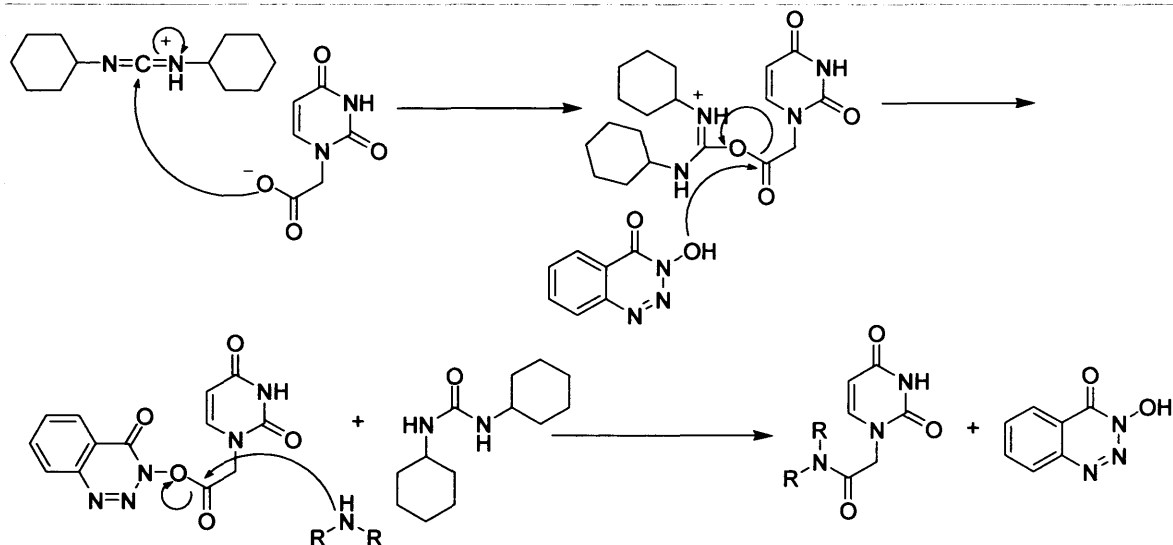
Scheme 4-19: Coupling of 1-carboxymethyluracil to secondary amines ($n=2,2$)

The mechanism of this reaction is as follows with the initial reaction of carbodiimide activation as described in Scheme 4-8 followed by reaction with DhbtOH to give an activated ester intermediate which then undergoes nucleophilic attack by the amine to release the desired amide.^{96, 97}

⁹⁵ Wenninger, D.; Seliger, H. Synthesis and Hybridization Properties of Modified Oligonucleotides With PNA-DNA Dimer Blocks. *Nucleosides Nucleotides* **1997**, *16*, 977-980.

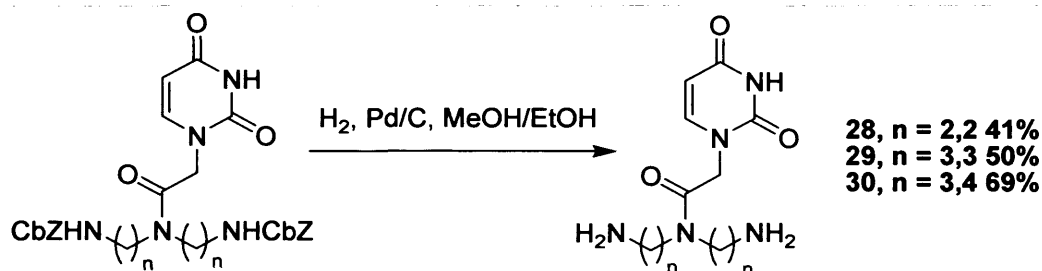
⁹⁶ König, W.; Geiger, R. A New Method for Synthesis of Peptides - Activation of Carboxy Group with Dicyclohexylcarbodiimide and 3-Hydroxy-4-Oxo-3,4-Dihydro-1,2,3-Benzotriazine. *Chemische Berichte-Recueil* **1970**, *103*, 2034-&.

⁹⁷ Atherton, E.; Holder, J. L.; Meldal, M.; Sheppard, R. C.; Valerio, R. M. Peptide-Synthesis .12. 3,4-Dihydro-4-Oxo-1,2,3-Benzotriazin-3-Yl Esters of Fluorenylmethoxycarbonyl Amino-Acids as Self-Indicating Reagents for Solid-Phase Peptide-Synthesis. *J. Chem. Soc., Perkin Trans. 1* **1988**, 2887-2894.



Scheme 4-20: Mechanism of coupling with DCC and DhbtOH

4.3.1.3 Deprotection of acylated primary amines - removal of the Cbz group

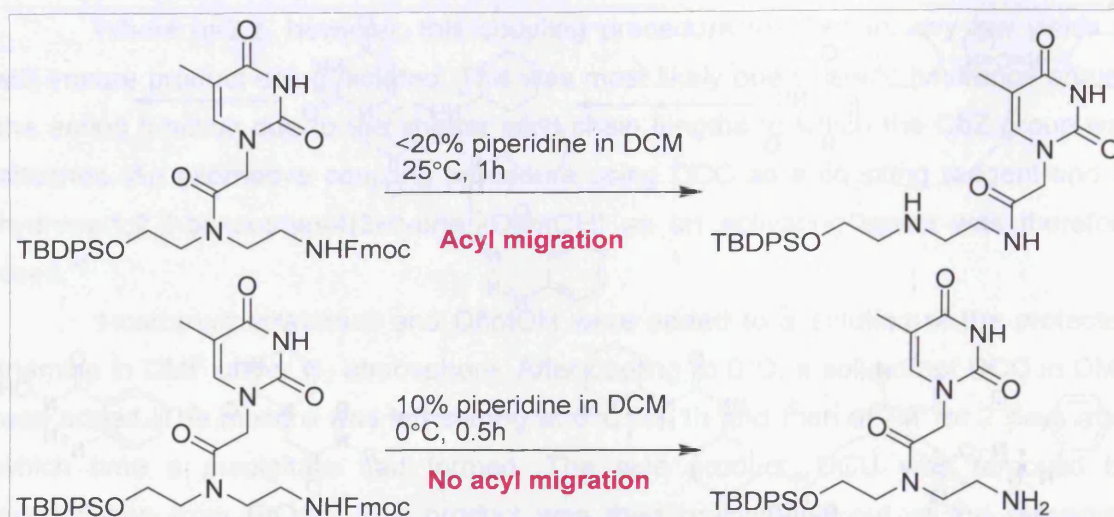
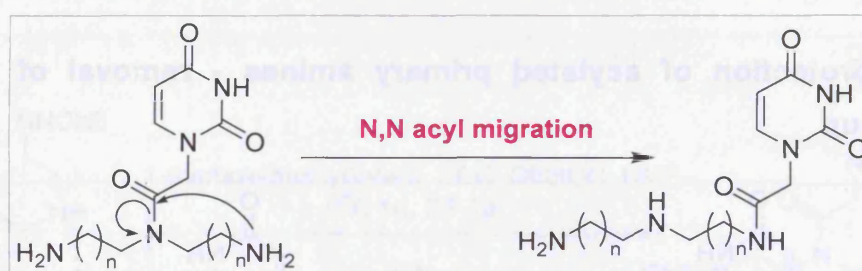


Scheme 4-21: Deprotection of primary amines

Removal of the Cbz group can be easily achieved by hydrogenation.⁹¹ However, this must be carried out selectively in the presence of the uracil ring which may also be hydrogenated at the double bond. It has been shown previously that no hydrogenation of the uracil ring occurs when 5% Pd/C is used as a catalyst.⁹⁸ Under these conditions, using MeOH:EtOH as solvent, selective hydrogenation using a hydrogen balloon was successful.

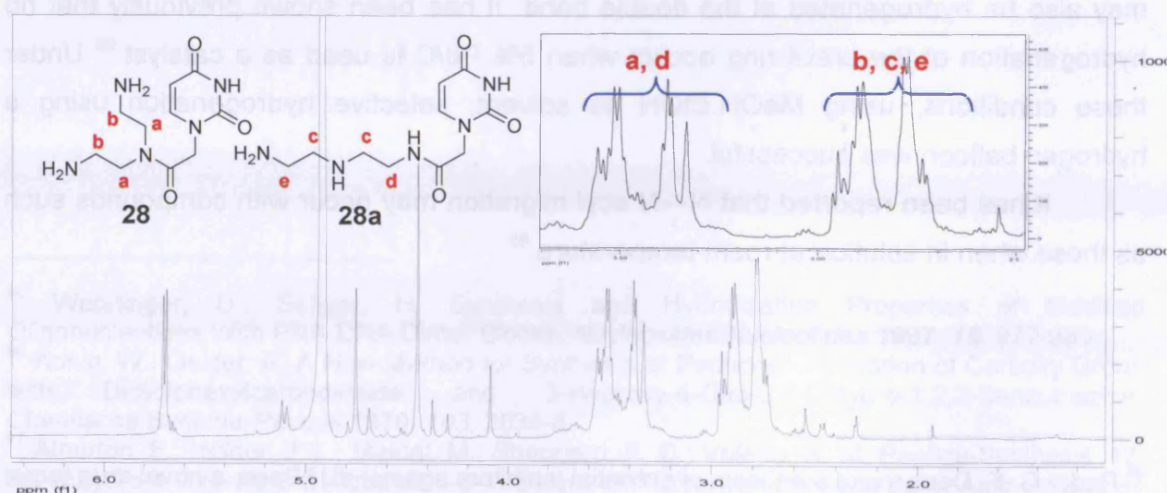
It has been reported that N→N acyl migration may occur with compounds such as these when in solution at room temperature.⁹⁵

⁹⁸ Ruda, G.-F. Design and synthesis of potential inhibitors against dUTPase, a novel drug target for the control of protozoal and bacterial infections. In *Welsh School of Pharmacy*; University of Wales, Cardiff: Cardiff, 2005.

Scheme 4-22a: N,N acyl migration reported by Wenniger *et al.*,⁹⁵

Scheme 4-23b: N,N acyl migration

NMR analysis of the products of this reaction as shown below, suggested that acyl migration to the terminal amino group had taken place to some extent, leading to a mixture of products (**28**, **28a** and **29**, **29a**). This was seen by the fact that the $\text{CH}_2\text{Nuracil}$ peaks and CH_2NH_2 peaks were not pronounced triplets as previously observed and instead were a mixture of multiplets. Peaks corresponding to the two isomers could also be seen in the ^{13}C NMR.

Figure 4-1: NMR analysis of **28**. Inset: expansion of $\text{CH}_2\text{Nuracil}$ and CH_2NH_2 peaks

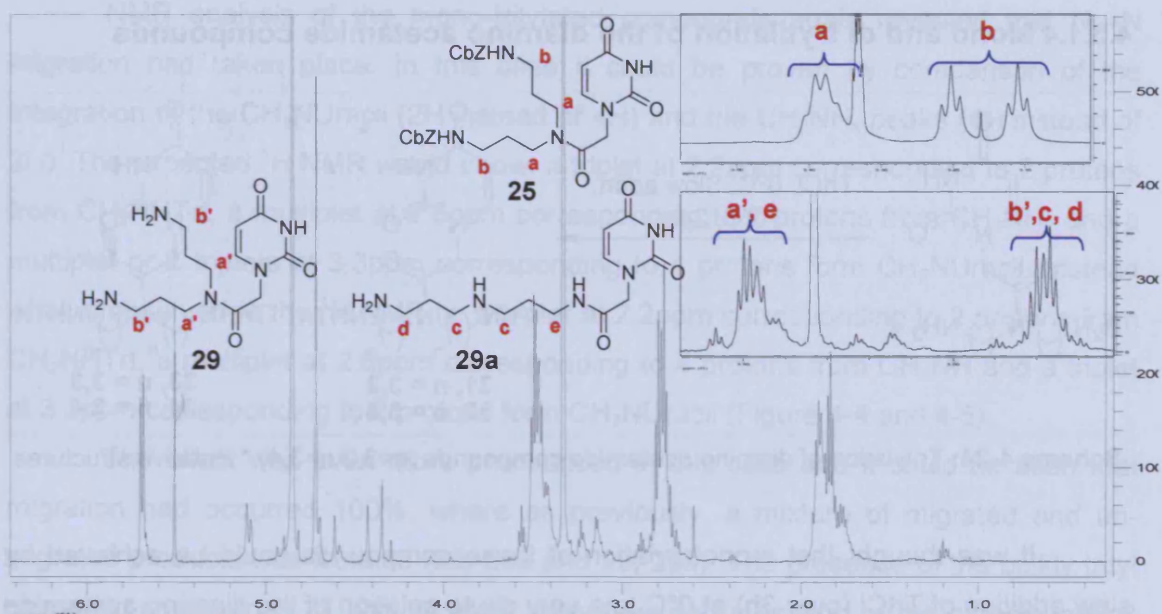


Figure 4-2: NMR analysis of **29**. Inset: (top) expansion of CH_2NHCbz and $\text{CH}_2\text{Nuracil}$ peaks from **25**, clear triplets can be seen (bottom) expansion of $\text{CH}_2\text{Nuracil}$ and CH_2NH_2 peaks from **29**, triplets are no longer pronounced

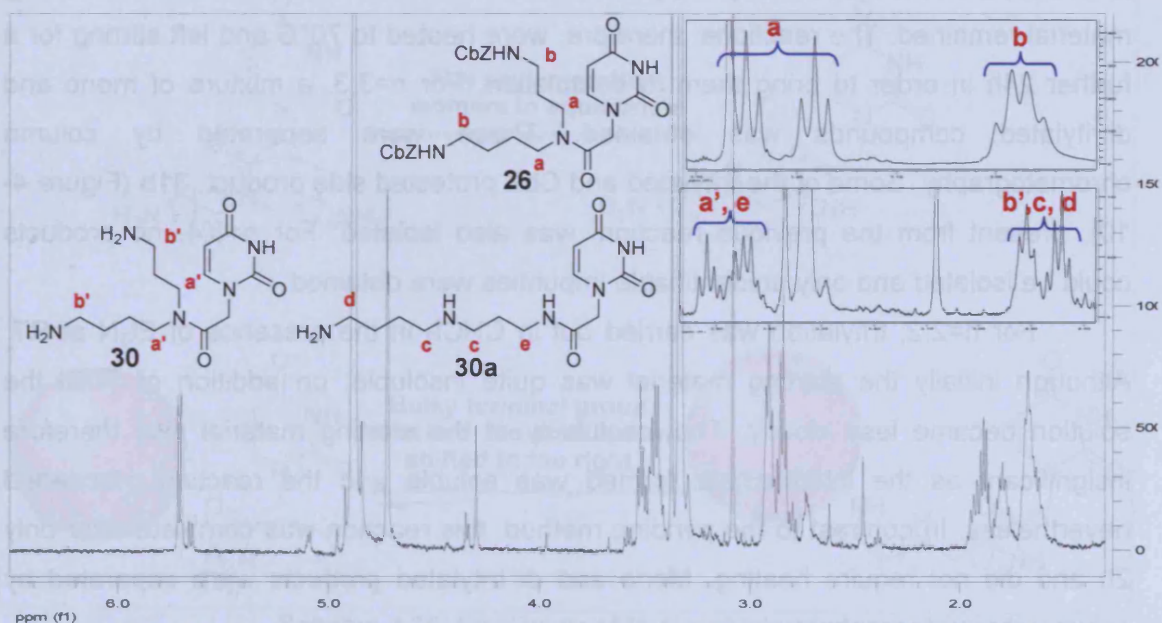
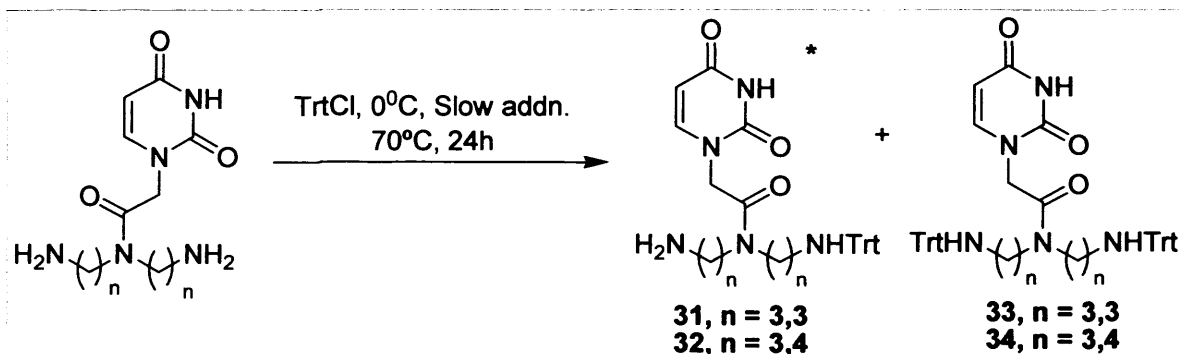


Figure 4-3: NMR analysis of **30**. Inset: (top) expansion of CH_2NHCbz and $\text{CH}_2\text{Nuracil}$ peaks from **26**, clear triplets can be seen (bottom) expansion of $\text{CH}_2\text{Nuracil}$ and CH_2NH_2 peaks from **30**, triplets are no longer pronounced

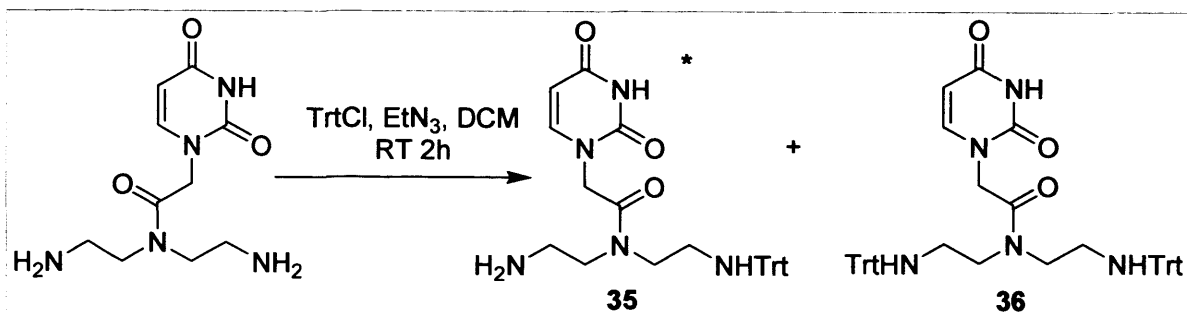
It is probable that the two isomers of **28** and **29** are interconverting structures in equilibrium and that this equilibrium is shifted to the right by the addition of the trityl group to one of the terminal amines. As explained in section 4.3.1.4, the presence of the bulky trityl group would favour the isomer in which the uracil acetamide is on the terminal nitrogen due to steric hindrance which is shown to be the evident case.

4.3.1.4 **Mono and di tritylation of the diamino acetamide compounds**

Scheme 4-24: Tritylation of diamino acetamide compounds (n=3,3 n=3,4) * Putative structures

It was thought that monotritylation of these compounds could be achieved by slow addition of TrtCl (over 3h) at 0°C to a very dilute solution of the diamino acetamide compound. For n=3,3 and n=3,4, tritylation was attempted in this way. Pyridine was used as a solvent due to the insolubility of the compounds in DCM. This reaction, however proceeds more slowly in pyridine than in DCM and after 24h, a lot of starting material remained. The reactions, therefore, were heated to 70°C and left stirring for a further 24h in order to bring them to completion. For n=3,3, a mixture of mono and ditritylated compounds was obtained. These were separated by column chromatography. Some of the tritylated and CbzZ protected side product, **31b** (Figure 4-10), present from the previous reaction, was also isolated. For n=3,4, no products could be isolated and only unidentifiable impurities were obtained.

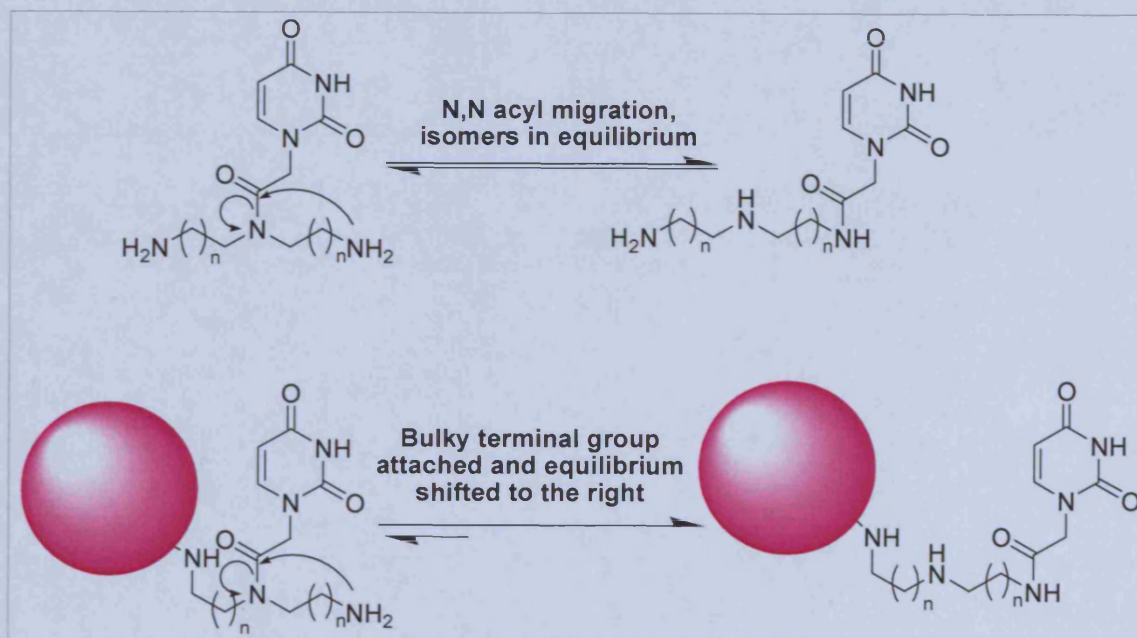
For n=2,2, tritylation was carried out in CHCl₃ in the presence of Et₃N at RT. Although initially the starting material was quite insoluble, on addition of TrtCl the solution became less cloudy. The insolubility of the starting material was therefore insignificant as the intermediate formed was soluble and the reaction proceeded nevertheless. In contrast to the pyridine method, this reaction was complete after only 2h and did not require heating. Mono and di tritylated products were separated by column chromatography.



Scheme 4-25: Tritylation of diamino acetamides (n=2,2) * Putative structure

NMR analysis of the mono-tritylated compounds again revealed that N→N migration had taken place. In this case it could be proven by comparison of the integration of the CH₂NUracil (2H instead of 4H) and the CH₂NH_x peaks (4H instead of 2H). The expected ¹H NMR would show: a triplet at 2.2ppm corresponding to 2 protons from CH₂NHTrt, a multiplet at 2.6ppm corresponding to 2 protons from CH₂NH₂ and a multiplet or 2 triplets at 3.3ppm corresponding to 4 protons from CH₂NUracil. Instead what is observed in the ¹H NMR is: a triplet at 2.2ppm corresponding to 2 protons from CH₂NHTrt, a multiplet at 2.6ppm corresponding to 4 protons from CH₂NH and a triplet at 3.3ppm corresponding to 2 protons from CH₂NUracil (Figure 4-4 and 4-5)

The effect was even more pronounced in this case and it could be seen that migration had occurred 100%, where as previously, a mixture of migrated and unmigrated products was isolated (**28**, **28a** and **29**, **29a**). The presence of the bulky trityl groups in compounds **31** and **35** most likely favoured migration of the carboxymethyl uracil to the terminal N for steric reasons.



Scheme 4-26: Equilibrium of N, N acyl migration

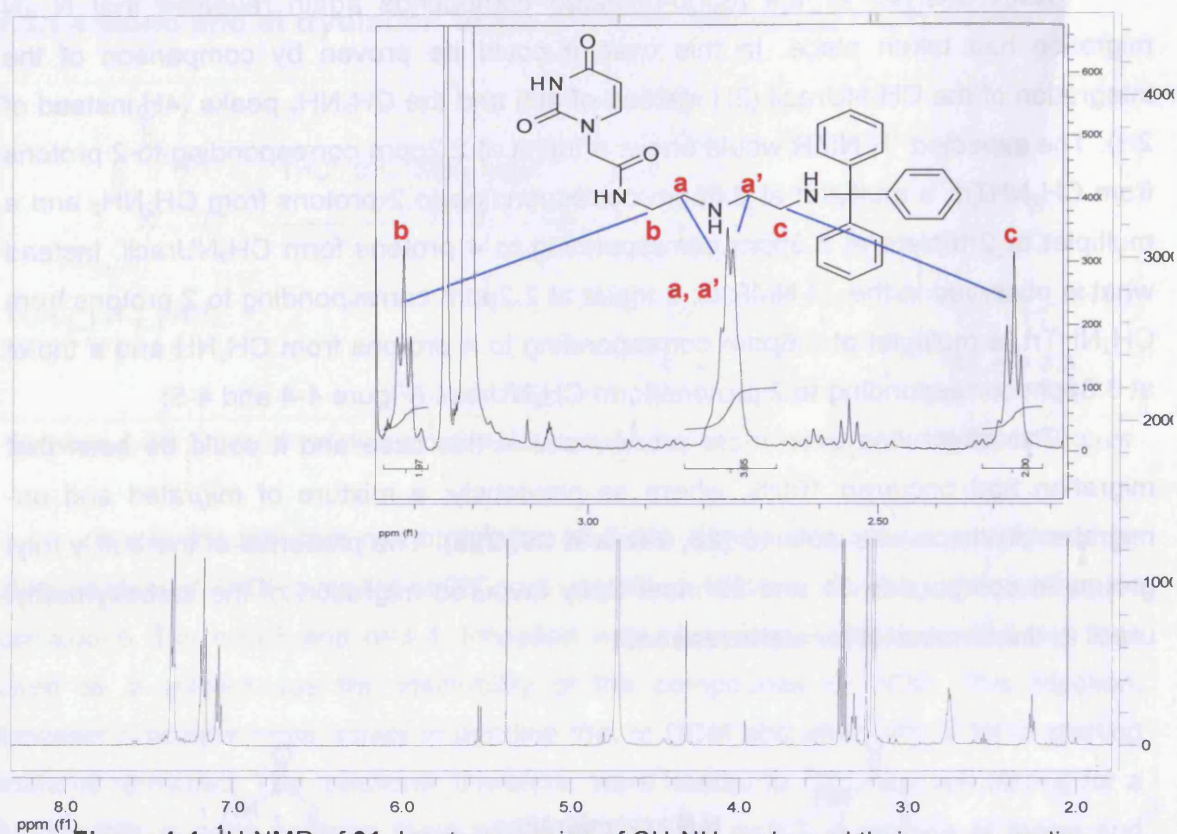


Figure 4-4: ^1H NMR of **31**. Inset: expansion of CH_2NH peaks and their corresponding integrations

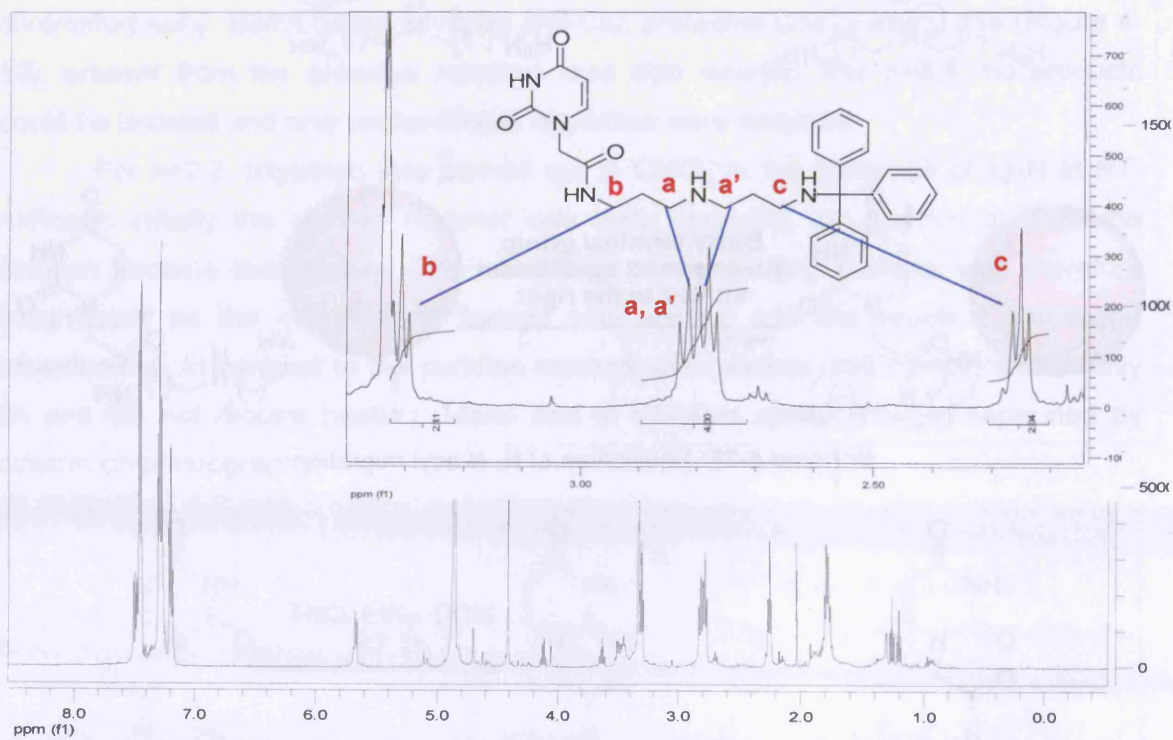
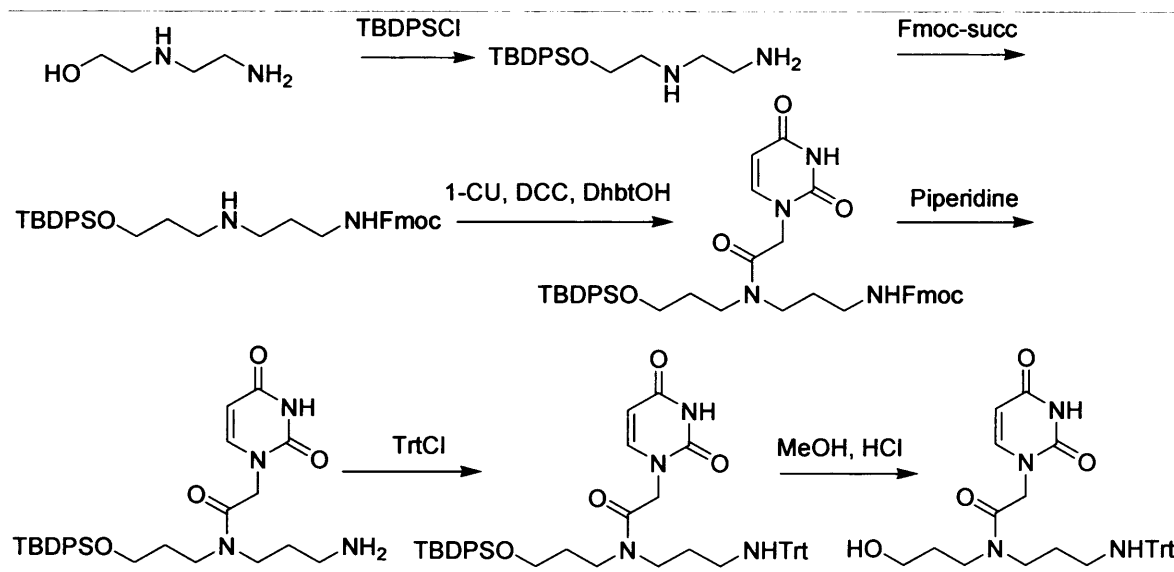


Figure 4-5: ^1H NMR of **33**. Inset: expansion of CH_2NH peaks and their corresponding integrations

4.3.2 Hydroxy(triphenylmethyl)amino dialkyl chain derivatives

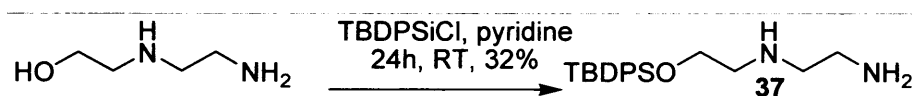
Once again, for these compounds, the terminal functional groups must first be protected in order to couple the secondary amine to 1-carboxymethyluracil. The protecting groups must be orthogonal in order that they be selectively cleaved at the end. The initial strategy was to use that of Wenniger *et al*;⁹⁵ That is to first protect the hydroxyl function with the TBDPS group which is cleaved under acidic conditions or by TBAF. Fmoc-succinimide can then be used to selectively protect the terminal amino group. After amide coupling has been carried out, the Fmoc group can be cleaved. The amino group then tritylated and finally the TBDPS group cleaved using TBAF.



Scheme 4-27: Strategy of Wenniger *et al*;

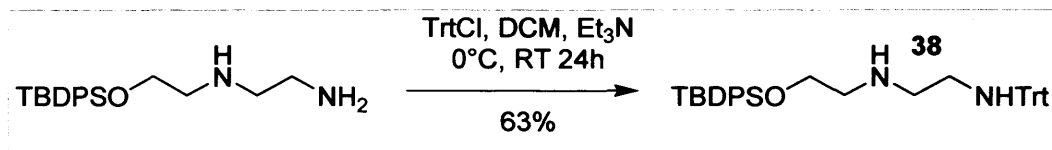
If, however we can use the trityl moiety as a protecting group for the terminal amino group in the beginning, this would eliminate 2 steps from the synthesis. It was also thought this would be a way in which to avoid acyl migration from occurring as the amino group would be protected throughout the synthesis and a deprotection step would not be necessary. The modified overall synthetic strategy is shown in Scheme 4-13.

4.3.2.1 Protection of the hydroxyl moiety



Scheme 4-28: Protection with the TBDPSi group

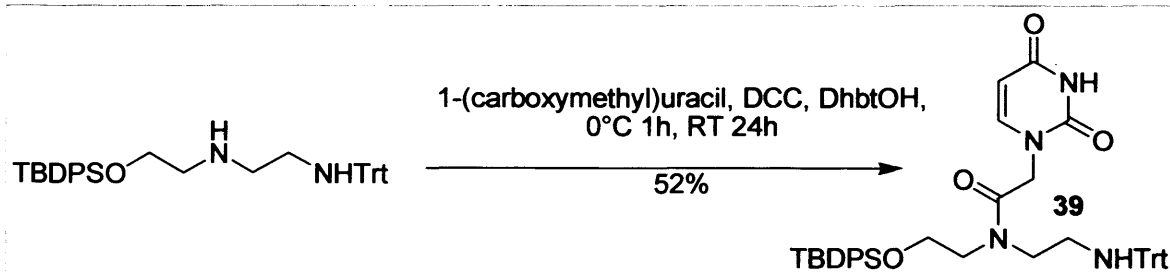
As mentioned previously, (4.2.3.1) the TBDPS group is a good protecting group for selectively protecting hydroxyl groups over amines. The reaction was carried out simply by adding TBDPSCI to N-(2-hydroxyethyl)ethylenediamine under N₂ using dry pyridine as the solvent.⁹⁵



Scheme 4-29: Tritylation of primary amine

Selective tritylation was carried out by slow addition of a dilute solution of TrtCl to **38** at 0°C followed by addition of Et₃N. The terminally substituted product was confirmed by a change in shift of the CH₂NH₂ protons by 0.5 ppm but no change in shift for the CH₂NHCH₂ peaks.

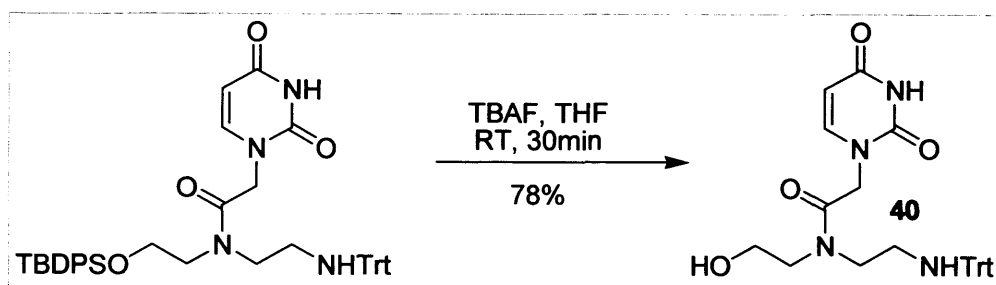
4.3.2.2 Coupling to 1-carboxymethyluracil



Scheme 4-30: Coupling to 1-carboxymethyluracil

Coupling to 1-carboxymethyluracil was carried out by the DCC/DhbtOH method described in section 4.3.1.2 and the mechanism is shown in Scheme 4-20. The pure product was precipitated from MeOH.

4.3.2.3 Deprotection – removal of the TBDPS group



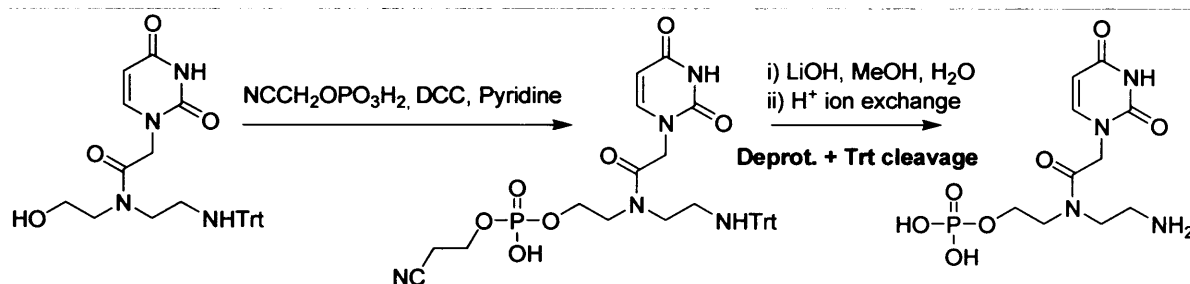
Scheme 4-31: Removal of the TBDPSiCl protecting group

As described before, the TDBPSiCl group can be cleaved in mild conditions using HCl in MeOH or TBAF. It was thought that in this case, however, the Trt group might also be cleaved under the acidic conditions used previously. The method of using TBAF to cleave the TBDPS group was therefore employed and the product was obtained after purification by column chromatography.

4.4 Tritylamino phosphate dialkyl chain derivatives

It was thought that one of the branched chains of these compounds might be orientated in such a way in the active site of the enzyme as to interact with the phosphate binding site. Therefore a phosphate moiety was attached to the hydroxyl group of **40** to probe for interactions and to investigate as to whether this would increase binding affinity of the molecules.

A phosphate with protecting groups that could be cleaved selectively in the presence of the Trt groups was needed. It was at first thought that 2-cyanoethyl protected phosphates, which can be deprotected in basic conditions,⁹⁹ would be useful in this case as the Trt group is stable under basic conditions. However, all literature methods involved purification on acidic ion exchange columns⁹⁹ in which the Trt group would almost certainly be cleaved off. This method was therefore rejected.

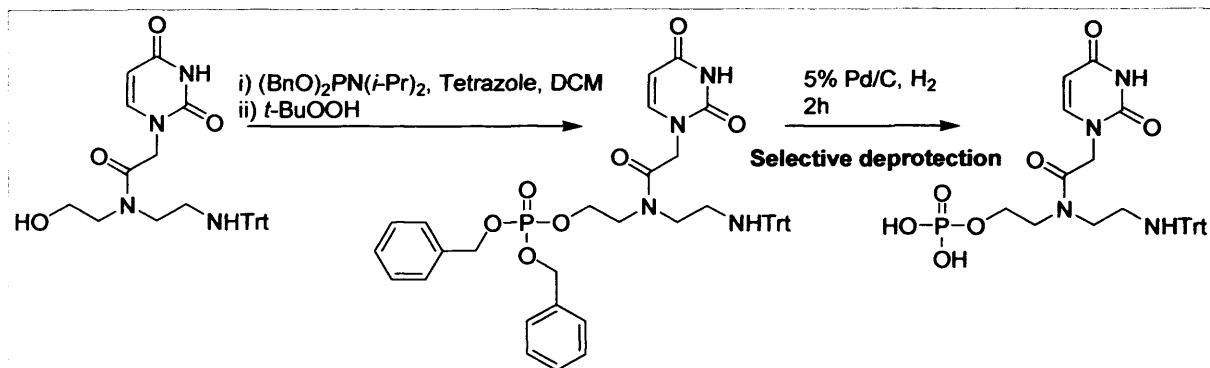


Scheme 4-32: Use of cyanoethyl protected phosphates

Benzyl protected phosphates are deprotected by hydrogenation.¹⁰⁰ This is by far the simplest method of phosphate ester synthesis as purification is carried out simply by filtration through celite. Although the Trt group is also considerably labile under hydrogenation conditions, the benzyl groups are much more labile and it has been shown previously within the group that selective cleavage of these benzyl groups can be carried out in the presence of the Trt group under mild conditions.⁹⁸

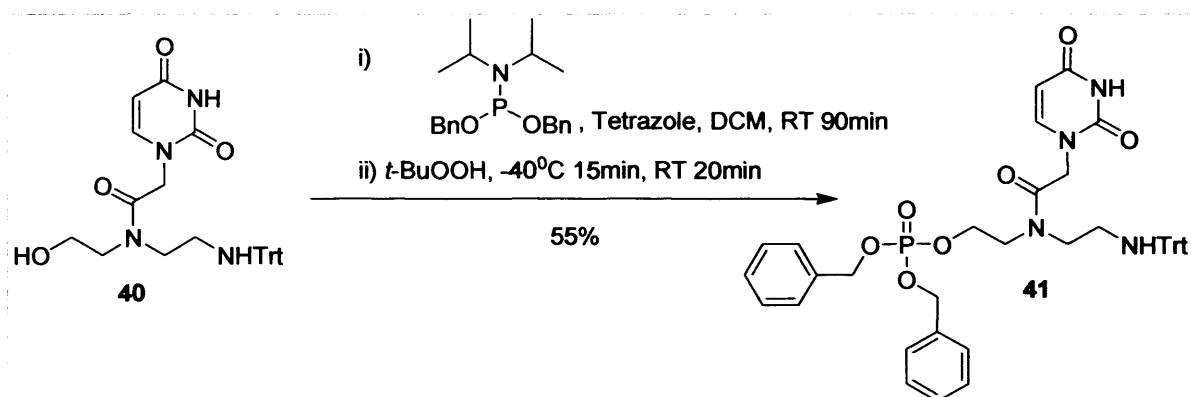
⁹⁹ Tener, G. M. 2-cyanoethyl Phosphate and its Use in the Synthesis of Phosphate Esters. *J. Am. Chem. Soc.* **1961**, *83*, 159-168.

¹⁰⁰ Yu, K. L.; Fraser-Reid, B. A Novel Reagent for the Synthesis of Myo-inositol Phosphates - N,N-Diisopropyl Dibenzyl Phosphoramidite. *Tetrahedron Lett.* **1988**, *29*, 979-982.



Scheme 4-33: Use of benzyl protected phosphates

4.4.1 Synthesis of benzyl protected phosphate ester



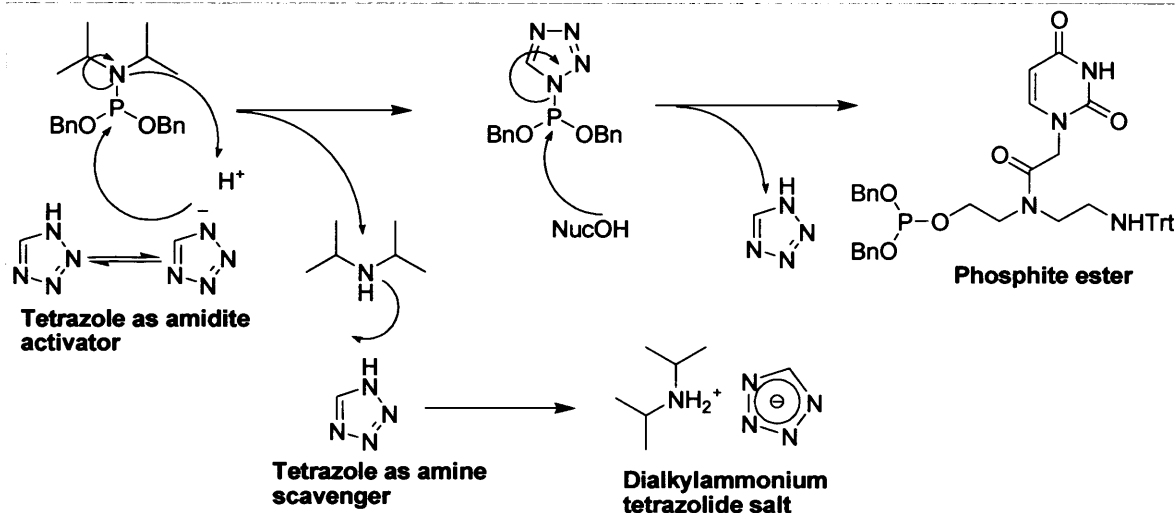
Scheme 4-34: Synthesis of benzyl protected phosphate ester

The synthesis was carried out by reacting **40** with *N,N*-diisopropyl dibenzyl phosphoramidite to form the intermediate phosphite ester by displacement of the $\text{N}(\text{i-Pr})_2$ moiety.¹⁰⁰ The reaction was carried out in the presence of an excess of 1-*H*-tetrazole which is thought to act as both an activator of the phosphoramidite and as a scavenger of the generated amine (scheme 4-33).¹⁰¹ A precipitate forms during the course of the reaction, shown to be the dialkylammonium tetrazolide salt, the formation of which may drive the reaction.¹⁰²

Compound **40** was treated with an excess of phosphoramidite at RT in the presence of an excess of tetrazole. After 90 min the reaction was complete.

¹⁰¹ Hayakawa, Y.; Kataoka, M. Preparation of short oligonucleotides via the phosphoramidite method using a tetrazole promoter in a catalytic manner. *J. Am. Chem. Soc.* **1997**, *119*, 11758-11762.

¹⁰² Chow, C. P.; Berkman, C. E. Synthesis of *N*-phosphoryl amino acids via phosphoramidite amine-exchange. *Tetrahedron Lett.* **1998**, *39*, 7471-7474.

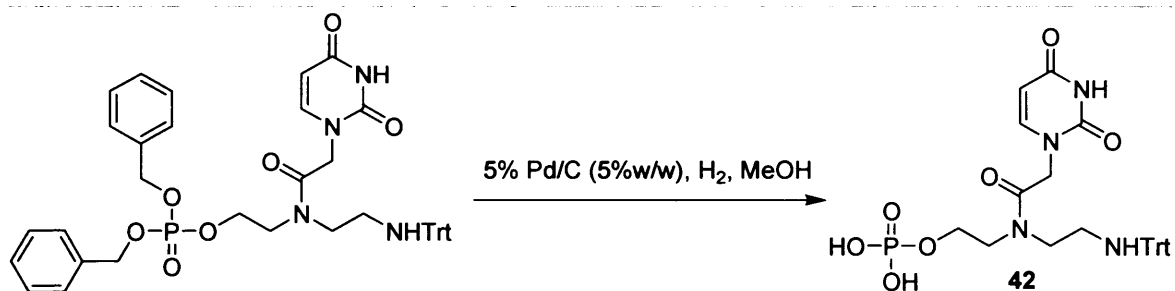


Scheme 4-35: Mechanism of tetrazole mediated phosphate formation¹⁰²

Following the generation of this phosphite ester, oxidation to the phosphate ester was then carried out in situ using *t*-butylhydroperoxide as an oxidising agent. *t*-BuOOH was added to the solution at -40°C , which was allowed to remain stirring at this temperature for 15 min and a further 40 min at RT. The pure product was isolated in an overall 55% yield after purification by column chromatography.

4.4.2 Deprotection of the benzyl phosphate ester

Removal of the benzyl protecting groups was carried out by selective hydrogenation in mild conditions. 5% Pd/C in 5% w/w was sufficient to cleave the benzyl groups from the molecule without cleaving the Trt group.

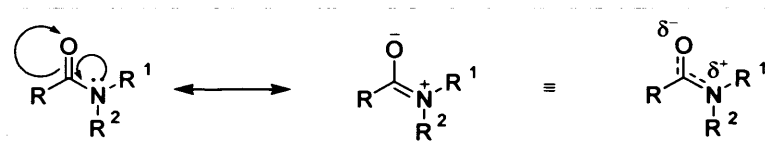


Scheme 4-36: Cleavage of benzyl protecting groups from phosphate ester

The reaction was firstly attempted in a THF:H₂O, 50:50 mixture as solvent. However, no product was isolated and this was thought to be due to the insolubility of the starting material. The reaction was then repeated using MeOH as solvent and hydrogenation was successful. The catalyst was removed by filtration through celite but washing with DMF was necessary as the product was highly insoluble in MeOH, EtOH, H₂O, CHCl₃ and acetone.

4.5 Restricted rotation around the amide bond and variable temperature NMR

Rotation about single bonds is normally very fast in contrast to rotation about double bonds which is normally very low or non-existent. The C-N bond in an amide has partial double bond character due to delocalisation of the lone pair on the nitrogen into the carbonyl group.



Scheme 4-37: Delocalization in an amide group

Often, slow rotation around the amide bond can mean that two isomers, or more specifically rotamers, *cis* and *trans* exist. Both of these rotamers can often be seen by NMR spectroscopy and the ratio in which they exist can be measured from the integration of the relevant peaks. Normally, where R are large substituents, the *trans* conformation would be the more stable. The rate at which the two isomers interchange, however depends on the energy of activation (E_a) of their rotation.

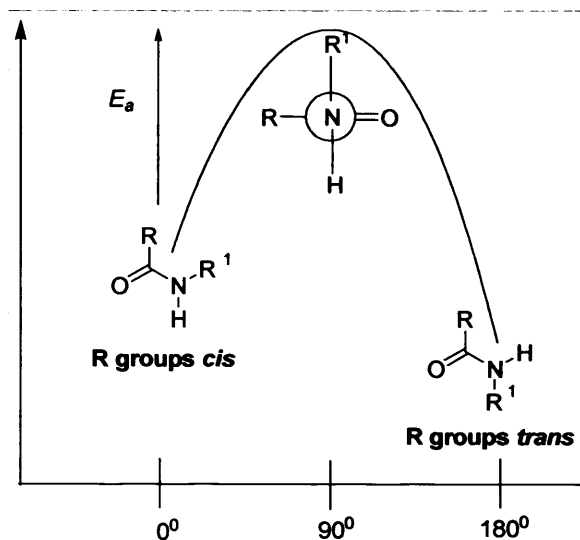


Figure 4-6: Energy profile diagram of rotation about amide bond

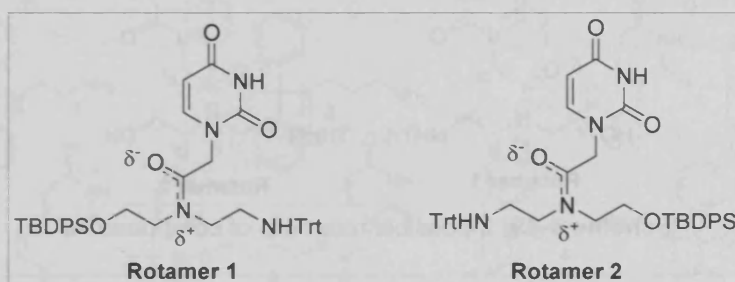
The energy of activation is the energy which is required to overcome the barrier to rotation. Not only does this depend on the R groups, but according to the Arrhenius equation, the rate at which rotation occurs also depends on temperature.

$$k = Ae^{\left(\frac{-E_a}{RT}\right)}$$

Equation 1 : (k = rate coefficient, A = pre-exponential factor, E_a = activation energy, $R = 8.314 \text{ J K}^{-1} \text{ mol}^{-1}$, T = temperature in Kelvin)

Increasing the temperature of the system can supply the molecules with sufficient energy to overcome the barrier of rotation. This is the basis for variable temperature NMR. Carrying out NMR experiment at a higher temperature will supply energy to the system such that free rotation about the amide bond becomes easier. The two isomers interconvert more rapidly and the structures are averaged out. The result is that the NMR peaks converge and the splitting is reduced.

Peak splitting due to restricted rotation around the amide bond was quite evident in some of the compounds synthesised. The effect was especially pronounced in compounds **39** and **40**. With compound **39** all peaks were evidently split and the presence of two isomers if not two compounds was obvious. From integration of the peaks it was calculated that at RT the isomers existed in a ratio of 2:3.



Scheme 4-38: 2 possible rotamers of compound **39**

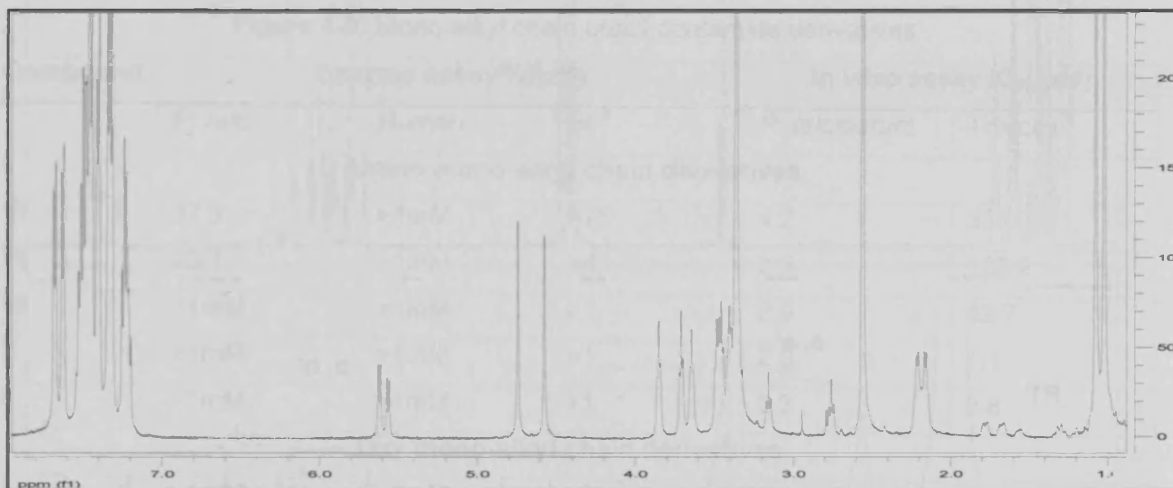
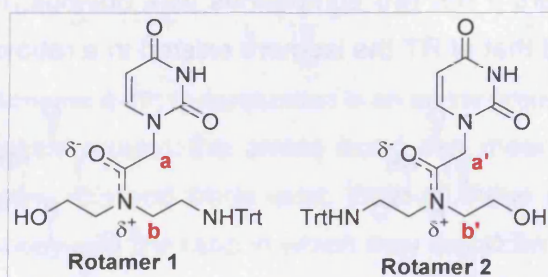


Figure 4-7: $^1\text{H-NMR}$ of compound **39**

After desilylation, removal of the bulky protecting group probably reduced the barrier to rotation significantly as the peak splitting of compound **40** was not as noticeable but was still present. To prove that the peak splitting was due to the presence of two isomers and not due to two different compounds being formed, a variable temperature NMR experiment was carried out on compound **40**.

The experiment was carried out in CD₃OD at RT and then at 40°C. In the event of unrestricted rotation, the protons in position 'a' would be expected to resonate as a singlet (e.g compound 1). However, in this case, two singlets were observed. On heating, the peaks converged and the splitting of N-1(CH₂) (a, a' Scheme 4-39) reduced from 0.04ppm to 0.01ppm. The protons in position 'b' would be expected to resonate as 2 sets of triplets in the case of unrestricted rotation. In this case, four sets of triplets were observed. Once again, however, these CH₂ started to converge on application of heat to the sample. This proved that peak splitting was due to restricted rotation around the amide bond.



Scheme 4-39: 2 possible rotamers of compound 40

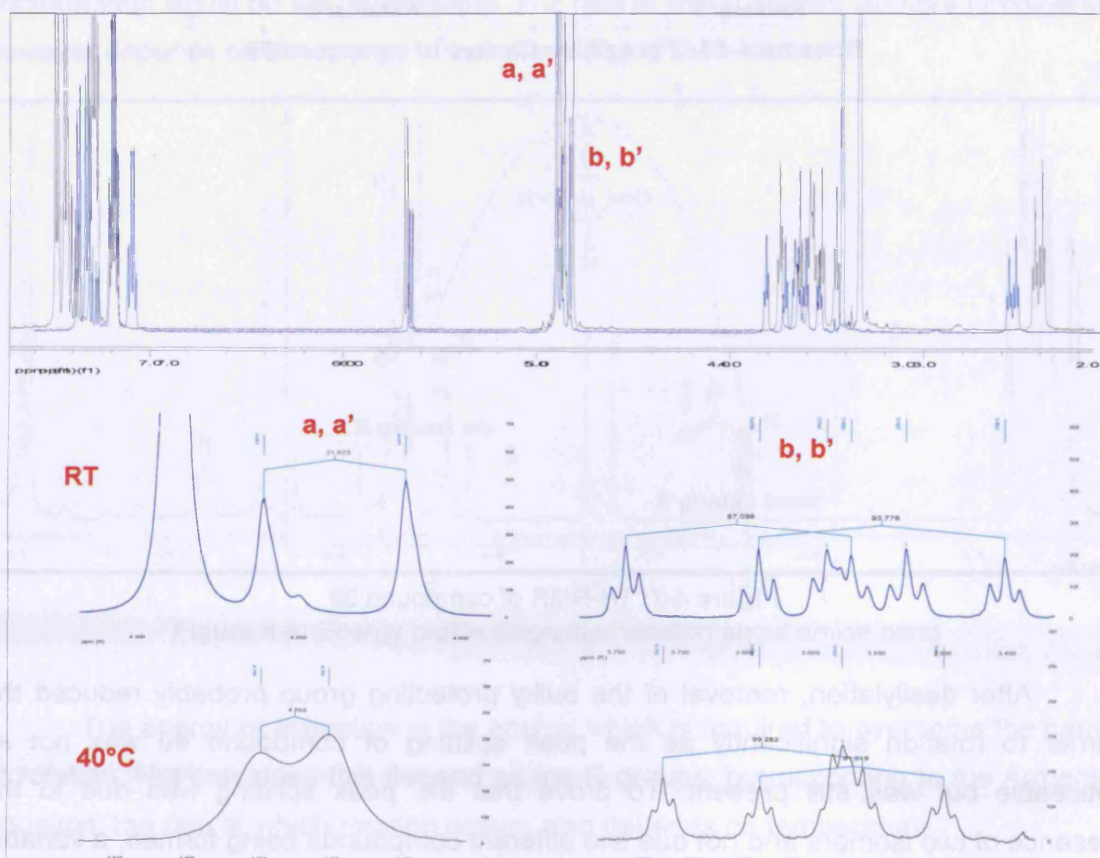


Figure 4-8: ¹H-NMR of 40. Top: Full spectrum of 40 at RT (blue) and at 40°C (black). Bottom: Expansion of CH₂ multiplets at RT (blue) and at 40°C (black). Experiments were carried out in MeOD

4.6 Biological results: Trimeric dUTPases and *P. falciparum* parasites

As the design of these compounds was based on lead inhibitors of the *P. falciparum* dUTPase, they were tested on this (trimeric) form of the enzyme initially. They were also tested against the human dUTPase enzyme to determine selectivity. For assay procedures see appendix 1.

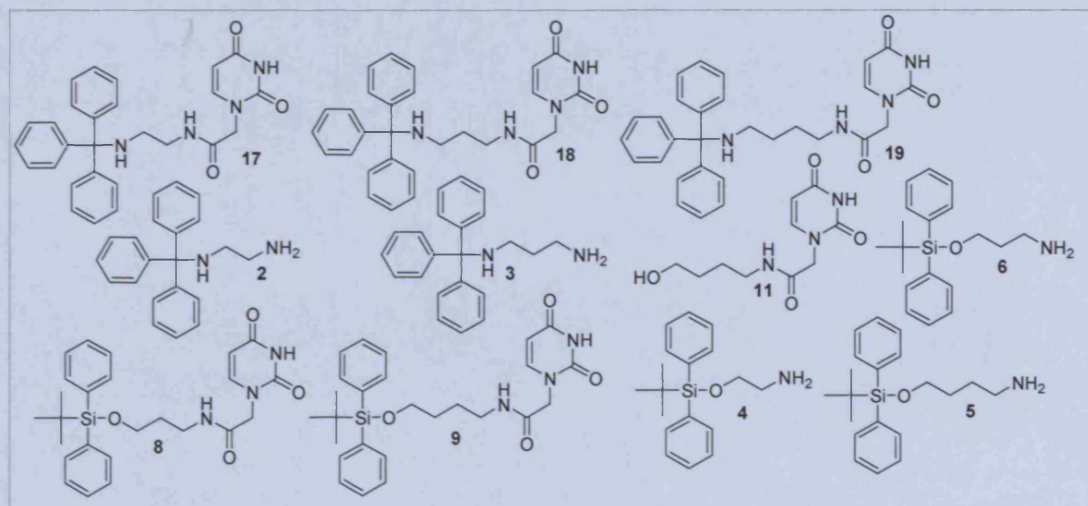


Figure 4-9: Mono-alkyl chain uracil acetamide derivatives

Compound	Enzyme assay K_i (μM)			In vitro assay IC_{50} (μM)	
	<i>P. falc</i>	Human	SI ^a	<i>P. falciparum</i>	Toxicity ^b
Amino mono-alkyl chain derivatives					
17	37.3	>1mM	>26	4.2	53.0
18	23.1	>1mM	>43	2.5	102.2
19	>1mM	>1mM	>1	2.9	42.7
2	>1mM	>1mM	>1	2.0	1.1
3	>1mM	>1mM	>1	2.3	8.8
Oxy mono-alkyl chain derivatives					
8	>1mM	>1mM	>1	4.6	88.9
9	>1mM	>1mM	>1	3.7	33.4
4	>1mM	>1mM	>1	>83.0	>373
5	>1mM	>1mM	>1	1.2	6.3
6	>1mM	>1mM	>1	1.4	4.1
11	>1mM	>1mM	>1	1.0	4.0

Table 4-2: Biological results of mono-alkyl chain derivatives against the trimeric dUTPase and in vitro results against malaria parasites. a) SI=selectivity index [K_i (humandUTPase)/ K_i (PfdUTPase)] b) Toxicity tests were carried out L6 cells

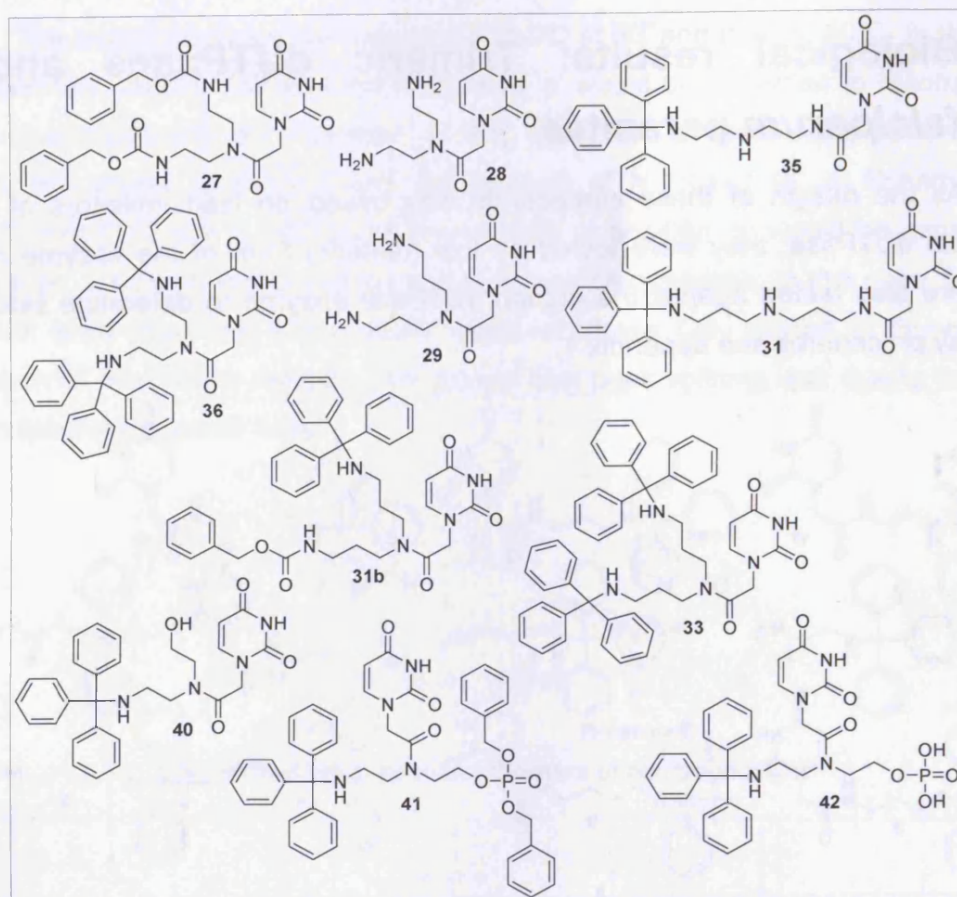


Figure 4-10: Di-alkyl chain uracil acetamide derivatives

Compound	Enzyme assay K_i (μ M)			In vitro assay IC_{50} (μ M)	
	<i>P. falc</i>	Human	SI ^a	<i>P. falciparum</i>	Toxicity ^b
Diamino di-alkyl chain derivatives					
27	>1mM	>1mM	>1	>9	>172.0
28	>1mM	>1mM	>1	>19.6	>352.6
35	>1mM	>1mM	>1	4.48	52.7
36	>1mM	>1mM	>1	0.4	>121.64
29	>1mM	>1mM	>1	15.4	>317.7
31	>1mM	>1mM	>1	3.9	76.7
31b	>1mM	>1mM	>1	0.5	43.2
33	>1mM	>1mM	>1	0.3	>117.2
Oxy amino di-alkyl chain derivatives					
40	>1mM	>1mM	>1	5.6	nd
41	>1mM	>1mM	>1	nd	nd
42	>1mM	>1mM	>1	nd	nd

Table 4-3: Biological results of di-alkyl chain derivatives against the trimeric dUTPase and in vitro results against malaria parasites. a) SI=selectivity index [K_i (humandUTPase)/ K_i (PfdUTPase)] b) Toxicity tests were carried out on L6 cells

4.6.1 Results and discussion

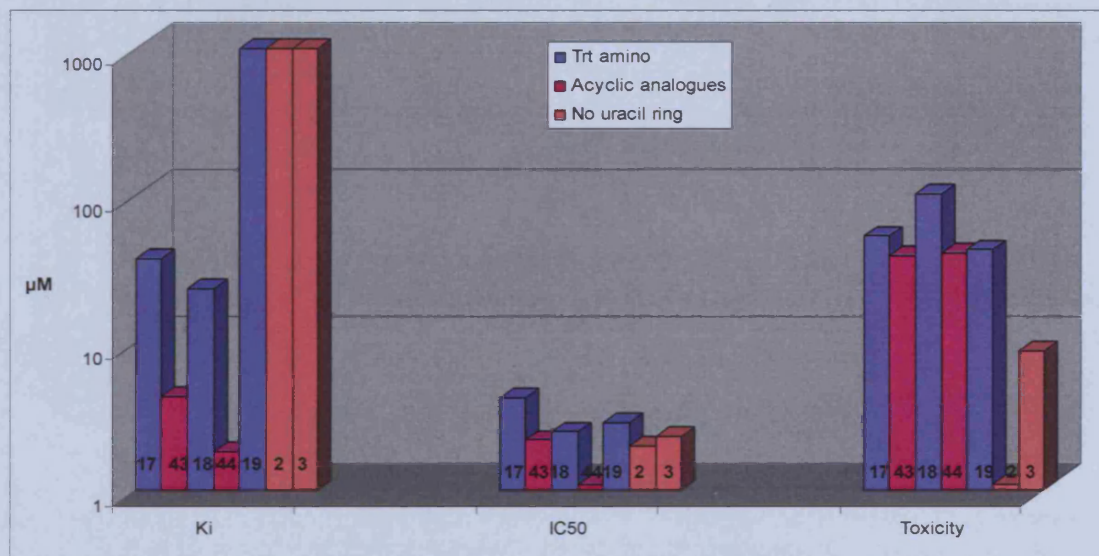


Figure 4-11: Inhibitory activity of Trt-amino uracil acetamides on PfdUTPase and on *P. falciparum* parasites compared with their acyclic analogues

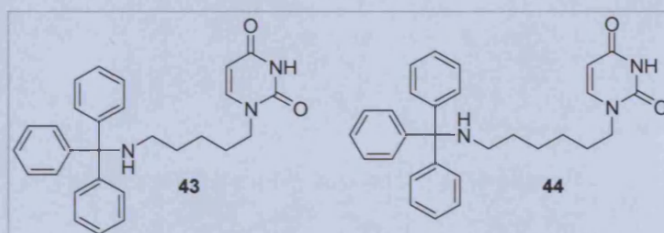


Figure 4-12: Acyclic analogues **43** and **44**

Two of the Trt-amino uracil acetamide compounds **17** and **18** exhibited weak but selective inhibition of the PfdUTPase enzyme ($K_i = 37.3, 23.1 \mu\text{M}$ respectively). However, the activity of these compounds against the enzyme was somewhat diminished in comparison with their acyclic analogues **43** and **44** ($K_i = 4.29, 1.84 \mu\text{M}$ respectively). It would therefore seem that introduction of an amide bond is unfavourable for the inhibitory action of these nucleoside derivatives against the PfdUTPase.

Despite their lack of activity as inhibitors of the dUTPase enzyme, some of these compounds show quite potent anti-parasitic activity *in vitro*. Compounds **17**, **18** and **19** exhibit inhibition of parasite growth at concentrations similar or equivalent to their acyclic analogues ($\text{IC}_{50} = 4.2, 2.5, 2.9 \mu\text{M}$ compared to 2.2 and $1.1 \mu\text{M}$). These compounds may, therefore be exerting their effect on a different target that has not yet been identified. Compounds **2** and **3** that do not contain the uracil ring inhibit parasite growth, however they also inhibit the growth of mammalian cells and are therefore more than likely generally toxic.

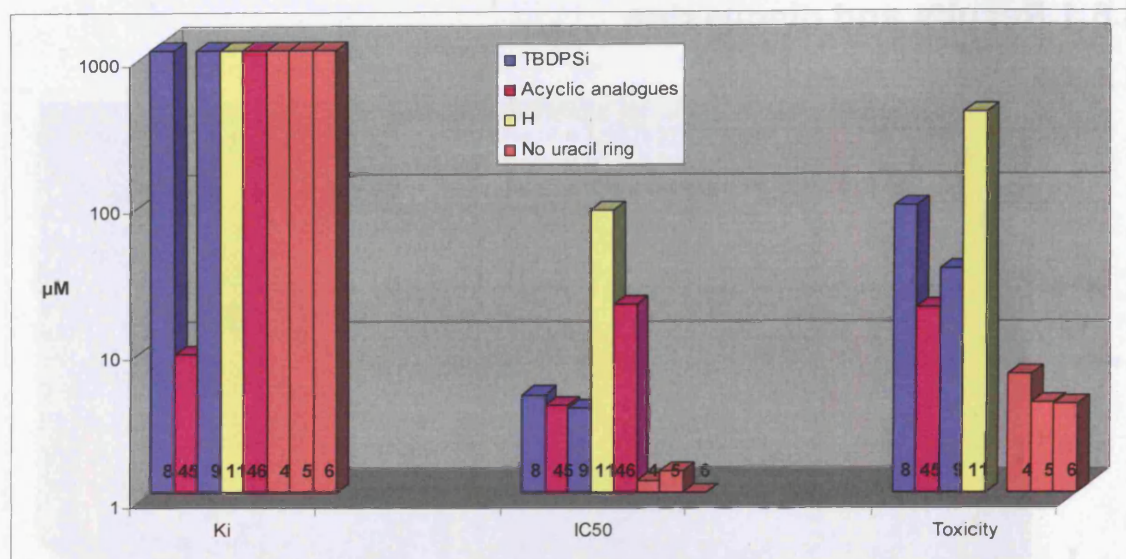


Figure 4-13: Inhibitory activity of TBDPS-oxy uracil acetamides on PfDUTPase and on *P. falciparum* parasites compared with their acyclic analogues

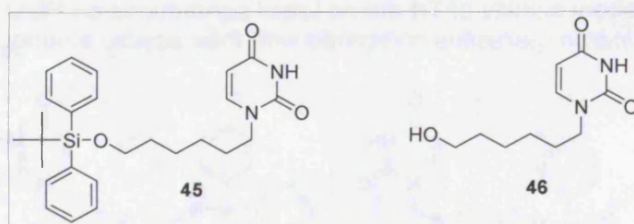


Figure 4-14: Acyclic analogues **45** and **46**

For the TBDPS-oxy uracil acetamide derivatives, dUTPase inhibition is completely lost and they show no enzyme inhibition at concentrations greater than 1mM. This is in contrast to the acyclic analogue **45** ($K_i = 8.74 \mu\text{M}$), showing that the introduction of an amide bond is detrimental to PfDUTPase enzyme inhibition.

Once more, however, the compounds show inhibition of parasite growth at concentrations similar to or lower than their acyclic analogues ($\text{IC}_{50} = 4.6$ and $3.7 \mu\text{M}$ compared to $3.9 \mu\text{M}$). For compounds **8** and **9**, the selectivity over mammalian cell growth inhibition is retained showing that the compounds are not generally toxic. This is further proof that these compounds may be exerting their activity by means of a different target to the dUTPase enzyme. However, as seen by the loss of activity of compound **11** ($\text{IC}_{50} = 83 \mu\text{M}$), the presence of the uracil ring is still required for *in vitro* activity suggesting that the target may still be a uracil binding protein.

A similar phenomenon is observed with the di-alkyl chain derivatives in that they show no inhibition of the dUTPase enzymes but they are selectively active *in vitro*. In fact, they are ten fold more potent than their mono-alkyl chain equivalents *in vitro* but only when the terminal amino groups are protected by Trt or Cbz groups.

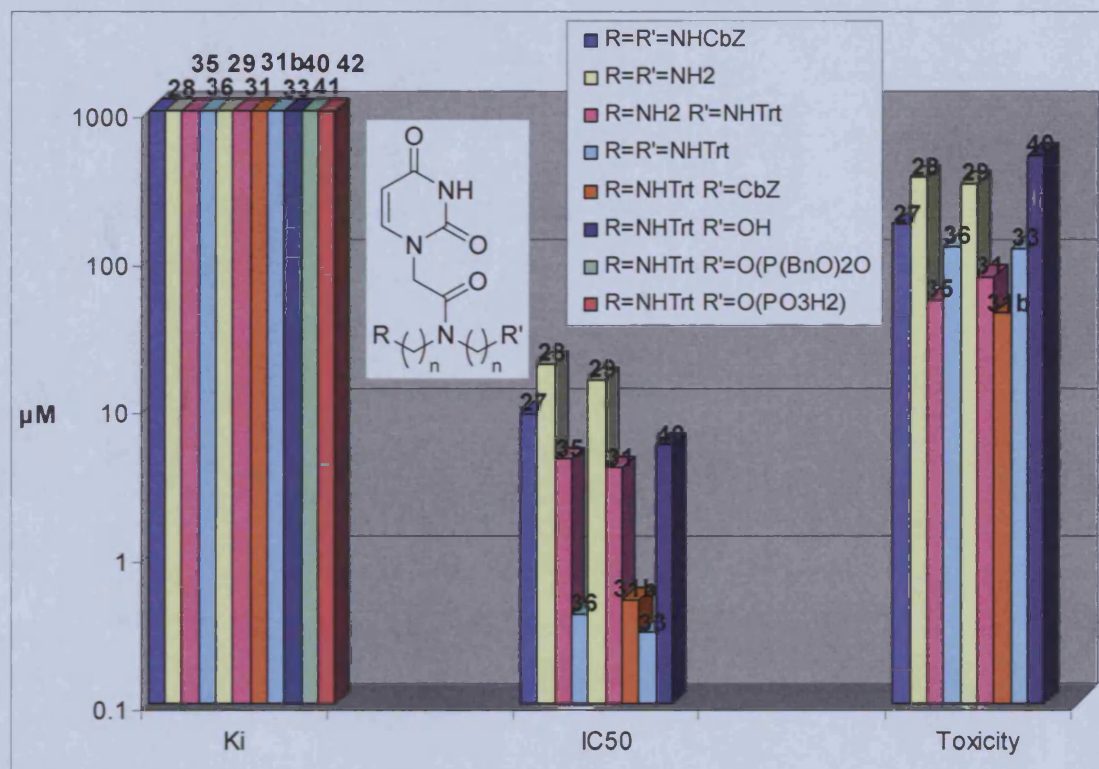


Figure 4-15: Inhibitory activity of the branched chain uracil acetamide derivatives on PfdUTPase and *P. falciparum* parasites

The most potent of the di-alkyl chain derivatives are those with two Trt groups attached (**36**, $\text{IC}_{50} = 0.4\mu\text{M}$ and **33**, $\text{IC}_{50} = 0.4\mu\text{M}$), followed by compound **31b** ($\text{IC}_{50} = 0.5\mu\text{M}$) which has one Trt group and one CbZ group attached. The loss of one lipophilic protecting group results in a ten fold decrease in activity (**35**, $\text{IC}_{50} = 4.48\mu\text{M}$, **31**, $\text{IC}_{50} = 3.9\mu\text{M}$ and **40** $\text{IC}_{50} = 5.6\mu\text{M}$) and the loss of both lipophilic groups results in at least a further ten fold reduction in activity *in vitro* (**28**, $\text{IC}_{50} = >19.6\mu\text{M}$ and **29**, $\text{IC}_{50} = 15.4\mu\text{M}$). Interestingly, compounds **27** ($\text{IC}_{50} = >9\mu\text{M}$) which has two CbZ groups is also quite inactive *in vitro*, therefore, at least one Trt group is required for *in vitro* activity.

Overall, the addition of the second alkyl chain to the uracil acetamide compounds results in a ten fold increase in *in vitro* activity, only if the second lipophilic group is attached. The extra chain itself does not bare much effect on the activity of the compounds. A correlation between lipophilicity and anti parasitic activity can be seen. It would be reasonable to say that the presence of the Trt groups aids the transport of the compounds across the membrane of the parasite. However, as the target of these compounds is not known, the effect of the increased potency due to the extra Trt group can not be as yet attributed with certainty to membrane permeability or to a specific effect on the target within the parasite.

4.7 Biological results: Dimeric dUTPases and trypanosome parasites

The uracil acetamide compounds were also tested for anti-trypanosome activity. The inhibition of growth of *T. cruzi*, *T. brucei* and *L. donovani* was measured. For procedures see appendix 1.

Compound	<i>L. donovani axen.</i> (amastigote form) IC ₅₀ µM	<i>T. brucei rhod.</i> (blood stream trypomastigotes) IC ₅₀ µM	<i>T. cruzi</i> (blood stream trypomastigotes) IC ₅₀ µM	Toxicity (L6 cells) IC ₅₀ µM
Mono-alkyl chain derivatives				
17	19.6	8.8	42.0	53.0
18	30.9	18.4	23.5	102.2
19	29.6	1.5	29.6	42.7
2	26.5	0.5	6.4	1.1
3	26.2	0.5	2.0	8.8
8	>64	16.3	37.4	88.9
9	15.6	6.0	16.9	33.4
4	13.4	0.7	0.2	6.3
5	25.5	0.6	5.7	4.1
6	12.8	0.4	4.6	4.0
11	>124	26.9	>124	>373
Di-alkyl chain derivatives				
27	Nd	118.6	>57	>172.0
28	Nd	199.3	>117.5	>352.6
35	Nd	16.8	36.8	52.7
36	Nd	20.8	>40.6	>121.6
29	Nd	147.3	>105.9	>317.6
31	Nd	45.4	>57.1	76.7
31b	Nd	24.8	45.5	43.2
33	Nd	19.0	39.1	>117.2
40	Nd	83.2	60.2	99.5
41	Nd	18.3	Nd	21.0
42	Nd	0.3	Nd	>155.6

Table 4-4: In vitro activities of the uracil acetamide compounds against trypanosome parasites

4.7.1 Results and discussion

Compounds **2**, **3**, **4**, **5** and **6** (IC_{50} = 0.5, 0.5, 0.7, 0.6 and 0.4 μ M respectively) seem to inhibit the growth, in particular of the *T. brucei* parasite. These compounds do not contain the uracil moiety. Their selectivity over mammalian cells, however is still quite low and they are therefore most probably too generally toxic to pursue further.

The phosphate compound **42** (IC_{50} = 0.3 μ M) exhibits promising activity against the *T. brucei* parasites. As this is an unprotected phosphate, it is surprising that this compound can cross the membrane of the parasite as it would normally be charged under physiological conditions. This compound may be acting on a membrane bound protein on the parasite, its activity against the dUTPase enzyme has not yet been determined. The benzyl ester equivalent, **41** (IC_{50} = 18.3 μ M) is not significantly active, however, neither is the free hydroxyl compound **40** (IC_{50} = 83.2 μ M). Therefore, the phosphate moiety plays a significant role in the activity of this compound.

4.8 General discussion

A number of chemical properties of the uracil acetamide compounds were explored in more detail to investigate the observed activity, or lack thereof of these compounds and to attempt to ascertain a reason why these compounds may not bind in the active site of the PfdUTPase as efficiently as their acyclic counterparts.

Conformational effects

The conformational effect of the insertion of an amide bond was firstly investigated. Conformational analyses of uracil acetamide **18** and the acyclic analogue **44** were first simply carried out *in vacuo* using Moloc.¹⁰³ Moloc is a molecular modelling package obtained from Gerber Molecular Design. It uses the MAB force field to calculate descriptions of molecular geometries and energies which is modelled by the following expression:

$$E = E_b + E_v + E_r + E_p + E_{14} + E_{in} + E_{bb}$$

Where:

E_b = bond stretching energy, E_v = valence angle bending energy

E_r = dihedral angle distortion energy, E_p = pyrimidality deformation energy

$E_{14} + E_{in}$ = dispersion interaction energies, E_{bb} = hydrogen bonding energy

¹⁰³ Gerber, P. R.; Muller, K. MAB, A Generally Applicable Molecular-Force Field for Structure Modeling in Medicinal Chemistry. *J. Comput.-Aided Mol. Des.* **1995**, *9*, 251-268.

The results showed that overall, the molecules could adopt a similar conformation *in vacuo*. The uracil ring, however was turned in the opposite direction in compound **18**. This was probably due to the fact that if the conformation was as in **44**, then there is the possibility of an unfavourable interaction between the O-2 of the uracil ring and the carbonyl oxygen of the amide bond.

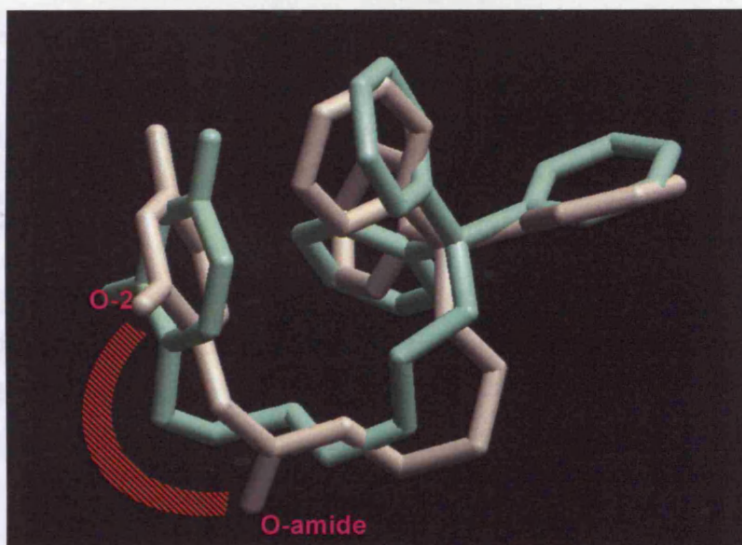
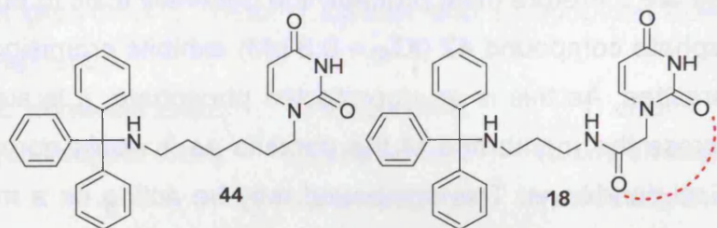


Figure 4-16: Superimposition of lowest energy conformation of compound **44** (lime) and compound **18** (pink) as calculated *in vacuo* using Moloc

Docking studies were attempted on the compounds. Previous attempts to dock compound **18** into the active site of the enzyme using the program FlexX were unsuccessful. The docking algorithm produced no results suggesting that when the protein is not flexible, the compounds do not in fact fit into the active site.

Docking studies were then attempted using the program GOLD. GOLD allows for more protein flexibility than FlexX. Uracil acetamide compound **18** and the acyclic analogue **44** were docked into the active site. The best ranked conformations according to Goldscore were visualised and superimposed in the active site using VMD 1.8.4 (Figure 4-17). Both compounds superimposed well over each other, however they did not superimpose over the crystal structure ligand. Rather, both compounds docked by GOLD in different positions in the active site to the crystal structure, rendering the results quite inconclusive as regards protein – ligand interaction.

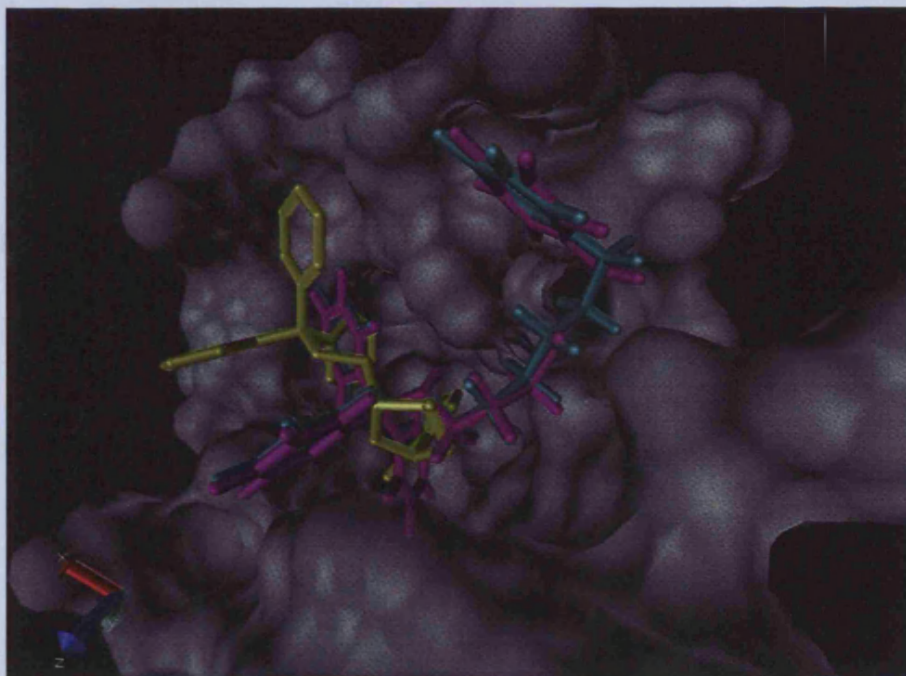


Figure 4-17: Docking of compounds **18** (purple) and **44**(cyan) into PfdUTPase active site by GOLD. Also shown is the reference molecule WSP869 (yellow)

Following the lack of success with automated docking procedures, compound **18** and **44** were placed manually into the active site of the enzyme. This was carried out using Sybyl 7.2. The uracil rings of compounds **18** and **44** were superimposed over the uracil ring of reference molecule WSP869 (Figure 2-26 and 2-25) and the active site later added. The placement of the compounds in the active site could then be visualised.

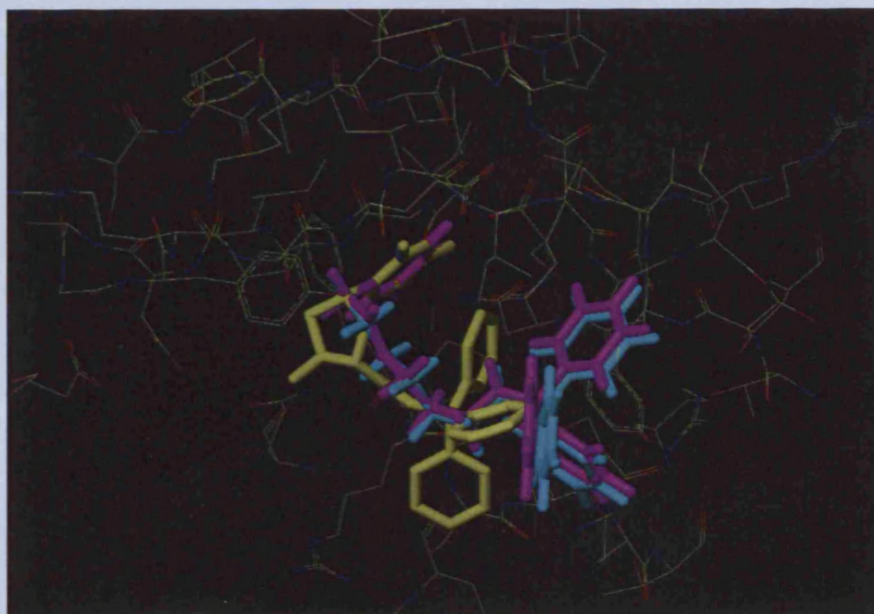


Figure 4-18: Manual docking of compounds **18** (purple) and **44** (cyan) in active site of PfdUTPase superimposed over reference molecule WSP869 (yellow)

Finally, compound **18** was minimised in the binding pocket using the MAB force field in Moloc. The purpose of this force field calculation was to investigate any large conformational change resulting from an undesired interaction between the ligand and the protein. However, no large change was observed and the compound could be visualised within the active site of the PfdUTPase in a binding mode similar to the crystal structure reference molecule.

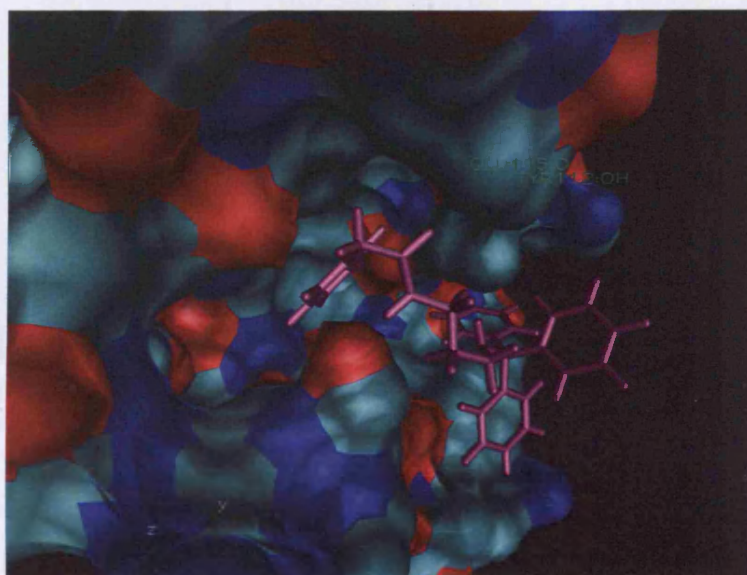


Figure 4-19: Compound **18** in active site of PfdUTPase after Moloc minimization

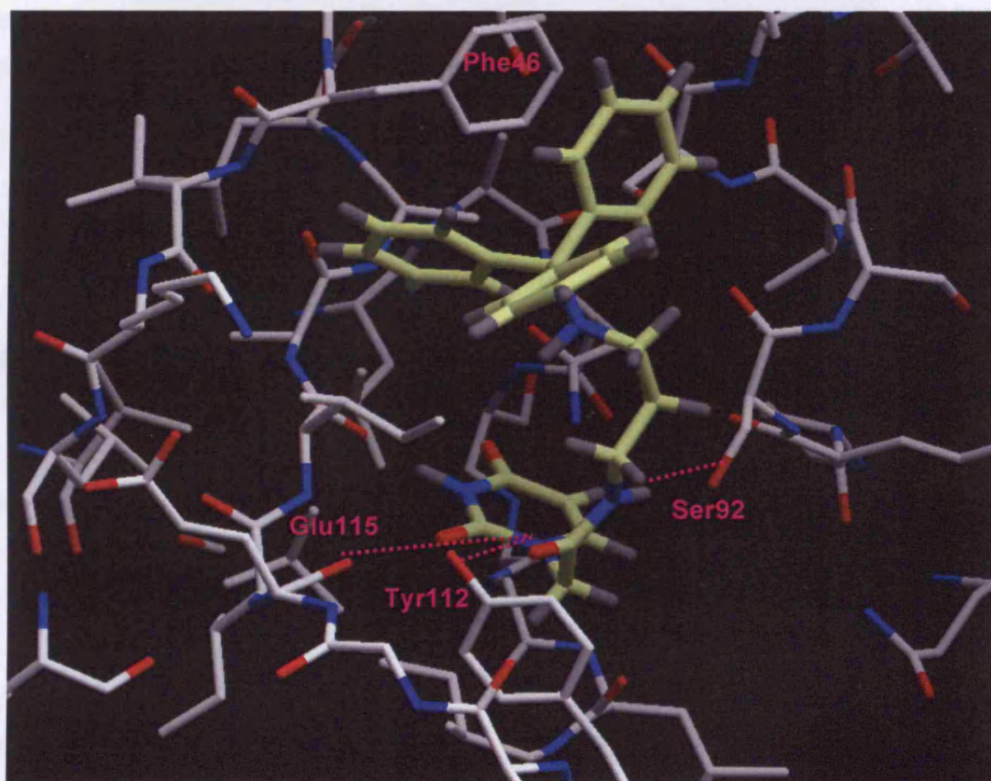


Figure 4-20: Possible interactions of compound **18** in PfdUTPase active site

When the uracil ring of compound **18** is bound in the correct pocket, the interactions that could be postulated are shown in Figure 4-20 and 4-21. It is possible that there might be some repulsive interaction between the carbonyl oxygen of the amide bond and the backbone oxygen of Glu115 or the side chain phenol of Tyr112 (Figure 4-21). The NH of the amide bond of compounds **18** was seen to lie very close to the OH of Ser92. Although there could be a hydrogen bond between the NH and OH of Ser92, there could also be a steric clash between them. The trityl moiety of the compound **18**, however, seems to be in a favourable orientation to form a π -stacking interaction with Phe46.

However, the carbonyl of the side chain and the O-2 of the uracil ring are in close proximity which may also give rise to a repulsive interaction in the bound conformation of compound **18**. This could play a factor in decreased binding of the uracil acetamide compounds. As this conformation would not be one of the low energy conformations of the molecule in solution, the compounds would have to overcome an energy barrier to adopt it and this may be one reason for their low affinity for the enzyme. In fact, the energy difference between the two conformations as calculated using the Tripos force field is 7.5kcal/mol.

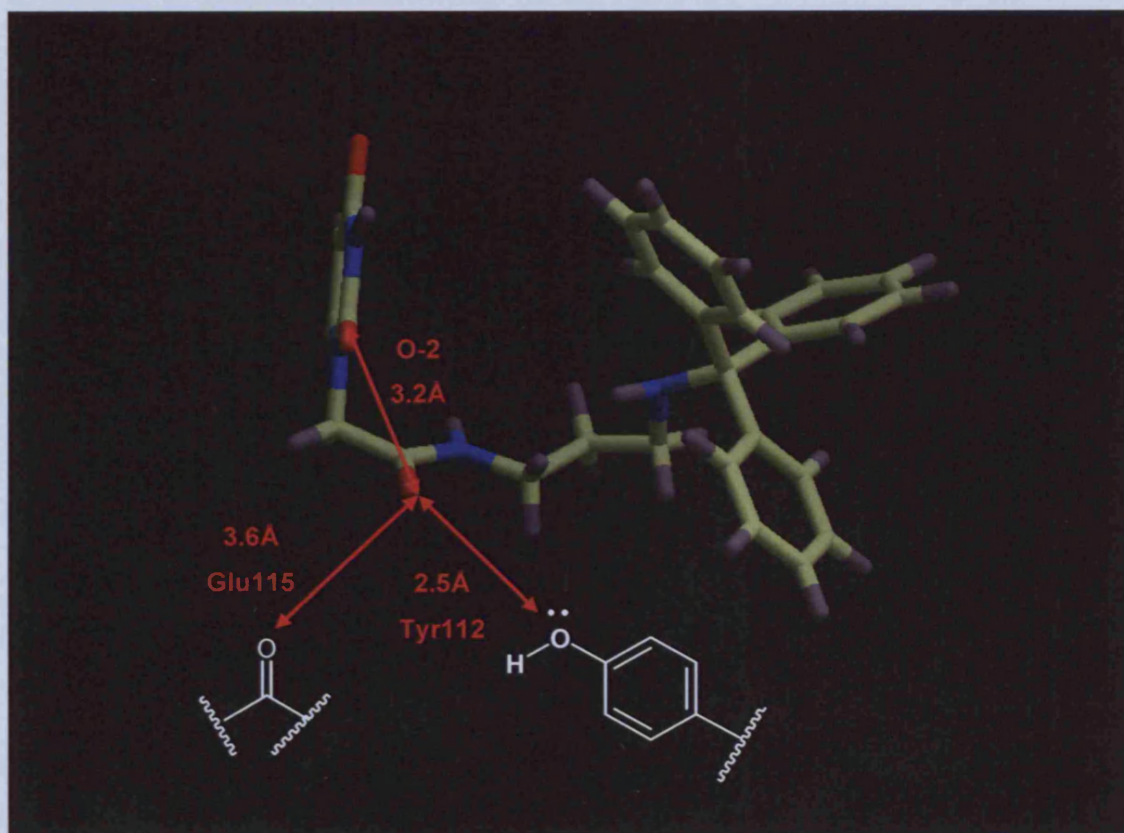


Figure 4-21: Possible repulsive interactions to the carbonyl oxygen of the amide bond on uracil acetamide compounds in the PfdUTPase active site

pKa calculations

Using ACD labs 7.0 /pK_aDB, the pK_a values of some of the compounds were evaluated and compared to that of the analogues in which the amide bond was absent. The most noticeable change was the pK_b of the N-3 of the uracil ring which was reduced from approximately 9.2 to 8.5. Although, the localised dielectric constant of the active site of the protein is not known, it can be estimated this difference would lead to a ten fold increase in the concentration of the deionised species of the uracil acetamides over the aliphatic derivatives. It has been shown in the crystal structure of the PfdUTPase that the N-3 of the uracil ring hydrogen bonds to the main chain CO of Ile117 and that this is an important interaction for maintaining selectivity over cytosine in which the N-3 is not a HBD. The presence of the deionised species would therefore result in an unfavourable electrostatic interaction with this residue and therefore result in decreased binding affinity. The presence of the electron withdrawing amide bond, or most probably any electron withdrawing group next to the N-1 of the uracil ring could therefore apparently be unfavourable as it reduces the pK_b of the N-3 by electron delocalisation, though it is unlikely that this is the main contributing factor to the loss in activity of the uracil acetamides.

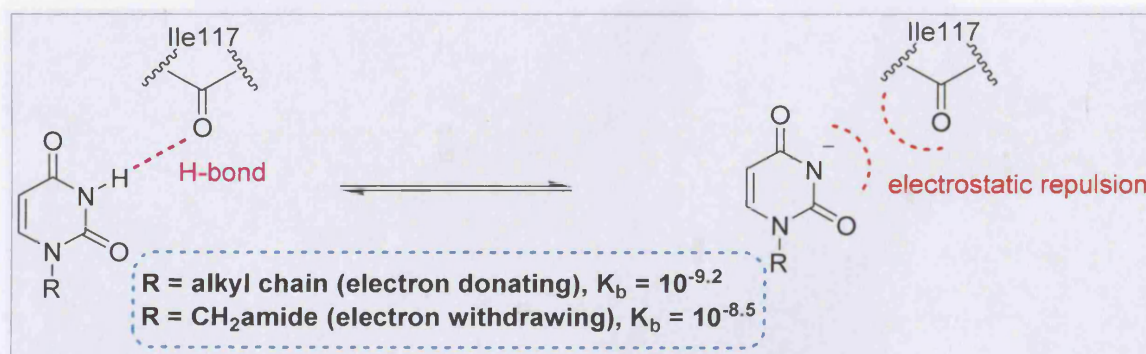


Figure 4-22: pK_b of N-3 of the uracil ring and effect of electron donating or electron withdrawing group to the N-1 position

LogD calculations

The logD values of some of the uracil acetamide compounds were calculated using ACD labs 7.0/logD software and in the case of the single chain derivatives were compared to their aliphatic analogues. The results are shown in Table 4.5. for the mono chain derivatives, the LogD values are decreased quite significantly compared to the aliphatic chain derivatives. For general drug design, this is advantageous as drug-like molecules should generally have a LogD value of less than 5 to aid their oral bioavailability.¹⁰⁴

The LogD values of the di-alkyl chain derivatives **33** and **34**, however are quite high, due to the presence of the two large lipophilic trityl groups. Although the LogD values do not seem to correlate with enzyme inhibition, there seems to be a relationship between lipophilicity and inhibition of parasite growth. This could be due to increased membrane permeability of the compounds. Once inside the cell, however, the mechanism by which the compounds exert their activity is not yet known.

Compounds (aliphatic analogues)	K _i (μM)	IC ₅₀ (μM)	LogD calculated at pH7
17	37.3	4.2	2.89
(43)	(4.3)	(2.2)	(4.28)
18	23.1	2.5	3.10
(44)	(1.8)	(1.1)	(4.78)
8	>1mM	4.6	1.33
(45)	(8.7)	(3.9)	(2.96)
33	>1mM	0.3	8.67
36	>1mM	0.4	9.57

Table 4-5: Calculated LogD values for selected compounds at pH7

¹⁰⁴ Lipinski, C. A.; Lombardo, F.; Dominy, B. W.; Feeney, P. J. Experimental and computational approaches to estimate solubility and permeability in drug discovery and development settings. *Advanced Drug Delivery Reviews* **1997**, 23, 3-25.

4.9 Conclusions

In this part of the project, series of mono alkyl chain and dialkyl chain tritylamino and hydroxyl derivatised uracil acetamides were successfully synthesised. Difficulties included selective protection and deprotection of hydroxyl functions over amines and of primary amines over secondary amines, effective amide bond formation and elucidation of unexpected structures.

The biological assays of these uracil acetamide compounds show that these compounds are not potent inhibitors of the dUTPase enzymes. Therefore, introduction of an amide bond at the β -C to the N-1 of the uracil ring results in a loss of activity against the PfdUTPase enzyme. This may be due to the energy barrier which the low energy conformation of the uracil acetamide compounds must overcome to adopt the required binding conformation. It has also been shown that the introduction of an electron withdrawing group at the N-1 position of the uracil ring has the effect of lowering the pK_b of the N-3 which also may reduce the ability of these compounds to bind in the active site of the PfdUTPase.

The uracil acetamide compounds, however, retain good activity *in vitro*. Their mode of action has not yet been ascertained, however, there does seem to be a correlation between lipophilicity and anti-plasmodial activity.

5 Acyclic uridine analogues

5.1 Acyclic uridine analogues

The elucidation of the crystal structure of the PfdUTPase enzyme with a previously synthesised novel inhibitor bound in the active site was published in 2005.⁵⁷ This provided a foundation for the use of structure based design approaches to the design of inhibitors of the PfdUTPase enzyme. Previously, inhibitor design was mainly analogue based. The use of the program GRID¹⁰⁵ to probe for interactions in the PfdUTPase active site was therefore employed. Potential inhibitors were then docked and modelled in the active site using FlexX and subsequently synthesised if possible.

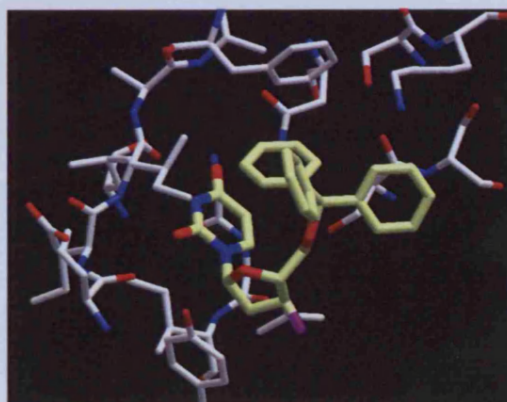
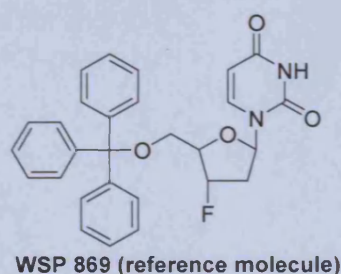


Figure 5-1: Previously synthesised inhibitor WSP869 in the active site of the PfdUTPase

WSP869 was a uridine analogue, however, acyclic nucleoside analogues, previously synthesised by the group also showed good and selective inhibition of the PfdUTPase enzyme.⁷⁵ The preliminary scaffold for the set of uridine analogues discussed in this chapter was based upon these acyclic nucleoside analogues.

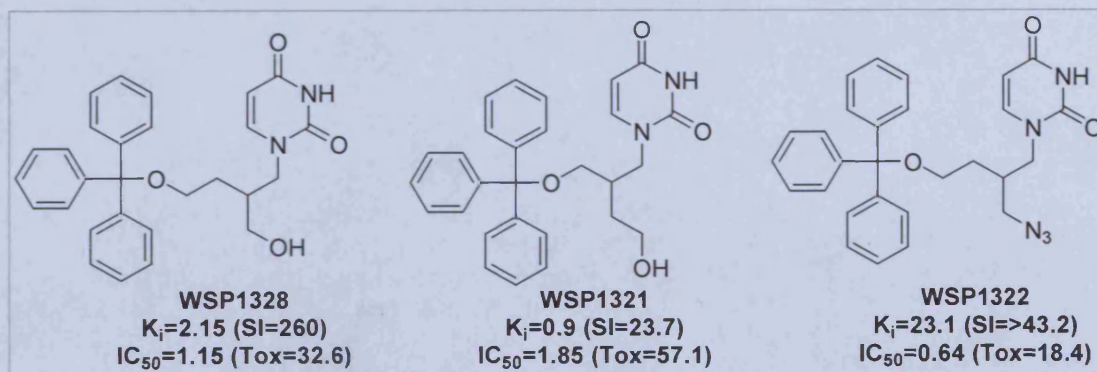


Figure 5-2: Some of the previously synthesised acyclic PfdUTPase inhibitors

5.2 GRID calculations on *P. falciparum* dUTPase enzyme

The program GRID is a computational procedure for determining energetically favourable binding sites on molecules of known structure.¹⁰⁵ GRID has been applied to structure based design¹⁰⁶ and has also been used to understand structural differences relating to enzyme selectivity.¹⁰⁷

GRID computes the interaction of a probe or probes with a protein of known structure at sample positions throughout and around the macromolecule, giving an array of energy values. Energetically favourable binding sites for each probe are shown by contours mapped on to the surface of the protein.

For the purpose of this study, GRID was used to probe the active site of the *P. falciparum* dUTPase enzyme for energetically favourable interactions. Docking of the previously synthesised inhibitor WSP1328 (Figure 5-2) and subsequent superimposition of this molecule into the GRID calculated structure, revealed several interesting implications. This then allowed for determination of some possible advantageous modifications that could be made to the previously synthesised acyclic inhibitors. These modifications would then generate new lead compounds that would, hopefully, have increased activity against the enzyme by interacting with the GRID proposed energetically favourable binding sites.

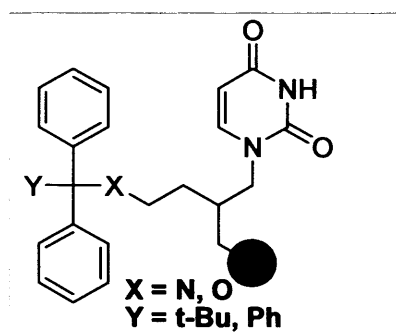


Figure 5-3: Proposed modified inhibitors (X = N, O)

¹⁰⁵ Goodford, P. J. A Computational-Procedure for Determining Energetically Favorable Binding-Sites on Biologically Important Macromolecules. *J. Med. Chem.* **1985**, *28*, 849-857.

¹⁰⁶ von Itzstein, M.; Wu, W. Y.; Kok, G. B.; Pegg, M. S.; Dyason, J. C.; Jin, B.; Phan, T. V.; Smythe, M. L.; White, H. F.; Oliver, S. W.; Colman, P. M.; Varghese, J. N.; Ryan, D. M.; Woods, J. M.; Bethell, R. C.; Hotham, V. J.; Cameron, J. M.; Penn, C. R. Rational Design of Potent Sialidase-Based Inhibitors of Influenza-Virus Replication. *Nature* **1993**, *363*, 418-423.

¹⁰⁷ Kastenzholz, M. A.; Pastor, M.; Cruciani, G.; Haaksma, E. E. J.; Fox, T. GRID/CPCA: A new computational tool to design selective ligands. *J. Med. Chem.* **2000**, *43*, 3033-3044.

The PDB file was loaded and the area over which the calculations were to be carried out was defined manually. This is possible in GRID by using the 'grid box' or 'cage' which is an interactive 3D cube that can be visualised in Gview and toggled around the area in which the calculations are to take place.

Several single atom and multi atom probes (Table 5-1) were used and their subsequent binding pockets shown at a given energy level.

Probe name	Description	Energy (kcal)	Probe name	Description	Energy (kcal)
C3	Methyl CH ₃	-2.47	N:	sp ³ N with lone pair	-5.93
N:#	sp N with lone pair	-7.49	N:=	sp ² N with lone pair	-7.90
N1	Neutral flat NH e.g. amide	-6.66	N1+	sp ³ amine NH cation	-7.49
N1:	sp ³ NH with lone pair	-7.49	NH=	sp ² NH with lone pair	-7.90
N2	Neutral flat NH ₂ e.g. amide	-7.93	N1=	sp ² amine NH cation	-7.90
N2=	sp ² amine NH ₂ cation	-7.93	N2:	sp ³ NH ₂ with lone pair	-6.15
O1	Alkyl hydroxy OH	-5.40	OH	Phenyl or carboxy OH	-5.42
O-	sp ² phenolate oxygen	-4.08	O	sp ² carbonyl oxygen	-4.01
O::	sp ² carboxy oxygen atom	-4.36	O=	O of sulphate or sulphonamide	-3.93
OES	sp ³ ester oxygen atom	-1.33	OC2	Ether or furan oxygen	-2.61
OS	O of sulphone or sulphoxide	-4.50	ON	Oxygen of nitro group	-4.50
PO4H	PO ₄ H phosphate anion	-6.77	S1	Neutral SH group	-5.53
F	Organic fluorine atom	-2.45	Cl	Organic chlorine atom	-3.80
Br	Organic bromine atom	-5.13	I	Organic iodine atom	-6.63
BOTH	The amphipathic probe	-0.39	DRY	The hydrophobic probe	-0.50
COO-	Aliphatic anionic carboxy group	-7.88	AR.COO-	Aromatic anionic carboxy group	-7.12
CONH2	Aliphatic neutral amide group	-7.53	AR.CONH2	Aromatic neutral amide group	-7.30
CONHR	Aliphatic neutral amide group	-7.75	AR.CONHR	Aromatic neutral amide group	-7.30
AMIDINE	Aliphatic cationic amidine group	-10.0	AR.AMIDINE	Aromatic cationic amidine group	-10.08

Table 5-1: Tables of probes used and their equivalent symbols and energies at which contours were shown

Nitrogen probes

In the case of the amino probes, where the nitrogen could potentially act as a hydrogen bond acceptor (HBA) and a hydrogen bond donor (HBD) such as in Figure 5-4, a large contour of binding potential could be seen where the end of the branch chain would be thought to sit.

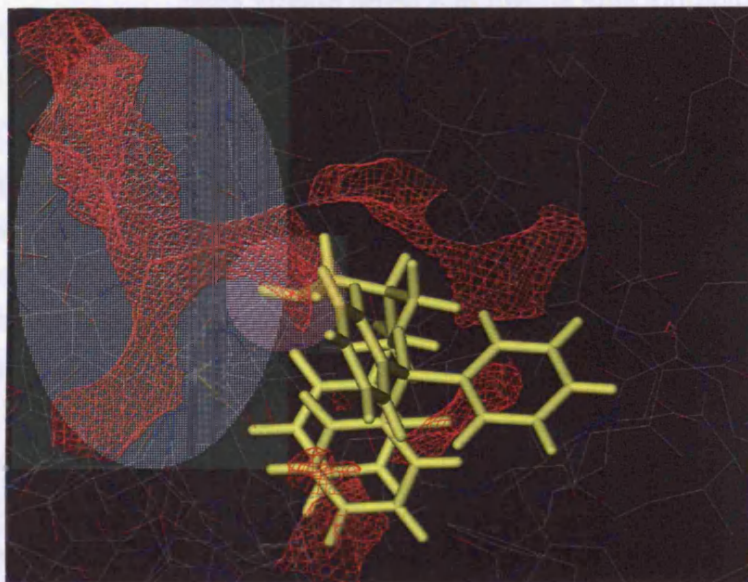


Figure 5-4: GRID calculations for N1: probe at an energy of -7.5kcal. (Side chain highlighted in pink bubble and interaction area highlighted in blue bubble)

This was also true for amino probes in which the nitrogen could potentially act as only a hydrogen bond donor as shown in Figure 5-5.

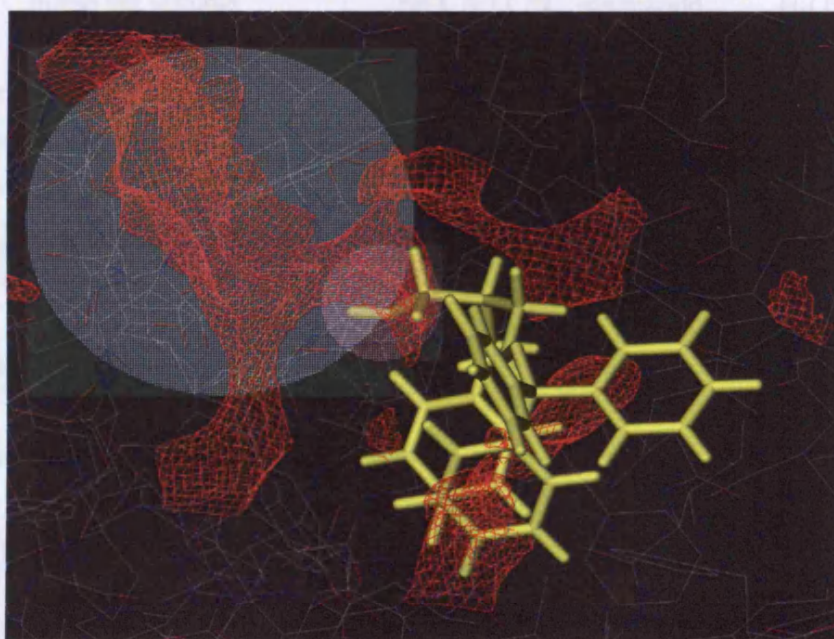


Figure 5-5: GRID calculations for N1= probe at an energy of -7.9kcal. (Side chain highlighted in pink bubble and interaction area highlighted in blue bubble)

However, when the nitrogen of the amino probe had a lone pair but no hydrogen, i.e could potentially act solely as a hydrogen bond acceptor and not as a donor, the same contour could be seen but was greatly reduced in surface area and energy.

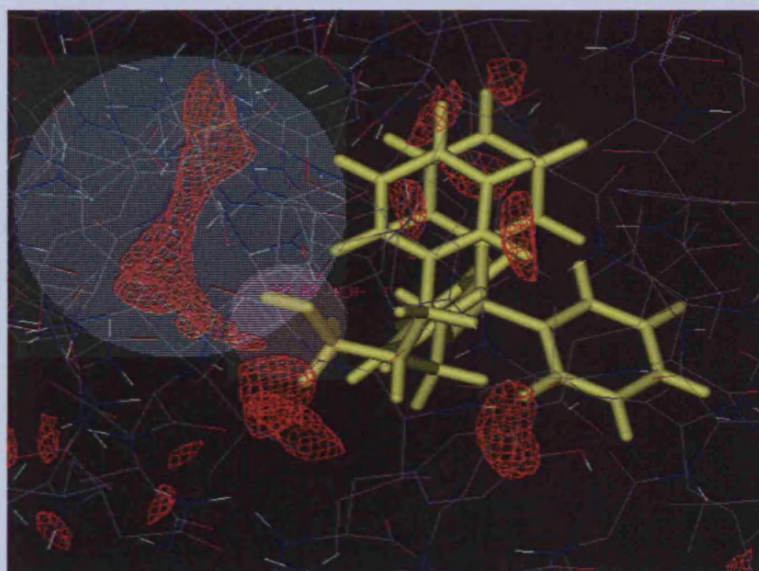


Figure 5-6: GRID calculations for N: probe at an energy of -5.9kcal. (Side chain highlighted in pink bubble and interaction area highlighted in blue bubble)

The assumption could therefore be made that an amino group that could act as a hydrogen bond donor, such as a primary or secondary amine or amide, at the end of the branch chain could lead to possible interactions between the molecule and active site. The larger, multi-atom amidine probes also seemed to bind in this region favourably and therefore would also be well tolerated.

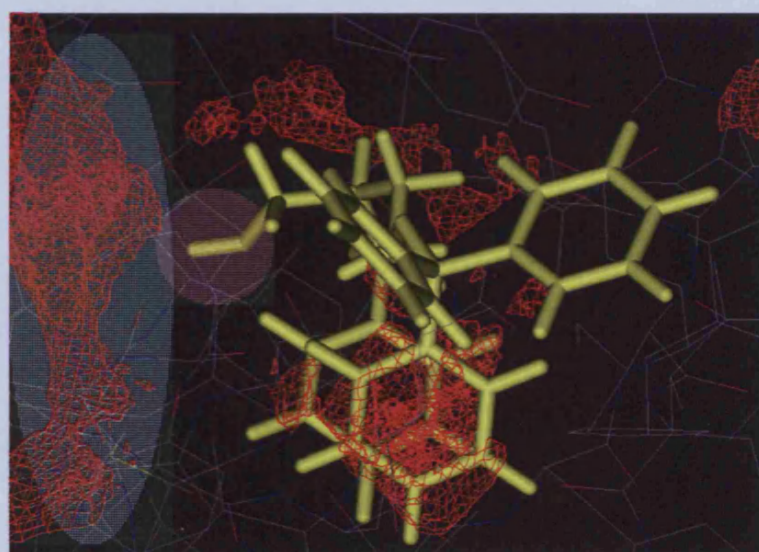


Figure 5-7: GRID calculations for the AMIDINE probe at an energy of -10.0kcal. (Side chain highlighted in pink bubble and interaction area highlighted in blue bubble)

Oxygen probes

The carbonyl oxygen probes showed a banana shape favourable binding contour approximately 2.0 Å distance from C-10 and C-11 of the inhibitor.

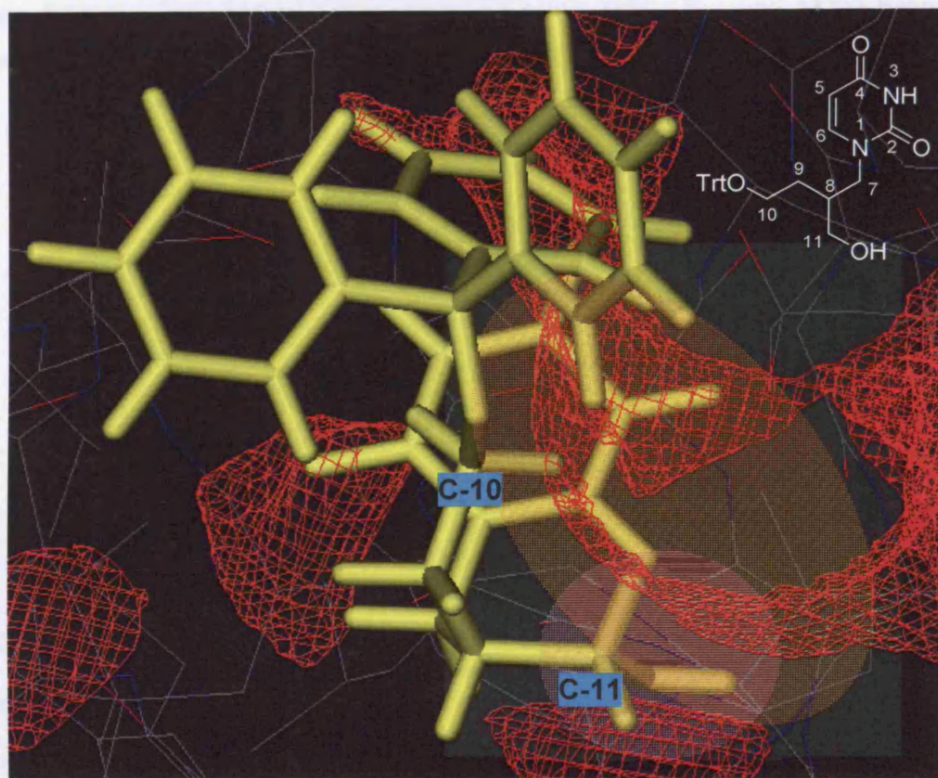


Figure 5-8: GRIND calculations for O probe at an energy of -4.01kcal. (Side chain highlighted in pink bubble and interaction area highlighted in orange bubble)

This is due to the presence of the Ser92 residue of the protein, whose side chain could act as a HBD. These results would suggest that the presence of a carbonyl oxygen that could act as a HBA on either C-10 or C-11 of WSP1328 would lead to an extra hydrogen bond within the active site providing the conformation of the molecule would not change significantly with this modification.

Other probes

Other calculations were also carried such as halogen atoms, amphipathic, hydrophobic, phosphate groups and multi atom probes. SH probes (Figure 5-9) and other HBD donating probes showed similar results to those of the amino probes. The phosphate probes showed a large contour in what would normally be the phosphate binding region of the active site (Figure 5-10) and the hydrophobic probes showed a contour around where the trityl moiety of the inhibitors are thought to bind (Figure 5-11). The halogen probes showed that it could be possible to replace some of the hydrogens on the molecule if necessary (Figure 5-12) and the multi atom probes suggested that quite a large group could be tolerated at G (Figure 5-14).

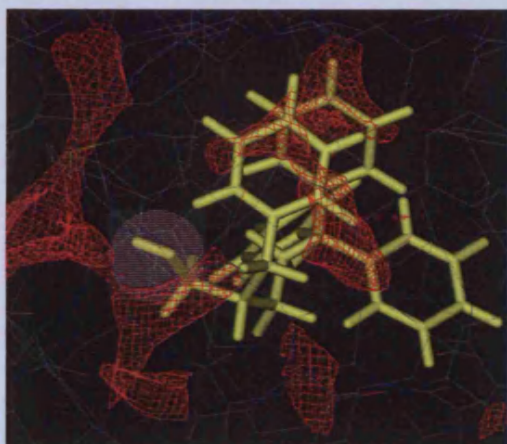


Figure 5-9: SH probe energy -5.5kcal

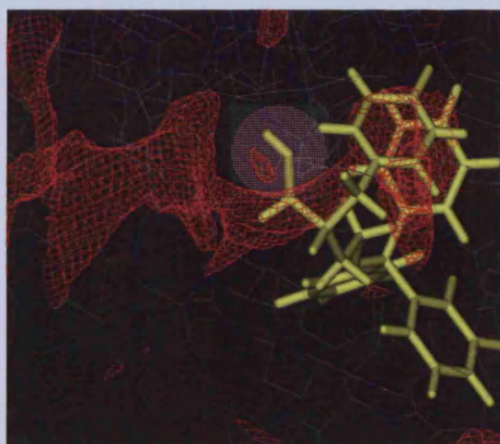


Figure 5-10: PO4H probe energy -6.8kcal

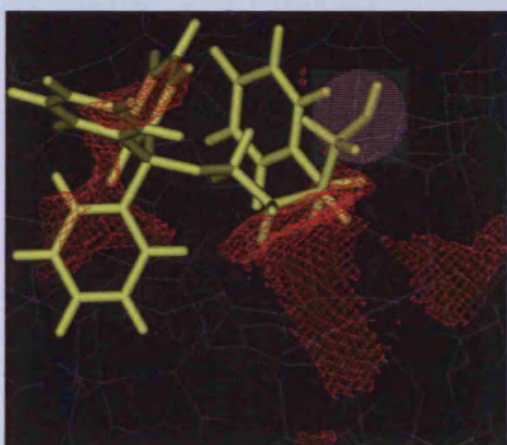


Figure 5-11: DRY probe energy -0.5kcal

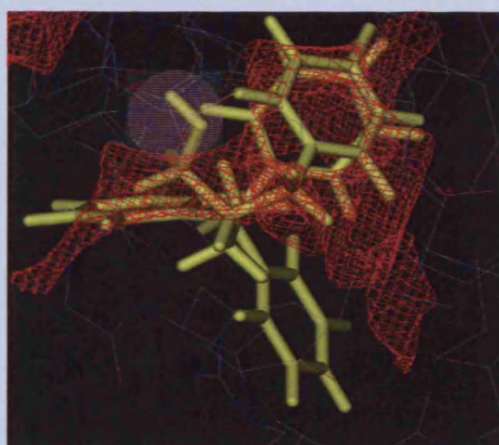


Figure 5-12: Cl probe energy -3.8kcal

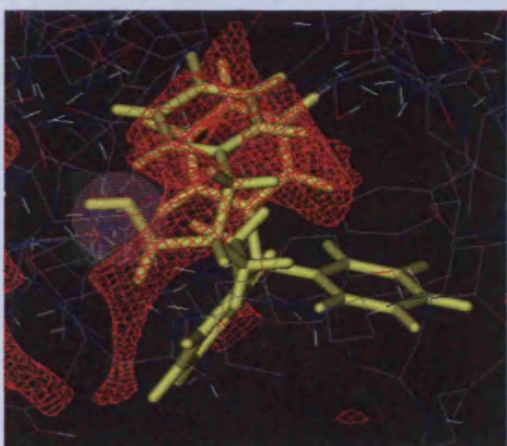


Figure 5-13: C3 probe energy -2.5kcal

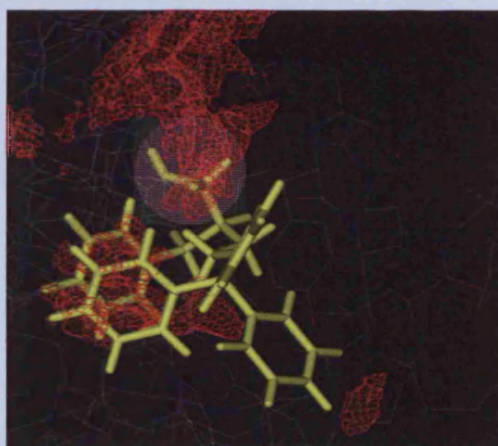


Figure 5-14: CONHR probe energy -7.8kcal

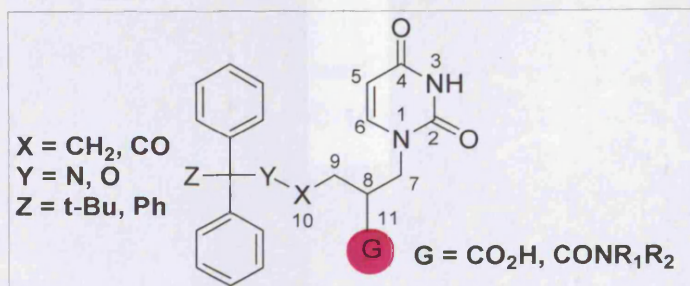


Figure 5-15: Proposed modified compounds

In summary, the main points noted from The GRID calculations are as follows:

- 1 A carbonyl oxygen attached to position 10 or 11 in the molecules could hydrogen bond to the side chain of Ser92 in the active site and therefore would have a favourable interaction.
- 2 The modified group G (Figure 5-15) should retain good hydrogen bond donating ability. This is probably due to Asp109 whose negatively charged side chain could act as a hydrogen bond acceptor. There does not seem to be great restriction on the size of G, however, the molecules are already of high molecular weight, therefore a small substitution such as an amine, amide or amidine would be ideal.
- 3 The molecules are currently synthesised as a mixture of enantiomers. Of the two enantiomers, however, the *S* may be more active. This is due to the presence of Tyr 112 which is 3.8 Å from the chiral carbon and may sterically hinder the side chain of the *R* enantiomer from sitting in the active site.

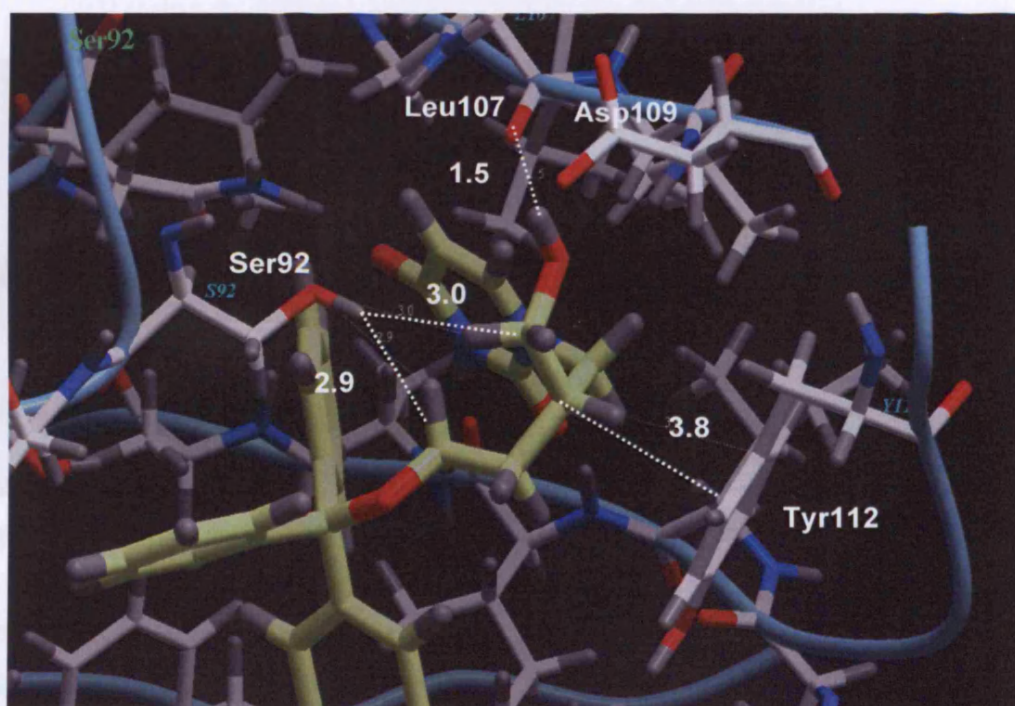


Figure 5-16: Summary of GRID calculations

5.3 Docking of proposed compounds into PfdUTPase

Some compounds with the general structure of the proposed compounds shown in Figure 5-15 were docked into the active site of the PfdUTPase using FlexX. FlexX is a docking program that takes into account the flexibility for the ligand but not that of the molecule¹⁰⁸ and is described in more detail in Chapter 6.

The compounds shown in Figure 5-17 were drawn and minimised using Sybyl 6.9.1. The active site of the protein was defined as being 8Å around the reference molecule (inhibitor bound in crystal structure PDB entry 1VYQ) and the compounds were docked using FlexX.

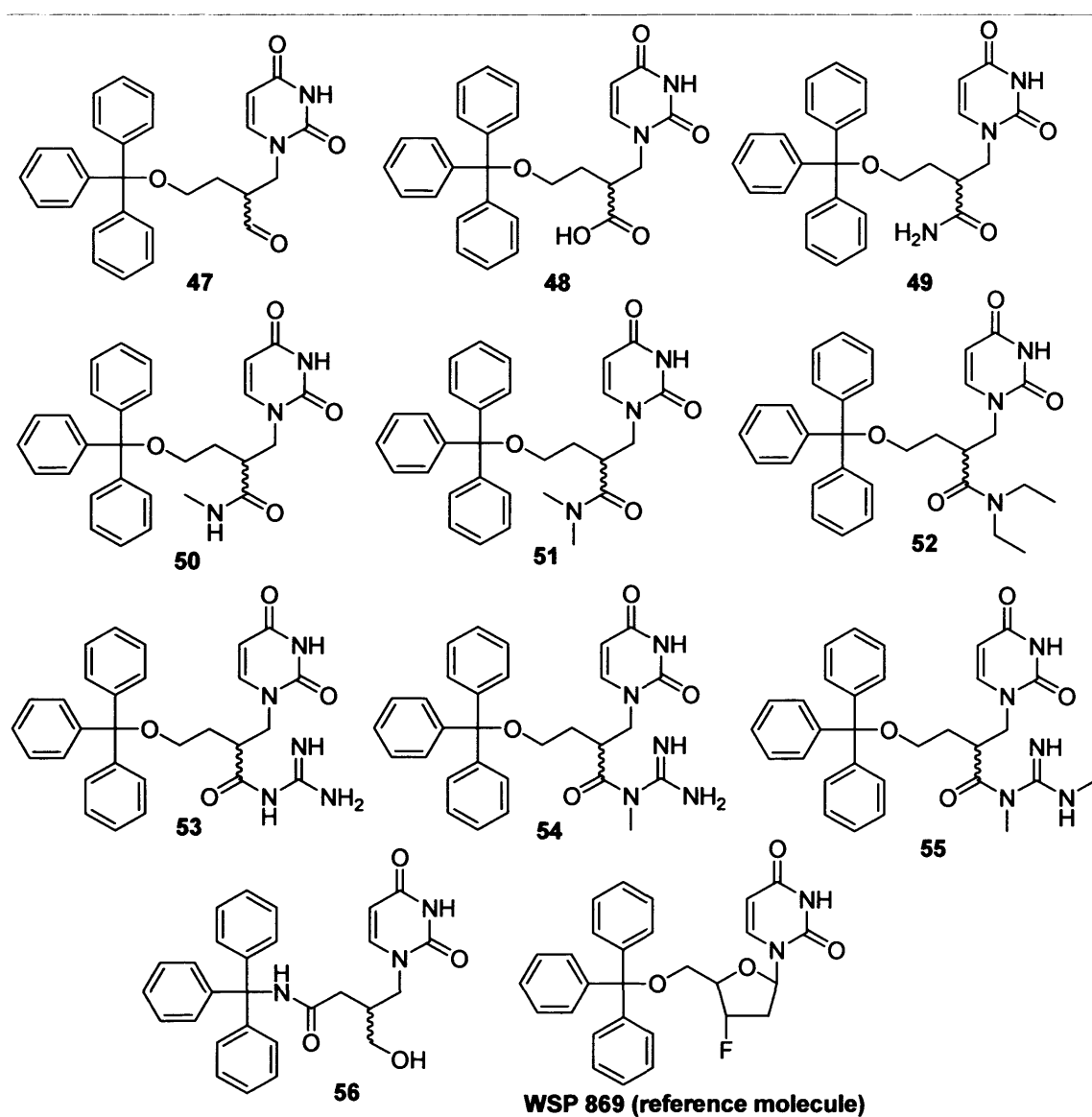


Figure 5-17: Branched acyclic derivatives which were docked into the active site of PfdUTPase

¹⁰⁸ Rarey, M.; Kramer, B.; Lengauer, T.; Klebe, G. A Fast Flexible Docking Method using an Incremental Construction Algorithm. *J. Mol. Biol.* **1996**, *261*, 470-489.

The results for each compound docked were listed in order of increasing energy which was calculated by FlexX as described in Chapter 6.

Compound	Number of conformations generated		Energy of highest scoring conformation (kcal mol ⁻¹)	
	S	R	S	R
47	30	No solution	- 59	No solution
48	30	8	- 62	- 58
49	30	21	- 59	- 58
50	30	23	- 62	- 61
51	24	30	- 54	- 54
52	27	1	- 57	- 38
53	30	25	- 65	- 70
54	30	23	- 65	- 54
55	4	4	- 75	- 62
56	30	30	- 60	- 55

Table 5-2: Results of compounds 47-56 docked into the active site of the PfdUTPase

The best results were superimposed in the active site of the molecule using Visual Molecular Dynamics (VMD) 1.8.4 software (Figure 5-18).

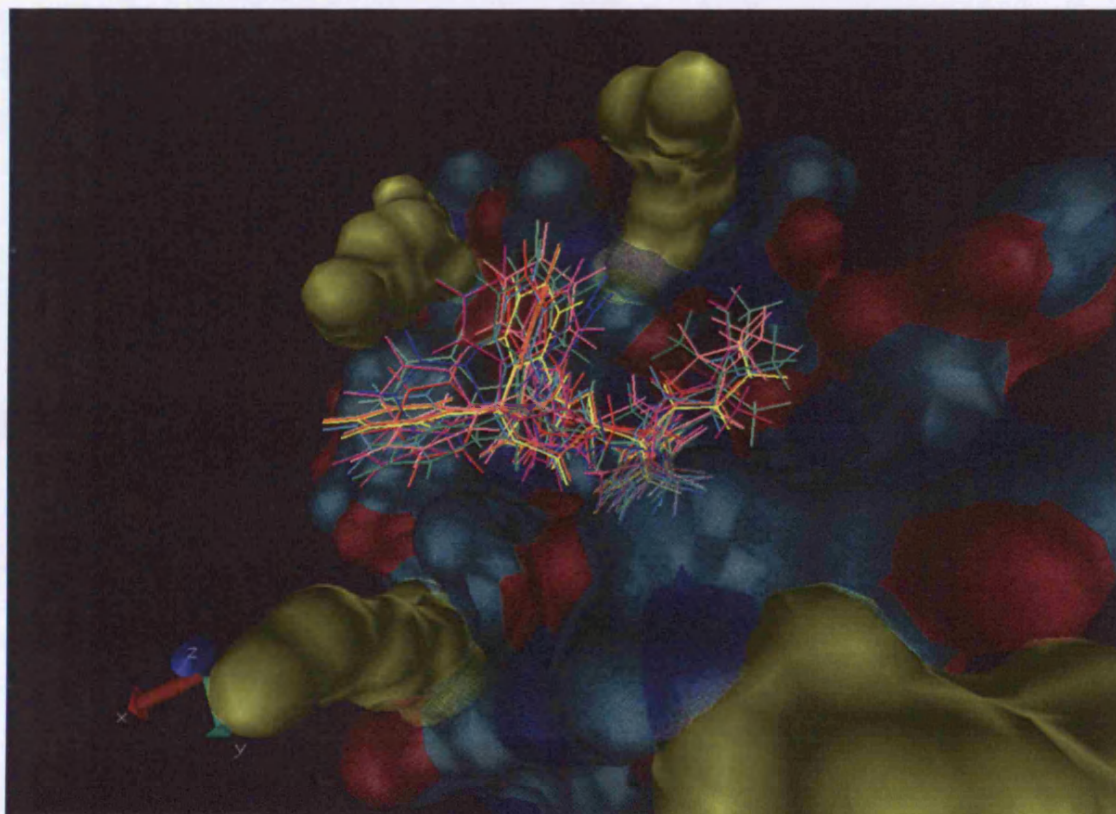


Figure 5-18: Compounds 47 (blue), 48 (red), 49 (orange), 50 (yellow), 51 (green), 52 (pink), 53 (cyan), 54 (purple), 55 (lime), 56 (mauve). All are shown in S configuration

The *R* and *S* enantiomers of each compound were drawn, minimised and docked separately in order to investigate the effect of the stereochemistry of the compounds. In agreement with the GRID calculations, the *S* enantiomers docked much more successfully and with better superimposition over the reference molecules than the *R* enantiomers. For compound **47**, the *R* enantiomer did not dock at all. In compounds **48** – **55** the Trt moiety of the *R* enantiomer is displaced. The amide functionality superimposes over the sugar and alkyl chain of the reference molecule and the Trt moiety moves towards the phosphate binding region of the active site. (Figure 5-19 – 5-21) in the *R* enantiomer solutions.

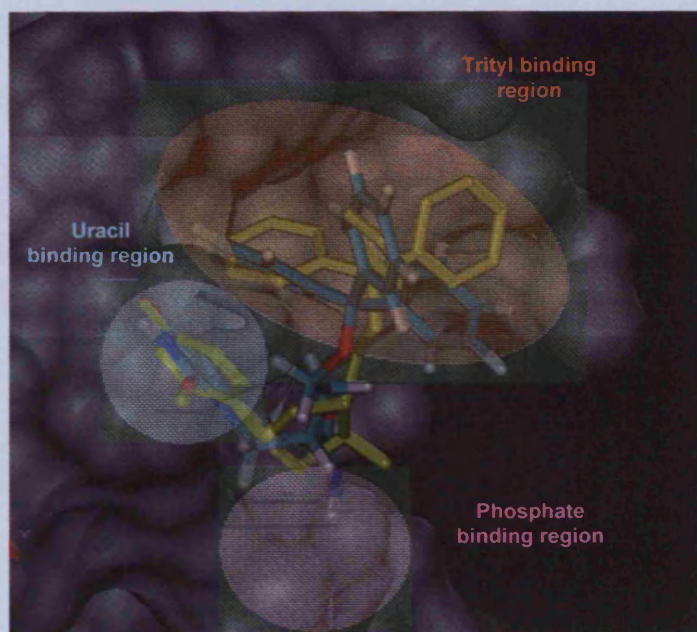


Figure 5-19: *S* enantiomer of **49** and reference molecule (yellow) in the PfdUTPase active site

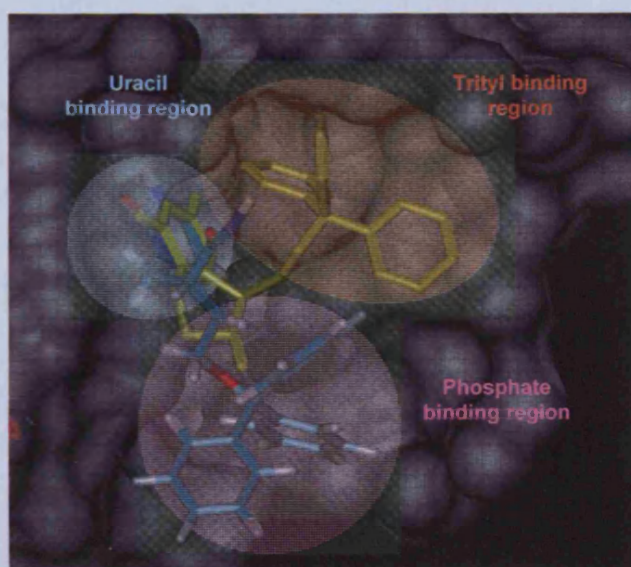


Figure 5-20: *R* enantiomer of **49** and reference molecule (yellow) in the PfdUTPase active site

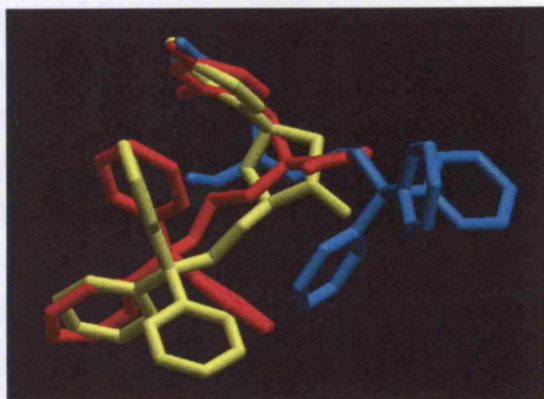


Figure 5-21: *R* - **49** (blue), *S* - **49** (red) and reference molecule wsp 869 (yellow) superimposed using Molsoft ICM-Browser-pro

The size of the substituents at position 11 (G in Figure 5-15) also effects the way in which the compounds dock into the active site. All of the conformations generated from compounds **47** and **48** and more than half of the conformations generated from compounds **49**, **50** and **51** dock with good superimposition over the reference molecule and in the correct orientation in the active site. As the substituents get larger, however, trityl displacement becomes more common. For compounds **52** and **54**, only two of the conformations dock with the correct orientation, for compound **53**, only four of the conformations dock in the correct orientation and for compound **55**, only one of the four generated conformations dock in the correct orientation. In all of the remaining conformations, one, two or all of the phenyl rings of the trityl moiety are displaced to accommodate the bulky substituents present. Therefore, when $G = \text{CONHR}_1\text{R}_2$, R_1 and $\text{R}_2 = \text{H}$ or Me is well tolerated (Figure 5-22), R_1 and $\text{R}_2 = \text{Et}$, amidine or Me -amidine is reasonably tolerated (Figure 5-23) and R_1 and $\text{R}_2 = \text{di-Me-amidine}$ is poorly tolerated (Figure 5-24).

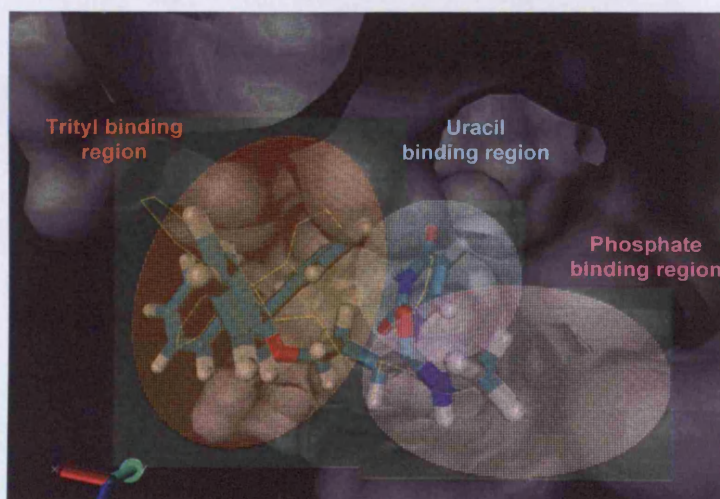


Figure 5-22: Compound **50** in active site. $\text{R}_1 = \text{H}$, $\text{R}_2 = \text{Me}$. G well tolerated. 30 conformations generated. Ref. molecule shown in yellow

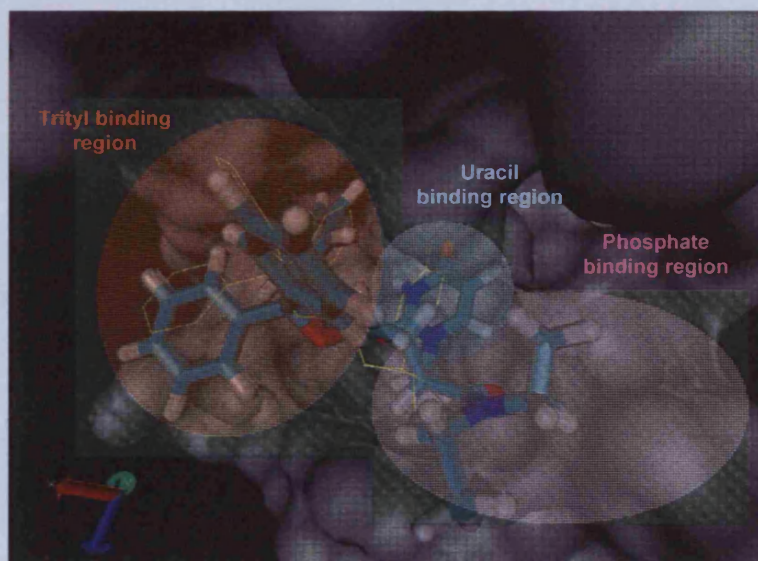


Figure 5-23: Compound **52** in active site. $R_1 = R_2 = \text{Et}$. G reasonably tolerated. Uracil ring slightly displaced, 27 conformations generated. Ref. molecule shown in yellow.

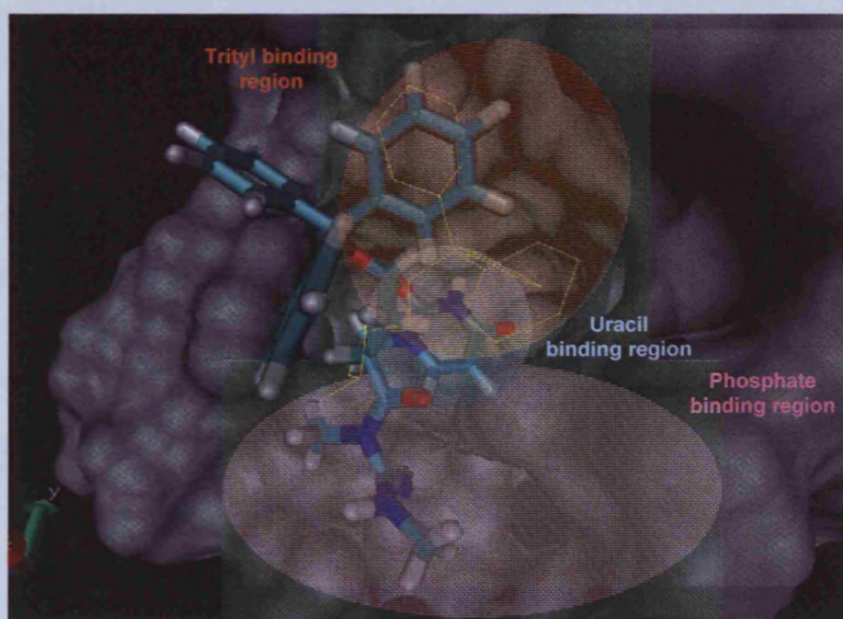


Figure 5-24: Compound **55** in active site. G = di-methylamidine. G not well tolerated. Trityl displaced and only 4 conformations generated. Ref. molecule shown in yellow

Compound **56**, in which there is a Trt-amide moiety, also docks with good superimposition into the active site and therefore this modification may be well tolerated within this group of compounds. The carbonyl oxygen points toward Ser 92, the residue with which it might form a hydrogen bond (Figure 5-25).

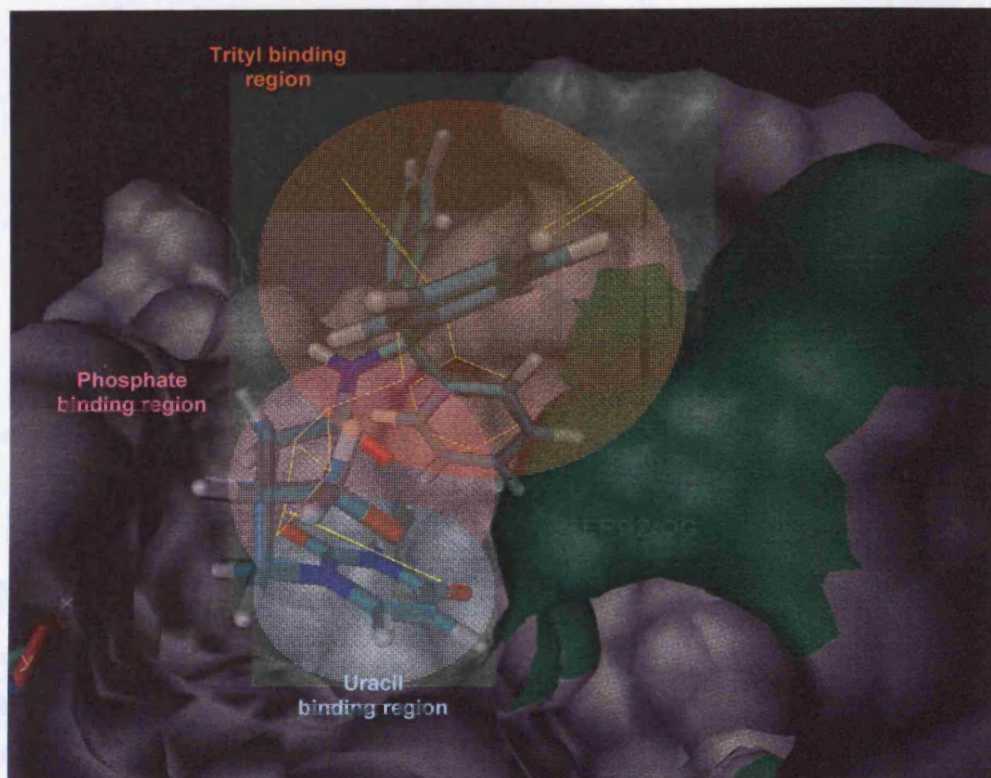


Figure 5-25: Compound **56** and reference molecule (yellow) in PfdUTPase active site Ser 92 shown in green

5.4 Modifications at position 11

The synthesis of these compounds started from the branched, acyclic uridine analogues **57** and **72** kindly provided by our partner, Medivir. As it was previously shown that compounds containing the TBDPS group were equipotent against the enzyme as compounds with the Trt moiety, compound **57** was used to synthesise TBDPSO derivatives. TrtNH derivatives were synthesised from intermediate **72**.

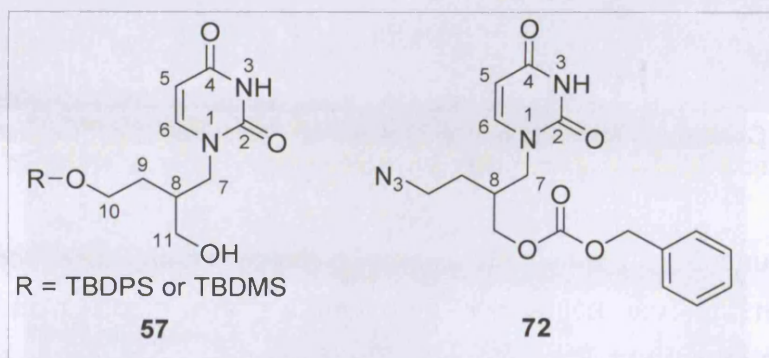
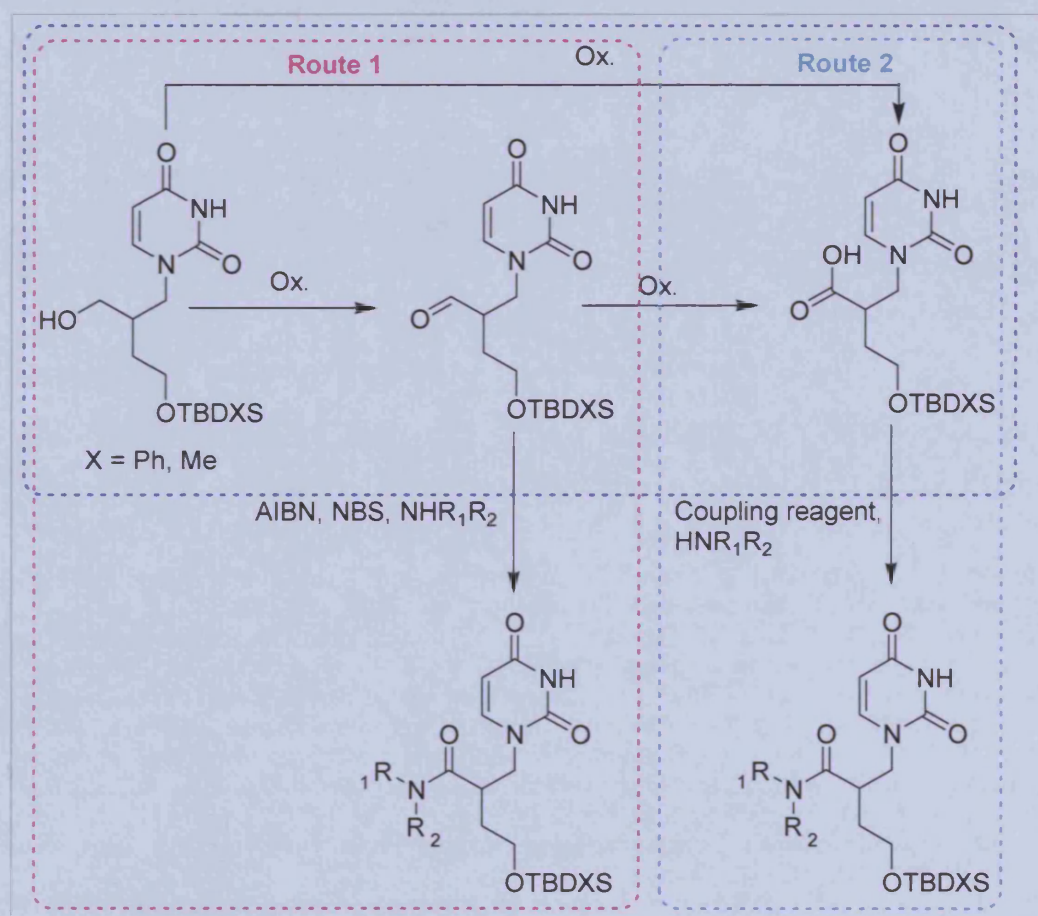


Figure 5-26: Intermediates **57** and **72** provided by Medivir

5.4.1 TBDPS-O derivatives

The overall synthetic strategy for the TBDPS-O derivatives is shown in Scheme 5-1. The first step required the oxidation of **57** to an acid, either through a two step oxidation *via* the aldehyde or by direct oxidation to the acid. Subsequent amide formation could then be achieved using suitable coupling reagents. Alternatively, oxidative amidation of aldehydes by a radical mechanism involving N-bromosuccinimide (NBS) and azobisisobutyronitrile (AIBN) as a radical initiator to form amides directly has also been documented.^{109, 110} This methodology was also investigated.



Scheme 5-1: Synthetic strategies for the synthesis of the branched TBDPS-O derivatives

¹⁰⁹ Markó, I. E.; Mekhalfia, A. Radical Mediated Oxidations in Organic-Chemistry .3. An Efficient and Versatile Transformation of Aldehydes into Amides. *Tetrahedron Lett.* **1990**, *31*, 7237-7240.

¹¹⁰ Fan, C. A.; Tu, Y. Q.; Song, Z. L.; Zhang, E.; Shi, L.; Wang, M.; Wang, B. M.; Zhang, S. Y. An efficient total synthesis of (+/-)-lycoramine. *Org. Lett.* **2004**, *6*, 4691-4694.

5.4.1.1 Oxidation of the primary alcohol at position 11

Various methods of oxidation of intermediate **57** to either the aldehyde or the acid (Scheme 5-2) were attempted as shown in Table 5-3. The oxidation procedure was not trivial and problems were encountered with many of the standard oxidation procedures as described below.

Method	Desired product	Result
PDC/DMF ^{111, 112}	Acid	Bromocresol green staining showed acid on TLC. Product could not be isolated from chromium salts.
PCC/DCM ¹¹³	Aldehyde	Product could be seen by TLC but could not be isolated from chromium salts.
CrO ₃ , H ₅ IO ₆ , wet ACN ^{114, 115}	Acid	Silanol group did not withstand conditions
Swern ^{116, 117}	Aldehyde	Decomposition of product occurred. Uracil base and α,β -unsaturated aldehyde were isolated.
TPAP, NMO, DCM ^{118, 119, 120}	Aldehyde	30% - 40% yield
BAIB, TEMPO, ACN/H ₂ O ¹²¹	Acid	85% yield

Table 5-3: Attempted procedures for oxidation at position 11

¹¹¹ Corey, E. J.; Schmidt, G. Useful Procedures for the Oxidation of Alcohols Involving Pyridinium Dichromate in Aprotic Media. *Tetrahedron Lett.* **1979**, 399-402.

¹¹² Czernecki, S.; Georgoulis, C.; Stevens, C. L.; Vijayakumaran, K. Pyridinium Dichromate Oxidation - Modifications Enhancing Its Synthetic Utility. *Tetrahedron Lett.* **1985**, 26, 1699-1702.

¹¹³ Corey, E. J.; Suggs, J. W. Pyridinium Chlorochromate - Efficient Reagent for Oxidation of Primary and Secondary Alcohols to Carbonyl-Compounds. *Tetrahedron Lett.* **1975**, 2647-2650.

¹¹⁴ Zhao, M. Z.; Li, J.; Song, Z. G.; Desmond, R.; Tschaen, D. M.; Grabowski, E. J. J.; Reider, P. J. A novel chromium trioxide catalyzed oxidation of primary alcohols to the carboxylic acids. *Tetrahedron Lett.* **1998**, 39, 5323-5326.

¹¹⁵ Yamazaki, S. Chromium(VI) oxide-catalyzed benzylic oxidation with periodic acid. *Organic Letters* **1999**, 1, 2129-2132.

¹¹⁶ Omura, K.; Swern, D. Oxidation of Alcohols by Activated Dimethyl-Sulfoxide - Preparative, Steric and Mechanistic Study. *Tetrahedron* **1978**, 34, 1651-1660.

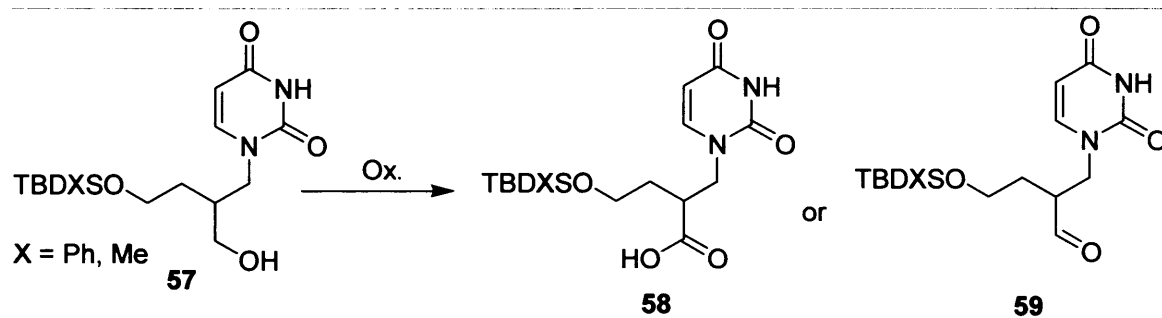
¹¹⁷ Mancuso, A. J.; Huang, S. L.; Swern, D. Oxidation of Long-Chain and Related Alcohols to Carbonyls by Dimethyl-Sulfoxide Activated by Oxalyl Chloride. *J. Org. Chem.* **1978**, 43, 2480-2482.

¹¹⁸ Griffith, W. P.; Ley, S. V. TPAP: Tetra-n-propylammonium perruthenate, a mild and convenient oxidant for alcohols. *Aldrichimica Acta* **1990**, 23, 13-19.

¹¹⁹ Ley, S. V.; Norman, J.; Griffith, W. P.; Marsden, S. P. Tetrapropylammonium Perruthenate, Pr₄n⁺Ruo₄⁻, Tpap - a Catalytic Oxidant for Organic-Synthesis. *Synthesis-Stuttgart* **1994**, 639-666.

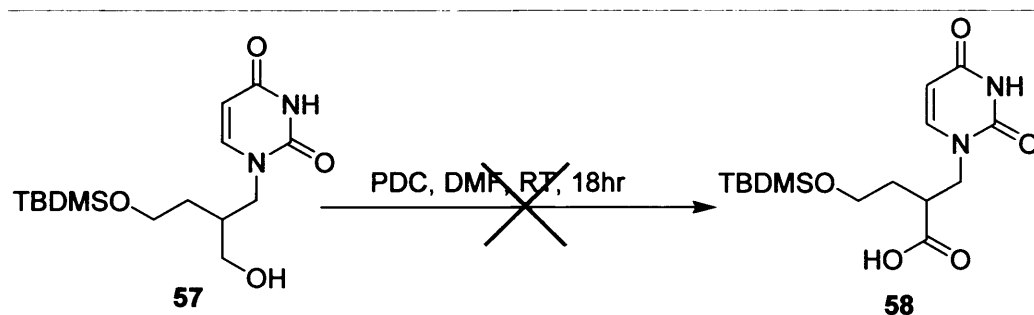
¹²⁰ Sharpless, K. B.; Akashi, K.; Oshima, K. Ruthenium Catalyzed Oxidation of Alcohols to Aldehydes and Ketones by Amine-N-Oxides. *Tetrahedron Lett.* **1976**, 2503-2506.

¹²¹ DeMico, A.; Margarita, R.; Parlanti, L.; Vescovi, A.; Piancatelli, G. A versatile and highly selective hypervalent iodine (III)/2,2,6,6-tetramethyl-1-piperidinyloxy-mediated oxidation of alcohols to carbonyl compounds. *J. Org. Chem.* **1997**, 62, 6974-6977.



Scheme 5-2: Oxidation of 57

PDC in DMF

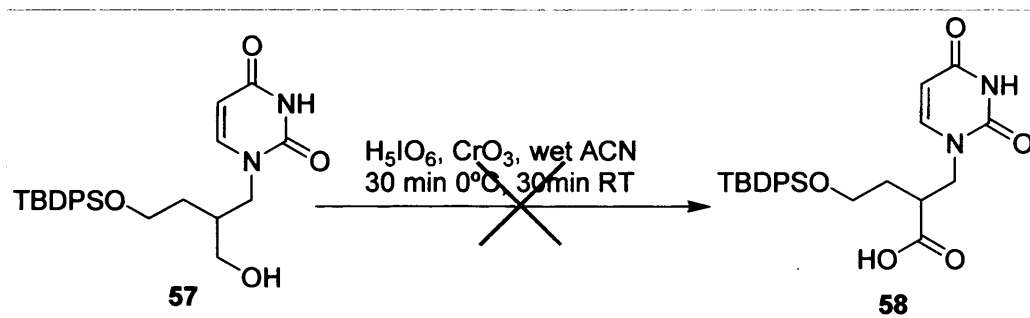


Scheme 5-3: Oxidation of 57 using PDC in DMF

Initially, direct oxidation of **57** to the acid was attempted using the widely known pyridinium dichromate (PDC)/DMF methodology¹¹¹ following the procedure of Xing *et al.*¹²² The TBDMS alcohol was used. The reaction was left stirring overnight and the presence of an acid could be seen by TLC using bromocresol green staining. The carboxylate was extracted into a saturated NaHCO₃ solution which was then acidified to pH 2 and an extraction with diethyl ether was then carried out. However, bromocresol green staining showed that the acid remained in the aqueous layer with the PDC. The product could not be separated from the PDC by washing with ether, ethyl acetate, DCM or MeOH. The product could not be identified by NMR, as no peaks were observed in the processed spectra. This was probably due to the interference of the paramagnetic chromium species with accurate shimming.

¹²² Xing, X. C.; Fichera, A.; Kumar, K. Simple and efficient method for the resolution of all four diastereomers of 4,4,4-trifluorovaline and 5,5,5-trifluoroleucine (vol 67, pg 1722, 2002). *J. Org. Chem.* **2002**, *67*, 8290-8290.

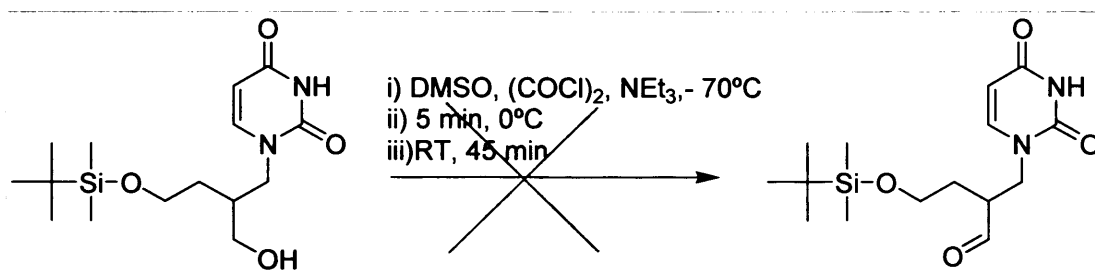
precipitate. The precipitate was removed and identified by ^1H NMR as starting material in which the TBDPS group had been cleaved. The filtrate was starting material and the silanol by-product. The TBDPS protecting group was cleaved under the reaction conditions.



Scheme 5-5: Oxidation of **57** using chromium trioxide and periodic acid

Swern oxidation

The oxidation of **57** was then attempted using the Swern procedure^{116, 117} which seemed attractive as it excluded the use of metal complex oxidising agents and was carried out in non-acidic conditions.



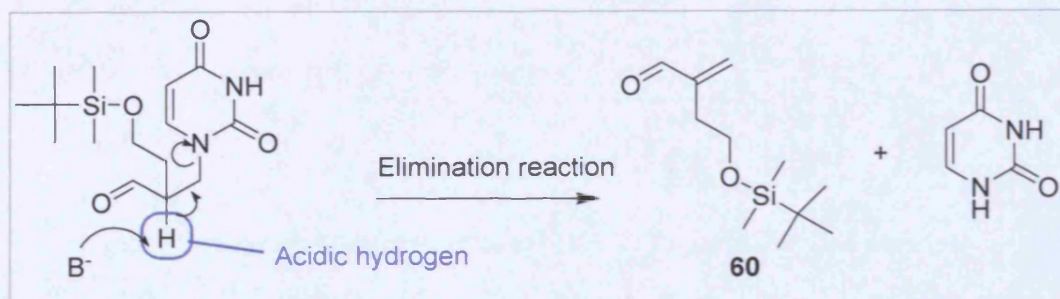
Scheme 5-6: Oxidation of **57** via the Swern procedure

The procedure was carried out according to Bundy *et al.*¹²³ However, following purification by column chromatography **59** was isolated in very low yield. The main product isolated, which was identified by NMR and a peak at 214 by mass spectrometry, was the α,β -unsaturated aldehyde **60** and uracil. The loss of pyrimidine base from nucleoside analogues under the oxidising conditions of NaIO_4 and RuCl_3 has been reported in the literature.¹²⁴ In this case, loss of nucleoside base probably occurred through an elimination, similar to a reverse Michael addition reaction to

¹²³ Bundy, G. L.; Banitt, L. S.; Dobrowolski, P. J.; Palmer, J. R.; Schwartz, T. M.; Zimmermann, D. C.; Lipton, M. F.; Mauragis, M. A.; Velely, M. F.; Appell, R. B.; Clouse, R. C.; Daus, E. D. Synthesis of 2,4-di-1-pyrrolidinyl-9H-pyrimido 4,5-b indoles, including antiasthma clinical candidate PNU-142731A. *Org. Process Res. Dev.* **2001**, *5*, 144-151.

¹²⁴ Singh, A. K.; Varma, R. S. Ruthenium Tetraoxide - a Mild Reagent for the Oxidation of 2',3'-O-Isopropylidene Purine Nucleosides. *Tetrahedron Lett.* **1992**, *33*, 2307-2310.

release uracil and compound **60**. This was probably due to the acidic nature of the hydrogen atom at position 8 and the fact that uracil is a good leaving group. The reaction may have proceeded through a base catalysed mechanism. Et_3N or the sulphur ylide intermediate produced during the reaction may have had the required basicity to abstract this proton and cause the elimination reaction to occur. In any case, compound **59** was not stable under the Swern oxidation conditions.

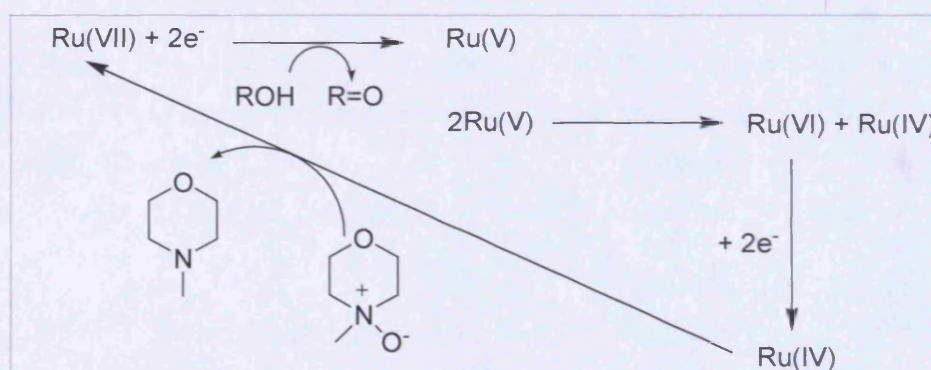


Scheme 5-7: Proposed mechanism for the elimination reaction under Swern conditions

TPAP, NMO

Ruthenium catalysed oxidation of alcohols to aldehydes and ketones by amine-*N*-oxides is a mild, effective and well documented oxidation procedure.¹²⁰ The tetrahedral perruthenate ion $[\text{Ru}(\text{VII})\text{O}_4]^-$ is a milder oxidant than ruthenium tetroxide $[\text{Ru}(\text{VIII})\text{O}_4]$. Particularly effective is the tetrapropylammonium salt of this species as it is soluble in many organic solvents. Catalytic tetrapropylammonium perruthenate (TPAP) and *N*-methylmorpholine-*N*-oxide (NMO) is a widely used procedure for the oxidation of alcohols to aldehydes. Many functionalities, including the TBDPS protecting group, are stable under these conditions and TPAP operates at room temperature and is devoid of obnoxious or explosive side products.^{118,119}

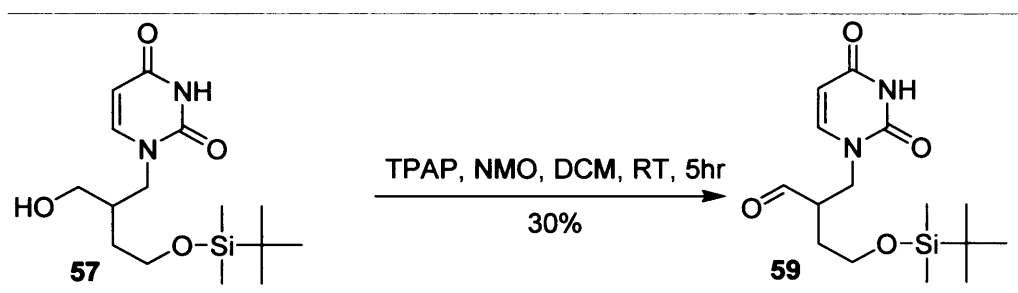
TPAP is an overall three electron oxidant and a postulated reaction sequence for $[\text{Ru}(\text{VII})\text{O}_4]^-$ is the following:



Scheme 5-8: Mechanism of TPAP catalysed oxidation

This procedure was therefore attempted according to the conditions used by Marcos *et al.*¹²⁵ The removal of water of crystallisation of the NMO and also the water formed during the reaction was obligatory to maintain good catalytic turnovers and this was best achieved by adding 3Å molecular sieves. The exclusion of water is also the main determining factor in preventing further oxidation to carboxylic acids.¹¹⁹

After stirring the reaction for 5h at RT, the desired aldehyde product **59** was isolated in 30% yield. This yield could not be improved by increasing the reaction time to overnight or by increasing the mol% of catalyst from 0.05% to 0.10%. There was no evidence from NMR or mass spectrometry that elimination had taken place.



Scheme 5-9: Oxidation of **57** to aldehyde **59** using TPAP and NMO

TEMPO, BAIB

In an effort to increase the yield of the first step of the synthesis of these compounds, a final oxidation procedure using a hypervalent iodine method was attempted. This procedure which utilised [bis(acetoxy)-iodo]benzene (BAIB) in excess and a catalytic amount of 2,2,6,6-tetramethylpiperidine-1-oxyl (TEMPO) was originally reported by De Mico *et al.*¹²¹ to oxidise alcohols to aldehydes and ketones. The procedure was then modified by Epp *et al.*¹²⁶ to prepare nucleoside-5'-carboxylic acids in the presence of high concentrations of water.

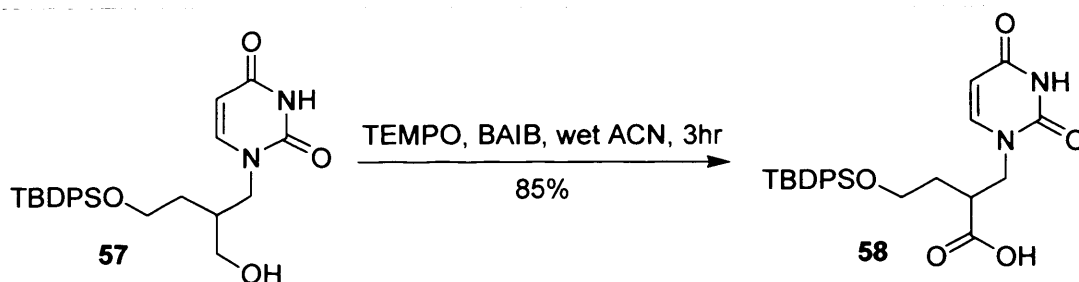
The advantages to this method included fast reaction times, ease of purification of the final carboxylic acid, stability of various protecting groups (including the TBDMS group), and the absence of inorganic salts. The side products of the reaction are iodobenzene, which can be removed in an ether wash, and acetic acid which can be removed under vacuum. The fact that the nucleoside derivatives had already been shown to be stable under these conditions was also promising.

The reaction was carried out in a 1:1 mixture of ACN/H₂O and left stirring for 3 h. The desired acid was isolated in 85% yield after trituration from diethyl ether.

¹²⁵ Marcos, I. S.; Garcia, N.; Sexmero, A. J.; Basabe, P.; Diez, D.; Urones, J. G. Synthesis of (+)-agelasine C. A structural revision. *Tetrahedron* **2005**, *61*, 11672-11678.

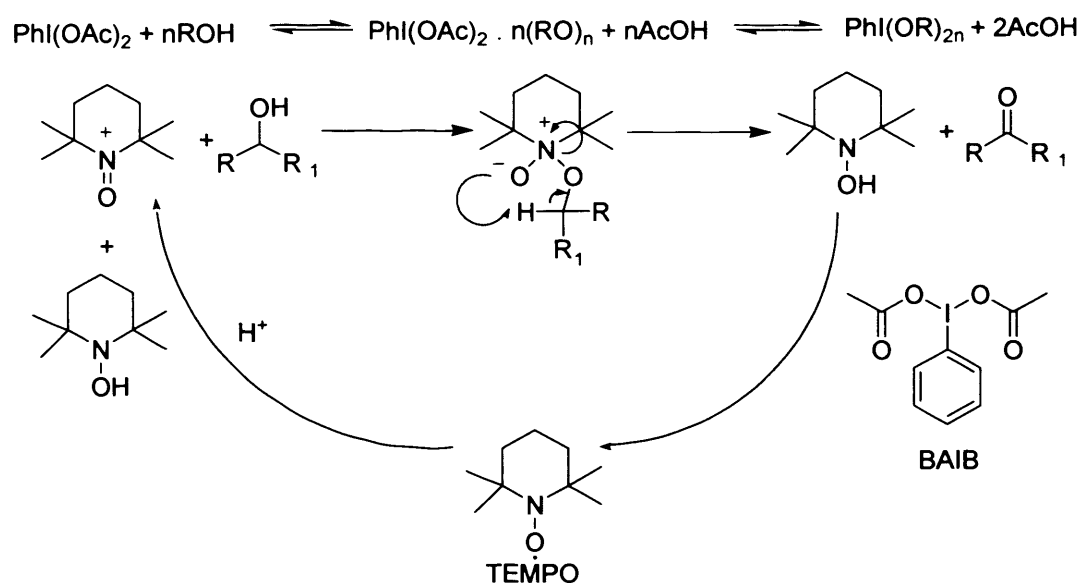
¹²⁶ Epp, J. B.; Widlanski, T. S. Facile preparation of nucleoside-5'-carboxylic acids. *J. Org. Chem.* **1999**, *64*, 293-295.

The pure product was identified by NMR and mass spectrometry.



Scheme 5-10: Oxidation of **57** to acid **58** using TEMPO and BAIB

The mechanism of the reaction is as follows:



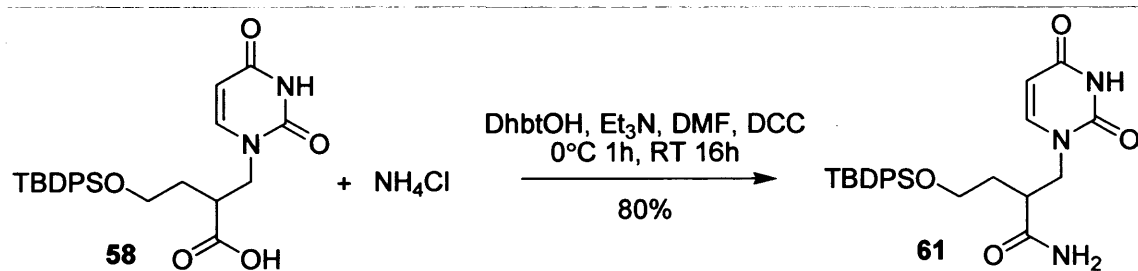
Scheme 5-11: Mechanism of oxidation by TEMPO and BAIB^{121, 127}

After a ligand exchange around the iodine of BAIB, the generated acetic acid catalyses the disproportionation of TEMPO to the hydroxylamine and oxoammonium salt. The oxoammonium salt is the species responsible for the oxidation of the alcohols while being, itself, reduced to hydroxylamine. The role of BAIB is to regenerate TEMPO.

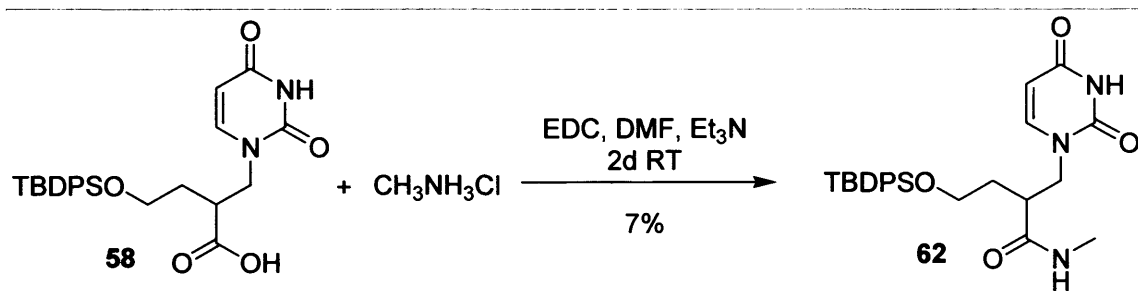
¹²⁷ de Souza, M. V. N. The use of TEMPO (2,2,6,6-tetramethylpiperidine-N-oxyl) for the oxidation of primary and secondary alcohols. *Quim. Nova* **2004**, *27*, 287-292.

5.4.1.2 Amide coupling to carboxylic acid **58**

Coupling of various substituted amines to the carboxylic acid moiety of **58** was then attempted (Route 2, Scheme 5-1). Initially, two methods were tried. The first was using the DCC, DhbtOH method as described in section 4.3.1.2 and the second was using EDC as a coupling reagent as described in section 4.2.3.2. In the case where the hydrochloric salt of the amine was used, Et₃N was used as the neutralising base. For the initial, trial reaction, more success was achieved with the former methodology.



Scheme 5-12: Amide coupling to acid **58** using DCC and DhbtOH



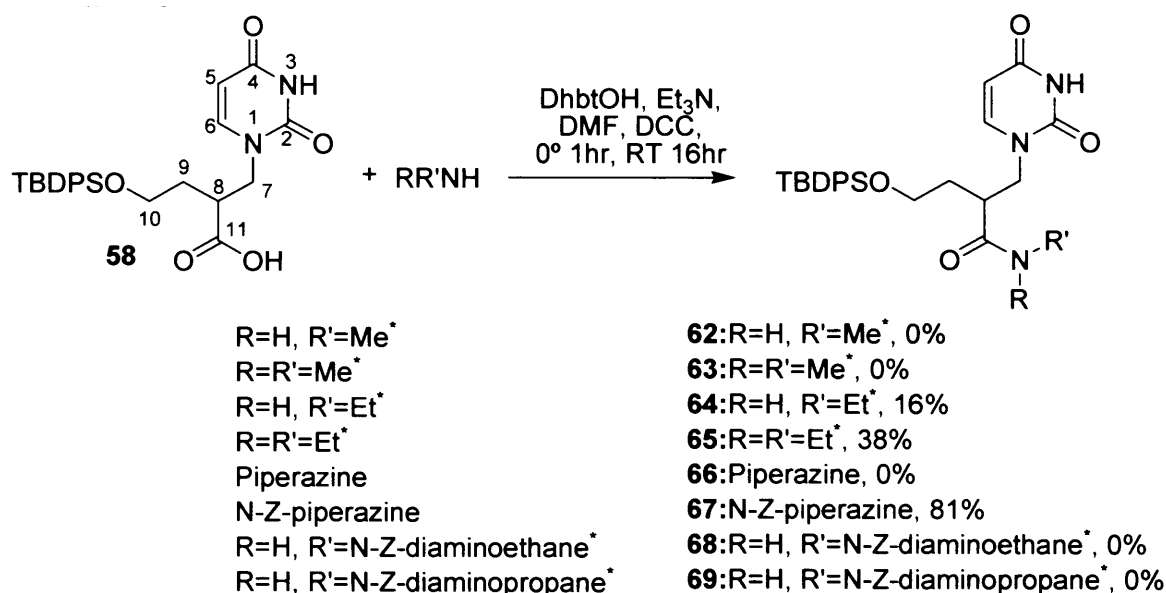
Scheme 5-13: Amide coupling to acid **58** using EDC

Using DCC as a coupling reagent in the presence of DhbtOH as an additive, it seemed that higher yields could be obtained. This methodology was therefore used to synthesise a small library of amides in a parallel fashion, using a Radley's low temperature carousel. Eight reactions were carried out simultaneously, varying the amine used. In cases where the hydrochloric salt of the amine was used, Et₃N was used as the neutralizing base. The acid, amine and DhbtOH were placed in the carousel reaction tubes with 2-3mL DMF and cooled to 0°C while stirring. The Et₃N was then added if necessary, followed by DCC. The reactions were stirred at 0°C for 1h and then at RT overnight. The precipitates which formed during the reactions were filtered off and identified to be the side product DCU. The solvent was evaporated under reduced pressure. In some cases, more DCU was removed by precipitation from acetone. The products were purified by column chromatography.

Compounds **64**, **65** and **67** were isolated in varying yields (Scheme 5-14). These compounds were characterised by ^1H and ^{13}C NMR, low resolution and high resolution mass spectrometry.

Unfortunately, products **62**, **63**, **66**, **68** and **69** could not be isolated. In all cases, a product that seemed to be the starting alcohol **57** by NMR, was isolated. No peaks corresponding to the amine substituents could be seen and there was no carbonyl peak in the ^{13}C spectra at 172 ppm, which had been present in the starting material. The integration of the peaks in the 3.5-3.9 ppm region of the ^1H NMR spectra was between 5 and 6. This would correspond to protons attached to carbon 7, 10 and 11 for the alcohol **57**, but should only integrate to 4 for the carbonyl compounds, corresponding to the protons at positions 7 and 10. The proton attached to carbon 8 usually resonates at approximately 2 ppm and moves downfield to approximately 3 ppm in the carbonyl compounds. This peak appeared at 2.2 ppm in this case. Neither the alcohol **57** nor the products **62**, **63**, **66**, **68**, and **69** could be seen by mass spectrometry.

Therefore 3 compounds (**62**, **65**, **67**) were successfully synthesised and isolated in sufficient quantity to submit for biological evaluation. However, there was no conclusive evidence for the formation of compounds **62**, **63**, **66**, **68** and **69** and these compounds were not submitted for biological evaluation.



Scheme 5-14: Synthesis of amides **62-69** ⁺hydrochloride salt used

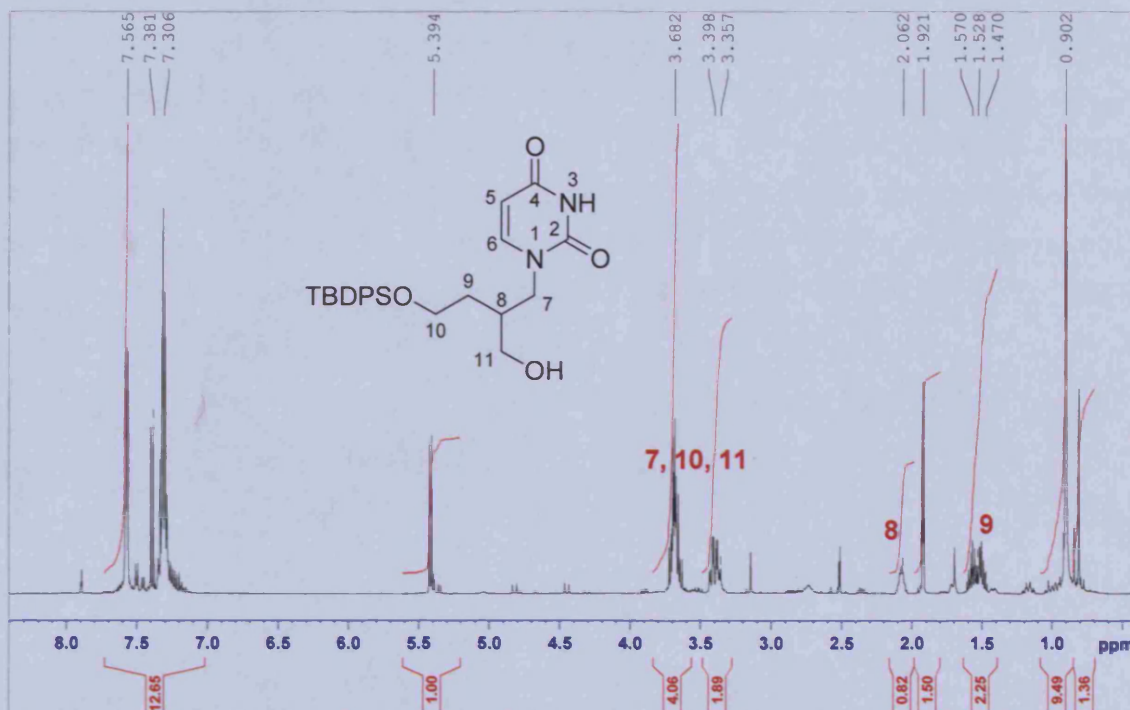
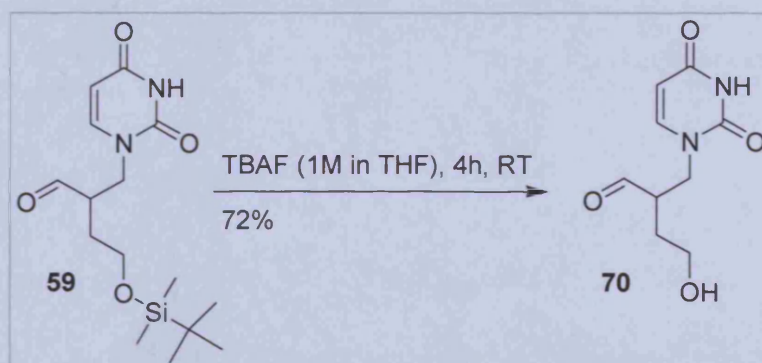


Figure 5-28: NMR of compound isolated from purification of compounds **62**, **63**, **66**, **68** and **69** and possible correlation to protons of alcohol **57**

5.4.1.3 Deprotection of aldehyde **59**

Although the amide coupling procedure described above was in some instances a success, some exploration into the synthesis of amides *via* route 1 (Scheme 5-1) was carried out. This procedure involved synthesis of amides directly from aldehyde **59** through oxidative amidation carried out *via* a radical mechanism.

In this case, the TBDPS protecting group had first to be replaced by the Trt group as it is quite labile under the AIBN/NBS conditions required for amide synthesis. The Trt group is more stable under these conditions.¹²⁸

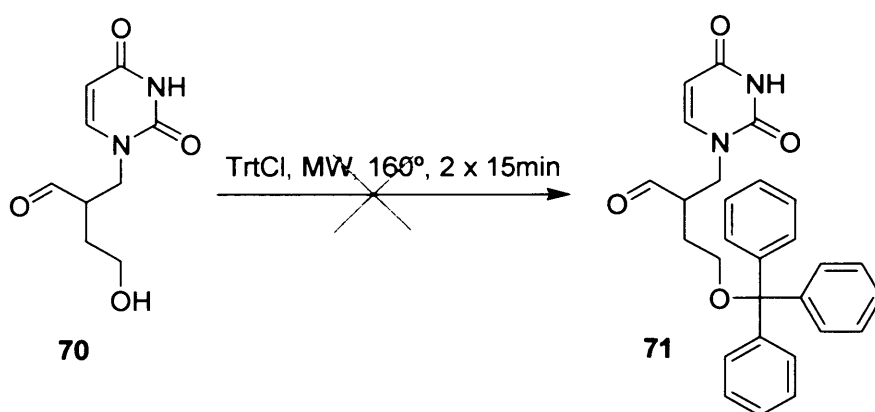


Scheme 5-15: Removal of the TBDPS group with TBAF

¹²⁸ Greene, T. W.; Wuts, P. G. M. *Protective Groups in Organic Synthesis*; 3rd ed.; John Wiley & Sons, 1999.

Deprotection of aldehyde **59** was therefore carried out using the TBAF method. Compound **59** was stirred in a 1M solution of TBAF in THF until the disappearance of starting material was observed by TLC. Following column chromatography, the product was isolated. The presence of TBAF could be seen by ^1H NMR and mass spectrometry and proved difficult to remove. The product could therefore have been isolated as the TBAF salt. The following tritylation step was carried out in any case.

5.4.1.4 Tritylation of alcohol **70**



Scheme 5-16: Unsuccessful tritylation of compound **70**

Compound **70** and TrtCl were dissolved in pyridine and exposed to microwave radiation at 160°C twice for 15min each time. However, though new spots were seen by TLC, after column chromatography only starting materials were isolated. No tritylated product was obtained. It was probable that the starting compound **70** was unreactive due to inter or intra molecular interaction between the alcohol and the aldehyde. Especially, in basic media, an intramolecular cyclisation to form a five membered ring could be envisaged, followed by oxidation in the MW reactor due to the presence of gas in the solvent.

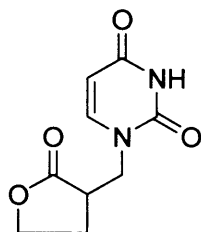
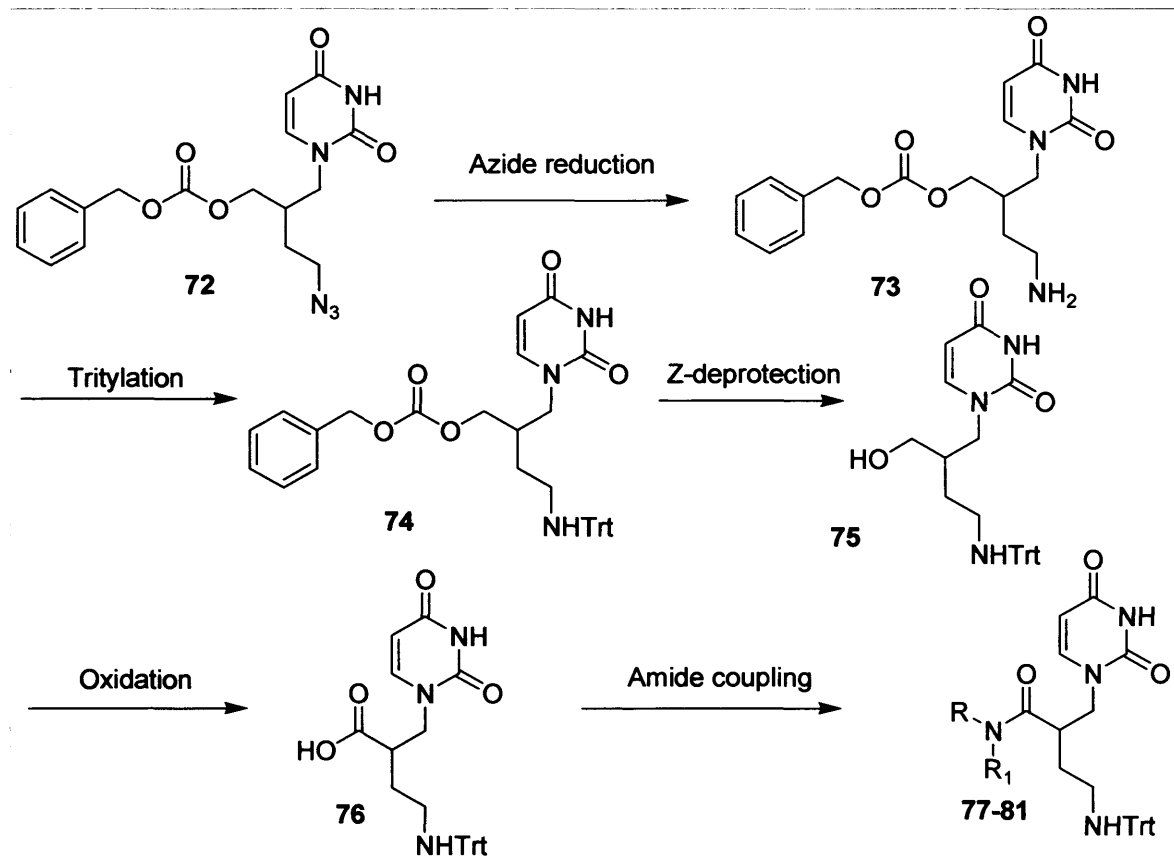


Figure 5-29: Possible cyclised product of aldehyde **70**

Due to lack of starting material and time constraints this method was therefore abandoned.

5.4.2 Triphenylmethylamino derivatives

Triphenylmethylamino derivatives were then synthesised from intermediate **72** (Figure 5-26) provided by Medivir as it was previously established that replacement of the TBDPS-O group with a Trt amino group increased the stability of the compounds in liver microsomes.⁷⁴ The overall synthetic strategy was as follows:



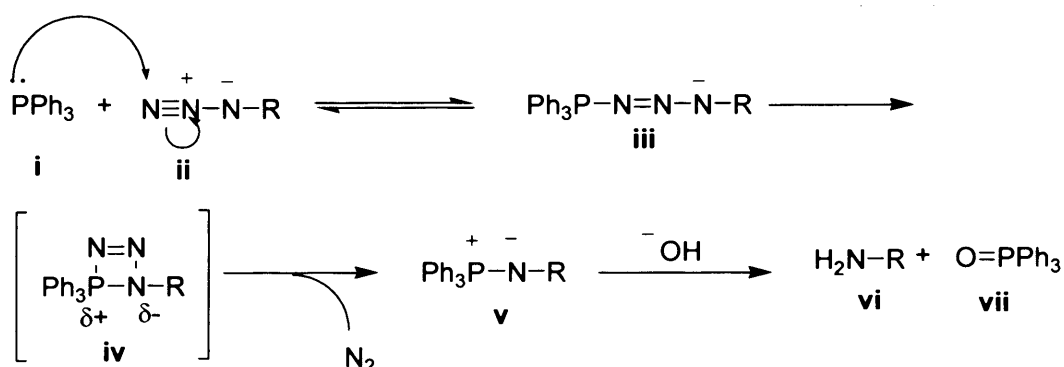
Scheme 5-17: Overall synthetic strategy for branched acyclic Trt amino nucleoside derivatives

5.4.2.1 Reduction of azide **72**

Reduction of azides to amines can be carried out using various methods. The most common are hydrogenation using Pt or Pd catalysts or reduction using lithium aluminium hydride or sodium borohydride.¹²⁹ Previously, in the group the reduction of azides in uridine derivatives by catalytic hydrogenation was attempted. 5% Pd/C was utilized. However, this resulted in reduction of the uracil ring and none of the desired amine was isolated.⁹⁸ The Staudinger reaction is an alternative, mild and selective route to convert azides to amines using triphenylphosphine and ammonium hydroxide.¹²⁹

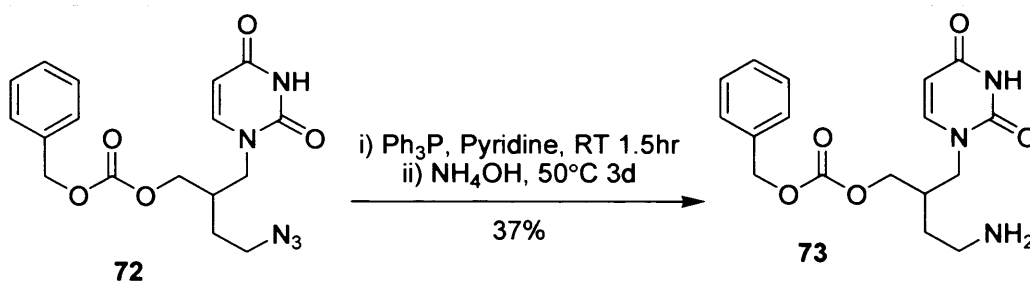
¹²⁹ Scriven, E. F. V.; Turnbull, K. Azides - Their Preparation and Synthetic Uses. *Chem. Rev.* **1988**, *88*, 297-368.

This method has also been used on nucleoside derivatives effectively¹³⁰ and was therefore the method of choice in this case. The mechanism of the reaction is as follows:



Scheme 5-18: Mechanism of the Staudinger reaction¹³¹

The lone pair of electrons on the phosphine **i** attack the terminal nitrogen atom of the azide **ii** to yield the linear triamine phosphazide intermediate **iii**. This intermediate undergoes intramolecular rearrangement *via* a four membered transition state **iv** to yield the iminophosphorane **v** with loss of N_2 . The iminophosphorane then undergoes hydrolysis to release the desired amine **vi** and triphenylphosphine oxide **vii**.¹³¹



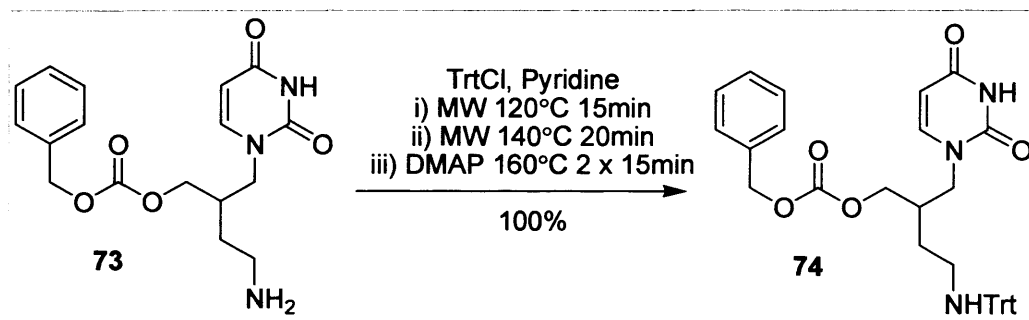
Scheme 5-19: Reduction of azide **72** to amine **73** under Staudinger conditions

The reaction was carried out according to Vanheusden *et al.*¹³⁰ However, hydrolysis of the iminophosphirane intermediate proved difficult. The intermediate **v** was probably stabilised due to interaction of the phenyl rings with the Cbz protecting group in place. Longer reaction times and heating was required. After purification by column chromatography, the pure amine **73** was isolated in 37% yield.

¹³⁰ Vanheusden, V.; Munier-Lehmann, H.; Froeyen, M.; Dugue, L.; Heyerick, A.; De Keukeleire, D.; Pochet, S.; Busson, R.; Herdewijn, P.; Van Calenbergh, S. 3'-C-branched-chain-substituted nucleosides and nucleotides as potent inhibitors of Mycobacterium tuberculosis thymidine monophosphate kinase. *J. Med. Chem.* **2003**, *46*, 3811-3821.

¹³¹ Lin, F. L.; Hoyt, H. M.; van Halbeek, H.; Bergman, R. G.; Bertozzi, C. R. Mechanistic investigation of the Staudinger ligation. *J. Am. Chem. Soc.* **2005**, *127*, 2686-2695.

5.4.2.2 Tritylation of amine 73

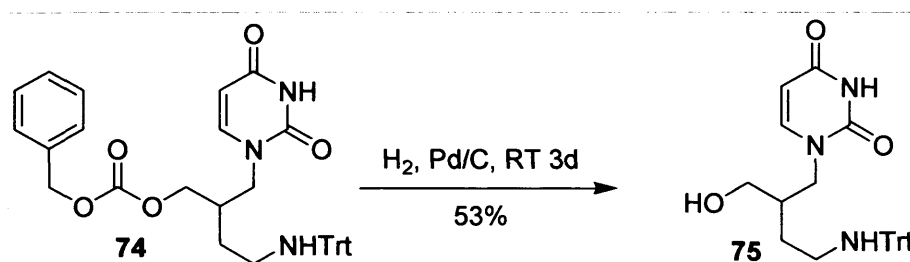


Scheme 5-20: Tritylation of amine 74

The next step of the synthesis was tritylation of the amino group. This was carried out in the microwave reactor in pyridine solvent. After exposure of the TrtCl and amine **73**, dissolved in pyridine, to MW radiation at 120°C for 15min and then at 140°C for a further 20min, starting material could still be seen by TLC. A catalytic amount of DMAP was added to the reaction mixture which was then exposed to microwave radiation for a further 15min at 160°C and the reaction went to completion. In fact, the optimal conditions found were DMAP, TrtrCl and amine dissolved in pyridine and exposed to MW radiation twice at 160°C for 15min. By TLC it could be seen that the reaction had gone to completion. After purification by column chromatography the tritylated compound was isolated in 100% yield.

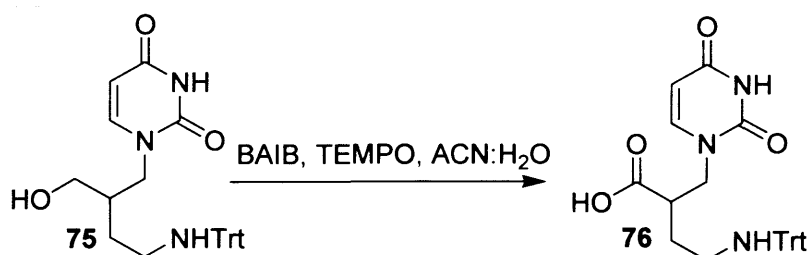
5.4.2.3 Deprotection – cleavage of the benzyl carbonate protecting group

Cleavage of the benzyl carbonate protecting group can be carried out by hydrogenolysis. This had to be carried out selectively in the presence of the Trt moiety which is also labile by hydrogenolysis.



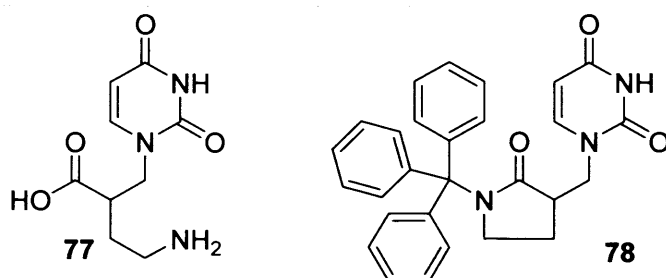
Scheme 5-21: Cleavage of the benzyl carbonate protecting group by hydrogenolysis

The reaction was carried out using 5% Pd/C catalyst and hydrogen filled balloons. After stirring for 2d at RT, starting material could still be seen by TLC. Fresh catalyst was added and the mixture was stirred again overnight after which time the catalyst was filtered off through celite. After purification by column chromatography the desired product was isolated in 53% yield.

5.4.2.4 Oxidation of alcohol **75**

The oxidation of alcohol **75** was carried out according to the BAIB, TEMPO procedure described in section 5.4.1.1. Formation of a new spot which stained with bromocresol green could be seen by TLC. However, this ran very close to BAIB which also stained with bromocresol green. The product, was slightly more lipophilic than the previous acid **58** and as a result, purification by column chromatography was necessary.

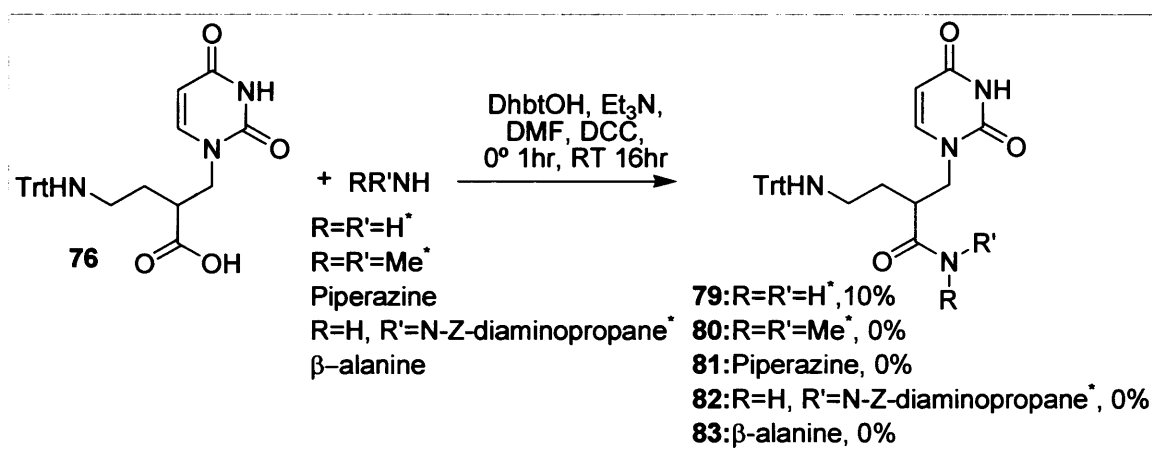
Analysis of the isolated product by electrospray mass spectrometry was complicated. Traces of the peak at 469 for compound **76** could be seen in negative mode. The fragment **77**, with molecular weight 227, due to loss of the trityl group, was the main peak in negative mode, supporting evidence that acid **76** had been made. The presence of the trityl peaks in the ^1H NMR, however, was proof that the trityl group was not cleaved in the main product and that **77** was a product of fragmentation during the electrospray process. In positive ion electrospray mass spectrometry, the Trt cation was the overwhelming main peak, however traces of the cyclised product **78** could also be seen. This product, however, may have formed during the electrospray process.



In the ^1H NMR spectrum of the purified product in CDCl_3 , a broad peak could be seen at 9.39 ppm which corresponded to the acidic OH. The characteristic carbonyl peak at 172 ppm in the ^{13}C spectrum could also be seen. Despite the presence of some contaminant peaks in the ^1H NMR spectrum which could not be identified, compound **76** was used to carry out the next step in the synthesis.

5.4.2.5 Amide coupling to carboxylic acid **76**

Amide bond formation was carried out in a parallel synthesis fashion in the Radley's low temperature carousel using DCC as a coupling reagent and DhbtOH as an additive as described in section 5.4.1.2.



Scheme 5-23: Amide coupling to carboxylic acid **76** *HCl salt used

Disappointingly, only amide **79** was isolated. Although, from the reaction utilising piperazine, some of compound **84** shown below was also isolated.

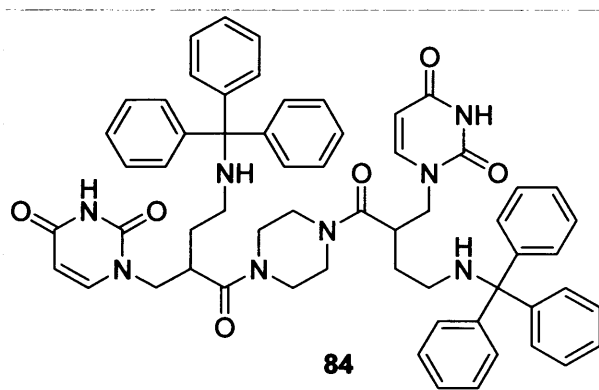


Figure 5-31: Compound **84**

For amide **82**, only starting material was isolated after column chromatography. Some of the amide **80** could be detected by mass spectrometry in one of the isolated fractions, but subsequent column chromatography resulted in isolation of unidentifiable products and DCC. This was likewise with amides **81** and **83**. Initially, peaks corresponding to the molecular weights of the products could be seen by mass spectrometry but subsequent column chromatography on silica resulted in isolation of unidentifiable side products. It was therefore thought that these compounds are unstable to purification by column chromatography on silica gel. Alternatively, the starting material **76** was decomposing under these conditions. It is possible that intramolecular amide bond formation was taking place instead, to give compound **78**.

5.5 Modifications at position 10

As suggested by the GRID calculations carried out, described in section 5.2, a modification in which a carbonyl oxygen was attached to C-10 of this class of branched acyclic inhibitors, may also be advantageous to the binding of the inhibitors in the PfdUTPase active site as it may also interact with Ser92 (Figure 5-16 and 5-25). The Trt-amide compound **56** docked well into the active site using FlexX. The attempted synthesis of this compound was therefore carried out from intermediate **57** supplied by Medivir.

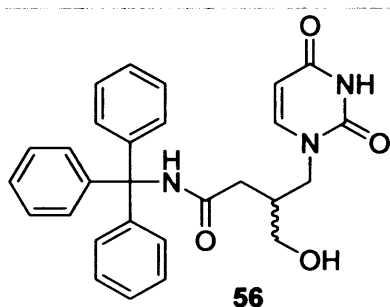
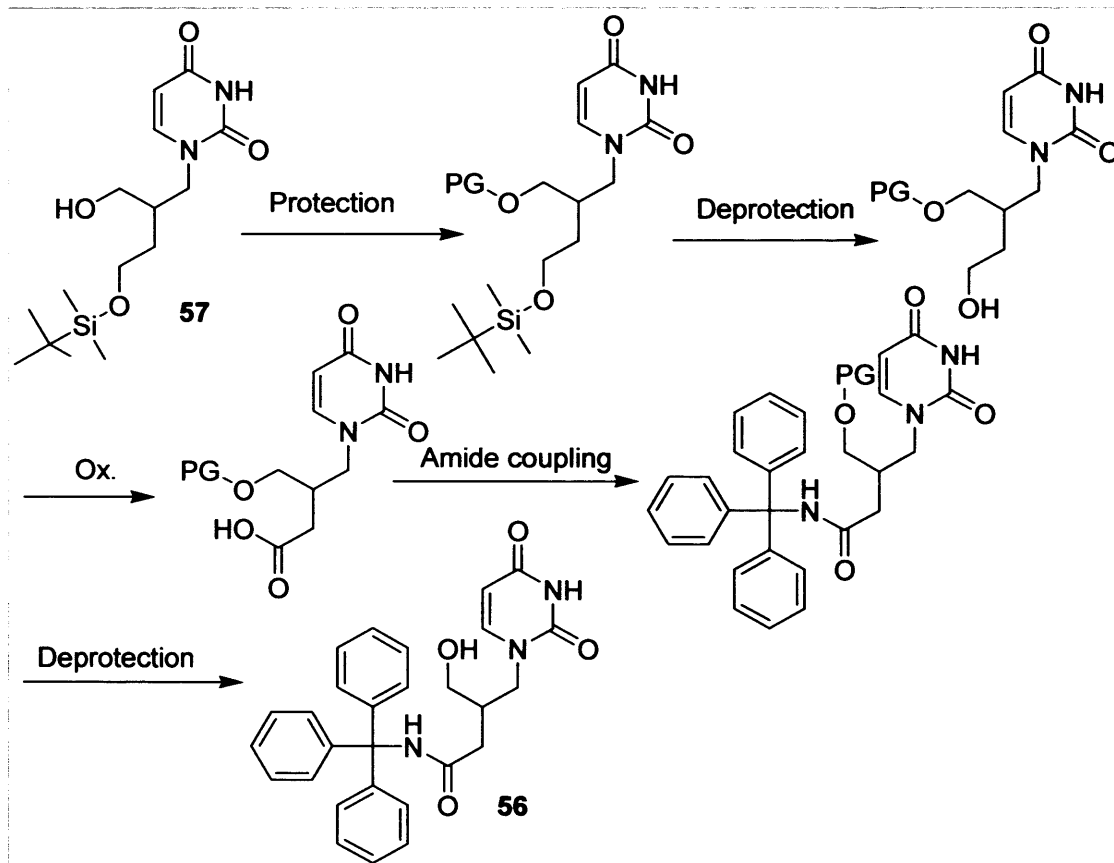


Figure 5-32: Trt-amide compound **56**

The overall synthetic strategy was as follows:



Scheme 5-24: Overall synthetic strategy for Trt-amide derivative **56**

5.5.1 Orthogonal protection of compound 57

The initial challenge in the synthesis of compound **56** was to find a protecting group for the free hydroxyl moiety of compound **57** that was orthogonal to the TBDMS group. Benzyl ethers seemed suitable as they are stable to the acidic or TBAF conditions required to cleave the TBDMS group.¹²⁸ Substituted benzyl ethers are more readily cleaved under oxidative conditions using DDQ^{132, 133} than their unsubstituted counterparts, a procedure to which other functionalities in the molecule should be stable.

The 4-methoxyphenylmethyl (4-MPM) protecting group was used in this case. Alcohol **57** was protected using NaH and 4-MPMCl.¹³⁴ The procedure was carried out according to Ueda *et al.*¹³⁵

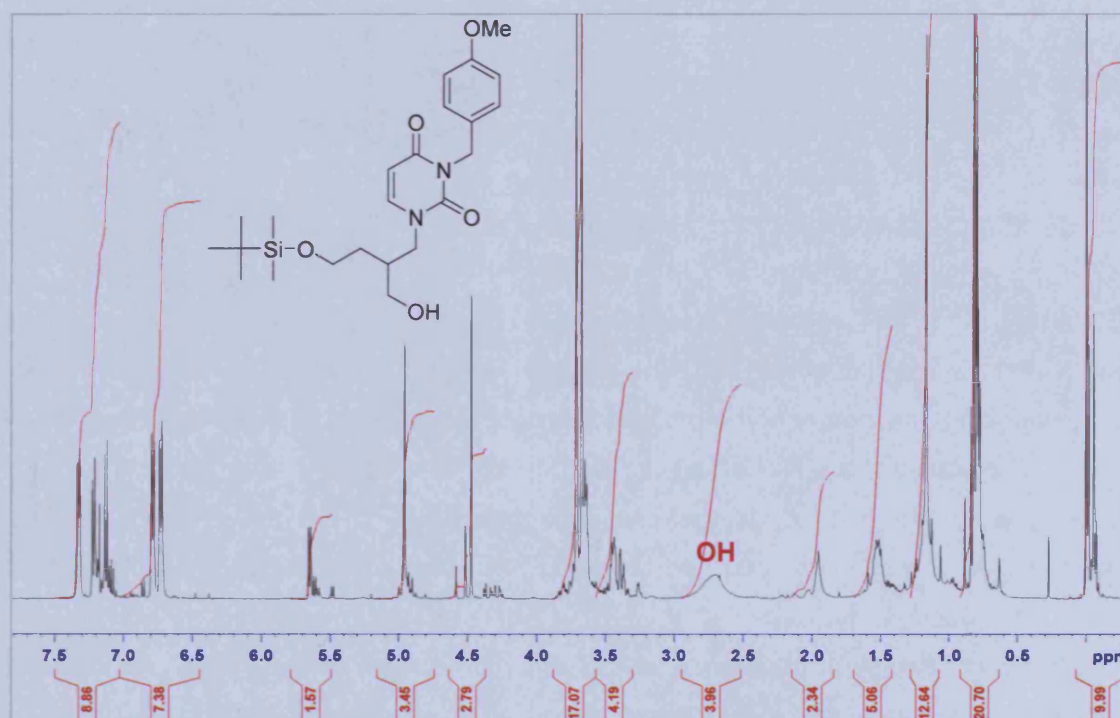


Figure 5-33: ¹H-NMR of 4-MPM protected compound **85**

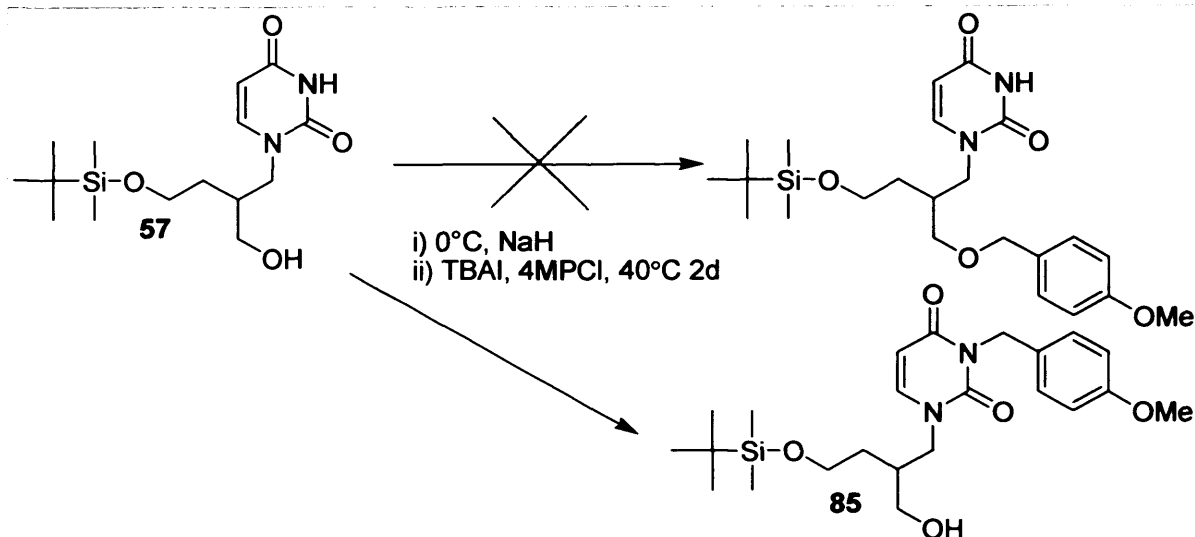
¹³² Horita, K.; Yoshioka, T.; Tanaka, T.; Oikawa, Y.; Yonemitsu, O. On the Selectivity of Deprotection of Benzyl, Mpm (4-Methoxybenzyl) and Dmpm (3,4-Dimethoxybenzyl) Protecting Groups for Hydroxy Functions. *Tetrahedron* **1986**, *42*, 3021-3028.

¹³³ Oikawa, Y.; Yoshioka, T.; Yonemitsu, O. Specific Removal of Ortho-Methoxybenzyl Protection by Ddq Oxidation. *Tetrahedron Lett.* **1982**, *23*, 885-888.

¹³⁴ Marco, J. L.; Huesorodriguez, J. A. Synthesis of Optically Pure 1-(3-Furyl)-1,2-Dihydroxyethane Derivatives. *Tetrahedron Lett.* **1988**, *29*, 2459-2462.

¹³⁵ Ueda, T.; Feng, F.; Sadamoto, R.; Niikura, K.; Monde, K.; Nishimura, S. I. Synthesis of 4-fluorinated UDP-MurNAc pentapeptide as an inhibitor of bacterial growth. *Org. Lett.* **2004**, *6*, 1753-1756.

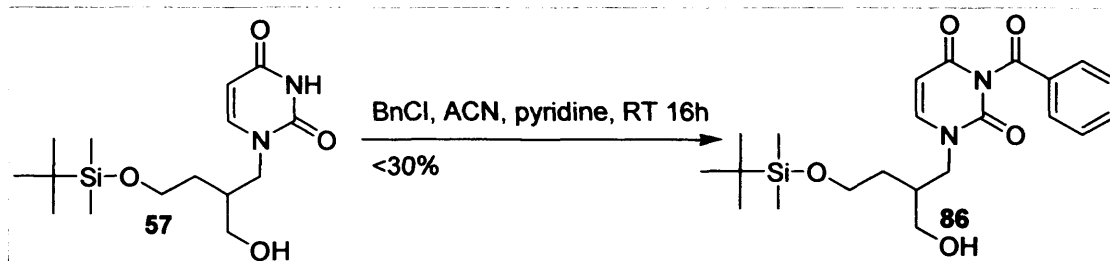
The $^1\text{H-NMR}$ of the crude product in CDCl_3 however, showed the presence of a broad OH peak at 2.71 ppm and the absence of the uracil N(3)H, normally resonating at 8 ppm. This was suggestive of the fact that the 4-MPM group was actually attached to the N-3 of the uracil ring and not the hydroxyl function.



Scheme 5-25: 4-MPM protection of alcohol 57

In fact, calculation of the expected pK_a values of the heteroatoms of molecule 57 using ACD/ pK_a DB version 7.07 showed that the expected pK_a of N(3)H was 9.5 while that of the OH was 14.5. It was therefore most likely that the NaH deprotonated the N-3 of the uracil ring instead of the alcohol, resulting in 4-MPMCl reaction at the N-3 position and attachment of the protecting group here and not at the desired position.

Protection of the N-3 of the uracil ring using the benzoyl (Bz) group which can subsequently be cleaved in the presence of MeNH_2 in EtOH is possible. The benzoylation procedure was carried out using BzCl in ACN and pyridine according to a modified procedure of Kumar *et al.*¹³⁶ in an effort to initially protect the N-3 position. The reaction, however, was low yielding and purification difficult. This method was therefore abandoned and an alternative protecting group strategy sought.

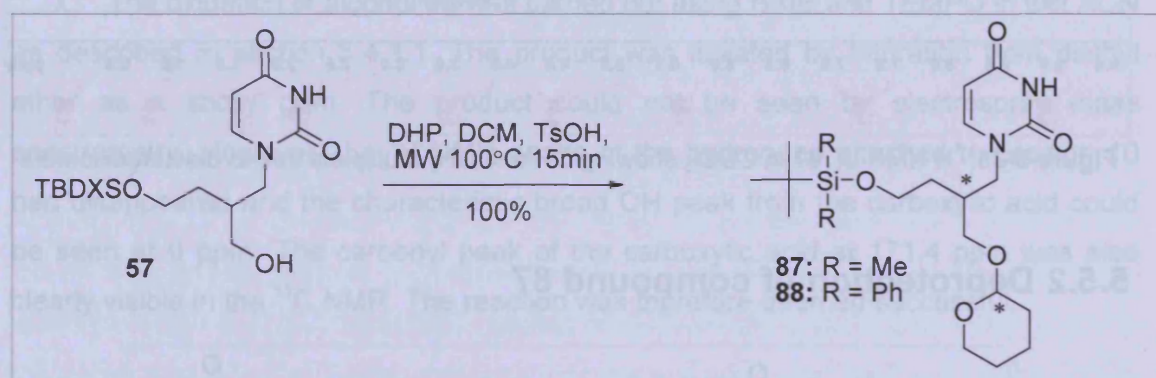


Scheme 5-26: Attempted benzoyl protection at N-3

¹³⁶ Kumar, T. S.; Madsen, A. S.; Wengel, J.; Hrdlicka, P. J. Synthesis and hybridization studies of 2'-amino- α -L-LNA and tetracyclic "locked LNA". *J. Org. Chem.* 2006, 71, 4188-4201.

The second attempt at orthogonal protection of the alcohol **57** involved the use of the tetrahydropyranyl (THP) protecting group as this can be cleaved under mild conditions in which the Trt group should be stable.¹²⁸ It is also stable to the oxidation conditions of BAIB and TEMPO.¹²⁶ However, it does limit the deprotection step of the TBDMS group to the use of TBAF, as under acidic conditions, the THP group would be cleaved. Another disadvantage of THP as a protecting group is the formation of diastereoisomers as THP contains a chiral centre.

The THP ether of compound **57** was prepared according to the procedure of Takayama *et al*,¹³⁷ initially. However, the isolated yield could be improved and the reaction time lowered by using microwave radiation. After exposure to microwave radiation at 100°C for only 15min, no starting material could be seen by TLC and the desired THP ether was isolated in quantitative yield.



Scheme 5-27: THP protection of alcohol **57** * = chiral centre

The presence of two chiral centres now meant that the product existed as four stereoisomers. This complicated the NMR spectra of the product as the different diastereoisomers resonate at different frequencies. Nearly all peaks were therefore solved as complicated multiplets.

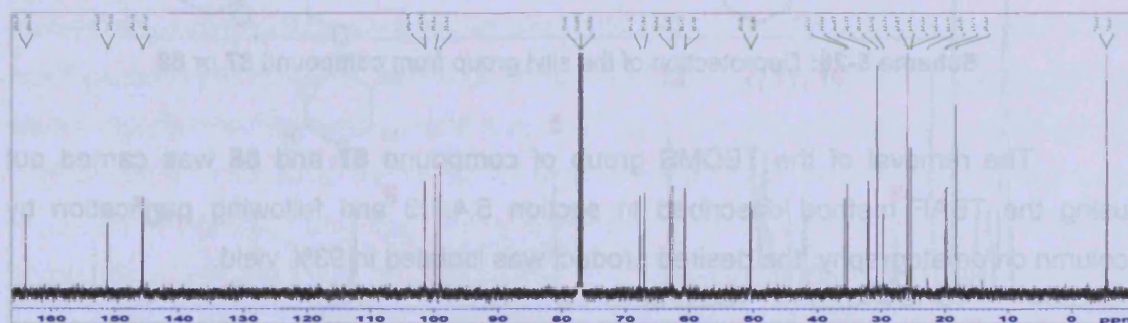


Figure 5-34: ^{13}C NMR of **87**. Peaks are multiplets

¹³⁷ Takayama, H.; Fujiwara, R.; Kasai, Y.; Kitajima, M.; Aimi, N. First asymmetric total synthesis of Us-7 and-8, novel D-seco corynanthe-type oxindole alkaloids from *Uncaria attenuata*: Structure revision of Us-7 and determination of absolute stereochemistry. *Organic Letters* **2003**, *5*, 2967-2970.

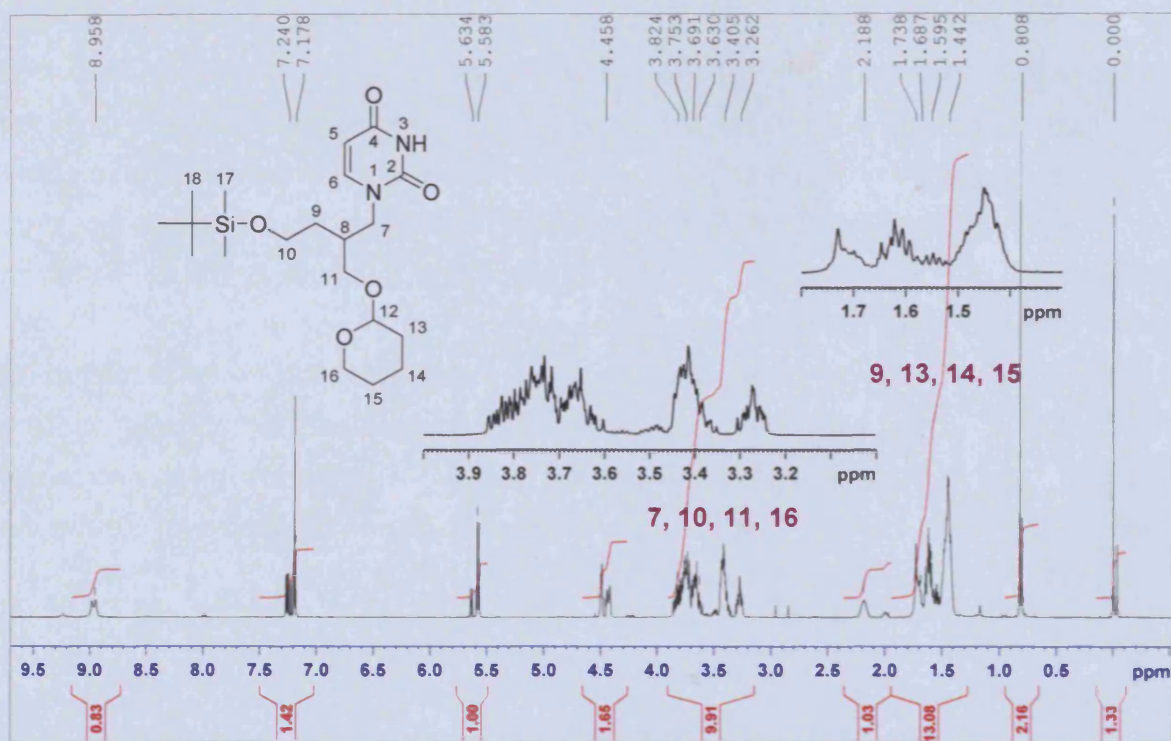
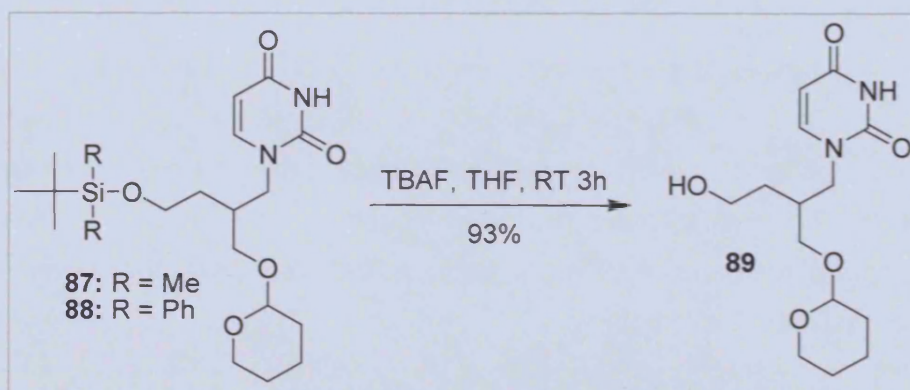


Figure 5-35: ^1H NMR of **87** in CDCl_3 showing CH and CH_2 multiplets due to diastereoisomers

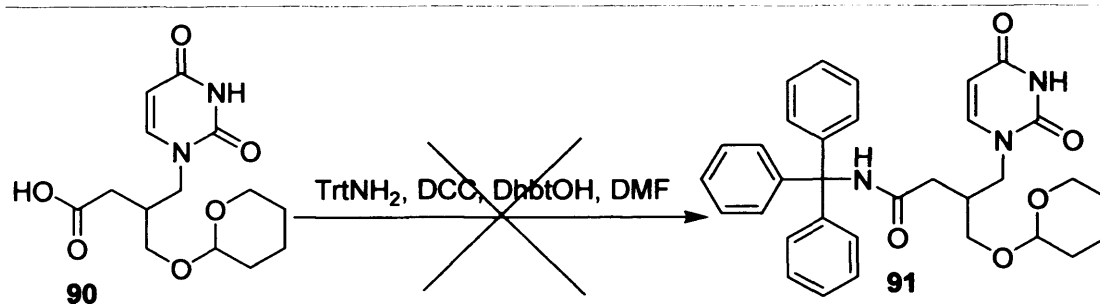
5.5.2 Deprotection of compound **87**



Scheme 5-28: Deprotection of the silyl group from compound **87** or **88**

The removal of the TBDMS group of compound **87** and **88** was carried out using the TBAF method described in section 5.4.1.3 and following purification by column chromatography, the desired product was isolated in 93% yield.

5.5.4 Amide coupling



Scheme 5-30: Amide coupling to acid **90**

The next step of the synthesis then involved the coupling of acid **90** to triphenylmethylamine and formation of the trityl amide **91** which in the final step needed to be deprotected to give the final compound **56**.

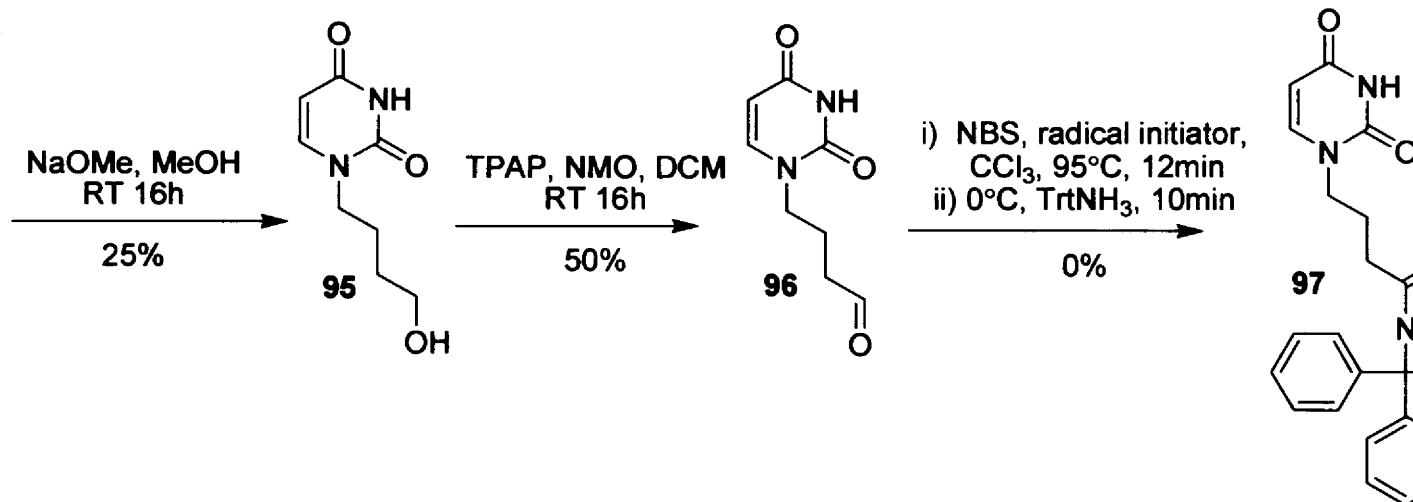
The amide coupling was attempted using the previously described method of DCC as a coupling reagent and DhbtOH as an additive. The crude product was purified by column chromatography but the product **91** could not be detected in any of the fractions by mass spectrometry or NMR. The starting tritylamine, DCU and DhbtOH were isolated and the final fraction collected seemed to be the starting acid **90** but some unidentifiable contaminant peaks were present in the 0.5-2.0 ppm region of the ^1H NMR spectrum.

It is probable the triphenylmethylamine is too sterically hindered by the three phenyl rings to act as a nucleophile and attack the intermediate formed in the coupling reaction, preventing the reaction from being successful.

5.6 Single chain derivatives

An effort was made to identify some chemistry that might be used successfully in the synthesis of trityl amide derivatives. As the amide coupling procedure was unsuccessful, it was thought that this might be achievable through the previously discussed AIBN, NBS method. However, due to the limited availability of the starting material **57** provided by Medivir, the chemistry was first attempted on more easily synthesised single chain derivatives. The comparison of the activity of unbranched chain derivatives against the enzyme to the activity of the branched chain derivatives would also be interesting for further SAR investigations.

The overall synthetic strategy for the single chain derivatives was as follows:

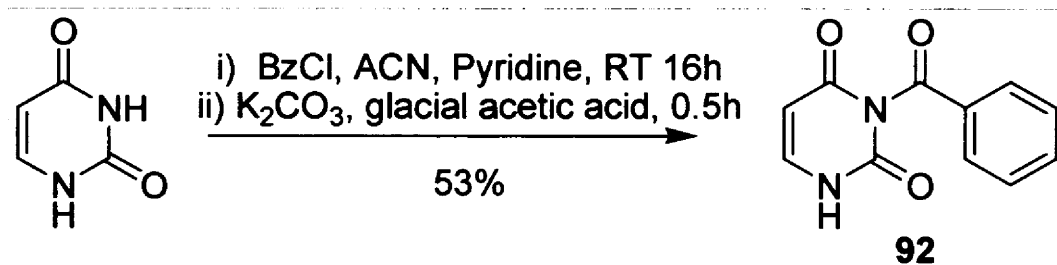


Scheme 5-31: Overall synthetic strategy for single chain trityl amide

The synthesis of **95** was carried out according to the procedure of Ng *et al.*⁷⁴ from uracil and the mono protected diol intermediate **93** previously synthesized. The group. Oxidation of the alcohol was then carried out using the TPAP method previously described to give aldehyde **96**. The radical oxidative amidation reaction was then attempted.

5.6.1 Synthesis of N-3 - benzoyl uracil

To avoid N-3 alkylation, the uracil was protected at the N-3 position. This was achieved by a two step procedure consisting of N-1,N-3 double protection with benzoyl chloride in pyridine, followed by selective N-1 deprotection carried out using K₂CO₃ in ACN. The pure product was recrystallised from acetone/H₂O 1:1 in 53% overall yield.

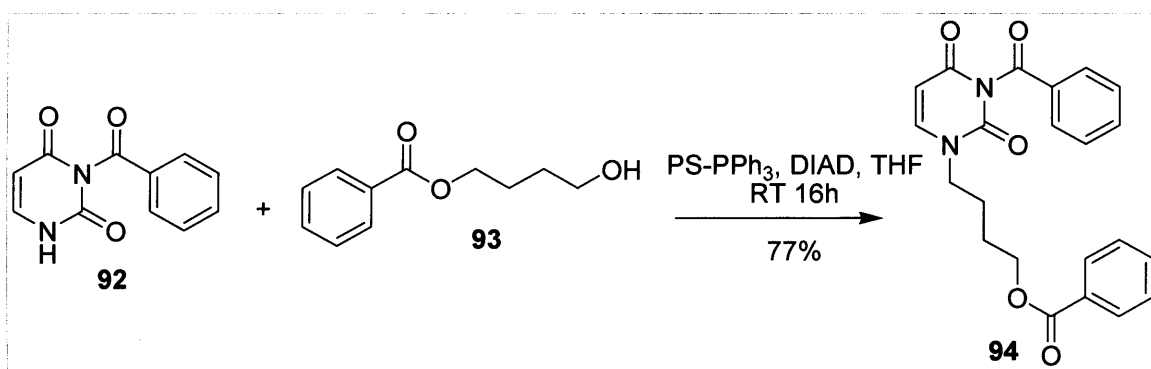


Scheme 5-32: Synthesis of N-3 protected uracil

¹³⁸ Frieden, M.; Giraud, M.; Reese, C. B.; Song, Q. L. Synthesis of 1-(hydroxymethyl)cyclobutyl -uracil, -thymine and -cytosine. *Journal of the Chemical Society Perkin Transactions 1* **1998**, 2827-2832.

5.6.2 Coupling to protected diol 93

Compound **92** was then coupled to the mono protected diol intermediate **93** which was previously synthesised in the group. The coupling procedure was carried out using Mitsunobu methodology on polymer supported PPh_3 according to the procedure of Hernández *et al.*¹³⁹ The use of polymer supported PPh_3 avoided the contamination of the product with the side product triphenylphosphine oxide which can be sometimes difficult to remove. The reaction was shaken as opposed to conventional stirring so as to avoid destruction of the polymer beads. Following purification by column chromatography on silica gel, the product was isolated in 77% yield.

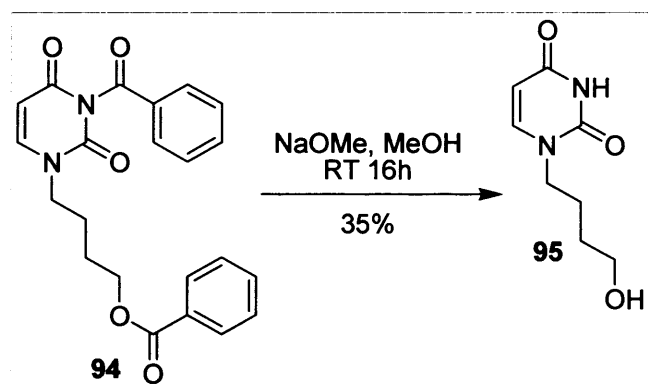


Scheme 5-33: Mitsunobu coupling of protected uracil **92** and protected diol **93**

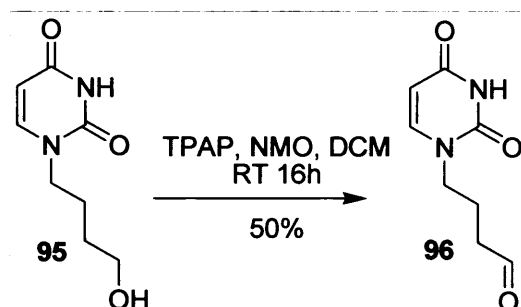
5.6.3 Deprotection of compound 94

Both of the benzoyl groups were cleaved from compound **94** simultaneously by stirring the compound in MeOH with NaOMe at room temperature overnight. Following purification by column chromatography, the pure product was isolated but in a low yield of 35%. It was thought that this was due to the formation of salts which were retained on the silica gel. Neutralising the product with Dowex H^+ resin before purification should solve this problem and increase yield.

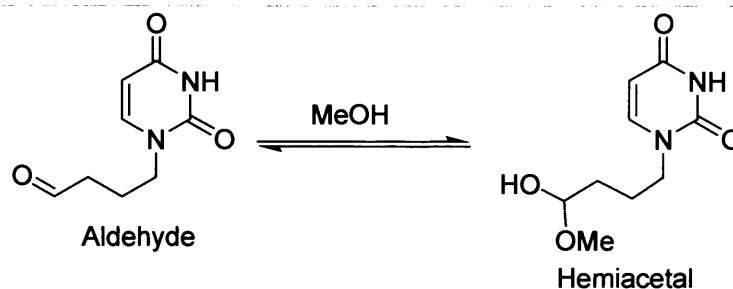
¹³⁹ Hernández, A. I.; Balzarini, J.; Karlsson, A.; Camarasa, M. J.; Perez-Perez, M. J. Acyclic nucleoside analogues as novel inhibitors of human mitochondrial thymidine kinase. *J. Med. Chem.* **2002**, *45*, 4254-4263.

Scheme 5-34: Deprotection of compound **94**

5.6.4 Oxidation of alcohol **95**

Scheme 5-35: Oxidation of alcohol **95** by TPAP, NMO method

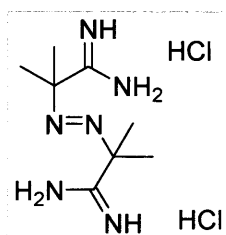
The alcohol **95** was oxidised to the corresponding aldehyde using the TPAP and NMO method described previously. Following column chromatography on silica gel, the product was isolated in 50% yield. The product was identified by $^1\text{H-NMR}$. However, the characteristic peaks of the hemi-acetal product could be seen by $^1\text{H-NMR}$ at 3.21 ppm and 4.45 ppm, as well as the aldehyde peak at 9.60 ppm. This may have been due to the fact that CD_3OD was the solvent used, therefore creating a hemi-acetal and aldehyde equilibrium.



Scheme 5-36: The equilibrium between aldehyde and hemiacetal

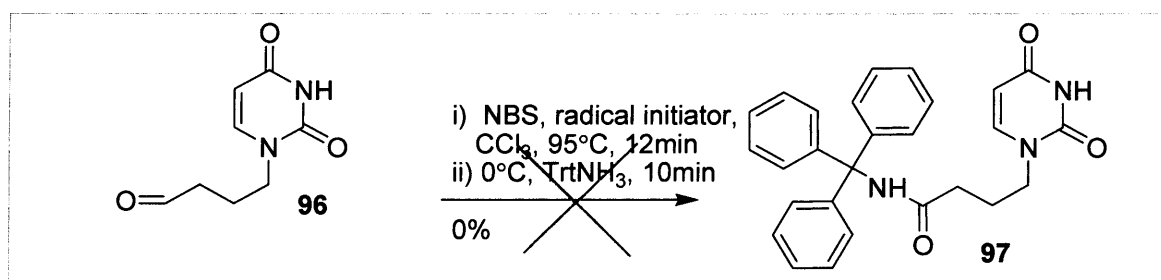
5.6.5 Oxidative amidation by a radical mechanism

The oxidative amidation procedure described previously was attempted using aldehyde **96**. The mechanism of this reaction normally proceeds through initial formation of the acid bromide¹⁴⁰ through a radical mechanism followed by nucleophilic attack of the amine to form the amide.¹⁰⁹ Conventionally, AIBN is the radical initiator of choice. However, due to the explosive nature of this compound, it was not commercially available. A safer alternative, 2,2'-azo-bis-(2-methylpropionamide) dihydrochloride was used.



Scheme 5-37: 2,2'-azo-bis-(2-methylpropionamide) dihydrochloride

The radical initiator, NBS and the aldehyde **96** were dissolved in CCl_4 and heated to 95°C for 12min. The reaction was cooled to 0°C in an ice bath and tritylamine was added. The reaction was allowed to come to room temperature and stirred for a further 10min.¹⁰⁹ Following aqueous work up, however, only starting tritylamine was isolated from the organic layer. The aqueous layer was found to contain aldehyde **96** and NBS. None of the trityl amide **97** was isolated.



Scheme 5-38: Oxidative amidation through a radical mechanism

¹⁴⁰ Cheung, Y. F. N-Bromosuccinimide - Direct Oxidation of Aldehydes to Acid Bromides. *Tetrahedron Lett.* **1979**, 3809-3810.

5.7 Biological results

The following compounds are currently awaiting biological evaluation:

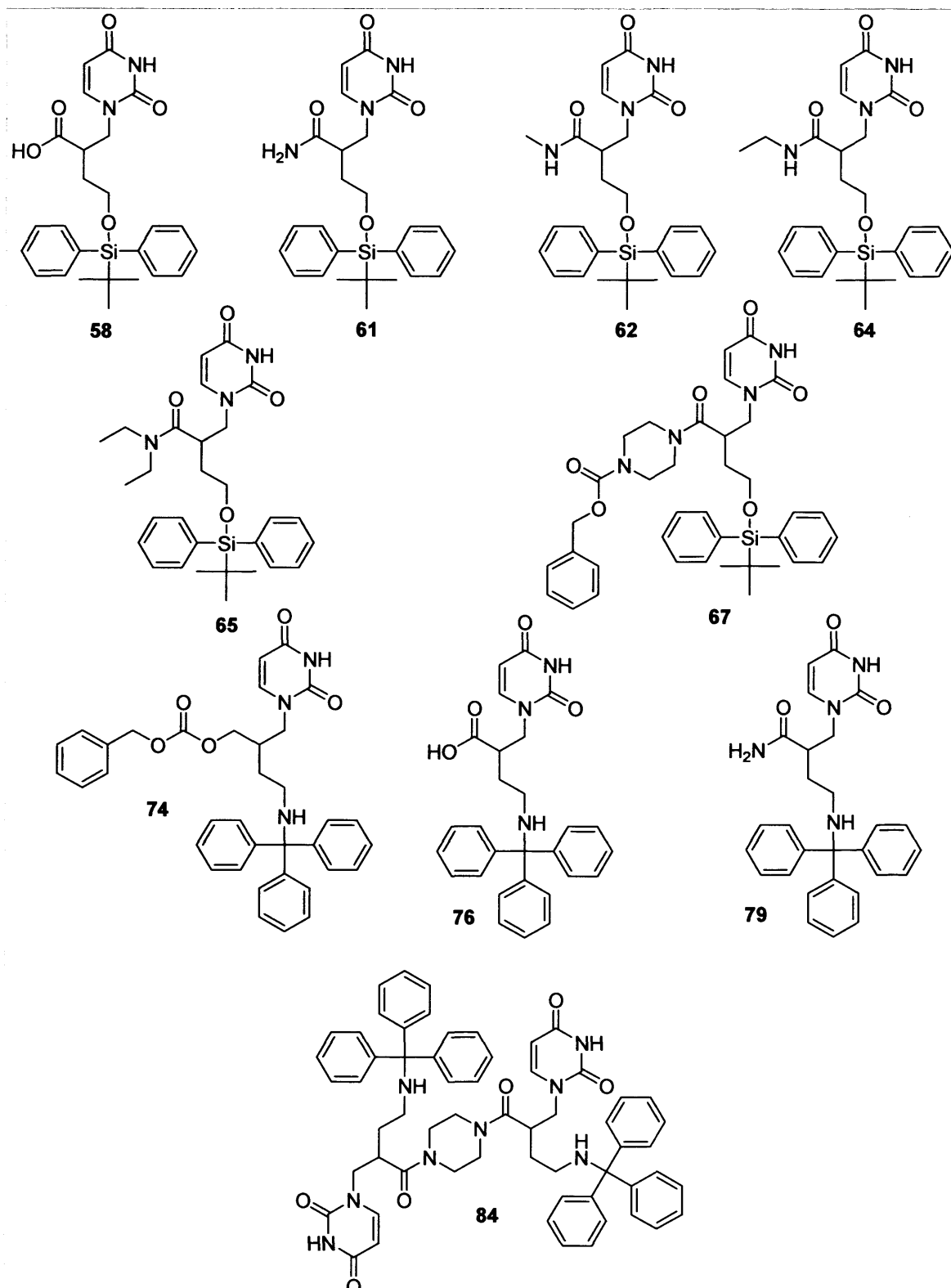


Figure 5-37: Acyclic uridine analogues currently awaiting biological evaluation

5.8 Discussion

GRID calculations carried out on the PfdUTPase enzyme suggested that compounds such as those shown in Figure 5-38 would hold favourable interactions within the active site. The most favourable interactions, most likely would be due to

1. Hydrogen bonding between the carbonyl oxygen at position 10 or 11 with the side chain of Ser92.
2. Hydrogen bonding between the NH moiety of G and the negatively charged side chain of Asp109.

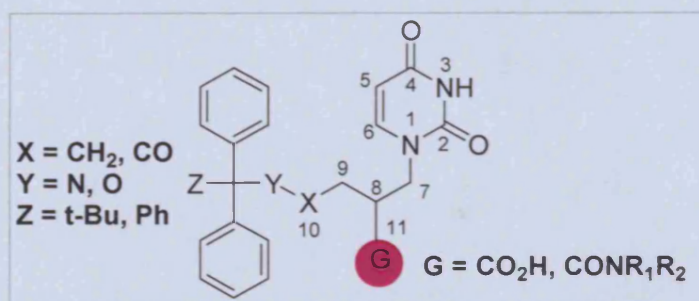


Figure 5-38: Composed proposed by GRID

Additionally, GRID calculations also suggested that the *S* enantiomer of these branched compounds would bind more favourable than the *R* enantiomer if the trityl moiety is to bind in the usual trityl binding pocket. This is due to the presence of Tyr112, sterically hindering the binding of the side of the *R* enantiomer. This theory was supported by subsequent docking studies in which many of the *R* enantiomers of the docked compounds either did not dock into the active at all or did so in a conformation in which the trityl moiety was displaced to the phosphate binding region of the active site and the side chain was positioned in the trityl binding pocket. (Figure 5-19 and 5-20)

It remains to be seen, however, whether GRID calculations and docking studies will correlate with biological data and what the implications are that result from the modifications carried out.

5.9 Conclusion

The elucidation of the crystal structure of the PfdUTPase enzyme provided an excellent chance for the use of structure based design approaches to the design of inhibitors of the PfdUTPase enzyme. GRID calculations which were carried out seemed to correlate well with docking studies using FlexX.

The syntheses of the proposed compounds proved challenging. Many oxidation procedures were attempted, eventually leading to a successful reaction. Orthogonal protecting group strategies also initially required some careful thought but finally were achieved.

Amide coupling was the final step and proved to be successful only in a few cases using the conditions reported. The reaction conditions used seemed to be quite unpredictable depending on the substrate. Purification of the final amides also proved to be problematic. However, it has been shown that the amide coupling procedure is possible, nevertheless, this crucial step requires optimisation which due to time constraints was not feasible.

6 Uracil amino acid conjugates as inhibitors of the *Trypanosoma Cruzi* dUTPase enzyme¹⁴¹

6.1 Probing of the *T. cruzi* active site

It has been shown that relative to other eukaryotic dUTPase enzymes, α,β -imido-dUTP is a strong inhibitor of the dimeric enzymes, it has therefore been proposed that the triphosphate moiety is necessary for inhibition of the dimeric enzymes.⁷³ This has been emphasised by the previously described tritylated inhibitors synthesised by the group that inhibit the trimeric enzymes but not the dimeric enzymes. As described in section 2.3.4, in contrast to the trimeric enzymes where a glycine-rich site for phosphate binding is common, the phosphates in the dimeric enzymes are held in place with hydrogen bonds to charged side chains.^{52, 65}

Although α,β -imido-dUTP inhibits the dimeric enzymes, it is not a good drug candidate as it is non-specific and would not cross the cell membrane of the parasite as it is a charged molecule. The purpose of this study was to probe the active site of the *T. cruzi* enzyme by designing libraries of potential inhibitors, docking them into the *T. cruzi* active site and comparing their docking scores as calculated by the docking programme FlexX.¹⁰⁸ The synthesis of the compounds with the lowest (largest minus) scores would then be attempted.

Analogues of the natural substrate for the enzyme, where various amino acids were in place of the tri-phosphate moiety were thought to be a good starting point for design of possible inhibitors as they had potential for a wide range of structural and functional variability and were synthetically viable. It was thought that the polar amino acids might act as good substituents, which would exert selectivity for the dimeric dUTPases due to the presence of many charged and polar residues in their phosphate binding domains compared to the trimeric forms.

¹⁴¹ Mc Carthy, O. K.; Schipani, A.; Musso Buendía, A.; Ruiz-Perez, L. M.; Kaiser, M.; Brun, R.; Gonzalez-Pacanowska, D.; Gilbert, I. H. Design, synthesis and evaluation of novel uracil amino acid conjugates for the inhibition of *Trypanosoma cruzi* dUTPase. *Bioorg. Med. Chem. Lett.* **2006**, *16*, 3809-3812.

Figure 6-1 shows the general structure of the compounds to be docked. R and R' were side chains of a number of natural amino acids, varying in size, lipophilicity and charge.

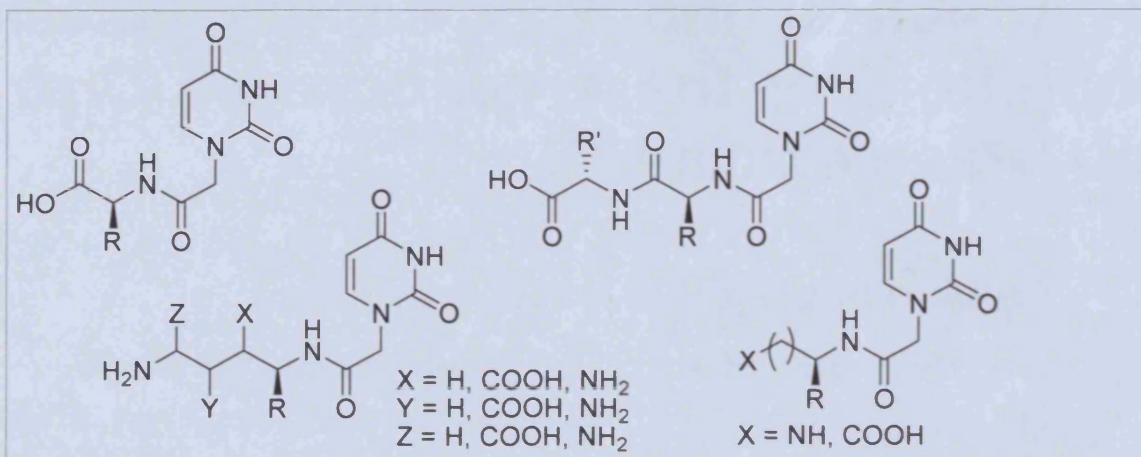


Figure 6-1: Generic structures of compounds to be docked. R, R' = various side chains of natural amino acids

The crystal structure of the dimeric *T. cruzi* dUTPase in its native and complexed form has been published.⁵² A detailed description of the secondary and tertiary structure of the enzyme can be found in section 2.3.2. In summary, the enzyme exists in two forms. With no substrate bound, the enzyme exists in an open conformation (native PDB 1OGL). Binding of the substrate induces substantial structural changes to the enzyme, causing it to bury the substrate in the enzyme core. When complexed with substrate, it therefore exists in a closed conformation (complexed PDB 1OGK).

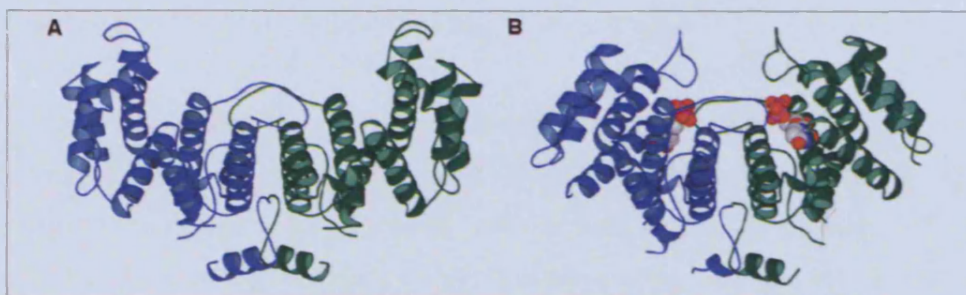


Figure 6-2: a) open (native) conformation and b) closed (complexed) conformation of the *T. cruzi* dUTPase⁵²

A detailed description of the *T. cruzi* active site, in the presence of dUDP as a substrate, is given in section 2.3.4 (Figure 2-20). The most important residues for interaction with dUDP are Asn26, Gln22 and Trp 61 which hydrogen bond to the uracil ring; Met26 which caps the uracil ring; Asn201, Phe84 and His83 which interact with the deoxyribose moiety and Trp62, Tyr209, Arg204, Lys197, Asn224, Lys216, Glu49,

Glu52 and Glu77, all of which form an intricate network of hydrogen bonds to which the phosphate groups are tightly positioned.⁵² The presence of the uracil moiety in these compounds is an essential starting point as the enzyme is very selective towards dUTP over other nucleotide bases (see Table 2-1).

6.2 Molecular modelling studies

For the purpose of this study, docking was carried out on the closed form of the enzyme as it is in this form that most of the protein – ligand interactions can be seen.

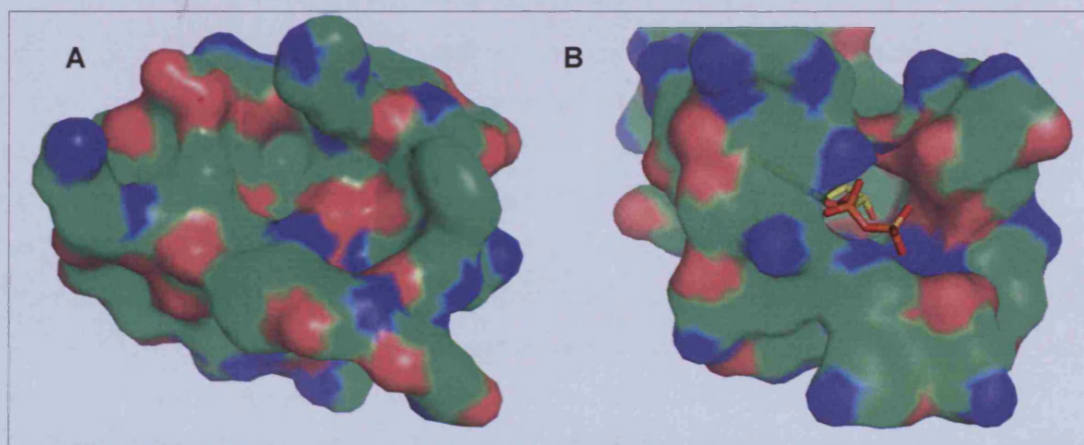


Figure 6-3: Surface representations of the TcdUTPase active sites in the A) open and B) closed forms

The presence of Mg^{2+} ions is also required for enzyme activity. The crystal structure, however, was obtained in the absence of Mg^{2+} ions to prevent substrate hydrolysis. Mg^{2+} ions are therefore not present in the docking models used.

The absence of water molecules from the receptor ligand complex is another simplification made to the docking models. This assumption was made on the basis that if water molecules are to be taken into account in the binding of the substrate to the ligand, they need to be considered as discrete entities, this strategy cannot be employed using FlexX. Additionally, a ligand which replaced bound water molecules might also be an advantage as this may actually decrease binding energy.

The most restrictive limitation of FlexX is that it does not take into account the flexibility of the protein. However, previous studies carried out in the group confirmed that FlexX was a satisfactory program for docking studies of this nature and was therefore the program used for the purpose of this study.

6.2.1 FlexX

FlexX is the docking programme used in this study. It is a programme which takes into account the flexibility of the ligand but not the receptor. The docking method it uses is based on an incremental construction algorithm.¹⁰⁸

The incremental construction strategy consists of three phases 1) base selection 2) base placement and 3) complex construction.

In the first phase a base or anchor fragment of the ligand is chosen automatically by the programme or it can be defined manually by the user.¹⁴²

The docking algorithm is quite sensitive to the selection of the base fragment as it is the core onto which the rest of the ligand is to be built. It must be large enough to make numerous and specific interactions with the protein so that a definite preference for binding orientation can be resolved. However, the larger the fragment, the more conformations in which it may exist, depending on its conformational flexibility. This increases run times significantly. The best base fragment therefore has the maximum number of interaction points and the fewest number of alternative conformations. The uracil ring was therefore the ideal selection for the base fragment as it is a small, rigid heterocycle with a fixed orientation in the active site due to a specific network of hydrogen bonds. It was manually defined as the base fragment in this case.

The placing of the base fragment uses a technique called pose clustering. The ligand is assumed to be a rigid object with defined interaction points. The interaction surface of the receptor is also represented as finite sets of interaction points. A transformation takes place by superimposing three interaction sites of the ligand onto three interaction sites of the receptor. Once all possible transformations have been identified, they are checked for angular constraints and for atom collision.

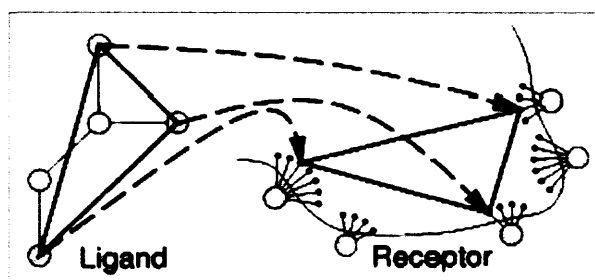


Figure 6-4: Pose clustering¹⁰⁸

¹⁴² Rarey, M.; Kramer, B.; Lengauer, T. Multiple automatic base selection: Protein-ligand docking based in incremental construction without manual intervention. *J. Comput.-Aided Mol. Des.* **1997**, *11*, 369-384.

The remaining parts of the ligand are divided up into small fragments and 'grown' onto the base fragment. The incremental construction is formulated as a tree search problem. The first sets of branches represent each partial placement of the base fragment. Each fragment is then added to each placement in the same order to produce the following sets of branches, one after another. A node in the tree represents a placement of a connected part of the ligand.

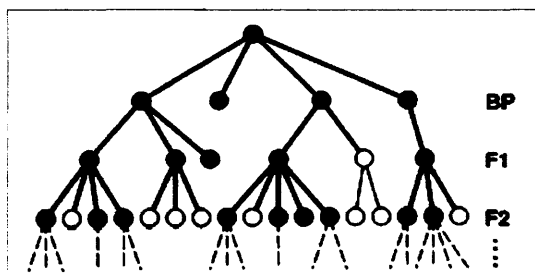


Figure 6-5: Search tree during complex construction algorithm, BP = placing of base fragment, F1 = placing of fragment 1, F2 = placing of fragment 2¹⁰⁸

A box hashing technique is used in detecting ligand receptor overlap and also in searching for new interactions. Placements are optimised using a weighted superposition of points. In this method l_i are fitted onto r_i so that $\sum w_i(l_i - r_i)^2$ is minimised where:

l_i is the interaction centre on the ligand

r_i is the interaction point on the receptor

$-w_i$ is the energy contribution of the interaction, given optimal geometry

All placements produced are ranked by energy, and in a greedy heuristic method, only the k (usually set to 500) best partial placements are used for the next step. This reduces run time and prevents the algorithm from getting stuck in local minima.

As mentioned above, FlexX takes into account the conformational flexibility of the ligand. The programme assigns a set of up to 12 preferred dihedral angles to each acyclic bond in the ligand, and systematically generates any low energy conformations of the ligand. FlexX assigns the most highly populated dihedral angles for each fragment according to the Cambridge Structural Database.

Both the interaction type and scoring function used by FlexX are based on work by Böhm and Klebe.¹⁴³ An interaction type (Table 6-1) and an interaction geometry is assigned to each interacting group of the molecule. The interaction geometry consists of the interaction centre c , an interaction radius r , and an interaction surface which has

¹⁴³ Böhm, H.-J. The development of a simple empirical scoring function to estimate the binding constant for a protein-ligand complex of known three-dimensional structure. *J. Comput.-Aided Mol. Des.* **1994**, *8*, 243-256.

the shape of a sphere, cone, capped cone or spherical rectangle and has radius r around c (Figure 6-6). An interaction between two groups A and B is formed if 1) the interaction types of A and B are compatible and 2) The interaction centre of A lies approximately on the interaction surface of B and vice versa.

Interaction group (A)	Complimentary interaction group (B)
H-acceptor	H-donor
Metal acceptor	Metal
Aromatic-ring atom, methyl, amide	Aromatic-ring-centre

Table 6-1: Interaction types in FlexX

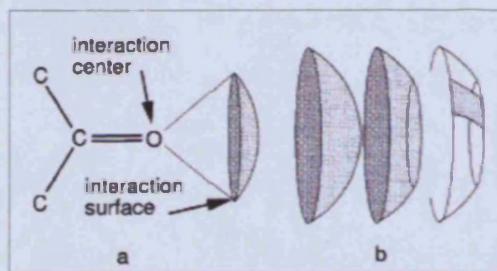


Figure 6-6: Interaction geometries in FlexX

The scoring function used to rank solutions is an estimate of the free binding energy ΔG of the protein-ligand complex. The equation is as follows:¹⁰⁸

$$\Delta G = \Delta G_0 + \Delta G_{rot} \times N_{rot} + \Delta G_{hb} \sum_{\text{neutral H-bonds}} f(\Delta R, \Delta \alpha) + \Delta G_{io} \sum_{\text{ionic int.}} f(\Delta R, \Delta \alpha) + \Delta G_{aro} \sum_{\text{aro. int.}} f(\Delta R, \Delta \alpha) + \Delta G_{lipo} \sum_{\text{lipo. cont.}} f'(\Delta R)$$

N_{rot} is the number of rotatable bonds that are immobilized in the complex

ΔG_0 , ΔG_{rot} , ΔG_{hb} , ΔG_{io} are adjustable parameters taken as developed by Bohm¹⁴³

ΔG_{aro} accounts for the interactions of aromatic groups, and is set to -0.7 kJ/mol

ΔG_{lipo} is a modified term that is calculated as a pairwise sum over all atom-atom contacts

$f(\Delta R, \Delta \alpha)$ is a scaling function that penalizes deviations from ideal geometry

$$\Delta R = R - R_0$$

R is the distance between the atom centres

R_0 is the ideal value, which is assumed to be the sum of both van der Waals radii plus 0.6Å

As with any docking programme, FlexX has limitations. The most severe restriction placed on FlexX is receptor rigidity. The advantage however is greatly reduced run times and it can be regarded as a reasonable approximation where the input structure is given in the bound state.

FlexX is limited to medium sized ligands. This is a limitation resulting from the greedy heuristic strategy used. Assumptions that become more and more unrealistic as the number of fragments increases. It has been shown, however, that ligands with 17 rotatable bonds are manageable. This number is sufficient for most practical purposes in drug design and certainly for the purpose of this study.

6.2.2 Results and discussion of docking studies

6.2.2.1 Docking study 1

Compounds with the following generic structure were docked into the closed form of the *T. cruzi* dUTPase active site. In this study amino acids of various sizes and lipophilic character were used to investigate steric tolerance. (Figure 6-7)

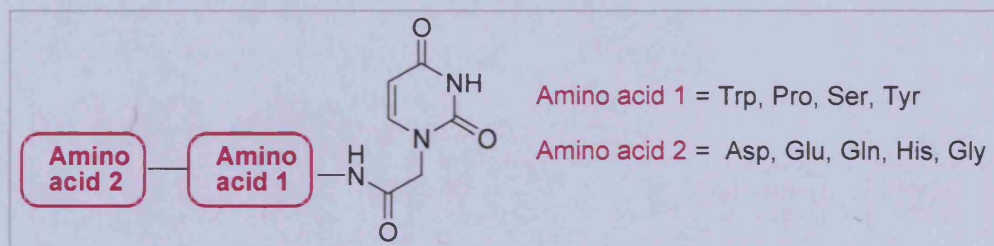


Figure 6-7: Compounds docked in docking study 1

Results showed that only amino acids with small side chains were tolerated in amino acid position 1. All compounds except compound **98** docked outside the active site as their side chains were too bulky.

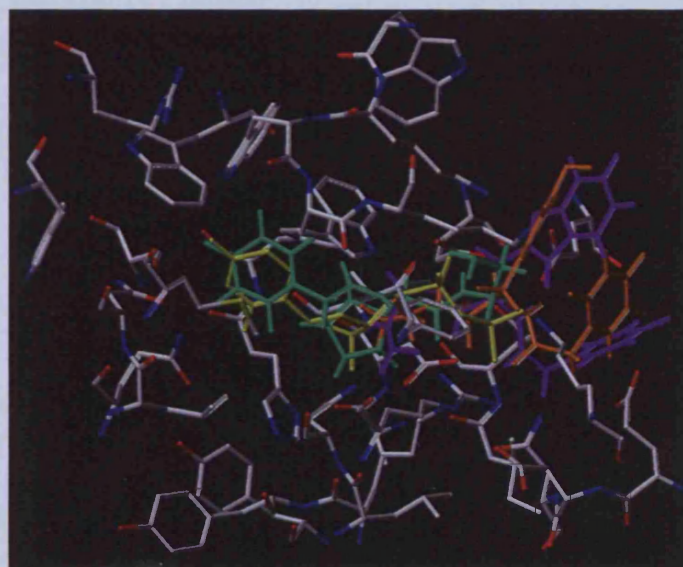
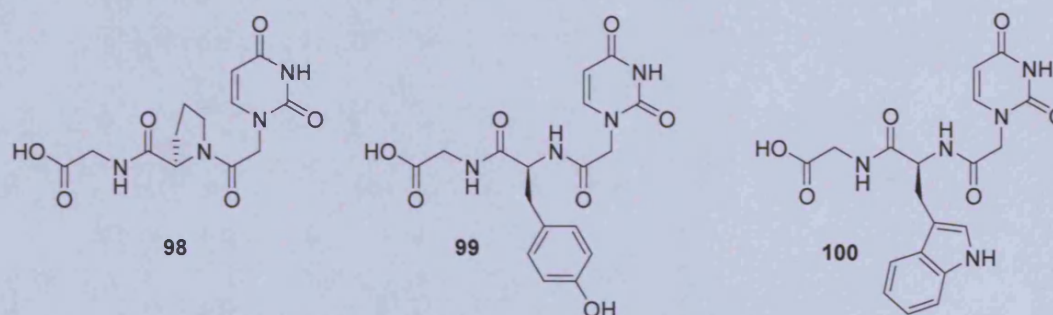


Figure 6-8: Superimposition of some of the compounds docked in docking study 1. dUDP (yellow), 98 (green), 99 (orange), 100 (violet)

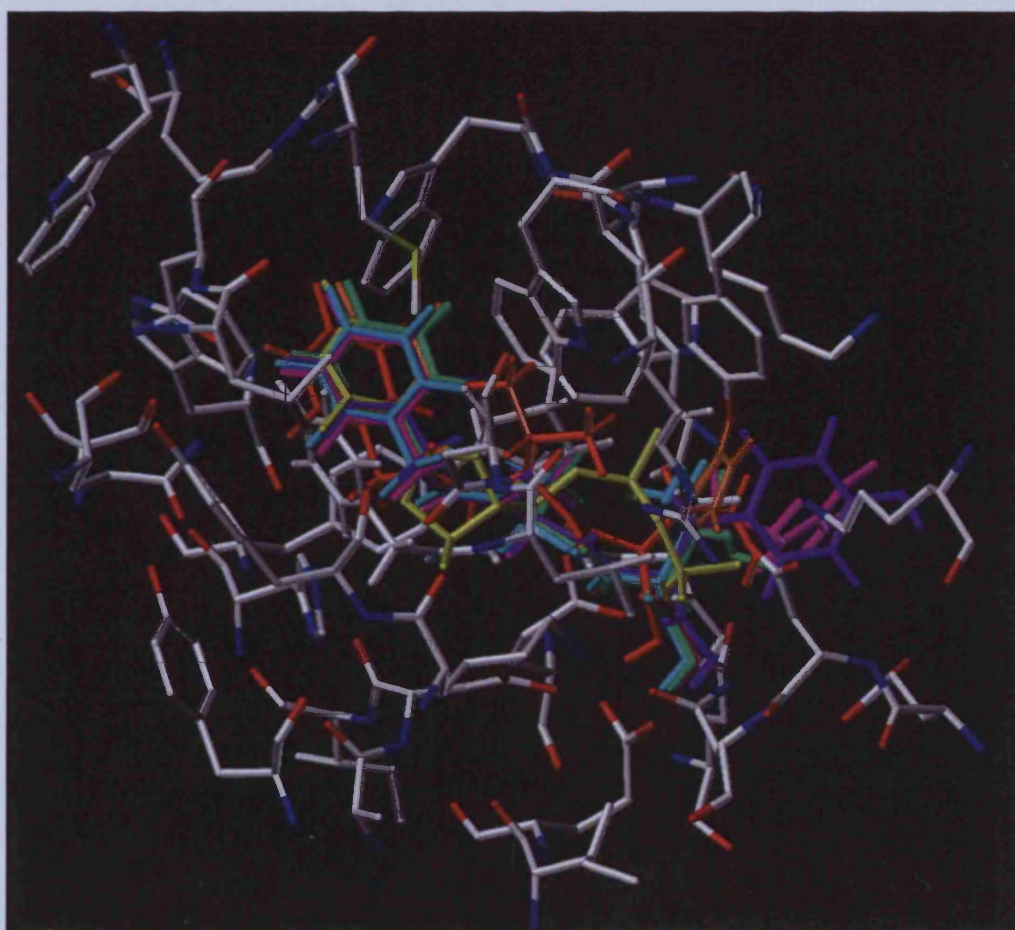
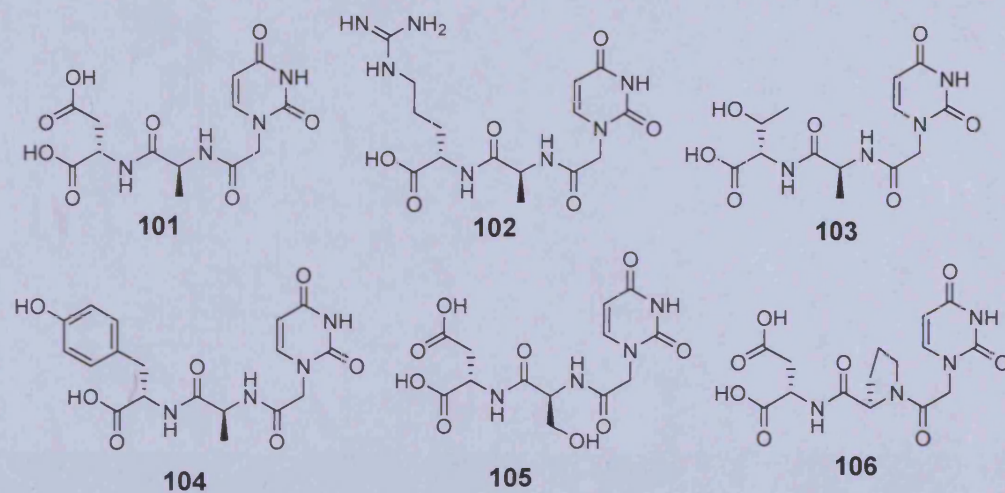


Figure 6-10: Docking study 2a. Superimposition of some of the best scoring compounds docked in docking study 2. dUDP (yellow), 101 (green), 102 (magenta), 103 (orange), 104 (purple), 105 (red/orange), 106 (white)

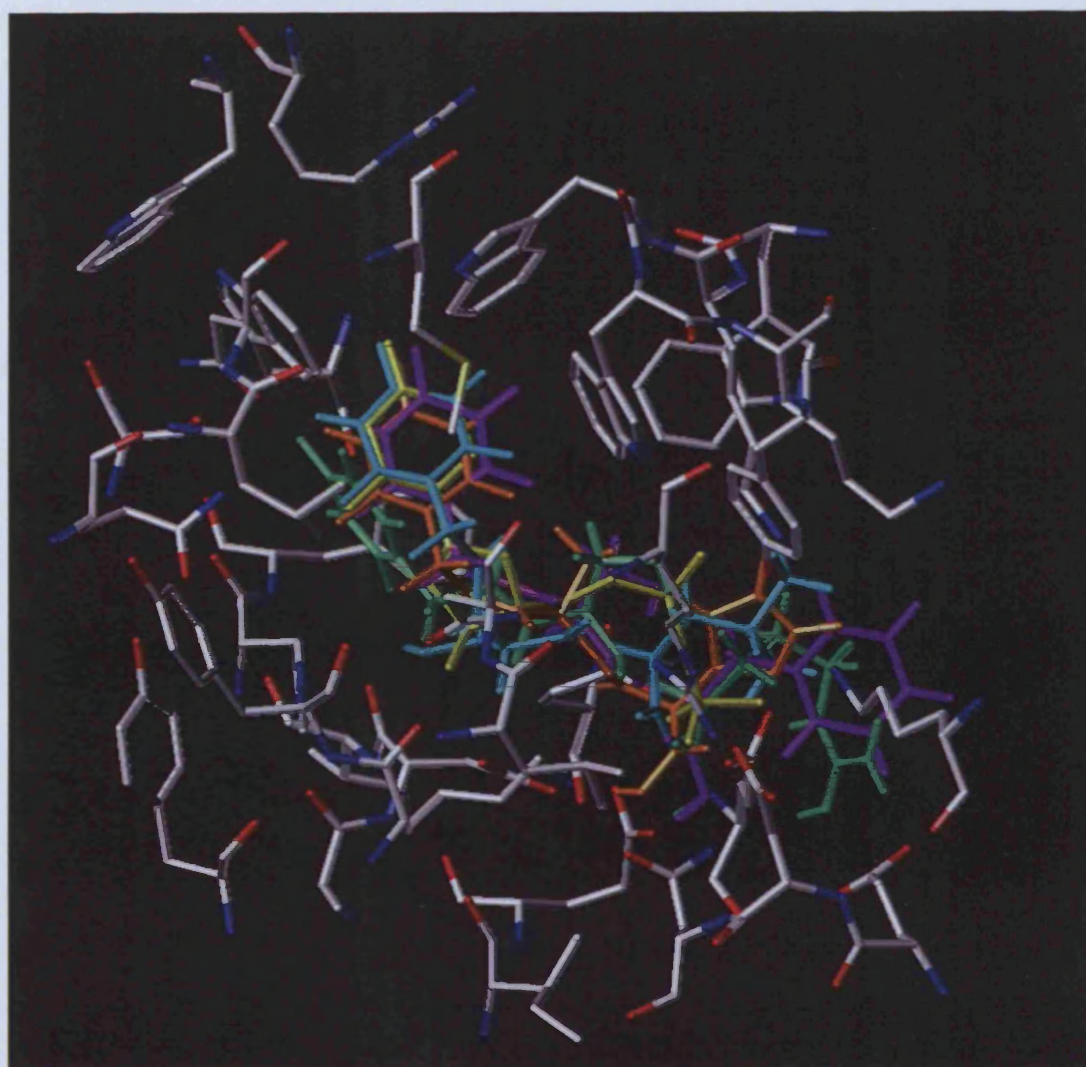
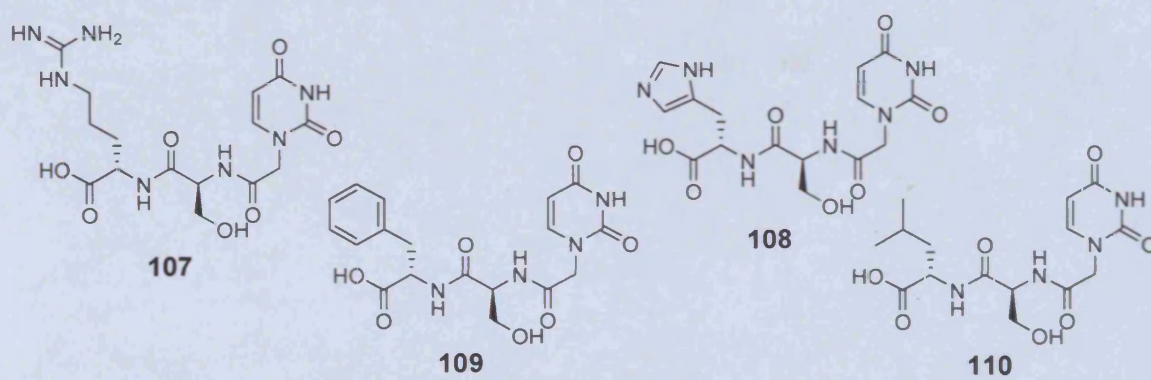


Figure 6-11: Docking study 2b. Superimposition of some of the best scoring compounds docked in docking study 2. dUDP (yellow), 107 (green), 108 (orange), 109 (violet), 110 (cyan)

6.2.2.3 Docking study 3

In the third docking study, optimal chain length and charge was investigated. The terminal group was either a simple amino acid with no side chain or an unbranched diamine of various chain length. The following structures were docked into the active site of the enzyme.

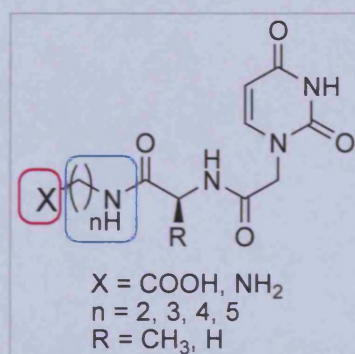


Figure 6-12: Generic structure of compounds docked in docking study 3

Results showed that compounds with $n=3$ had the best superimposition over the natural dUDP substrate and mimicked best the dUDP size. Where $n=4/5$, however, the chain terminus could extend out to within interaction distance of a Lys, Asn and Arg side chain in the active site. The best scoring compounds had carboxylic acid terminals. This was probably due to the interaction with either the Arg or Asn residue which was common to all of the ligands containing the carboxylic group and which would alter the calculated energy favourably.

Compound	X	n	R	Score (-)	Compound	X	n	R	Score (-)
126	COOH	3	CH ₃	37.9	132	NH ₂	2	CH ₃	32.6
127	COOH	4	CH ₃	37.1	133	NH ₂	3	CH ₃	30.7
128	COOH	5	CH ₃	36.9	134	NH ₂	4	CH ₃	29.9
129	COOH	2	CH ₃	32.8	135	NH ₂	5	CH ₃	26.3
130	COOH	4	H	36.7	136	COOH	3	H	32.3
131	NH ₂	3	H	35.1	137	NH ₂	4	H	31.7

Table 6-3: Docking scores of compounds docked in docking study 3

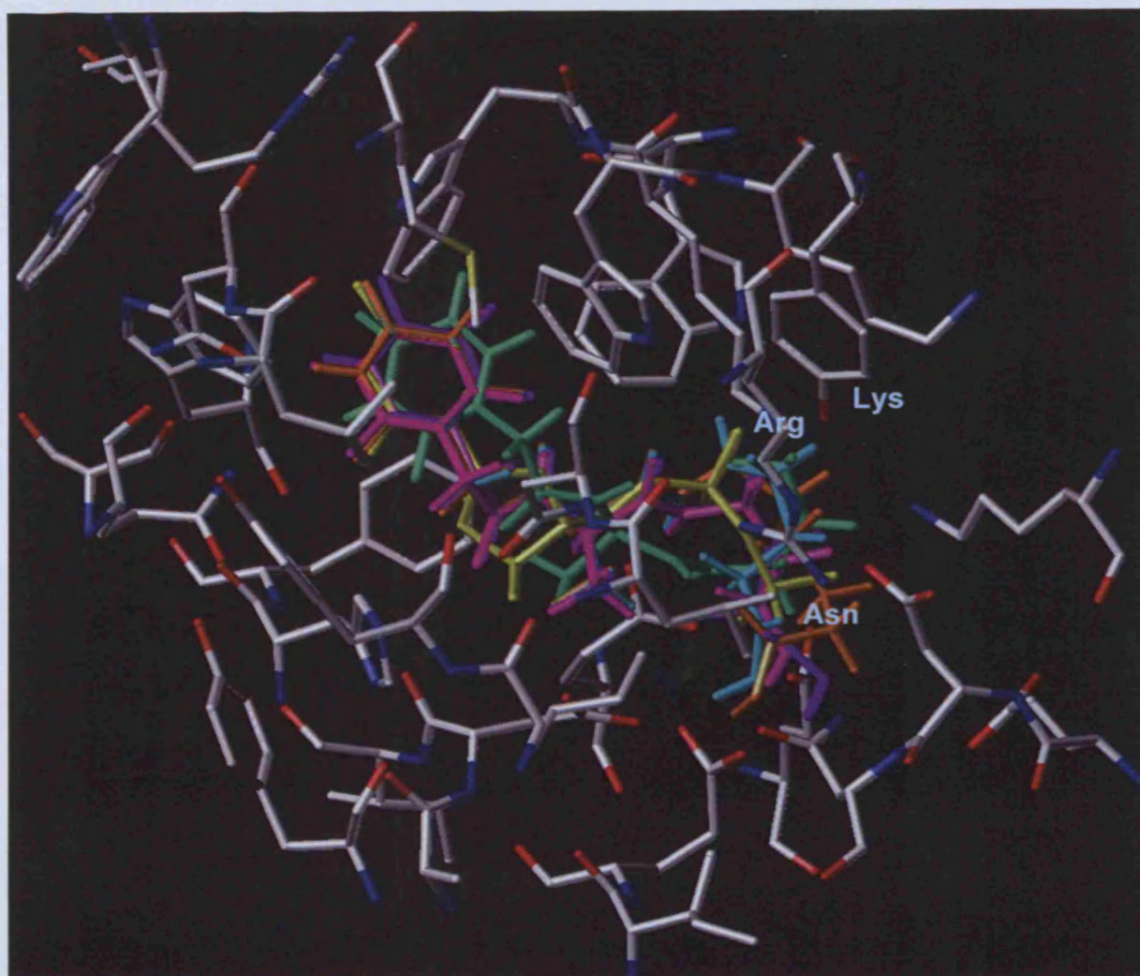


Figure 6-13: Superimposition of some compounds docked in docking study 3. dUDP (yellow), 132 (green), 129 (orange), 126 (violet), 127 (cyan), 128 (magenta)

6.2.2.4 Docking study 4

To further probe for interactions around the *T. cruzi* dUTPase active site, compounds with the following generic structure were docked into the closed form of the enzyme. Although the structures of these compounds deviated quite considerably from the amino acid backbone previously used, it was thought that comparatively it would prove interesting to investigate the effect of changing positions of positively or negatively charged side chains.

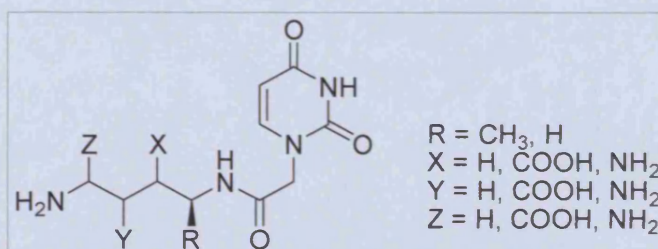


Figure 6-14: Generic structure of compounds docked in docking study 4

These compounds docked with the lowest (highest minus) scores and also had the best superimposition in the docking studies performed. In general, the docking scores improved when X = COOH or Y = COOH or X = Y = COOH, supporting the fact that a terminal COOH group was advantageous for binding.

Comp.	X	Y	Z	R	Score (-)	Comp.	X	Y	Z	R	Score (-)
138	H	CO ₂ H	CO ₂ H	CH ₃	45.0	150	H	CO ₂ H	NH ₂	H	46.9
139	H	CO ₂ H	NH ₂	CH ₃	45.3	151	H	NH ₂	CO ₂ H	H	46.4
140	CO ₂ H	H	H	CH ₃	41.5	152	H	H	CO ₂ H	H	44.3
141	CO ₂ H	CO ₂ H	H	CH ₃	41.0	153	CO ₂ H	NH ₂	H	H	44.1
142	NH ₂	CO ₂ H	H	CH ₃	39.1	154	CO ₂ H	CO ₂ H	H	H	43.6
143	H	H	CO ₂ H	CH ₃	36.8	155	CO ₂ H	H	H	H	42.3
144	NH ₂	H	CO ₂ H	CH ₃	35.9	156	NH ₂	CO ₂ H	H	H	41.9
145	H	NH ₂	CO ₂ H	CH ₃	35.9	157	H	CO ₂ H	H	H	41.5
146	H	CO ₂ H	H	CH ₃	35.1	158	CO ₂ H	H	NH ₂	H	40.0
147	CO ₂ H	H	NH ₂	CH ₃	34.4	159	NH ₂	H	CO ₂ H	H	37.1
148	CO ₂ H	H	CO ₂ H	CH ₃	26.2	160	CO ₂ H	H	CO ₂ H	H	35.5
149	H	CO ₂ H	CO ₂ H	H	50.6						

Table 6-4: Docking scores of compounds docked into active site in docking study 4

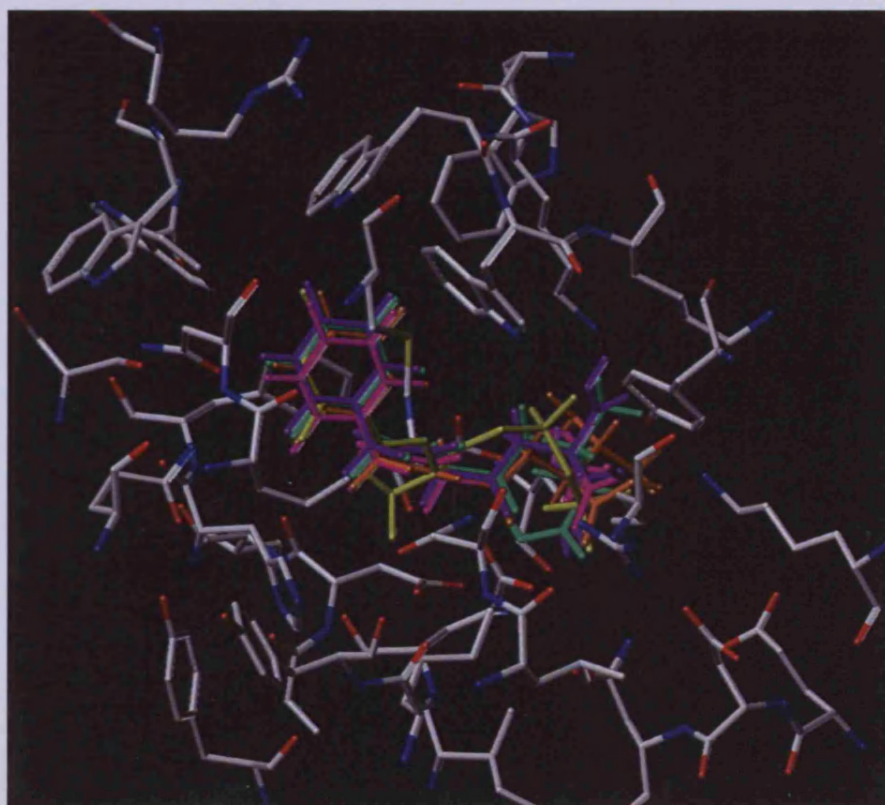


Figure 6-15: Superimposition of some of the compounds docked in docking study 4. dUDP (yellow), 136 (green), 135 (orange), 134 (violet), 142 (magenta)

6.2.2.5 Docking study 5

For comparison, the best scoring compounds were docked into the open form of the *T. cruzi* enzyme. Their superimposition was measured by manually placing the dUDP ligand in the active site with the same coordinates as those given for the complexed form. However, the scores obtained were very low. None of the compounds docked with superimposition over the natural ligand dUDP and many compounds did not dock inside the active site at all and produced no conformations.

Compound	Score (-)	Compound	Score (-)
127	26.8	137	19.7
134	23.9	150	19.2
111	22.3	101	18.6
113	22.3	139	18.4
102	21.4	128	17.7
159	21.1	138	17.3
143	20.1	147	12.9
107	19.9		

Table 6-5: Docking scores from attempted docking into open form of active site

6.3 Solid phase amino acid uracil acetamide synthesis

Following molecular modelling and docking studies as discussed previously, amino acid uracil acetamide derivatives were synthesised to investigate their anti-parasitic action and inhibitory activity against dUTPase enzymes, especially against that of the *T. cruzi* parasite.

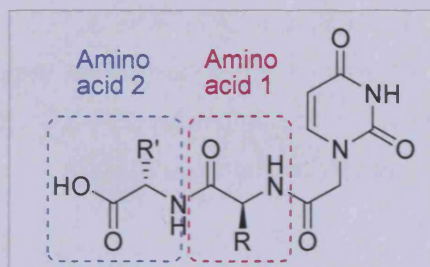


Figure 6-16: General structure of amino acid uracil acetamide conjugates

These amino acid uracil conjugates are similar to PNAs (peptide nucleic acids) which are oligonucleotides with peptide bonds in place of the sugar and phosphate backbone. They are normally synthesised as DNA mimics and can bind sequence specifically to DNA and RNA. They have several unique properties and much of the methodology utilised for their synthesis could be applied to these compounds.^{144, 145, 146}

To synthesise these compounds, a solid phase combinatorial strategy was used (Scheme 6-1). Solid phase peptide synthesis was first introduced by Merrifield¹⁴⁷ and the general concept depends on the attachment of the substrate to a solid, insoluble and filterable polymer. The advantages of this method include ease of purification and possibility of semi-automation resulting in combinatorial libraries being synthesised in a short amount of time.

Wang resin was chosen for its ability to attach carboxylic acids and to release them again under acidic conditions milder than those needed for Merrifield resin.¹⁴⁸

¹⁴⁴ Nielsen, P. E.; Egholm, M.; Berg, R. H.; Buchardt, O. Sequence-Selective Recognition of DNA by Strand Displacement with a Thymine-Substituted Polyamide. *Science* **1991**, *254*, 1497-1500.

¹⁴⁵ Kosynkina, L.; Wang, W.; Liang, C. T. A convenient synthesis of chiral peptide nucleic acid(PNA) monomers. *Tetrahedron Lett.* **1994**, *35*, 5173-5176.

¹⁴⁶ Corradini, R.; Sforza, S.; Dossena, A.; Palla, G.; Rocchi, R.; Filira, F.; Nastri, F.; Marchelli, R. Epimerization of peptide nucleic acids analogs during solid-phase synthesis: optimization of the coupling conditions for increasing the optical purity. *J. Chem. Soc., Perkin Trans. 1* **2001**, *1*, 2690-2696.

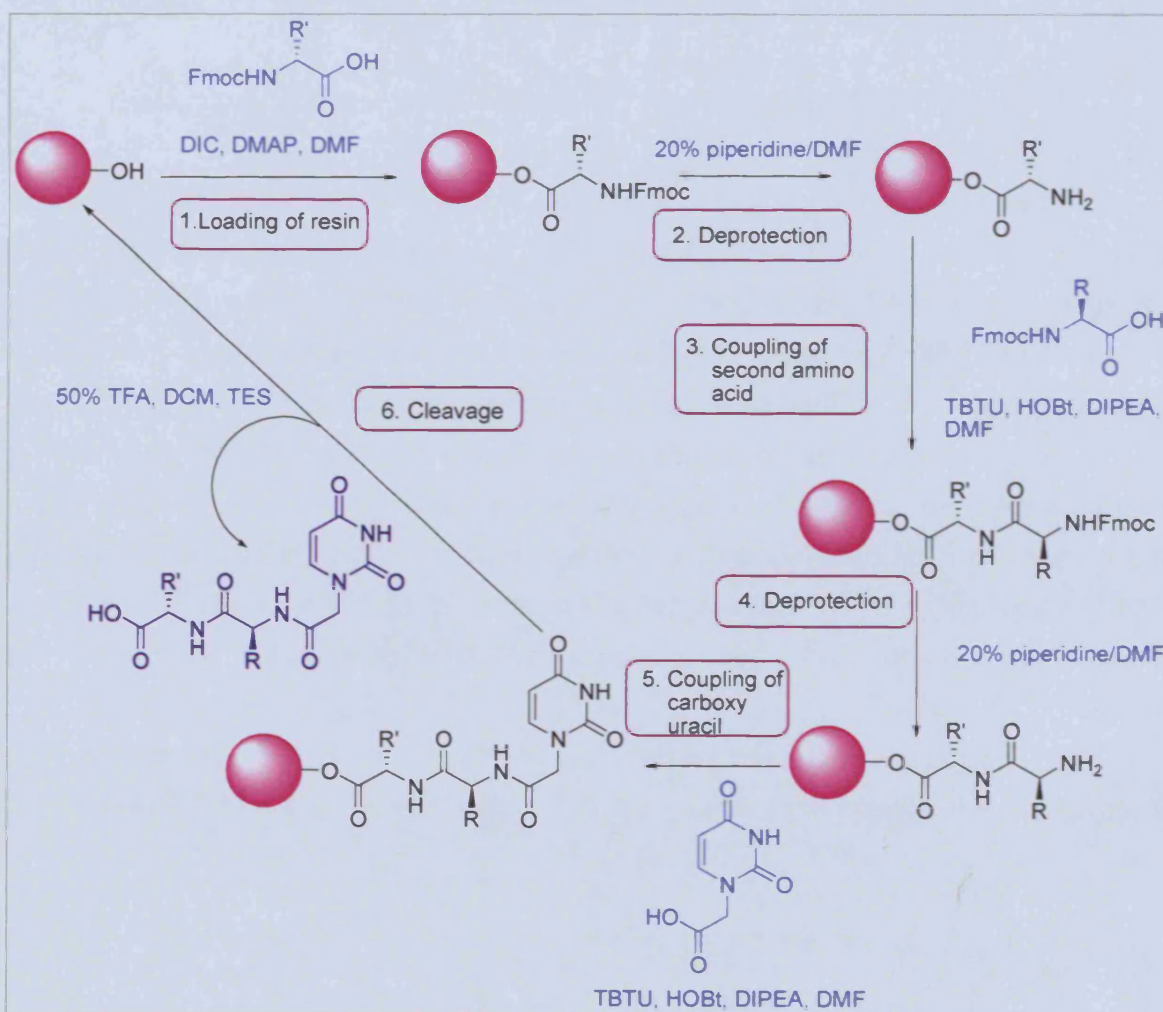
¹⁴⁷ Merrifield, R. B. Solid Phase Synthesis. I. The synthesis of a Tetrapeptide. *J. Am. Chem. Soc.* **1963**, *85*, 2149-2154.

¹⁴⁸ Wang, S.-S. Solid phase synthesis of protected peptide hydrazides. preparation and application of hydroxymethyl resin and 3-(*p*-benzyloxyphenyl)-1,1-dimethylpropyloxycarbonylhydrazide resin. *J. Org. Chem.* **1975**, *40*, 1235-1239.

All amino acids used were protected at the N positions by the base labile 9-fluorenylmethyl-oxycarbonyl (Fmoc) group to control the coupling reactions.

The side chains of the amino acids used were orthogonally protected with acid labile groups (*tert*-butyl for Asp, Glu, Thr and Tyr, Boc for Orn and Lys, Pbf for Arg and Trt for Asn, Gln and His) that were simultaneously cleaved by TFA upon cleavage of the product from the resin beads.

A semi-automated procedure was used where 16 compounds could be made at once. Reaction vials were placed in a modified shaker. A peristaltic pump was utilised to pump solvents through all vials simultaneously. Concurrent filtration was also achieved using a waste or collecting manifold and suction.



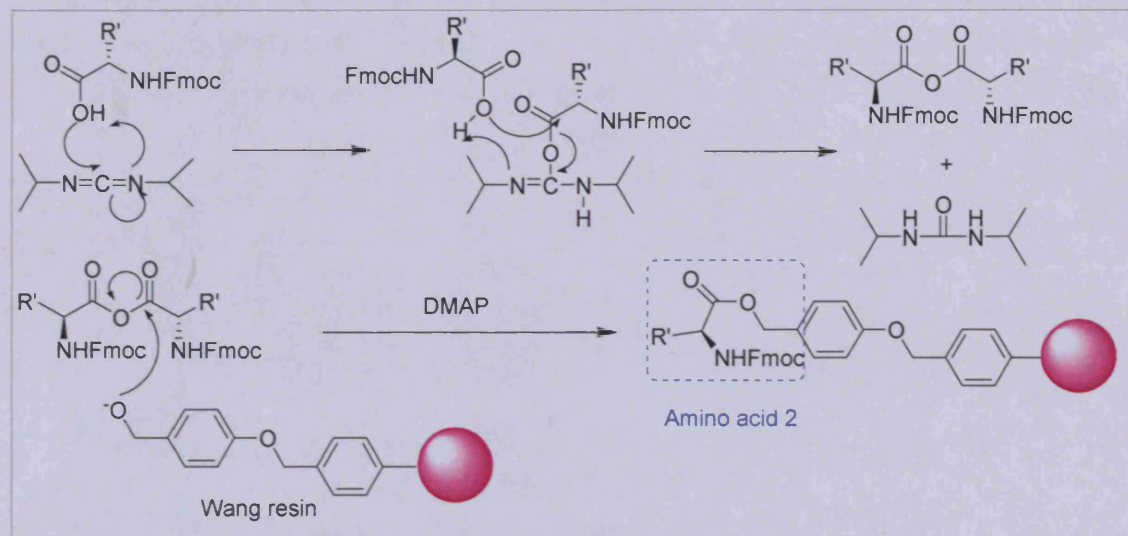
Scheme 6-1: Overview of solid phase synthetic strategy

6.3.3 Loading of resin

DIC/DMAP is used in this esterification reaction. The reaction proceeds via formation of the anhydride as shown in Scheme 6-2.

The resin must first be swelled in DMF before the reagents were added. This is essential for the free access of the functional groups to the polymer. The less the

reaction space is restricted by the polymeric support of the beads, the more favourable the reaction conditions and the higher the loading obtained.¹⁴⁹



Scheme 6-2: Loading of the resin

6.3.3.1 Estimation of level of first residue attachment

The resin loading (mg amino acid attached/g resin) was estimated manually. There are a number of reasons for this. The precise amount of functionality on the resin is not given by the manufacturer. Only a wide range of pre-measured loading values are given. The number of hydroxyl groups or reaction centres exposed on the surface of the beads may vary due to swelling conditions or amount of resin, therefore the quantity of first amino acid that becomes attached may vary.

An Fmoc UV absorbance test was used to monitor the attachment of the first amino acid to the resin. A weighed amount of resin was placed in a quartz cuvette in a solution of 20% piperidine in DMF. Under these conditions the Fmoc protected group of the attached amino acid is cleaved and its UV absorbance of the resulting dibenzofulvene (DBF) at 290nm is measured. Using the equation:

$$\text{Fmoc loading: mmole/g} = (\text{Abs}) / (1.65 \times \text{mg resin})^{150}$$

The Fmoc and therefore amino acid attachment can be calculated.

Conditions	Calculated resin loading (mg/g)
1 Hour (DMAP present)	0.03-0.16
Overnight (no DMAP)	0.35-0.51
Overnight (DMAP present)	0.8-1.2

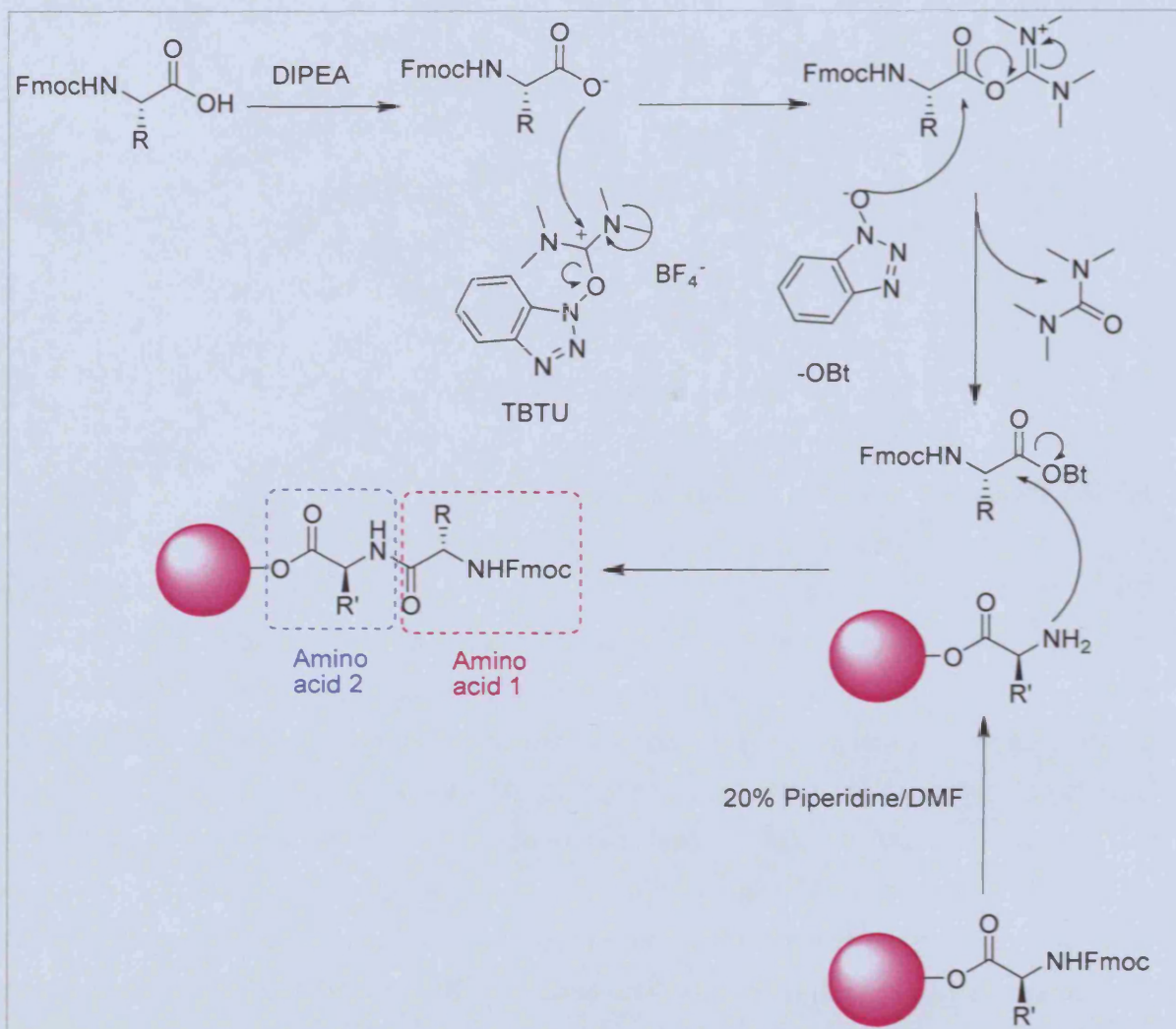
Table 6-6: Calculated resin loadings

Therefore the resin was loaded in the presence of DMAP overnight.

¹⁴⁹ Bayer, E. Towards the chemical synthesis of proteins. *Angew. Chem.* **1991**, *30*, 113-216.

6.3.4 Coupling to amino acids

Deprotection of the Fmoc protecting group was achieved by treating the derivatised resin beads with 20% piperidine in DMF. Subsequently coupling of the second amino acid was carried out using TBTU/ HOBt as coupling reagents.¹⁵¹ A proposed mechanism of activation is as follows:

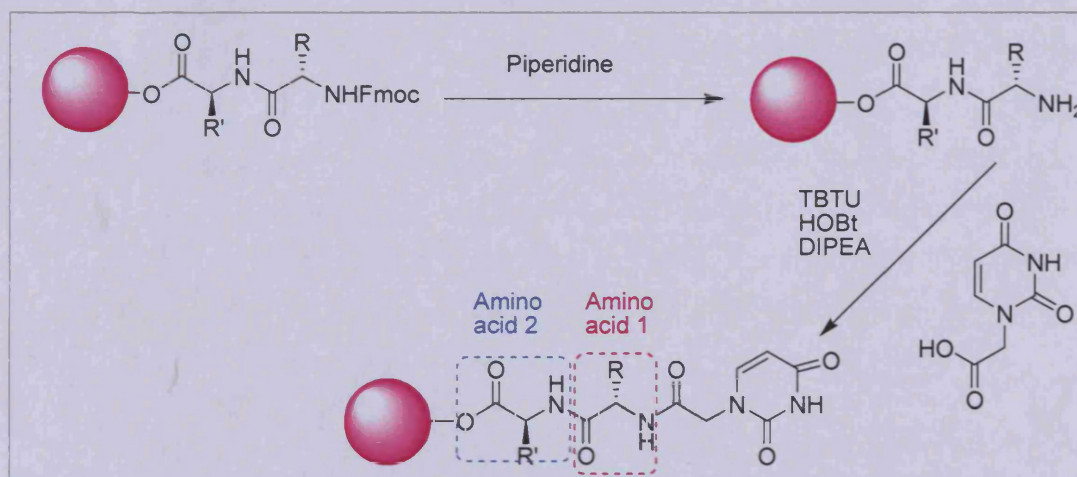


Scheme 6-3: Proposed mechanism of activation/coupling by TBTU/HOBt/DIPEA combination

Following a second deprotection step, 1-carboxymethyl uracil was then coupled on to the derivatised resin. The TBTU/HOBt/DIPEA method was again used. Coupling using the EDC method was also attempted, however, the ninhydrin test was positive (blue), indicating that a free amine was still present and that the coupling was not successful.

¹⁵⁰ Merck Bioscience 2002/2003, *Novabiochem catalogue*

¹⁵¹ Knorr, R.; Trzeciak, A.; Bannwarth, W.; Gillissen, D. New Coupling Reagents in Peptide Chemistry. *Tetrahedron Lett.* 1989, 30, 1927-1930.



Scheme 6-4: Coupling of carboxyuracil

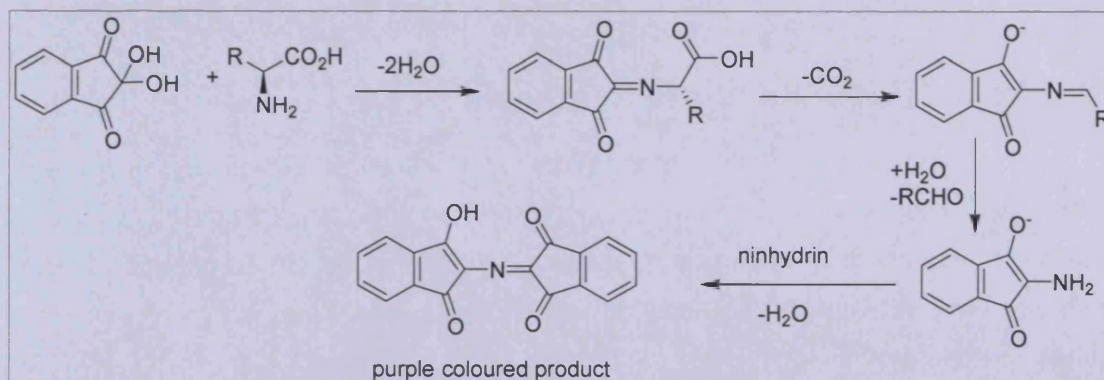
6.3.5 Monitoring of the reactions

One of most difficult problems encountered in solid phase synthesis is the monitoring of the reactions. The progress of the reactions cannot be assessed by conventional TLC, mass spec or NMR without first cleaving the product from the resin beads. Therefore different procedures must be used.

The deprotection and coupling reactions were monitored using a modified ninhydrin test. This is a simple colour change test, which can detect the presence or absence of free amines on the beads.¹⁵²

Deprotection of amino groups was monitored with a positive (blue resin beads) test, indicating that free amino groups were present. Coupling reactions were monitored with a negative (pink beads) test, showing all of the amino groups had reacted.

The ninhydrin reaction proceeds as follows:



Scheme 6-5: Mechanism of the ninhydrin test

¹⁵² Sarin, V., K.; Kent, S., B. H.; Tam, J., P.; Merrifield, R. B. Quantitative Monitoring of Solid-Phase Peptide Synthesis by the Ninhydrin Reaction. *Anal. Biochem.* **1981**, *117*, 147-157.

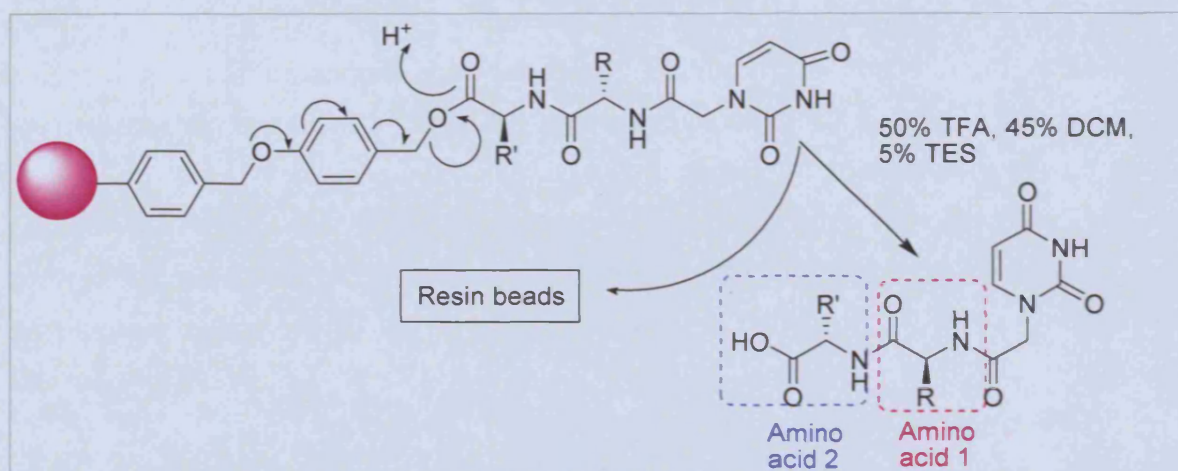
6.3.6 Cleavage from the resin beads

Wang resin is cleaved under acidic conditions. As standard cleavage procedures of 95% TFA in DCM¹⁵⁰ seemed to cause excess cleavage of peptide bonds in the molecule and resulted in undesired products, the cleavage conditions had to be optimised. Different cleavage conditions were attempted.

Cleavage procedure	Time (mins)	Conditions
Cleavage procedure A	60	95% TFA, 2.5% TES, 2.5% DCM
Cleavage procedure B	30	95% TFA, 2.5% TES, 2.5% DCM
Cleavage procedure C	60	50% TFA, 5% TES, 45% DCM
Cleavage procedure D	60	50% TFA, 2.5% TES, 47.5% DCM
Cleavage procedure E	30	50% TFA, 2.5% TES, 47.5% DCM

Table 6-7: Cleavage conditions attempted

50% trifluoroacetic acid (TFA) with the presence of a small amount of 5% triethylsilane (TES) as an alkyl scavenger in DCM (cleavage procedure C) was found to be the optimal conditions for release of the desired products^{147, 153} which were subsequently precipitated from cold ether after removal of the solvent *in vacuo*.



Scheme 6-6: Cleavage from resin beads

6.3.7 Results of solid phase synthesis

The compounds were characterised by low resolution and high resolution mass spectrometry and ¹H NMR. Compounds of greater than 90% purity, as evaluated by ¹H-NMR were submitted for biological evaluation. Only 11 of the 24 compounds whose syntheses were attempted were isolated in sufficient quantity and purity for biological assays.

¹⁵³ Pearson, D. A.; Blanchette, M.; Baker, M. L.; Guindon, C. A. Trialkylsilanes as Scavengers for the Trifluoroacetic acid Deblocking of protecting Groups in Peptide Synthesis. *Tetrahedron Lett* **89**, 30, 2739-2742.

Some of the compounds synthesised were not included in the docking studies but were synthesised never the less for comparative studies.

Compound	Amino acid 1	Amino acid 2	No. times synthesis attempted	Outcome
101	Ala	Asp	3	Tested in biological assays
102	Ala	Arg	3	No product isolated. NMR showed a mixture of carboxyuracil and compound 165
103	Ala	Thr	3	Tested in biological assays
104	Ala	Tyr	2	Tested in biological assays
111	Ala	His	2	Detected by mass spec but insufficiently pure by ¹ H NMR (peaks in 1-1.5ppm)
112	Ala	Phe	1	No product isolated, just carboxyuracil
113	Ala	Asn	3	Detected by mass spec but insufficiently pure by ¹ H NMR *
161	Ala	Gln	3	Tested in biological assays
162	Ala	Orn	1	Detected by mass spec but insufficiently pure by ¹ H NMR *
163	Ala	Lys	4	Tested in biological assays
164	Ala	Glu	4	Tested in biological assays
165	Ala	-	2	Detected by mass spec but insufficiently pure by ¹ H NMR *
166	Ala	Gly	1	Tested in biological assays
120	Gly	Asp	4	No product isolated, just carboxyuracil
121	Gly	Asn	3	No product isolated. NMR showed a mixture of carboxyuracil and compound 172
123	Gly	His	3	No product isolated. NMR showed a mixture of carboxyuracil and compound 172
124	Gly	Thr	3	Tested in biological assays
125	Gly	Arg	1	No product isolated
167	Gly	Gln	2	Detected by mass spec but insufficiently pure by ¹ H NMR *
168	Gly	Tyr	2	Tested in biological assays
169	Gly	Glu	4	Detected by mass spec but insufficiently pure by ¹ H NMR *
170	Gly	Orn	2	No product isolated, just carboxyuracil
171	Gly	Lys	3	Tested in biological assays
172	Gly	-	2	Tested in biological assays

Table 6-8: Compounds synthesised by solid phase methodology. * NMR showed a mixture of product, carboxyuracil and either compound 165 or 172

6.4 Biological results: Dimeric dUTPases and trypanosome parasites

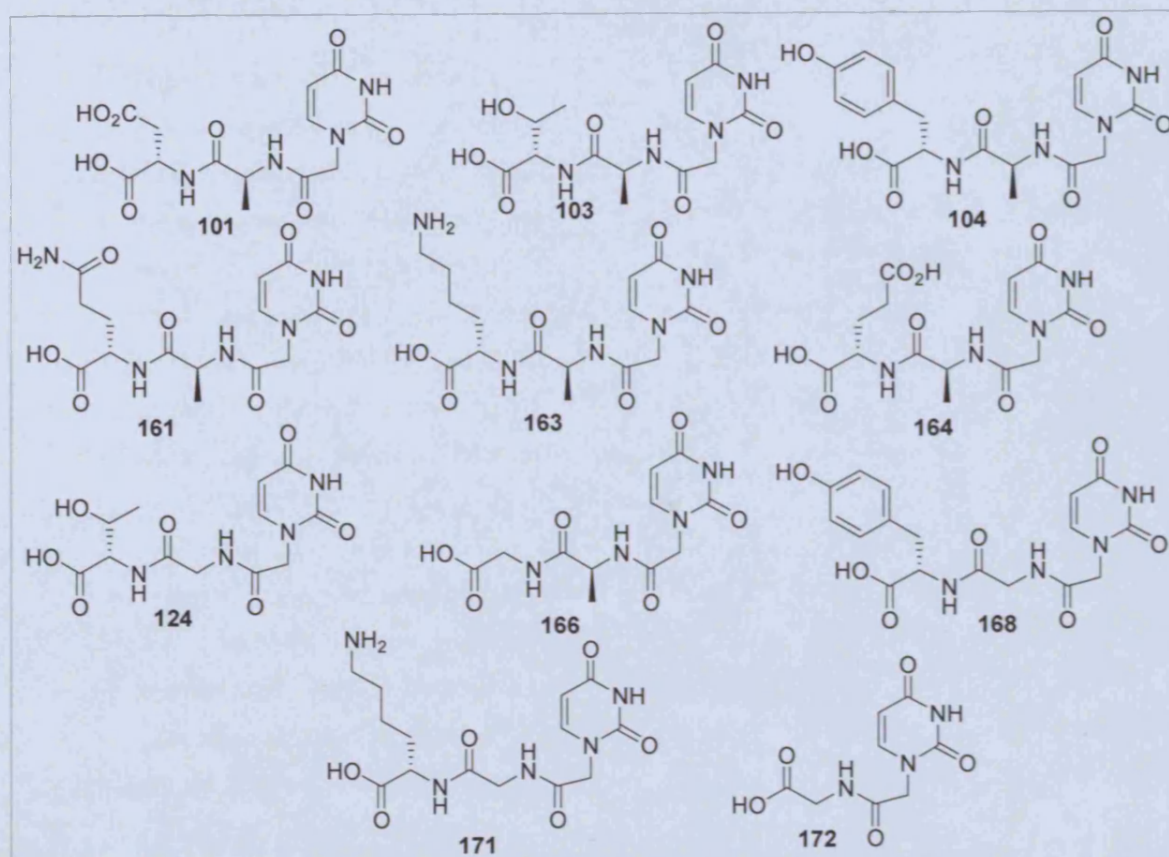


Figure 6-17: Uracil amino acid conjugates

Compound	Enzyme assays ($K_i = \mu\text{M}$)				<i>In vitro</i> assays ($\text{IC}_{50} = \mu\text{M}$)				
	<i>T. cruzi</i>	<i>L. maj.</i>	<i>P. falc.</i>	Hum.	<i>T. cruzi</i>	<i>T. bruc.</i>	<i>L. don.</i>	<i>P. falc</i>	Tox. ^a
101	>1mM	>1mM	>1mM	>1mM	>84	>252	>84	>84	>252
103	>1mM	>1mM	>1mM	>1mM	>87	>262	>87	>14	>262
104	>1mM	>1mM	>1mM	>1mM	>74	>222	45.8	>12	214.4
161	>1mM	>1mM	>1mM	>1mM	>81	>243	>81	>14	>243
163	>1mM	>1mM	>1mM	>1mM	>81	>243	>81	>13	>243
164	>1mM	>1mM	>1mM	>1mM	>81	>243	37.0	>13	210.4
166	>1mM	>1mM	>1mM	>1mM	>100	>301	69.7	>16	>301
124	>1mM	>1mM	>1mM	>1mM	>91	>274	>91	>15	>274
168	>1mM	>1mM	>1mM	>1mM	>76	>230	>76	>12	>230
171	>1mM	>1mM	>1mM	>1mM	>84	>253	>84	>14	>253
172	>1mM	>1mM	>1mM	>1mM	>132	>396	95.1	>22	>396
Standard	18.40 ^b	13.05 ^b	0.38 ^c	-	1.04 ^d	0.008 ^e	0.16 ^f	0.14 ^g	0.15 ^e

Table 6-9: Biological results of the uracil amino acid conjugates against the dimeric dUTPases and *in vitro* results against the trypanosome parasites. ^aToxicity tests were carried out on rat L6 cells ^bdUMP ^cDMT-dU ^dBenznidazole ^eMelarsoprol ^fMiltefosine ^gChloroquine ^ePodophyllotoxin

6.4.8 Results and discussion

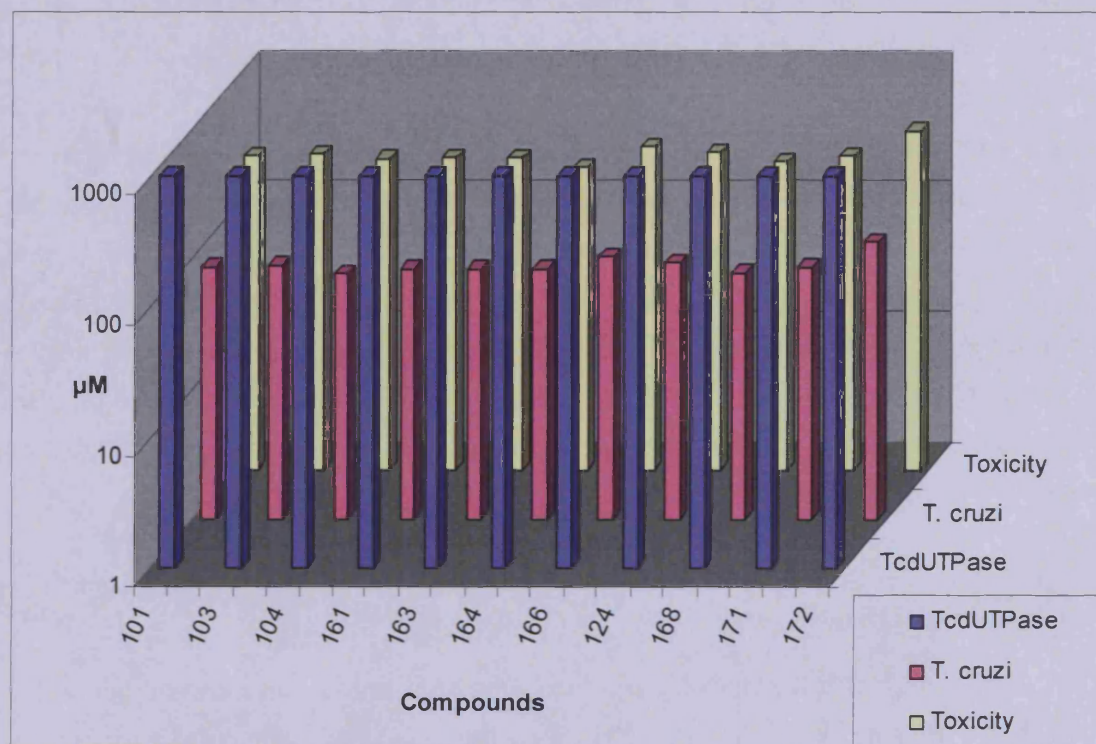


Figure 6-18: Inhibitory activity of the uracil amino acid conjugates against the dimeric enzymes and *T. cruzi* parasite

As can be seen from Table 6-9, none of the uracil amino acid conjugates synthesised inhibited the TcdUTPase enzyme at a concentration of 1mM. Neither did the compounds inhibit parasite growth at the maximum concentrations shown. In this case, molecular modelling studies did not correlate with biological data. There may be a number of possible reasons for this outcome.

Recently, the crystal structure of the dimeric *Campylobacter jejuni* dUTPase revealed the coordination of Mg^{2+} ions within the active site of the enzyme.⁶⁵ These ions are absent in the TcdUTPase crystal structure and it is unclear whether these Mg^{2+} ions are bound to the native enzyme but it is possible that the presence of these ions must be taken into account when designing inhibitors *in silico*.

As previously mentioned, FlexX does not take into account the flexibility of the protein in question. Although this approximation reduces run time significantly, in this case where binding of the ligand induces a large conformational change in protein structure it is possible that a docking program in which protein flexibility is taken into account should be used. It would be extremely challenging for a program to cope with the conformational flexibility shown by the dimeric dUTPases, however.

It is possible that for the dimeric dUTPases, the presence of the triphosphate moiety is essential for substrate or inhibitor binding itself. Two mechanisms of binding could be envisaged. Firstly, the uracil and deoxyribose moieties which bind to motifs from the rigid domain of protein would be recognised. The α , β and subsequently γ phosphates, which are recognized by mobile domain motifs, would then bond to the Mg^{2+} ions and respective amino acid side chains sequentially and induce 'active site closure'. Alternatively, the phosphate moieties would be recognised by the mobile domain first and then the protein would undergo such a conformational change as to encapsulate the uracil and sugar moieties. In the latter case, the phosphate moieties would be more essential for ligand recognition and therefore replacement of them would be detrimental to ligand recognition. This would explain the lack of activity of the uracil amino acid conjugates.

6.5 Conclusion

Following molecular docking and modelling studies that were carried out on the TcdUTPase enzyme using the program FlexX, several uracil amino acid conjugates were successfully synthesised by solid phase methodology. The sufficiently pure compounds were then tested for inhibition of the TcdUTPase and of parasite growth by our collaborators. Disappointingly, none of the compounds tested inhibited the dimeric dUTPase at concentrations greater than 1mM, nor did they inhibit parasite growth. Thus, the search so far for lead inhibitors of the dimeric dUTPase enzymes remains unsuccessful.

Molecular modelling studies did not correlate with biological data in this case. Many theoretical reasons may be envisaged for this. Ultimately, however, it is obvious from experimental biological data that the uracil amino acid compounds do not possess the required structure to bind to the open form of the enzyme sufficiently enough to induce the conformational change required for inhibition. Although the compounds docked with good superimposition and favourable binding energies into the TcdUTPase active site with FlexX, it is apparent that other factors such as protein flexibility and the presence of Mg^{2+} ions should be taken into account when designing competitive inhibitors for these enzymes *in silico*.

7 Conclusions

This project was divided into two main studies; firstly, the modification of known and selective inhibitors of the trimeric PfdUTPase in an effort to increase their potency for use as anti-malarials; secondly, the structure based design and synthesis of potential lead inhibitors of the dimeric TcdUTPase for use as trypanocides.

7.1 Trimeric PfdUTPase inhibitors for use as anti-malarials

The introduction of an amide bond into the scaffold of previously discovered selective inhibitors of the *Plasmodium falciparum* dUTPase led to the synthesis of a range of uracil acetamide derivatives. It was thought that through amide coupling methodology, a wide range of functional variability could be introduced to these molecules and therefore this modification would be advantageous for diversification studies and ultimately to increase the potency of our inhibitors.

Series of single chain and branched chain tritylamino and hydroxyl derivatised uracil acetamides were successfully synthesised. Selective protection and deprotection of polyamines and subsequent coupling to 1-methylcarboxy uracil was carried out to yield a wide range of these derivatives.

Unfortunately, these compounds were not potent inhibitors of the dUTPase enzymes. Introduction of an amide bond at the β -C to the N-1 of the uracil ring resulted in a loss of activity against the PfdUTPase enzyme. Molecular modelling and conformational studies showed that this may have been due to the fact that the low energy conformation of the uracil acetamide compounds must overcome an energy barrier to adopt the required binding conformation. Additionally, there may be an unfavourable interaction between the O-2 of the uracil ring and the carbonyl oxygen of the amide bond in the proposed bound conformation leading to a decrease in potency of these compounds.

The uracil acetamide compounds do retain good activity *in vitro*. Their mode of action has not yet been ascertained, nonetheless, it is known that the presence of the uracil ring and the trityl or TBDPS moieties are required for activity.

Following the elucidation of the crystal structure of the PfdUTPase enzyme with a known inhibitor bound, structure based drug design approaches utilising this information were employed. Attention was focused on known branched, acyclic PfdUTPase inhibitors as a starting point for further inhibitor development. Molecular probe interaction calculations carried out by GRID, followed by docking studies gave rise to some observations that were utilised in the design of potentially more potent dUTPase inhibitors. The synthesis of the proposed modified compounds was carried out from intermediates kindly provided by Medivir and the successfully synthesised compounds were submitted for biological evaluation, the results of which are being awaited.

7.2 Dimeric TcdUTPase inhibitors as trypanocides

The crystal structure of the dUTPase from *Trypanosoma cruzi* revealed that the enzyme undergoes an extremely significant conformational change on ligand binding. In the unliganded form, the active site is large and exposed relative to that of the liganded conformation in which the substrate is effectively buried by the active site. No selective inhibitors of this enzyme were known.

Molecular docking and modelling studies were therefore carried out on the closed form of the TcdUTPase enzyme using the program FlexX, leading to the design of several uracil amino acid conjugates that docked with good superimposition over the natural ligand and seemed to bind in the active site. Some of these compounds were successfully synthesised by solid phase methodology. The sufficiently pure compounds were then tested for inhibition of the TcdUTPase and of parasite growth. Disappointingly, none of the compounds tested inhibited the dimeric dUTPase at concentrations greater than 1mM, nor did they inhibit parasite growth. Thus, the search so far for lead inhibitors of the dimeric dUTPase enzymes remains unsuccessful.

Molecular modelling studies did not correlate with biological data in this case. Many theoretical reasons may be envisaged for this. Ultimately, however, it is obvious from experimental biological data that the uracil amino acid compounds do not possess the required structure to bind to the open form of the enzyme sufficiently enough to induce the conformational change required for inhibition. Although the compounds docked with good superimposition and favourable binding energies into the TcdUTPase active site with FlexX, it is apparent that other factors such as protein flexibility and the presence of Mg²⁺ ions should be taken into account when designing competitive inhibitors for these enzymes *in silico*.

8 Experimental I

8.1 General remarks

IR spectra were recorded at an FT-IR spectrometer 1600 from Perkin Elmer using the Diffuse Reflectance Accessory from Spectra Tech. (Refl.) and a potassium bromide pellet (KBr). The band positions were characterised by their wave numbers (ν/cm^{-1}) and assignment. (For IR values obtained *w*= weak strength signal, *m*= medium strength signal, *s* = strong signal)

Mass spectra were recorded at a Platform II mass spectrometer (Micromass) from Fisons, a Mariner mass spectrometer or at a MicroTOF mass spectrometer from Bruker Daltonics where ionisation was achieved in the positive and negative electrospray modes using a 1:1 mixture of acetonitrile and water plus 0.2% formic acid or a 95:5 mixture of methanol and water plus 0.2% formic acid as a mobile phase. *m/z* Values are given together with the assignment of ion peaks. High resolution mass spectra were recorded by the National Mass Spectrometry Service Centre in Swansea at a MAT 900 XLT high resolution double focussing mass spectrometer from Finnigan or by University of Birmingham at a Micromass LCT spectrometer. High resolution mass spectra were also recorded at a MicroTOF mass spectrometer from Bruker Daltonics. Accurate mass measurement was performed by peak matching.

¹H-NMR spectra were recorded at a Bruker 300 MHz NMR spectrometer or at a Bruker 500 MHz NMR spectrometer using the applied solvent simultaneously as internal standard. Chemical shifts (δ) are given in ppm together with the multiplicity, relative frequency, assignment and the coupling constants ($nJ(\text{H,H})/\text{MHz}$) of the observed signals. Chemical shifts for AB-systems are directly deduced from Mestre-C free software or Bruker Topspin programme. (For NMR values given *s* = singlet, *d* = doublet, *t* = triplet, *q* = quartet, *qn* = quintet, *m* = multiplet, *br* = broad)

¹³C-NMR spectra were recorded at a Bruker 300 MHz spectrometer or at a Bruker 500 MHz spectrometer using the applied solvent simultaneously as internal standard. Chemical shifts (δ) are given in ppm. Chemical shifts for AB-systems are directly deduced from Mestre-C free software or Bruker Topspin programme.

Purification by **column chromatography** was performed on Sorbosil C60A silica gel-40-60 μm from Merck. Flash chromatography was performed using the Flashmaster II from Jones Chromatography and Isolute® propylene columns which were prepacked with silica. Qualitative thin layer chromatography (TLC) was done on precoated aluminium sheets Silica gel 60 F254 from Merck. Compounds were detected either with ninhydrin, bromocresol green, iodine, KMnO_4 or 254 nm UV light.

Elemental analysis was carried out by the analytical and chemical consultancy services MEDAC LTD. Found percentage values are reported together with calculated values for different salt compositions as indicated by the preceding formula.

Melting points were determined with a Gallenkamp melting point apparatus and are not corrected.

Solvents and reagents were purchased from Sigma-Aldrich, Fluka or Lancaster and were used without further purification. Dry solvents were purchased in sure sealed bottles stored over molecular sieves. Deuterated solvents were purchased from Goss. Resins and amino acids were purchased from Novabiochem.

All **molecular modelling** was carried out on a silicon graphics work station or a Mac OS using SYBYL 6.9 or 7.2. **GRID** calculations were carried out on a windows operating system using software obtained from Molecular Discovery.

The numbering and nomenclature system used for the drawn structures in the following chapters is to aid NMR interpretation and is not effectively referring to IUPAC nomenclature.

8.2 General procedures

General procedure A: *tert*-Butyl diphenyl silylation of hydroxyl group using DMF and imidazole

TBDPSiCl (1.1 eq.) dissolved in DMF (0.2 mL/mmol) was added to a mixture of imidazole (2.2 eq.) and the alcohol (1 eq.) dissolved in DMF (0.1 mL/mmol) under N₂ or Ar atmosphere. The mixture was left stirring at RT until the disappearance of the starting material was observed by TLC.

General procedure B: *tert*-Butyl diphenyl silylation of hydroxyl group using pyridine

TBDPSiCl (1.1 eq.) dissolved in pyridine was added to the alcohol (1 eq.) dissolved in pyridine. The solution was stirred at RT under N₂ or Ar atmosphere until the disappearance of the starting material was observed by TLC.

General method C: EDC mediated coupling to form amide bonds

1-Carboxyuracil **1** (1.3 eq.) and EDC (1.4 eq.) dissolved in DMF (2 mL/mmol) was added to the amine (1 eq.) under N₂ or Ar atmosphere. The reaction was left at RT, usually overnight. The solvent was evaporated off and the crude purified by column chromatography.

General procedure D: Mono-tritylation of diamines

TrtCl (0.1 eq.) dissolved in DCM (2.5 mL/mmol) was added to the diamines in DCM (0.1 mL/mmol) and left stirring under N₂ at RT overnight. The mixture was poured into 50 mL ice water and extracted with ether (1 x 100 mL, 2 x 50 mL). The organic layer was washed with water (2 x 50 mL), brine (1 x 50 mL) and dried with MgSO₄. The solvent was evaporated off. The product was purified by flash chromatography.

General procedure E: Carbobenzoxy protection of terminal NH groups of triamines

The relevant triamine (1 eq.) and DMAP (0.2 eq.) were dissolved in DCM (0.7 mL/mmol). **23** (2 eq.) in DCM (1 mL/mol) was added under N₂ atmosphere. The reaction was left stirring overnight at 50°C. The solvent was evaporated off under reduced pressure and the product purified by flash chromatography.

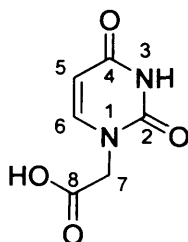
General procedure F: Removal of the Cbz protecting group by hydrogenation

5% Pd/C (0.1eq w/w) was preactivated with hydrogen in a round bottomed flask using a hydrogen balloon. The relevant protected amine dissolved in either MeOH or a 1:1 mixture of MeOH:EtOH was added. The mixture was flushed with hydrogen three times using a hydrogen balloon and finally left stirring under hydrogen until the disappearance of the starting material was observed by TLC. The catalyst was removed by filtration after flushing the system with N₂.

General procedure G: Removal of the silyl protecting group using TBAF

The relevant silyl protected alcohol was stirred in a solution of TBAF in THF (1M, 2.0mL/mmol eq) at RT until the disappearance of the starting material was observed by TLC.

8.3 (1) Synthesis of 1-carboxymethyluracil⁸⁰



Uracil (2.98 g, 26.64 mmol), chloroacetic acid (4.41g, 47.67mmol) and KOH (6.57 g, 117.12 mmol) were dissolved in 100 mL water and refluxed for 1h. The reaction mixture was cooled to room temperature and acidified to pH 2 with HCl (32% w/w in water). The mixture was left at 4°C overnight. The white precipitate formed was collected by filtration and washed with water (50 mL), ethanol (50 mL) and EtOAc (50 mL) to afford 3.16g of the product as a white powder.

Yield: 71%

Melting point: 287-290°C (Lit. 287°C⁸⁰)

R_f: 0.1 in CHCl₃/MeOH, 9:1

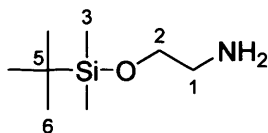
IR : (KBr)v_{max}/cm⁻¹ 3082.2 (*m*, OH), 1698.0 (*s*, CO₂H), 1402.6 (*m*, OH bending), 1280.8 (*m*, CO), 845.9 (*m*, ring CH)

¹H-NMR: (300 MHz, DMSO) δ 4.43 (2 H, *s*, C(7)H₂), 5.60 (1 H, *d* *J*=7.9, C(5)H), 7.62 (1 H, *d* *J*=7.9, C(6)H), 11.35(1 H, *s*, N(3)H), 13.13 (1 H, *br*, OH)

¹³C-NMR: (75 MHz, DMSO) δ 49.4 (C-7), 101.7 (C-5), 146.9 (C-6), 151.9 (C-2), 164.7(C-4), 170.4 (C-8)

LRMS (ES⁻): *m/z* = 168.8 [M-H]⁻

8.4 (3) Synthesis of 2-(*tert*-butyldimethylsilyloxy)-ethylamine



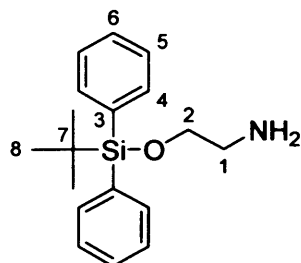
TBDMSiCl (2.47 g, 16.39 mmol) dissolved in DMF (4 mL) and imidazole (2.90 g, 42.61 mmol) were added to 1,2-ethanolamine (1.0 g, 16.39 mmol) under N₂ atmosphere. The reaction was left for 7 h at RT. The mixture was poured into 200 mL water and extracted with EtOAc (300 mL). The crude product was washed with 5% NaHCO₃ (50 mL) and dried with Na₂SO₄. The solvent was removed *in vacuo* and the product purified by column chromatography (CH₂Cl₂/MeOH 9:1). The product was isolated in low yield as a clear oil. (<250mg).

Yield: <10%

R_f: 0.5 in CHCl₃/MeOH, 9:1

¹H-NMR: (300 MHz, MeOD) δ 0.10 (6 H, s, 2 x C(3)H₃), 0.90 (9 H, s, 3 x C(6)H₃), 2.65 (2 H, m, C(1)H₂), 3.58 (2 H, m, C(2)H₂)

8.5 (4) Synthesis of 2-(*tert*-butyldiphenylsilyloxy) ethylamine



Compound **4** was prepared according to the general procedure A using TBDPSiCl (4.50 g, 18.59mmol), imidazole (2.91 g, 42.61mmol) and ethanolamine (1.00 g, 16.39 mmol) The reaction was repeated according to general procedure B using TBDPSiCl (3.90 g, 36.07mmol) and ethanolamine (2.00 g, 32.79 mmol) in pyridine (20 mL) The solvent was removed *in vacuo*. The crude was purified by flash chromatography (CH₂Cl₂/MeOH/NH₃100:0:0→95:4:1) to yield a yellow oil (3.7g for procedure B and 3.4g for procedure A)

Yield: 35% (method A), 38% (method B)

Melting point: 104-106°C

R_f: 0.5 in CH₂Cl₂/MeOH/NH₃ 95:4:1

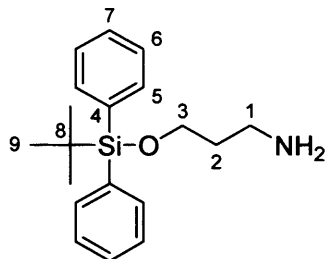
¹H-NMR: (300 MHz, MeOD) δ 1.10 (9 H, s, 3 x C(8)H₃), 2.76 (2 H, t J= 5.6 C(1)H₂), 3.70 (2 H, t J=5.6 C(2)H₂), 7.39-7.71 (10 H, m, 4 x C(4)H, 4 x C(5)H, 2 x C(6)H)

¹³C-NMR: (75 MHz, MeOD) δ 20.4 (C-7), 27.8 (3 x C-8), 44.9 (C-1), 66.9 (C-2), 129.2 (4 x C-5), 131.3 (2 x C-6), 135.1 (4 x C-4), 137.0 (2 x C-3)

LRMS (ES⁺): m/z= 300.2 [M+H]⁺, 600.3 2[M+H]⁺

HRMS (ES⁺): Found: 300.1792 [M+H]⁺ C₁₈H₂₆ONSi requires 300.1778

8.6 (5) Synthesis of 3-(*tert*-butyldiphenylsilyloxy)-propylamine



Compound **5** was synthesised according to the general procedure A using TBDPSiCl (12.10 g, 44.00 mmol), imidazole (6.00 g, 88.00 mmol) and 1-amino-3-propanol (3.00 g, 40.00 mmol). The mixture was poured into water (150 mL) and extracted with EtOAc (2 x 100 mL). The organic layer was washed with NaHCO₃ (100 mL), dried with MgSO₄ and the solvent was removed *in vacuo*. The product was purified by flash chromatography (CH₂Cl₂/MeOH/NH₃ 100:0:0→95:4:1) as a colourless oil (0.81 g).

Yield: 7%

R_f: 0.3 in CH₂Cl₂/MeOH/NH₃ 90:8:2

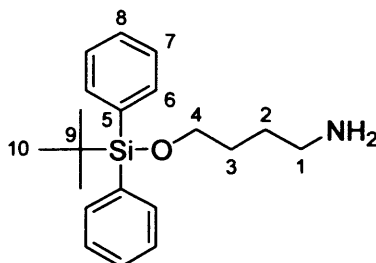
¹H-NMR: (300 MHz, MeOD) δ 0.95 (9 H, s, 3 x C(9)H₃), 1.71 (2 H, qn *J*= 6.5, C(2)H₂), 2.78 (2 H, t *J*=6.5, C(1)H₂), 3.73 (2 H, t *J*=6.5, C(3)H₂), 7.36 (10 H, m, 4 x C(5)H, 4 x C(6)H, 2 x C(7)H)

¹³C-NMR: (75 MHz, MeOD) δ 20.5 (C-8), 27.9 (3 x C-9), 36.5 (C-2), 40.3 (C-1), 63.6 (C-3), 129.3 (4 x C-6), 131.4 (2 x C-7), 135.2 (4 x C-5), 136.7-137.4 (2 x C-4)

LRMS (ES⁺): *m/z*= 314.2 [M+H]⁺, 627.9 2[M+H]⁺

HRMS (ES⁺): Found: 314.1935 [M+H]⁺ C₁₉H₂₈ONSi requires 314.1935

8.7 (6) Synthesis of 4-(*tert*-butyldiphenylsilyloxy)-butylamine



Compound **6** was synthesised according the general procedure A using TBDPSCI (10.19 g, 37.07 mmol), imidazole (5.08 g, 74.14 mmol) and 1-amino-4-butanol (3.00 g, 33.70 mmol). The mixture was poured into water (150 mL) and extracted with EtOAc (200 mL). The organic layer was washed with NaHCO₃, dried with MgSO₄ and the solvent was removed *in vacuo*. The product was purified by flash chromatography (CH₂Cl₂/MeOH/NH₃ 100:0:0→95:4:1) as a colourless oil (1.52 g).

Yield: 14%

R_f: 0.2 in CH₂Cl₂/MeOH/NH₃ 90:8:2

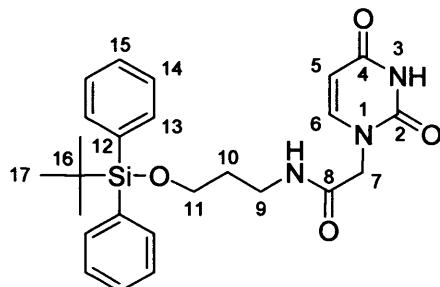
¹H-NMR: (300 MHz, MeOD) δ 1.05 (9 H, s, 3 x C(10)H₃), 1.61 (4 H, m, C(2)H₂, C(3)H₂), 2.63 (2 H, t J=6.7 C(1)H₂), 3.69 (2 H, m, C(4)H₂), 7.36-7.60 (10 H, m, 4 x C(7)H, 2 x C(8)H), 4 x C(6)H)

¹³C-NMR: (75 MHz, MeOD) δ 20.5 (C-9), 27.9 (3 x C-10), 30.5 (C-2), 31.5 (C-3) 42.8 (C-1), 65.0 (C-4), 129.3 (4 x C-7), 131.3 (2 x C-8), 135.3 (4 x C-6), 137.1 (2 x C-5)

LRMS (ES⁺): m/z= 328.2 [M+H]⁺

HRMS (ES⁺): Found: 328.2098 [M+H]⁺ C₂₀H₃₀ONSi requires 328.2091

8.8 (8) Synthesis of N-[3-(*tert*-butyldiphenylsilyloxy)-propyl] uracil acetamide



Compound **8** was synthesised according to general procedure C using carboxyuracil **1** (349 mg, 2.08 mmol), **5** (500 mg, 1.6mmol) and EDC (430 mg, 2.24 mmol). The product was purified by flash chromatography (CH₂Cl₂/MeOH 100:0→94:6) as a white solid (454 mg).

Melting point: 186°C

Yield: 61%

R_f: 0.5 in CH₂Cl₂/MeOH 90:10

¹H-NMR: (300 MHz, MeOD) δ 1.05 (9 H, s, 3 x C(17)H₃), 1.79 (2 H, qn *J*=6.5, C(10)H₂), 3.37 (2 H, m, C(9)H₂), 3.75 (2 H, t *J*=6.5, C(11)H₂), 4.35 (2 H, s, C(7)H₂), 5.67 (1 H, d *J*=7.9 C(5)H), 7.40 (6 H, m, 2 x C(15)H, 4 x C(14)H), 7.42 (1 H, d *J*=7.9, C(6)H), 7.68 (4 H, m, 4 x C(13)H)

¹³C-NMR: (75 MHz, DMSO) δ 18.8 (3 x C-17), 26.6 (C-16), 32.0 (C-10), 45.1 (C-9), 49.4 (C-7), 61.2 (C-11), 100.4 (C-5), 127.9 (2 x C-15), 129.8 (4 x C-14), 133.2 (4 x C-13), 135.0 (2 x C-12), 146.6 (C-6), 151.0, (C-2), 163.9 (C-4), 166.5 (C-8)

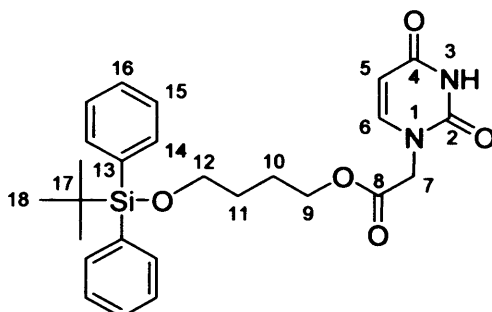
LRMS (ES⁻): *m/z*= 464.0 [M-H]⁻

HRMS (ES⁺): Found: 466.2159 [M+H]⁺ C₂₅H₃₂O₄N₃Si⁺ requires 466.2157

Analysis: Found: C, 64.4; H, 6.8; N, 8.9

Calc. for C₂₅H₃₁N₃O₄Si.0.1H₂O C, 64.2; H, 6.7, N, 9.0

8.9 (9) Synthesis of N-[4-(*tert*-butyldiphenylsilanyloxy)-butyl] uracil acetamide



Compound **9** was synthesised according to general procedure C using carboxyuracil **1** (349 mg, 2.08 mmol), **6** (523 mg, 1.6 mmol) and EDC (430 mgs, 2.24 mmol). The product was purified by flash chromatography (CH₂Cl₂/MeOH 100:0→93:7) as a white solid (522 mg).

Yield: 68%

Melting point: 174°C

R_f: 0.5 in CH₂Cl₂/MeOH 9:1

¹H-NMR: (300 MHz, MeOD) δ 1.05 (9 H, s, 3 x C(18)H₃), 1.63 (4 H, m, C(10)H₂ C(11)H₂), 3.23 (2 H, t *J*=6.5, C(12)H₂), 3.71 (2 H, t *J*=5.8, C(9)H₂), 4.41 (2 H, s, C(7)H₂), 5.65 (1 H, d *J*=7.7, C(5)H), 7.40 (6 H, m, 2 x C(16)H, 4 x C(15)H), 7.51 (1 H, d *J*=7.9, C(6)H), 7.66 (4 H, m, 4 x C(14)H)

¹³C-NMR: (75 MHz, MeOD) δ 20.4 (3 x C-18), 27.8 (C-17), 30.1, 31.3 (C-10, C-11), 40.8 (C-12), 51.6 (C-7), 65.0 (C-9), 102.6 (C-5) 129.2 (2 x C-16), 131.2 (4 x C-15), 135.4 (4 x C-14), 137.0 (2 x C-13), 148.3 (C-6), 153.1 (C-2) 156.7 (C-4) 169.5 (C-8)

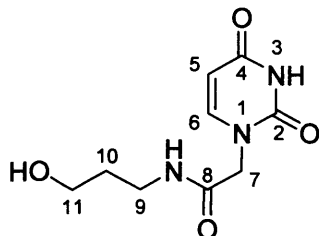
LRMS (ES⁻): *m/z*=478.2 [M-H⁻]

HRMS (ES⁺): Found: 480.2306 [M+H]⁺ C₂₆H₃₄O₄N₃Si⁺ requires: 480.2313

Analysis: Found: C, 64.4; H, 6.9; N, 8.7

Calc. for C₂₆H₃₃O₄N₃Si.0.2H₂O: C, 64.6; H, 7.0; N, 8.7

8.10 (10) Synthesis of N-(3-hydroxypropyl) uracil acetamide



HCl (1 ml, 10M, 10 mmol) was added to **8** (350 mg, 0.75 mmol) dissolved in 25 mL MeOH. The reaction was left stirring at RT for 1.5 h and monitored by TLC. The solvent was removed *in vacuo*. The crude was washed with EtOAc (20 mL) to remove the silanol. The product (100 mg) was obtained as a white solid.

Yield: 65%

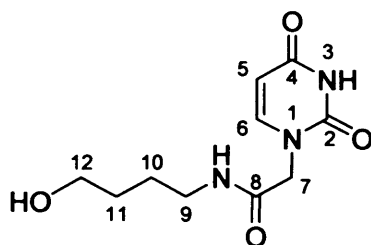
R_f: 0.2 in CH₂Cl₂/MeOH 90:10

¹H-NMR: (300 MHz, MeOD) δ 1.76 (2 H, qn *J*=6.6 C(10)H₂), 3.34 (2 H, m, C(9)H₂), 3.63 (2 H, t *J*=6.6 C(11)H₂), 4.45 (2 H, s, C(7)H₂), 5.70 (1 H, d *J*=7.8 C(5)H), 7.57 (1 H, d *J*=7.8 C(6)H)

¹³C-NMR: (75 MHz, MeOD) δ 33.5 (C-10), 38.0 (C-9), 51.7 (C-7), 60.7 (C-11), 102.6 (C-5), 148.3 (C-6)

LRMS (ES⁺): *m/z*= 227.0 [M]⁺

8.11 (11) Synthesis of N-(4-hydroxybutyl) uracil acetamide



HCl (1 ml, 10M, 10mmol) was added to **9** dissolved in MeOH. (25 mL) The reaction was left stirring a RT for 1.5 h and monitored by TLC. The solvent was removed *in vacuo*. The product was recrystallised from ethanol. Small white crystals formed, were filtered off, washed with ethanol (10 mL) and dried to afford compound **11** (70 mg)

Yield: 48%

Melting point: 193°C

R_f: 0.1 in CH₂Cl₂/MeOH 9:1

¹H-NMR: (300 MHz, MeOD) δ 1.59 (4 H, m, C(10)H₂, C(11)H₂), 3.26 (2 H, t *J*=6.5, C(9)H₂), 3.58 (2 H, t *J*=5.6, C(12)H₂), 4.42 (2 H, s, C(7)H₂), 5.69 (1 H, d *J*=7.9, C(5)H), 7.53 (1 H, d *J*=7.8, C(6)H)

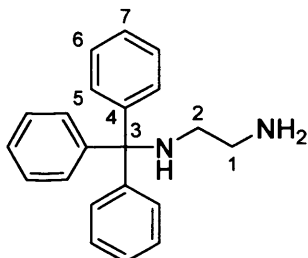
¹³C-NMR: (75 MHz, MeOD) δ 27.2, (C-11) 31.2 (C-10), 40.8 (C-9), 51.6 (C-12), 62.9 (C-7), 102.6 (C-5), 148.3 (C-6), 153.3 (C-2), 167.3 (C-4), 169.6 (C-8)

LRMS (ES⁻): *m/z*= 240 [M-H]⁻

Analysis: Found: C, 49.1; H, 6.2; N, 17.2

Calc. for C₁₀H₁₅O₄N₃·0.2H₂O: C, 49.1; H, 6.3; N, 17.2

8.12 (14) Synthesis of 2-(triphenylmethylamino) ethylamine



Compound **14** was synthesised according to the general procedure D using TrtCl (3.50 g, 12.55mmol) dissolved in DCM (30 mL) and ethylenediamine (8.4 mL, 125.55 mmol) dissolved in DCM (10 mL). Following the described work up, the product was purified by flash chromatography (CH₂Cl₂/MeOH/NH₃ 100:0:0→92:6.4:1.6) as a colourless oil (1.90 g)

Yield: 51%

R_f: 0.6 in CH₂Cl₂/MeOH/NH₃ 90:7:3

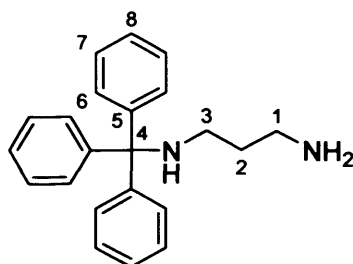
¹H-NMR: (300 MHz, MeOD) δ 2.14 (2 H, t *J*=6.2, C(2)H₂), 2.64 (2 H, t *J*=6.3, C(1)H₂), 7.19 (3 H, 3 x C(7)H), 7.29 (6 H, m, 6 x C(6)H), 7.5, (6 H, m, 6 x C(5)H)

¹³C-NMR: (75 MHz, MeOD) δ 43.4 (C-1), 47.6 (C-2), 83.3 (C-3), 127.7 (6 x C-5), 129.1 (3 x C-7), 129.7 (6 x C-6), 147.9 (3 x C-4)

LRMS (ES⁺): *m/z*= 303 [M+H]⁺

HRMS (ES⁺): Found: 303.1853 [M+H]⁺ C₂₁H₂₁N₂⁺ requires 303.1856

8.13 (15) Synthesis of 3-triphenylmethylamino propylamine



Compound **15** was synthesised according to the general procedure D using TrtCl (3.50 g, 12.55 mmol) dissolved in DCM (30mL) and diaminopropane (10.80 mL, 125.55 mmol) dissolved in DCM (10 mL). Following the described work up, the product was purified by flash chromatography (CH₂Cl₂/MeOH/NH₃ 100:0:0→92:6.4:1.6) to afford a colourless oil (807 mg).

Yield: 20%

R_f: 0.4 in CH₂Cl₂/MeOH/NH₃ 92:6.4:1.6

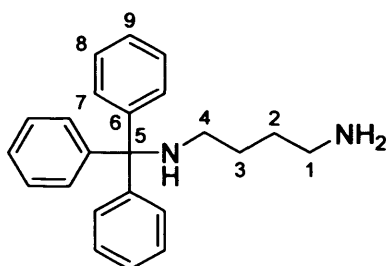
¹H-NMR: (300 MHz, MeOD) δ 1.63 (2 H, qn *J*=7.0, C(2)H₂), 2.15 (2 H, t *J*=7.0, C(3)H₂), 2.67 (2 H, t *J*=7.0, C(1)H₂), 7.15 (3 H, m, 3 x C(8)H), 7.24 (6 H, m, 6 x C(7)H), 7.42 (6 H, m, 6 x C(6)H)

¹³C-NMR: (75 MHz, MeOD) δ 35.1 (C-2), 41.4 (C-1), 43.3, (C-3), 72.6 (C-4), 127.7 (3 x C-8), 129.1 (6 x C-6), 130.3 (6 x C-7), 147.9 (3 x C-5)

LRMS (ES⁺): *m/z*= 317 [M+H]⁺

HRMS (ES⁺): Found: 317.2015 [M+H]⁺ C₂₂H₂₄N₂⁺ requires 317.2012

8.14 (16) Synthesis of 4-(triphenylamino)butylamine



Compound **16** was synthesised according to the general procedure D using TrtCl (3.50 g, 12.55 mmol) dissolved in DCM (30 mL) and 1,4-diaminobutane (12.62 mL, 125.55 mmol) dissolved in DCM (10 mL). Following the described work up, the product was purified by flash chromatography (CH₂Cl₂/MeOH/NH₃ 100:0:0→93:6.4:0.6) to afford a colourless oil (1.30 g)

Yield: 31%

Melting point: 63-64°C

R_f: 0.4 in CH₂Cl₂/MeOH/NH₃ 90:7:3

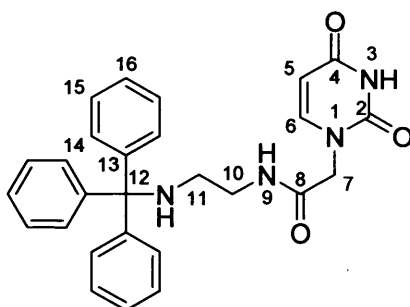
¹H-NMR: (300 MHz, MeOD) δ 1.51 (4 H, m, C(2)H₂C(3)H₂), 2.15 (2 H, t *J*=6.8, C(2)H₂), 2.60 (2 H, t *J*=6.8, C(1)H₂), 7.17 (3 H, m, 3 x C(9)H), 7.26 (6 H, m, 6 x C(8)H), 7.47, (6 H, m, 6 x C(7)H)

¹³C-NMR: (75 MHz, MeOD) δ 29.3 (C-2), 31.7 (C-3), 42.8 (C-1), 45.2 (C-4), 72.6 (C-5), 127.7 (3 x C-9), 129.1 (6 x C-8), 130.3 (6 x C-7), 147.9 (3 x C-6)

LRMS (ES⁺): *m/z*= 331 [M+H]⁺

HRMS (ES⁺): Found: 331.2005 [M+H]⁺ C₂₃H₂₇N₂⁺ requires 331.2169

8.15 (17) Synthesis of 1-[N-(2-triphenylmethylaminoethyl)-acetamide] uracil



Compound **17** was synthesised according to general procedure C using carboxyuracil (336 mg, 1.99 mmol) in DMF (10mL), **14** (500 mg, 1.66 mmol) dissolved in 1 mL DMF and EDC (430 mg, 2.24 mmol) in DMF (20 mL) was added. The product was purified by flash chromatography (CH₂Cl₂/MeOH 100:0→92:8) to yield a white solid (251 mg).

Yield: 33%

Melting point: 219°C

R_f: 0.4 in CH₂Cl₂/MeOH 95:5

¹H-NMR: (300 MHz, MeOD) δ 2.28 (2 H, t *J*=6.3, C(11)H₂), 3.37 (2 H, t *J*=6.3, C(10)H₂), 4.43 (2 H, s, C(7)H₂), 5.66 (1 H, d, *J*=7.9, C(5)H), 7.18 (1 H, m, C(6)H), 7.18 (3 H, m, 3 x C(16)H), 7.29 (6 H, m, 6 x C(15)H), 7.45, (6 H, m, 6 x C(14)H)

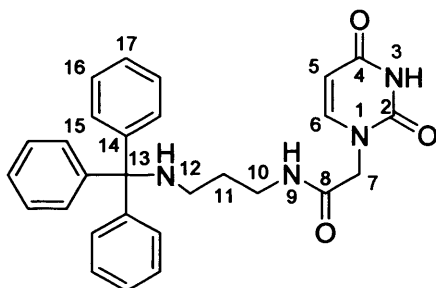
¹³C-NMR: (75 MHz, MeOD) δ 41.4 (C-10), 45.5 (C-11), 50.3 (C-7), 70.5 (C-12), 100.8 (C-5), 126.4 (6 x C-14), 128.1 (3 x C-16), 128.7 (6 x C-15), 145.4 (C-6), 146.4 (3 x C-13), 164.3 (C-4), 167.2 (C-8)

LRMS (ES⁻): *m/z*= 453 [M-H]⁺

Experimental I

HRMS (ES⁻): Found: 453.1940 [M+H]⁺ C₂₇H₂₅N₄O₃ requires 453.1927

8.16 (18) Synthesis of 1-[N-(3-triphenylmethylaminopropyl)-acetamide] uracil



Compound **18** was synthesised according to general procedure C using carboxyuracil (383 mg, 2.28 mmol), EDC (510 mg, 2.66 mmol) and **15** (600 mg, 1.90 mmol) dissolved in DMF (30 mL). The product was purified by flash chromatography (CH₂Cl₂/MeOH 100:0→92:8) to yield a white solid (376 mg)

Yield: 42%

Melting point: 189°C

R_f: 0.6 in CH₂Cl₂/MeOH 90:10

¹H-NMR: (300 MHz, CDCl₃) δ 1.62 (2 H, m, C(11)H₂), 2.13 (2 H, m, C(12)H₂), 3.31 (2 H, m, C(10)H₂), 4.18 (2 H, s, C(7)H₂), 5.61 (1 H, d *J*=7.8, C(5)H), 7.19 (1 H, m, C(6)H), 7.14 (3 H, m, 3 x C(17)H), 7.22 (6 H, m, 6 x C(16)H), 7.40, (6 H, m, 6 x C(15)H)

¹³C-NMR: (75 MHz, CDCl₃) δ 30.6 (C-11), 38.8 (C-12), 41.6 (C-10), 51.1 (C-7), 71.4 (C-13), 102.9 (C-5), 126.8 (3 x C-17), 128.3 (6 x C-15), 129.1 (6 x C-16), 145.7 (C-6), 146.4 (3 x C-14), 151.7 (C-2), 164.5 (C-4), 166.6 (C-8)

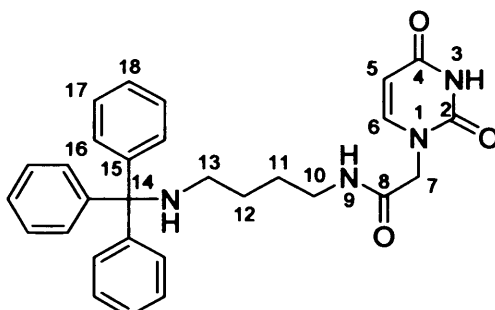
LRMS (ES⁺): *m/z*= 469 [M+H]⁺

HRMS (ES⁺): Found: 469.2239 [M+H]⁺ C₂₈H₂₈N₄O₃⁺ requires 469.2234

Analysis: Found: C, 69.2; H, 5.9; N, 11.4

Calc. for C₂₈H₂₈O₃N₄.1.0H₂O: C, 69.1; H, 6.2; N, 11.5

8.17 (19) Synthesis of 1-[N-(3-triphenylmethylaminobutyl)-acetamide] uracil



Compound **19** was synthesised according to general procedure C, using carboxyuracil (336 mg, 1.99 mmol) dissolved in DMF (10 mL), **16** (547 mg, 1.66 mmol) and EDC (430 mg, 2.24 mmol) in DMF (20 mL). The product was purified by flash chromatography (CH₂Cl₂/MeOH/NH₃ 100:0:0→92:6.4:1.6) to yield a white solid (206 mg).

Yield: 26%

Melting point: 180°C

R_f: 0.3 in CH₂Cl₂/MeOH 90:10

¹H-NMR: (300 MHz, CDCl₃) δ 1.57 (4 H, m, C(11)H₂, C(12)H₂), 2.19 (2 H, m, C(13)H₂), 3.27 (2 H, m, C(10)H₂), 4.29 (2 H, s, C(7)H₂), 5.75 (1 H, d *J*=7.9, C(5)H), 6.80 (1 H, m, N(9)H), 7.23 (3 H, m, 3 x C(18)H), 7.25 (1 H, m, C(6)H), 7.32 (6 H, m, 6 x C(17)H), 7.50, (6 H, m, 6 x C(16)H)

¹³C-NMR: (75 MHz, CDCl₃) δ 27.6, 28.6 (C-11, C-12), 40.4 (C-13), 43.6 (C-10), 51.3 (C-7), 71.3 (C-14), 102.9 (C-5), 126.7 (6 x C-16), 128.2 (3 x C-18), 129.0 (6 x C-17), 145.6 (C-6), 146.5 (3 x C-15), 151.5 (C-2), 164.1 (C-4), 166.4 (C-8)

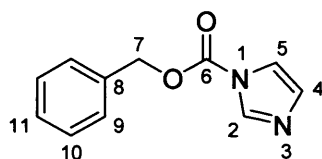
LRMS (ES⁺): *m/z*= 483 [M+H]⁺

HRMS (ES⁺): Found: 483.23996 [M+H]⁺ C₂₉H₃₀N₄O₃⁺ requires 483.2391

Analysis: Found: C, 71.4; H, 6.2; N, 11.4

Calc. for C₂₉H₃₀O₃N₄.0.3H₂O: C, 71.4; H, 6.3; N, 11.5

8.18 (20) Synthesis of carbobenzoxyimidazole⁹¹



Benzyl chloroformate (19.92 g, 117.23 mmol) was cooled to 0°C in an ice bath. Imidazole (15.96 g, 234.47 mmol) in DCM (70 mL) was added slowly. The reaction was left at RT for 15 min. The mixture was washed with citric acid (3 x 150 mL) and the organic layer was dried to give the pure product as a colourless oil (20.60 g). The product could not be detected by ES MS as it more than likely too unstable to the ionisation conditions.

Yield: 87%

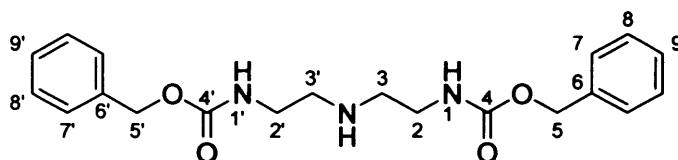
Melting point: 41°C

R_f: 0.7 in CH₂Cl₂/MeOH 90:10

¹H-NMR: (500 MHz, CDCl₃) δ 5.39 (2 H, s, C(7)H₂), 7.02, 7.49, (2 H, m, C(4)H, C(5)H), 7.34-7.43 (5 H, m, 2 x C(9)H, 2 x C(10)H, C(11)H), 8.20 (1 H, m, C(2)H)

¹³C-NMR: (125 MHz, CDCl₃) δ 70.3, (C-7), 117.6 (C-4), 128.8-129.6 (C-11, 2 x C-10, 2 x C-9), 131.1 (C-5), 134.4 (C-8), 137.6 (C-2), 149.1 (C-6)

8.19 (21) Synthesis of N¹,N^{1'}-(dicarbobenzoxy) diethylene triamine



Compound **21** was synthesised according to the general procedure E using diethylenetriamine (3.00 g, 29.08 mmol) and DMAP (0.70 mg, 5.74 mmol) dissolved in DCM (20 mL) and **20** (11.76 g, 58.16 mmol) in DCM (30 mL). The product was purified by flash chromatography (CH₂Cl₂/MeOH/NH₃ 100:0:0→90:8:2) to yield a white solid (3.80 g)

Yield: 35%

Melting point: 53-55°C

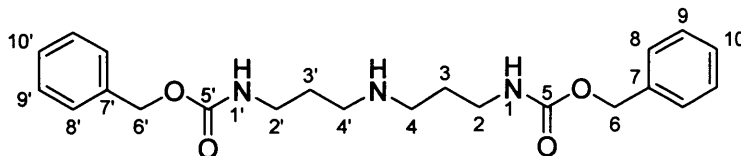
R_f: 0.9 in CH₂Cl₂/MeOH 80:18:2

¹H-NMR: (500 MHz, MeOD) δ 2.64 (4 H, t *J*=6.2, C(3)H₂, C(3')H₂), 3.19 (4 H, t *J*=6.2, C(2)H₂, C(2')H₂), 5.01 (4 H, s, C(5)H₂, C(5')H₂), 7.28 (10 H, m, C(9)H, 2 x C(8)H, 2 x C(7)H, C(9')H, 2 x C(8')H, 2 x C(7')H)

¹³C-NMR: (125 MHz, MeOD) δ 41.1 (C-3, C-3'), 49.5 (C-2, C-2'), 67.5 (C-5, C-5') 128.5-129.5 (C-9, 2 x C-8, 2 x C-7, C-9', 2 x C-8', 2 x C-7'), 138.3 (C-6, C-6'), 158.9 (C-4, C-4')

LRMS (ES⁺): *m/z*= 372.2 [M+H]⁺

8.20 (22) Synthesis of N¹N^{1'}-(dicarbobenzoxy)di(n-propyl) triamine



Compound **22** was synthesised according to the general procedure E using, Bis-(3-aminopropyl)amine (4.00 g, 30.48 mmol) and DMAP (10%w/w), DCM (150 mL) and **20** (12.32 g, 60.96 mmol) in DCM (200 mL). The reaction was left stirring for 4 d at 50°C. The product was purified by flash chromatography (CH₂Cl₂/MeOH/NH₃ 100:0:0→90:8:2) and subsequently recrystallised from EtOAc to yield a white solid (4.60 g)

Yield: 38%

Melting point: 208°C

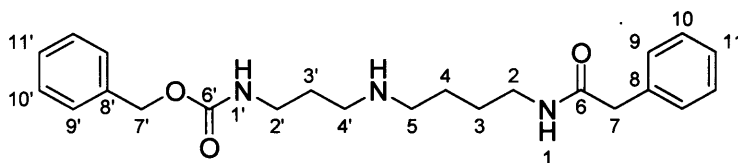
R_f: 0.4 in CH₂Cl₂/MeOH 75:25

¹H-NMR: (500 MHz, MeOD) δ 1.85 (4 H, qn *J*=7.0, C(3)H₂, C(3')H₂), 2.94 (4 H, t *J*=7.0, C(4)H₂, C(4')H₂), 3.25 (4 H, t *J*=7.0, C(2)H₂, C(2')H₂), 5.10 (4 H, s, C(6)H₂, C(6')H₂), 7.36 (10 H, m, C(10)H, 2 x C(9)H, 2 x C(8)H, C(10')H, 2 x C(9')H, 2 x C(8')H)

¹³C-NMR: (125 MHz, MeOD) δ 26.4 (C-3, C-3'), 38.8 (C-4, C-4'), 46.2 (C-2, C-2'), 65.9 (C-6, C-6') 126.6-128.8 (C-10, 2 x C-9, 2 x C-8, C-10', 2 x C-9', 2 x C-8'), 138.3 (C-7, C-7'), 158.9 (C-5, C-5')

LRMS (ES⁺): *m/z*= 399.4 [M+H]⁺

8.21 (23) Synthesis of N¹N^{1'}-dicarbobenzoxyspermidine



Compound **23** was synthesized according general procedure E using spermidine (0.70 g, 4.82 mmol) and DMAP (5% w/w) in DCM (30 mL) and **20** (1.95 g, 9.64 mmol) The reaction was heated to 50°C and left stirring for 3 d. The crude product was purified by column chromatography in (CH₂Cl₂/MeOH/NH₃ 100:0:0→90:8:2). The fractions containing the product were collected and washed with H₂O (30 mL) and HCl (20 mL, 0.5 M) solution. The precipitate collected was redissolved in MeOH:CHCl₃. The residue which was not soluble was filtered off and the filtrate was dried *in vacuo* to yield the pure product as a white solid (758 mg).

Yield: 38%

Melting point: 175-177°C

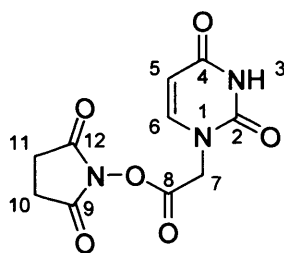
R_f: 0.6 in CH₂Cl₂/MeOH/NH₃ 80:16:4

¹H-NMR: (500 MHz, MeOD) δ 1.54-1.66 (4 H, m, C(3)H₂, C(3')H₂), 1.82 (2 H, qn *J*=7.1, C(4)H₂), 2.79-2.87(4 H, m, C(4')H₂, C(5)H₂), 3.14-3.25 (4 H, m, C(2)H₂, C(2')H₂), 5.09 (4 H, s, C(7)H₂, C(7')H₂), 7.33-7.37 (10 H, m, 2 x C(9)H, 2 x C(10)H, C(11)H, 2 x C(9')H, 2 x C(10')H, C(11')H)

¹³C-NMR: (125 MHz, MeOD) δ 26.0, 28.3, 29.4 (C-3, C-3', C-4), 38.9, 41.2 (C-5, C-4'), 47.2 (C-2, C-2'), 67.4 (C-7, C-7') 128.5-129.5 (C-11, 2 x C-10, 2 x C-9, C-11', 2 x C-10', 2 x C-9'), 138.5 (C-8, C-8'), 159.2 (C-6, C-6')

LRMS (ES⁺): *m/z*= 414.5 [M+H]⁺

8.22 (24) Synthesis of 1-carboxymethyluracil succinimidyl ester



1-Carboxymethyl uracil **1** (2.95 g, 17.35 mmol) and N-hydroxysuccinimide (2.21 g, 19.09 mmol) were dissolved in DMF (20 mL) and cooled to 0°C in an ice bath. A solution of DCC (3.94 g, 19.09 mmol) in DMF (5 mL) was added to the mixture under N₂ atmosphere. The solution was left stirring at 0°C for 3 h and then at RT for a further 24 h. The pure product was precipitated from MeOH to yield a white solid (4.70 g). The product could not be detected by ES MS as it was too unstable to ionization.

Yield: quantitative

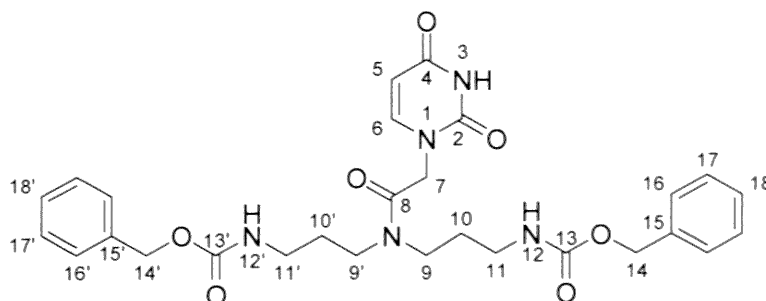
Melting point: 218-222°C

R_f: 0.2 in CH₂Cl₂/MeOH 80:18:2

¹H-NMR: (500 MHz, DMSO) δ 2.83 (4 H, s, C(10)H₂, C(11)H₂), 5.02 (2 H, s, C(7)H₂), 5.85 (1 H, d *J*=7.9, C(5)H), 7.74 (1 H, d *J*=7.9, C(6)H₂)

¹³C-NMR: (125 MHz, DMSO) δ 25.8 (C-10, C-11), 46.9 (C-7), 102.1 (C-5), 145.6 (C-6), 151.0 (C-2), 164.0 (C-4), 165.3 (C-8), 170.1 (C-9, C-12)

8.23 (25) Synthesis of 1-[N¹²N^{12'}-(dicarbobenzoxy)diaminodi (n-propyl)acetamide] uracil



22 (1.67 g, 6.26 mmol) and DMAP (10% w/w) were dissolved in DMF (10 mL). **24** (2.50 g, 6.26 mmol) was added under N₂ atmosphere. The reaction was heated to 60°C and left stirring for 4 d. The solvent was removed *in vacuo*. White crystals were recrystallised from EtOAc and were washed with H₂O (10 mL) to yield the pure product (2.37 g).

Yield: 69%

Melting point: 141-144°C

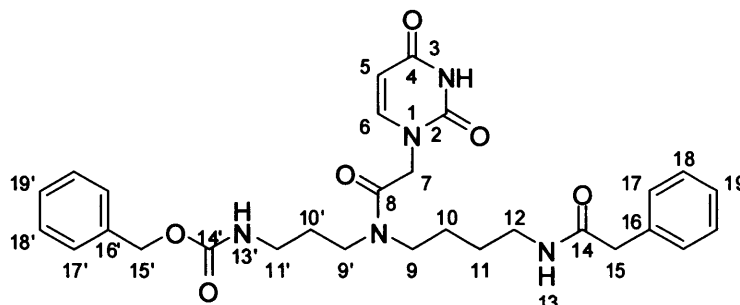
R_f: 0.4 in CH₂Cl₂/MeOH 90:10

¹H-NMR: (500 MHz, MeOD) δ 1.73, 1.88 (4 H, qn *J*=6.5, C(10)H₂ C(10')H₂), 3.11, 3.20 (4 H, 2 x t *J*= 6.5 C(9')H₂, C(9)H₂), 3.38 (4 H, m, C(11')H₂ C(11)H₂), 4.58 (2 H, s, C(7)H₂), 5.08 (4 H, 2 x s, C(14)H₂ C(14')H₂), 5.67 (1 H, d *J*=7.8 C(5)H), 7.28-7.35 (10 H, m, 2 x C(17)H, C(18)H, 2 x C(16)H, 2 x C(17')H, C(18')H, 2 x C(16')H), 7.43 (1 H, d *J*=7.8 C(6)H)

¹³C-NMR: (125 MHz, MeOD) δ 27.2, 28.2 (C-10, C-10'), 37.6 (C-9', C-9), 43.3 (C-11', C-11), 48.5 (C-7), 65.9 (C-14, C-14'), 100.6 (C-5), 127.3-128.0 (C-18, 2 x C-17, 2 x C-16, C-18', 2 x C-17', 2 x C-16'), 137.0 (C-15, C-15'), 146.6 (C-6), 151.4(C-2), 158.9 (C-13, C-13'), 165.4 (C-4), 167.2 (C-8)

LRMS (ES⁺): *m/z*= 552.4 [M+H]⁺

8.24 (26) Synthesis of N-(1-carboxymethyluracil)-N¹³N^{13'}-(dicarbobenzoxy) spermidine



A solution of **24** (430 mg, 0.72 mmol) in DMF (8 mL) was added to **23** (190 mg, 0.72 mmol) under N₂ atmosphere. The solution was heated to 70°C and DMAP (10% w/w) in DMF (2 mL) was added. The solution was left stirring at 70°C for 3 d. The solvent was vacuumed off under reduced pressure. On addition of EtOAc, a yellow oil formed which was removed by careful pipetting. Recrystallisation from EtOAc was carried out. The white crystals formed were washed with water (20 mL) and HCl solution (20 mL, 0.5M) to yield the pure product as a white solid (340 mg)

Yield: 89%

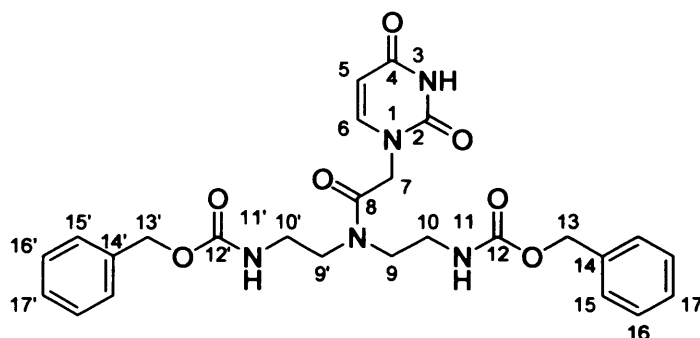
R_f: 0.4 in CH₂Cl₂/MeOH/NH₃ 90:9:2

¹H-NMR: (500 MHz, MeOD) δ 1.59, 1.70, 1.87 (6 H, m, C(10)H₂, C(10')H₂, C(11)H₂), 2.97 (4 H, m, C(9')H₂, C(9)H₂), 3.14-3.25 (4 H, 2 x t J=6.6, C(11')H₂, C(12)H₂), 4.30 (2 H, s, C(7)H₂), 5.09 (4 H, 2 x s, C(15)H₂, C(15')H₂), 5.64 (1 H, d J=7.8, C(5)H), 7.32-7.37 (10 H, m, 2 x C(17)H, 2 x C(18)H, C(19)H, 2 x C(17')H, 2 x C(18')H, C(19')H), 7.49 (1 H, d J=7.8, C(6)H)

¹³C-NMR: (125 MHz, MeOD) δ 28.2-30.6 (C-10, C-10', C-11), 45.8 (C-9', C-9), 46.6 (C-11', C-12), 57.0 (C-7), 67.7 (C-15, C-15'), 102.5 (C-5), 129.0-130.1 (C-19, 2 x C-18, 2 x C-17, C-19', 2 x C-18', 2 x C-17'), 138.5 (C-16, C-16'), 150.1 (C-6), 158.9 (C-14, C-14'), 168.8 (C-8)

LRMS (ES⁺): m/z= 556.2 [M+H]⁺

8.25 (27) Synthesis of 1-[N¹¹N^{11'}-(dicarbobenzoxy)diethyl acetamide]uracil



Compound **21** (1.53 g, 4.12 mmol) was dissolved in DMF (5 mL). 1-carboxymethyluracil (700 mg, 4.12 mmol) in DMF (5 mL) was added under N₂ atmosphere, followed by, DhbtOH (770 mg, 4.74 mmol) in DMF (5 mL). The solution was cooled to 0°C and DCC (1.02 g, 4.95 mmol) in DMF (5 mL) was added under N₂ atmosphere. The mixture was left stirring at 0°C for 1 h and then at RT for 48 h after which time a precipitate had formed. The solvent was evaporated off under reduced pressure and DCU was precipitated out using EtOAc. On addition of diethyl ether to the EtOAc solution, a further gel precipitate formed. This was collected by decantation. On evaporation of the remaining solvent, a foamy white solid formed and identified as the pure product (783 mg).

Yield: 36%

R_f: 0.4 in CH₂Cl₂/MeOH 90:10

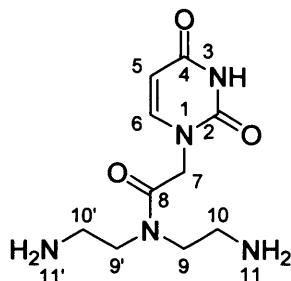
¹H-NMR: (500 MHz, MeOD) δ 3.25-3.30 (4 H, m, C(10)H₂, C(10')H₂), 3.40-3.45 (4 H, m, C(9)H₂, C(9')H₂), 4.57 (2 H, s, C(7)H₂), 5.10 (4 H, m, C(13)H₂, C(13')H₂), 5.65 (1 H, C(5)H), 7.25-7.39 (11 H, m, C(6)H, C(17)H, 2 x C(16)H, 2 x C(15)H, C(17')H, 2 x C(16')H, 2 x C(15')H)

¹³C-NMR: (125 MHz, MeOD) δ 39.4, 40.0 (C-10, C-10'), 44.2 (C-9, C-9'), 49.5 (C-7), 67.6 (C-13, C-13'), 102.2 (C-5), 129.0-130.0 (C-17, 2 x C-16, 2 x C-15, C-17', 2 x C-16', 2 x C-15'), 138.3 (C-14, C-14'), 147.9 (C-6), 154.7 (C-4), 159.0 (C-12, C-12')

LRMS (ES⁺): m/z= 524 [M+H]⁺

HRMS (ES⁺): Found: 546.1953 [M+Na]⁺ C₂₆H₂₉N₅O₇Na⁺ requires 546.1965

8.26 (28) Synthesis of 1-[diaminodiethylacetamide]uracil



Compound **28** was synthesised according to the general procedure F using **27** (500 mg, 0.956 mmol) dissolved in MeOH (15 mL) and 5% Pd/C (10% w/w). The catalyst was removed by filtration and the solvent evaporated off under reduced pressure to yield a sticky gel which was identified as a mixture of the product and the mono-protected side product. The mono-protected side product was removed by washing with DCM to yield the product as a cream/yellow solid (100 mg). By NMR, however it could be seen that some N,N acyl migration had occurred.

Yield: 41%

R_f: 0.2 in CH₂Cl₂/MeOH/NH₃ 80:16:4

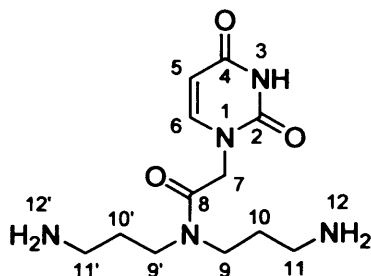
¹H-NMR: (500 MHz, MeOD) δ 2.70-2.97 (4 H, m, C(10)H₂, C(10')H₂), 3.30-3.59 (4 H, m, C(9)H₂, C(9')H₂), 4.46, 4.75(2 H, 2 x s, C(7)H₂), 5.70 (1 H, m, C(5)H), 7.53 (1 H, m, C(6)H)

¹³C-NMR: (125 MHz, MeOD) δ 39.8-41.2 (C-10, C-10'), 49.1-51.3 (C-9, C-9'), 102.2 (C-5), 147.9 (C-6), 154.7 (C-4), 159.0 (C-8)

LRMS (ES⁺): m/z= 256 [M+H]⁺

HRMS (ES⁺): Found: 256.1400 [M+H]⁺ C₁₀H₁₈N₅O₃⁺ requires 256.1404

8.27 (29) Synthesis of 1-[diaminodi(n-propyl)acetamide] uracil



Compound **29** was synthesised according the general procedure F using **25** (800 mg, 1.45 mmol) dissolved in EtOH:MeOH (50 mL) and 5% Pd/C (5% w/w). The catalyst was removed by filtration and the solvent was removed *in vacuo* to yield a white foamy solid (143 mg). By NMR it was observed that some acyl migration had occurred.

Yield: 35%

R_f: 0.2 in CH₂Cl₂/MeOH/NH₃ 80:16:4

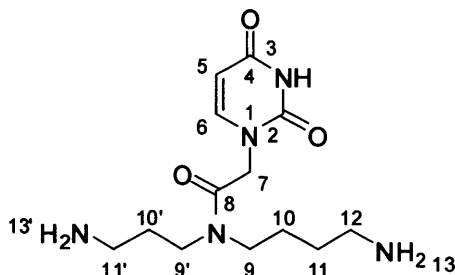
¹H-NMR: (500 MHz, MeOD) δ 1.78-1.94 (4 H, m, C(10)H₂, C(10')H₂), 2.70-2.83 (4 H, m, C(11)H₂, C(11')H₂), 3.40-3.51 (4 H, m, C(9)H₂, C(9')H₂), 4.34, 4.72 (2 H, 2 x s, C(7)H₂), 5.69 (1 H, m, C(5)H), 7.51 (1 H, d *J*=7.8, C(6)H)

¹³C-NMR: (125 MHz, MeOD) δ 25.1-26.0 (C-10, C-10'), 38.1-38.8 (C-11, C-11'), 45.1-45.7 (C-9, C-9'), 48.5 (C-7), 101.2 (C-5), 147.6 (C-6), 150.4 (C-2), 165.4 (C-4), 167.2 (C-8)

LRMS (ES⁺): *m/z*= 284 [M+H]⁺

HRMS (ES⁺): Found: 284.1715 [M+H]⁺ C₁₂H₂₂N₅O₃⁺ requires 284.1717

8.28 (30) Synthesis of N-(1-carboxymethyluracil) spermidine



Compound **30** was synthesised according the general procedure F using **26** (250 mg, 0.44 mmol) dissolved in MeOH (30 mL) and 5% Pd/C (5% w/w). The catalyst was removed by filtration and the solvent was removed *in vacuo* to yield a white foamy solid (90 mg). By NMR it was seen that N,N acyl migration had occurred to some extent.

Yield: 69%

R_f: 0.1 in CH₂Cl₂/MeOH/NH₃ 80:16:4

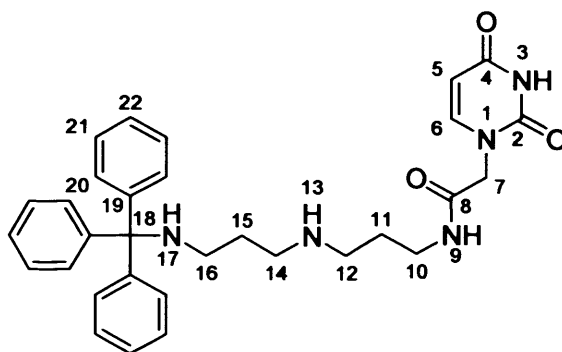
¹H-NMR: (500 MHz, MeOD) δ 1.67, 1.80, 1.90 (6 H, 3 x m, C(10)H₂ C(10')H₂, C(11)H₂), 2.82-2.92 (4 H, m, C(11')H₂, C(12)H₂), 3.41-3.53 (4 H, 2 x t J=6.6, C(9')H₂, C(9)H₂), 4.30, 4.72 (2 H, 2 x s, C(7)H₂), 5.65, 5.70 (1 H, d J=7.8 C(5)H), 7.52 (1 H, d J=7.8 C(6)H)

LRMS (ES⁺): m/z= 298 [M+H]⁺

8.29 (31), (31b) and (33) Synthesis of 1-[N,N⁺(triphenylmethyl)diaminodi(n-propyl)acetamide]uracil, 1-[N-(carboxybenzyl)-N-(triphenylmethyl)diaminodi(n-propyl) acetamide] uracil and 1-[N⁺(triphenylmethyl)diaminodi(n-propyl)acetamide]uracil

Compound **29** (140 mg, 0.49 mmol) and Et₃N (0.03 mg, 0.25 mmol) were dissolved in pyridine (50 mL). TrtCl (138 mg, 0.49 mmol) in pyridine (10 mL) was added over 3 h. After 1 h the solution had begun to turn cloudy. After addition had ceased the mixture was heated to 70°C, left stirring for 2 d and monitored periodically b TLC. The solvent was evaporated off under reduced pressure. The remaining starting material was removed by precipitation firstly form EtOH (10 mL) and subsequently EtOAc (10 mL). The remaining filtrate was purified by flash chromatography (CH₂Cl₂/MeOH/NH₃ 100:0:0→97:2.4:0.6) to yield **31** (fraction 5, 45 mg) as a yellow crystalline solid, **33** (fraction 2, 50 mg) as a white solid and **31b** (fraction 3, 25 mg) as a white crystalline solid.

31



Yield: 17%

Melting point: 103-105°C

R_f: 0.1 in CH₂Cl₂/MeOH/NH₃ 85:14:1

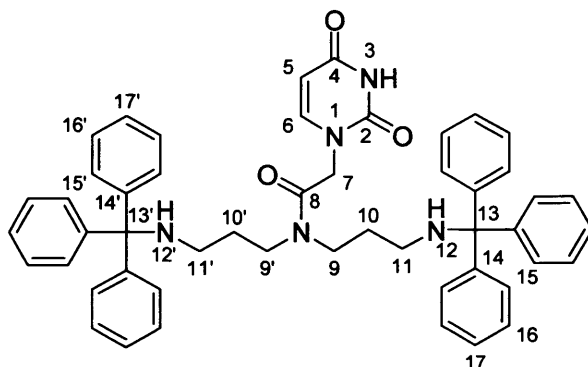
¹H-NMR: (500 MHz, MeOD) δ 1.75-1.80 (4 H, m, C(11)H₂, C(15)H₂), 2.23-2.29 (2 H, m, C(16)H₂), 2.75-2.81 (4 H, m, C(12)H₂, C(14)H₂), 3.37-3.51 (2 H, m, C(10)H₂), 4.41 (2 H, s, C(7)H₂), 5.67 (1 H, d *J*=7.9, C(5)H), 7.19-7.52 (16 H, m, 6 x C(20)H, 6 x C(21)H, 3 x C(22)H, C(6)H)

¹³C-NMR: (125 MHz, MeOD) δ 29.2, 30.0 (C-11, C-15'), 38.0 (C-16), 43.1 (C-12, C-14), 51.5 (C-7), 58.6 (C-10), 72.3 (C-18), 102.3 (C-5), 127.3-129.9 (6 x C-20, 6 x C-21, 3 x C-22), 147.9 (C-6), 147.4 (3 x C-19), 169.8 (C-8)

LRMS (ES⁺): m/z= 526 [M+H]⁺

HRMS (ES⁺): Found: 548.2639 [M+Na]⁺ C₃₁H₃₆N₅O₃Na⁺ requires 548.2632

33



Yield: 13%

Melting point: 162-165°C

R_f: 0.9 in CH₂Cl₂/MeOH/NH₃ 85:14:1

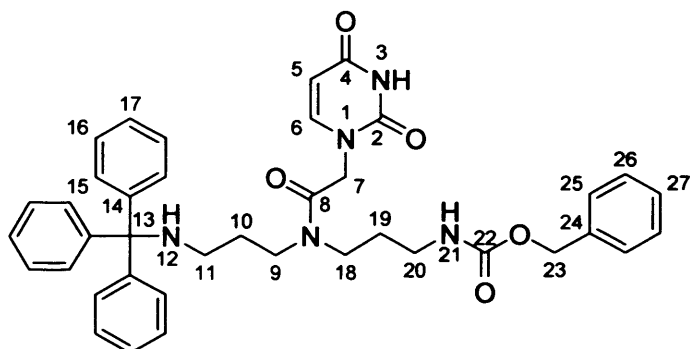
¹H-NMR: (500 MHz, CDCl₃) δ 1.72-1.82 (4 H, m, C(10)H₂, C(10')H₂), 2.13-2.23 (4 H, m, C(11)H₂, C(11')H₂), 3.35-3.39 (4 H, m, C(9)H₂, C(9')H₂), 4.22, 4.60 (2 H, 2 x s, C(7)H₂), 5.67 (1 H, d J=7.9, C(5)H), 7.16-7.20, 7.43-7.47 (30H, m, 6 x C(15)H, 6 x C(15')H, 6 x C(16)H, 6 x C(16')H, 3 x C(17)H, 3 x C(17')H), 7.30 (1 H, d J=7.9, C(6)H)

¹³C-NMR: (125 MHz, CDCl₃) δ 28.8-30.3 (C-10, C-10'), 40.9 (C-11, C-11'), 44.9, 45.7 (C-9, C-9'), 47.7(C-7), 71.5 (C-13, C-13'), 101.9 (C-5), 126.2-128.6 (6 x C-15, 6 x C-15', 6 x C-16, 6 x C-16'), 3 x C-17, 3 x C-17'), 145.3 (C-6), 145.7, 146.0 (3 x C-14, 3 x C-14'), 148.1 (C-2), 166.9 (C-4), 168.7 (C-8)

LRMS (ES⁺): m/z= 768 [M+H]⁺

HRMS (ES⁺): Found: 768.3904 [M+H]⁺ C₅₀H₅₀N₅O₃⁺ requires 768.3908

31b



Yield: 8%

Melting point: 91-95°C

R_f: 0.8 in CH₂Cl₂/MeOH/NH₃ 85:14:1

¹H-NMR: (500 MHz, MeOD) δ 1.69-1.86 (4 H, m, C(10)H₂ C(19)H₂), 2.13-2.52 (2 H, 2 x t *J*=6.4, C(11)H₂), 3.12-3.20 (2 H, 2 x m, C(20)H₂), 3.44-3.47(4 H, m, C(9)H₂ C(18)H₂), 4.52, 4.67 (2 H, 2 x s, C(7)H₂), 5.05, 5.08 (2 H, 2 x s, C(23)H₂), 5.67 (1 H, m C(5)H), 7.17-7.21, 7.44-7.48 (20 H, m, 6 x C(15)H, 6 x C(16)H, 3 x C(17)H, 2 x C(25)H, 2 x C(26)H, C(27)H), 7.33 (1 H, m, C(6)H)

¹³C-NMR: (125 MHz, MeOD) δ 28.8, 29.5, 29.8, 30.7 (C-10, C-19), 39.1, 39.3 (C-11, C-20), 42.3 (C-20), 45.1, 45.7 (C-9, C-18), 48.7 (C-7), 67.4 (C-23), 71.5 (C-13), 102.1 (C-5), 127.3-129.5 (6 x C-15, 6 x C-16, 3 x C-17, 2 x C-25, 2 x C-26, C-27), 147.6 (C-14), 148.1 (C-6), 157.2 (C-24), 166.9 (C-4), 168.4 (C-22), 168.7 (C-8)

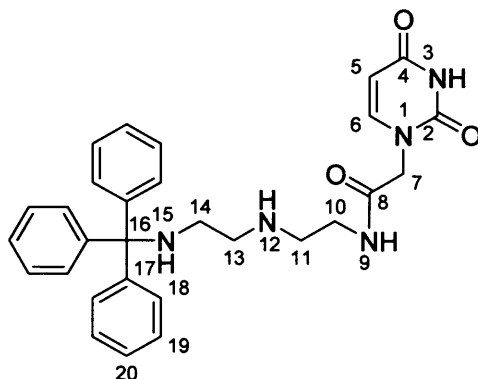
LRMS (ES⁺): *m/z*= 660 [M+H⁺]

HRMS (ES⁺): Found: 660.3187 [M+H⁺] C₃₉H₄₂N₅O₅⁺ requires 660.3180

8.30 Synthesis of 1-[N-di(triphenylmethylaminoethyl)acetamide]uracil (36) and 1-[N-(triphenylmethy-aminoethyl)-N-(aminoethyl)acetamide]uracil (35)

A suspension of **28** (100 mg, 0.39 mmol) in DCM (30 mL) was placed under N₂ atmosphere and Et₃N (80 mg, 0.78 mmol) in DCM (2 mL) was added followed by TrtCl (110 mg, 0.39 mmol) in DCM (10 mL). The solution which became cloudy was left stirring at RT for 2 h. The solvent was removed *in vacuo* and both mono and di tritylated products were observed by mass spectrometry. The crude was washed with diethyl ether and water and purified by flash chromatography (CH₂Cl₂/MeOH/NH₃ 100:0:0→80:18.6:0.4). The di-substituted product was collected as the first fraction and was precipitated from ether as a white solid (15 mg). The mono-substituted product was also collected as a white solid (11 mg).

35



Yield: 6%

R_f: 0.5 in CH₂Cl₂/MeOH/NH₃ 85:14:1

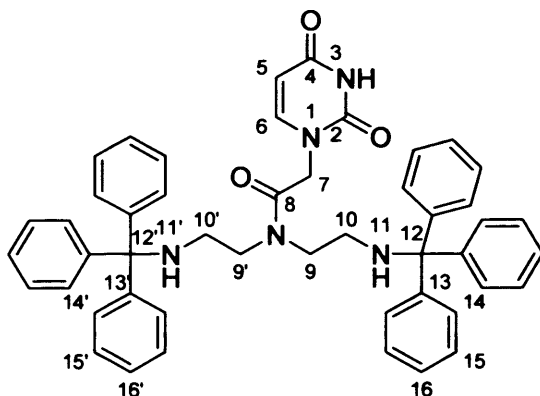
¹H-NMR: (500 MHz, MeOD) δ 2.39 (2 H, m, C(14)H₂), 2.88 (4 H, m, C(11)H₂, C(13)H₂), 3.42 (2 H, m, C(10)H₂), 4.45 (2 H, s, C(7)H₂), 5.67 (1 H, d *J*=7.9, C(5)H), 7.18-7.50 (16 H, m, 6 x C(18)H, 6 x C(19)H, 3 x C(20)H, C(6)H)

¹³C-NMR: (125 MHz, MeOD) δ 30.7 (C-14), 39.1, 43.2 (C-11, C-13), 51.4 (C-7), 54.8 (C-10), 72.1 (C-16), 102.3 4 (C-5), 127.5-129.9 (6 x C-18, 6 x C-19, 3 x C-20), 147.2 (3 x C-17), 147.8 (C-6), 170.2 (C-8)

LRMS (ES⁺): *m/z*= 498 [M+H]⁺

HRMS (ES⁺): Found: 498.2498 [M+H]⁺ C₂₉H₃₂N₅O₃⁺ requires 498.2500

36



Yield: 5%

R_f: 0.7 in CH₂Cl₂/MeOH/NH₃ 85:14:1

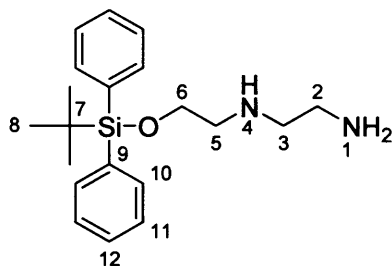
¹H-NMR: (500 MHz, CDCl₃) δ 2.21-2.28 (4 H, m, C(10)H₂, C(10')H₂), 3.26-3.38 (4 H, m, C(9)H₂, C(9')H₂), 4.04, 4.61 (2 H, 2 x s, C(7)H₂), 5.62 (1 H, d *J*=7.9, C(5)H), 7.08-7.40 (30H, m, 6 x C(14)H, 6 x C(14')H, 6 x C(15)H, 6 x C(15')H, 3 x C(16)H, 3 x C(16')H), C(6)H

¹³C-NMR: (125 MHz, CDCl₃) δ 41.7 (C-10, C-10'), 46.5 (C-9, C-9'), 48.0, 48.2 (C-7), 70.8, 71.1 (C-12, C-12'), 102.0 (C-5), 126.4-128.5 (6 x C-14, 6 x C-14', 6 x C-15, 6 x C-15', 3 x C-16, 3 x C-16'), 145.1 (C-6), 145.3, 145.8 (3 x C-13, 3 x C-13'), 150.5 (C-2), 162.9 (C-4), 166.7 (C-8)

LRMS (ES⁺): *m/z* = 740 [M+H]⁺

HRMS (ES⁺): Found: 740.3596 [M+H]⁺ C₄₈H₄₆N₅O₃⁺ requires 740.3595

8.31 (37) Synthesis of N-(tert-butylidiphenylsilyloxy)ethyl ethylenediamine



Compound **37** was synthesised according to general procedure B using N-(2-hydroxyethyl)ethylenediamine (2.13 mL, 21.07 mmol) in pyridine (20 mL), and *tert*-butyldiphenylsilyl chloride (5.50 mL, 21.15 mmol) in pyridine (30 mL). The reaction was left stirring at RT overnight. The solvent was removed *in vacuo* and the crude product was purified by column chromatography (CH₂Cl₂/MeOH/NH₃ 100:0:0 → 90:8:2) to yield the pure product as a yellow oil (2.27 g).

Yield: 32%

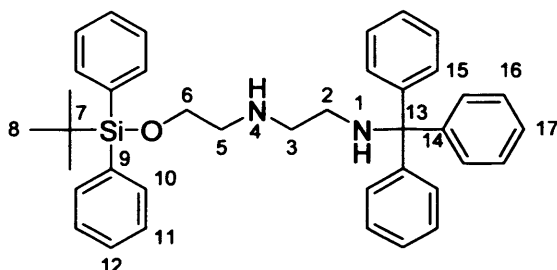
R_f: 0.7 in CH₂Cl₂/MeOH/NH₃ 80:18:2

¹H-NMR: (300 MHz, MeOD) δ 1.08 (9 H, s, 3 x C(8)H₃), 2.76, 2.80, 2.84 (6 H, 3 x t *J*=6.0, *J*=6.0, *J*=5.7, C(2)H₂, C(3)H₂, C(5)H₂), 3.81 (2 H, t *J*=5.7 C(6)H₂), 7.42-7.71 (10 H, m, 4 x C(10)H, 4 x C(11)H, 2 x C(12)H)

¹³C-NMR: (75 MHz, MeOD) δ 20.1 (C-7), 27.4 (3 x C-8), 41.1 (C-2), 50.5, 52.0 (C-3, C-5), 64.2 (C-6), 128.9, (4 x C-11), 131.1 (2 x C-12), 136.7 (4 x C-10), 134.6 (2 x C-9)

LRMS (ES⁺): *m/z*= 343.4 [M+H]⁺

8.32 (38) Synthesis of N-(*tert*-butyldiphenylsilyloxy) ethyl -N-(triphenylmethylamino)ethyl amine



A solution of **37** (500 mg, 1.46 mmol) in DCM (50 mL) was cooled to 0°C under N₂ atmosphere. TrtCl (407 mg, 1.46 mmol) in DCM (80 mL) was added slowly. The reaction was brought to RT and Et₃N was added (0.20 mL, 1.46 mmol). The reaction was left stirring at RT overnight over which time the solution turned cloudy. The solvent was removed *in vacuo*. The crude was redissolved in DCM (30 mL), washed with H₂O and dried with MgSO₄ to yield a sticky yellow oil (613 mg). This crude product was used for the subsequent synthetic step without further purification.

Yield: 72%

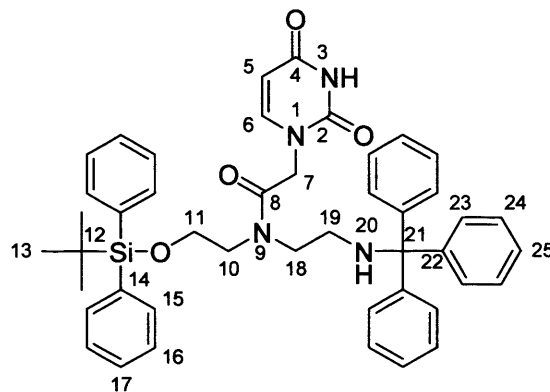
R_f: 0.6 in CH₂Cl₂/MeOH/NH₃ 95:4.5:0.5

¹H-NMR: (300 MHz, MeOD) δ 0.97 (9 H, s, 3 x C(8)H₃), 2.20 (2 H, t *J*= 6.2 C(2)H₂) 2.57, 2.61 (4 H, 2 x t, *J*= 6.2, *J*= 5.7, C(3)H₂, C(5)H₂), 3.70 (2 H, t *J*=5.7 C(6)H₂), 7.05-7.37 (25 H, m, 4 x C(10)H, 4 x C(11)H, 2 x C(12)H, 6 x C(15)H, 6 x C(16)H, 3 x C(17)H)

¹³C-NMR: (75 MHz, MeOD) δ 20.1 (C-7), 27.4 (3 x C-8), 44.2 (C-2), 50.7, 52.1 (C-3, C-5), 63.9 (C-6), 72.1 (C-13), 127.4, 130.5 (3 x C-17, 6 x C-16, 6 x C-15), 128.9, (4 x C-11), 130.5 (2 x C-12), 136.7 (4 x C-10), 134.6 (2 x C-9), 147.5 (3 x C-14)

LRMS (ES⁺): *m/z*= 585 [M+H]⁺

8.33 (39) Synthesis of 1-[N-(*tert*-butyldiphenylsilyloxy)ethyl- N-(triphenylmethylamino)ethyl-acetamide] uracil



Compound **38** (614 mg, 1.05 mmol) was dissolved in DMF (3 mL) and cooled to 0°C under N₂ atmosphere. A solution of **1** (180 mg, 1.05 mmol) and DhbtOH (200 mg, 1.21 mmol) in DMF (3 mL) was added while stirring under N₂ atmosphere followed by a solution of DCC (260 mg, 1.25 mmol) in DMF (6 mL). The mixture was left stirring at 0°C for 1 h and then at RT overnight. The solvent was evaporated off under reduced pressure. The crude was redissolved in DCM (30 mL) and washed with NaHCO₃ (3 x 30 mL), NaCl (2 x 30 mL) and dried with MgSO₄. The solvent was removed *in vacuo* and the pure product was precipitated from MeOH as a white solid (365 mg). NMR showed splitting of peaks due to restricted rotation about the amide bond.

Yield: 52%

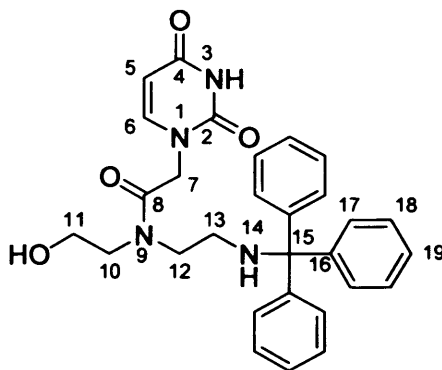
R_f: 0.8 in CH₂Cl₂/MeOH 95:5

¹H-NMR: (300 MHz, MeOD) δ 1.02, 1.08 (9 H, s, 3 x C(13)H₃), 2.15, 2.22 (2 H, m, C(19)H₂), 3.41, 3.47 (4 H, 2 x m, C(10)H₂, C(18)H₂), 3.71, 3.85 (2 H, m, C(11)H₂), 4.58, 4.75 (2 H, 2 x s, C(7)H₂), 5.56, 5.66 (1 H, 2 x d *J*=7.8, C(5)H), 7.20-7.69 (26 H, m, C(6)H, 4 x C(15)H, 4 x C(16)H, 2 x C(17)H, 6 x C(23)H, 6 x C(24)H, 3 x C(25)H)

¹³C-NMR: (75 MHz, MeOD) δ 19.8, 20.3 (C-12), 26.5, 27.0 (3 x C-13), 43.2, 43.6 (C-19), 47.3, 48.2 (C-10, C-18), 50.5, 51.6 (C-7), 63.7, 64.3 (C-11), 72.3 (C-21), 101.3 (C-5), 127.4-135.0 (2 x C-17, 4 x C-16, 4 x C-15, 6 x C-23, 6 x C-24, 3 x C-25, 2 x C-14), 147.5 (3 x C-22), 147.7 (C-6), 154.2 (C-2), 166.5 (C-4), 168.8 (C-8)

LRMS (ES⁺): *m/z*= 738 [M+H]⁺

8.34 (40) Synthesis of 1-[N-hydroxyethyl-N-(triphenylmethyl amino)ethyl-acetamide] uracil



Compound **40** was synthesised according to general procedure G using **39** (365 mg, 0.495 mmol) in THF (5 mL) and TBAF in THF (1.0 mL, 1.0 mmol). After 30mins, no starting material could be seen by TLC. The solvent was removed *in vacuo* and purified by flash chromatography (CH₂Cl₂/MeOH 100:0→95:5) and the pure product was isolated as a white solid (200 mg). NMR again showed peak splitting. It was proven, however, by variable temperature NMR that this was due to restricted rotation around the nitrogen bond as *J* C(7)H₂ reduced from 0.4 to 0.1 ppm on heating to 40°C.

Yield: 79%

R_f: 0.25 in CH₂Cl₂/MeOH 95:5

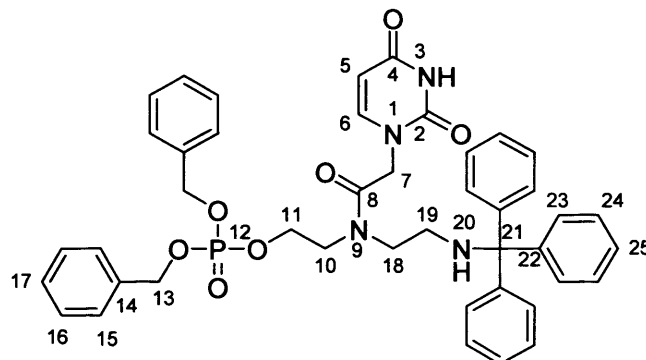
¹H-NMR: (300 MHz, MeOD) δ 2.38, 2.41 (2 H, 2 x t *J*=6.0, C(13)H₂), 3.45, 3.55 (4 H, 2 x m, C(10)H₂, C(12)H₂), 3.63, 3.73 (2 H, 2 x t *J*=5.4, C(11)H₂), 4.78, 4.79 (2 H, 2 x s, C(7)H₂), 5.57 (1 H, d *J*=7.9, C(5)H), 7.17-7.48 (16 H, m, C(6)H, 6 x C(17)H, 6 x C(18)H, 3 x C(19)H)

¹³C-NMR: (75 MHz, MeOD) δ 43.1, 43.7 (C-13), 48.7 (C-10, C-12), 50.4, 51.2 (C-7), 60.4 (C-11), 72.6 (C-15), 102.1 (C-5), 127.4, 128.9, 129.9 (6 x C-17, 6 x C-18, 3 x C-19,), 147.4 (3 x C-16), 147.9 (C-6), 152.9 (C-2), 166.9 (C-4), 169.7 (C-8)

LRMS (ES⁺): *m/z* = 499 [M+H]⁺

HRMS (ES⁺): Found: 499.2361 [M+H]⁺ C₂₉H₃₁N₄O₄⁺ requires 499.2340

8.35 (41) Synthesis of 1-[N-(dibenzylphosphoxy)ethyl-N-(triphenylmethylamino)ethyl acetamide] uracil



Compound **40** (60 mg, 0.12 mmol) and 1-H-tetrazole (0.45 M soln. in THF, 0.3 mL, 0.14 mmol) were partially dissolved in DCM (10 mL) under N₂ atmosphere. Dibenzyl N,N-diisopropyl phosphoramidite (249 mg, 0.72 mmol) in DCM (2 mL) was added and the solution became a little less cloudy though a precipitate still remained. The solution was left stirring at RT for 90 min, after which time the solution was clear. The solution was cooled to -40°C using CH₃CN/dry ice bath. *Tert*-BuOOH (70% in H₂O, 0.96 mmol) was added slowly to the solution which was left stirring at 40°C for 15 min and then allowed to come to RT over 20 min and finally was left stirring for a further 20 min under N₂ at RT. The solvent was removed *in vacuo*. The crude was washed with H₂O and redissolved in MeOH. On addition of diethyl ether a precipitate formed. This was shown by NMR to be a mixture of the phosphoramidite starting material and the desired product. After purification by flash chromatography (CH₂Cl₂/MeOH 100:0→90:10) the pure product was isolated as a white solid (50 mg). ¹³C NMR peaks did show splitting for up to 5 bonds from P.

Yield: 55%

R_f: 0.7 in CH₂Cl₂/MeOH 90:10

¹H-NMR: (300 MHz, MeOD) δ 2.35, 2.39 (2 H, 2 x t *J*=5.6, C(19)H₂), 3.39 (2 H, m, C(10)H₂), 3.47, 3.64 (2 H, m, C(18)H₂), 4.07, 4.16 (2 H, m, C(11)H₂), 4.57, 4.78 (2 H, 2 x s, C(7)H₂), 5.02, 5.07 (4 H, m, 2 x C(13)H₂), 5.59 (1 H, m, C(5)H), 7.18-7.47 (26 H, m, C(6)H, 2 x C(17)H, 4 x C(15)H, 4 x C(16)H, 3 x C(25)H, 6 x C(23)H, 6 x C(24)H)

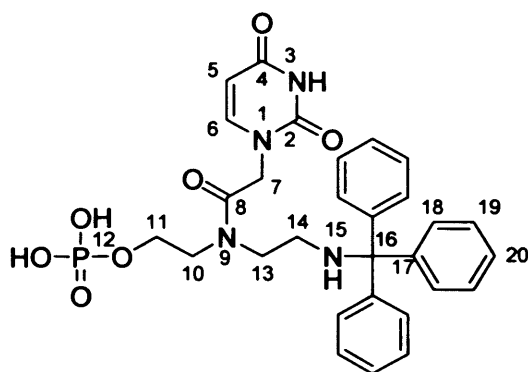
¹³C-NMR: (75 MHz, MeOD) δ 43.3, 43.8 (C-19), 47.8 (C-10), 48.1 (C-18), 49.9, 50.2 (C-7), 66.3, 66.4 (C-11), 71.0, 71.2 (C-13), 102.2 (C-5), 129.0-129.9 (6 x C-23, 6 x C-24, 3 x C-25), 137.0, 137.1 (2 x C-17, 4 x C-16, 4 x C-15, 2 x C-14), 147.3 (3 x C-22), 147.8 (C-6), 152.7 (C-2), 166.9 (C-4), 169.6, 169.7 (C-8)

³¹P-NMR: (202MHz, MeOD) δ 8.5 (P-12)

LRMS (ES⁺): m/z= 760 [M+H]⁺

HRMS (ES⁺): Found: 759.2911 [M+H]⁺ C₄₃H₄₄N₄O₇P⁺ requires 759.2942

8.36 (42) Synthesis of 1-[N-(phosphoxy)ethyl-N-(triphenylmethylamino) ethyl acetamide] uracil



Compound **41** (50 mg, 0.07 mmol) was dissolved in MeOH (15 mL) and placed first under vacuum and then N₂. 5% Pd/C (15 mg, 0.01 mmol) was added. The system was placed under vacuum and flushed with N₂ 3 times and finally placed under vacuum again. The system was exposed to H₂ by piercing the septum with a H₂ filled balloon. The solution was left stirring for 2 h. The solvent was removed *in vacuo*. The crude plus the catalyst was taken up in DMF (5 mL) and filtered through celite. The solvent was again removed *in vacuo* and the crude was again taken up in DMF (5 mL) and filtered through celite in order to remove catalyst. A white solid was obtained (19 mg).

Yield: 50%

R_f: 0 in CH₂Cl₂/MeOH 70:30

¹H-NMR: (300 MHz, MeOD) δ 2.29 (2 H, m, C(14)H₂), 3.38 (2 H, m, C(10)H₂), 3.69 (2 H, m, C(13)H₂), 3.86, 3.93 (2 H, m, C(11)H₂), 4.69, 4.72 (2 H, 2 x s, C(7)H₂), 5.57 (1 H, m, C(5)H), 7.18-7.44 (16 H, m, C(6)H, 6 x C(18)H, 6 x C(19)H, 3 x C(20)H)

¹³C-NMR: (75 MHz, MeOD) δ 42.1, (C-14), 46.1 (C-10), 47.9 (C-13), 49.0 (C-7), 62.2 (C-11), 70.1 (C-16), 100.5 (C-5), 127.8, 128.3, 128.4 (6 x C-18, 6 x C-19, 3 x C-20), 145.8 (3 x C-17), 146.8 (C-6), 151.0 (C-2), 163.9 (C-4), 167.0 (C-8)

LRMS (ES⁺): m/z= 580 [M+2H]⁺

HRMS (ES⁺): Found: 579.2009 [M+H]⁺ C₂₉H₃₂N₄O₇P⁺ requires 579.2003

9 Experimental II

9.1 GRID calculations

The PDB file 1VYQ was downloaded from the protein data bank. The reference molecule was removed by deleting all HETATM in the text file to create the file plasmlessligand.pdb. GRID was run from the directory in which the .pdb file was saved. GRIN calculations were run in order to prepare the protein for GRID calculations using the automatic filtering option. All GRIN warnings were ignored. Coordinates were defined in which the calculations were to be carried out as BOTX 26.34, BOTY -17.35, BOTZ -18.40, TOPX 42.56, TOPY -1.03, TOPZ -4.63. Default settings and keywords were used. The directive MOVE which controls the flexibility of the target was set to 0. This allowed for lone pairs and tautomeric hydrogens to move in response to the probe. The directive NPLA which determines the resolution of the computation i.e. the distance between each GRID point was set to 4, therefore, each GRID point in the defined region was 0.25Å apart. The directive LEVL which controls the amount of information in the the output file GRINLOUT was set to 3 and the directive ALMD was set to 1 which allowed for extra information to be written to the GRID output file GRIDKONT. The probes to be used were chosen, these are listed in table 5-1 and the GRID calculations were carried out and visualised using the integrated program using GVIEW.

9.2 FlexX docking

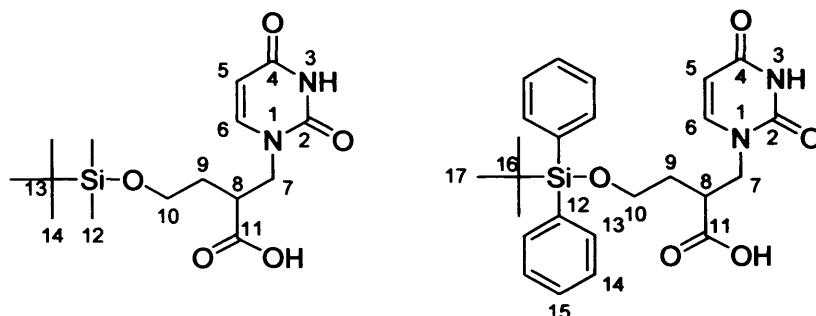
Compounds **47-56** were drawn and minimised using Sybyl 6.9.1. Minimisation was carried out using the TRIPOS force field in a dielectric constant of 80, the conjugated gradient method was used with a gradient of 0.05kcal/mol and 1000 iterations. Charges were not assigned as FlexX assigns formal charges to the ligand before docking calculations are carried out. The compounds were then docked using FlexX. The uracil ring was manually defined as the base fragment and the active site was defined as 8Å around the reference molecule. The conformations generated were ranked by FlexX by decreasing FlexX total score (increasing ΔG) and visualised using Sybyl 6.9.1 and VMD 1.8.4.

9.3 General procedures

General procedure H: Parallel amide synthesis using DhbtOH and DCC in a Radley's reduced temperature carousel

The relevant amine (1.2 eq), **58** (1 eq) and DhbtOH (1.2eq) was stirred in a Radley's threaded glass reaction tube in DMF (6 mL/mmol). Et₃N (1.5 eq) was added in cases where the hydrochloride amino salt was used. The reactions were cooled to 0°C under argon and DCC (1.2eq) in DMF (1 mL/mmol) was added. The reactions were stirred at 0°C for 1 h and then at RT overnight. The DCU precipitate which formed was removed by filtration and the crude mixtures were purified by flash chromatography on silica gel.

9.4 (58) 1-[2-(carboxy)-4-(*tert*-butyldiphenylsilyloxy)butyl]uracil or 1-[2-(carboxy)-4-(*tert*-butyldimethylsilyloxy)butyl]uracil



Method 1 PDC/DMF: Previously supplied intermediate TBDMS protected intermediate **57** (500 mg, 1.52 mmol) was dissolved in DMF (2 mL) under argon at RT. PDC (5.86 g, 7.61 mmol) in DMF (5 mL) was added. The solution was stirred overnight at RT. Bromocresol green stained TLC showed the presence of the acid on the base line as a bright yellow spot. Diethyl ether (30 mL) was added and the solution was washed with saturated NaHCO₃ (2 x 50 mL). The aqueous layer was acidified to pH 2 with 0.2 M HCl and extracted with diethyl ether (4 x 50 mL). The organic layer was dried with MgSO₄ and evaporated *in vacuo*. No product, however was isolated from this extraction. TLC stained with bromocresol green showed the acid was still present in the aqueous phase, however, separation from the excess PDC was not possible using any organic solvents. Furthermore, NMR analysis did not show the presence of any product.

Method 2 CrO₃, H₅IO₆, H₂O, ACN: A solution of CrO₃ (0.5 mg, 0.01 mmol) and H₅IO₆ (252 mg, 1.11 mmol) in ACN:H₂O 3:1 (1 mL) was added over 15 min using a syringe pump to a solution of TBDPS protected intermediate **57** (200 mg, 0.44 mmol) in ACN:H₂O 3:1 (1 mL) at 0°C. The reaction was stirred for 30min at 0°C and then allowed to warm to RT. The precipitate which had formed was filtered and identified as periodic acid. The solvent was removed from the filtrate and DCM (5 mL) was added to form an insoluble yellow gel which was removed by trituration. This insoluble material was identified by ¹H-NMR as starting material in which the silyl protecting group had been cleaved. The DCM soluble material was identified by ¹H-NMR as silanol. None of the desired product was isolated from the reaction.

Method 3 TEMPO, BAIB: The TBDPS protected intermediate **57** (1.5 g, 3.31 mmol), BAIB (2.35 g, 7.29 mmol) and TEMPO (104mg, 0.66 mmol) were dissolved in ACN:H₂O 1:1 (10 mL). The yellow solution was stirred at RT for 3 h. The solvent was removed under reduced pressure and the desired product was triturated from diethyl ether as a white solid (1.31 g).

Melting point: 65-66°C

Yield: 85%

R_f: 0 in CH₂Cl₂/MeOH 90:10

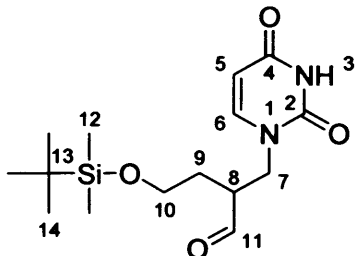
¹H-NMR: (500 MHz, CD₃CN) δ 1.01 (9 H, s, 3 x C(17)H₃), 1.75, 1.88 (2 H, m, C(9)H₂), 3.06 (1 H, m, C(8)H), 3.74 (2 H, m, C(7)H₂), 3.85-3.94 (2 H, m, C(10)H₂), 5.58 (1 H, d *J*=7.7 C(5)H), 7.43-7.68 (10 H, m, 2 x C(15)H, 4 x C(14)H, 4 x C(13)H), 7.76 (1 H, d *J*=7.7, C(6)H)

¹³C-NMR: (125 MHz, CD₃CN) δ 18.2 (C-16), 25.8 (3 x C-17), 31.7 (C-9), 40.8 (C-8), 49.8 (C-7), 61.0 (C-10), 100.4 (C-5), 127.5 (2 x C-15), 129.5 (4 x C-14), 135.0 (4 x C-13), 133.0 (2 x C-12), 146.1 (C-6), 150.8, (C-2), 164.2 (C-4), 174.6 (C-11)

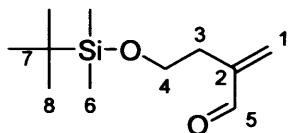
LRMS (ES⁺): *m/z*= 467.0 [M+H]⁺

HRMS (ES⁻): Found: 465.1834 [M-H]⁻ C₂₅H₂₈O₅N₂Si⁻ requires 465.1840

9.5 (59) 1-[2-(acetaldehyde)-4-(*tert*-butyldimethylsilyloxy)butyl] uracil



Method 1 Swern oxidation: Oxalyl chloride (212 mg, 1.67 mmol) was dissolved in DCM (10 mL) under argon and cooled to -70°C . DMSO (262 mg, 3.35 mmol) in DCM (5 mL) was added drop-wise so that the temperature remained constant. After 10 min, previously supplied intermediate **57** (500 mg, 1.52 mmol) in 3 mL DCM was added slowly. The reaction was left stirring for a further 15 min at -70°C and became cloudy. NEt_3 (616 mg, 6.09 mmol) was added at -70°C and the solution became clear. The solution was warmed to 0°C and stirred for 5 min. The mixture was then allowed to reach RT over 45 min. H_2O (20 mL) was added and separated from the organic layer which was washed with brine (2 x 75 mL), dried with MgSO_4 and evaporated *in vacuo*. A number of spots could be seen by permanganate stained TLC. A precipitate formed on addition of diethyl ether which was identified by $^1\text{H-NMR}$ as uracil. The diethyl ether filtrate showed to be a mixture of products which were purified by flash chromatography (EtOAc:Hexane 50:50 \rightarrow 90:10). The major product isolated, however was identified by $^1\text{H NMR}$ and mass spectrometry as the enal, **60** produced from a reverse Michael addition across the N-1, C-7 bond.



60

$^1\text{H-NMR}$: (500 MHz, CDCl_3) δ 0.05 (6 H, s, 2 x C(6)H₃), 0.91 (9 H, s, 3 x C(8)H₃), 2.30 (2 H, m, C(3)H₂), 3.71 (2 H, m, C(4)H₂), 6.01, 6.37 (2 H, 2 x s, C(1)H₂), 9.51 (1 H, s, C(5)H)

LRMS (ES^+): $m/z = 215.2$ [$\text{M}+\text{H}$] $^+$

Method 2 PCC, DCM: PCC (177 mg, 0.82 mmol) and TBDMS protected intermediate **57** were stirred in 3 mL dry DCM with 3 Å molecular sieves (120 mg) under argon at RT overnight. No starting material could be seen by TLC. The solution was filtered through celite to remove the catalyst which was further washed with DCM (300 mL). However, no product was isolated from the filtrate. The product could not be isolated from the chromium salts.

Method 3 TPAP, NMO: Previously supplied TBDMS intermediate **57** (100mg, 0.30 mmol) and 3Å molecular sieves (112 mg) were stirred in dry DCM (1 mL) under argon at RT. *N*-metylmorpholine-*N*-oxide (53 mg, 0.46 mmol) in DCM (0.5 mL) was added, followed by tetrapropylammonium peruthenate (5 mg, 0.02 mmol) in DCM (1 mL). The solution was left stirring for 5 h. The solvent was evaporated under reduced pressure and the crude residue was purified by flash chromatography (EtOAc/Hexane 0:100→50:50) to yield the product as a white solid (50 mg).

Yield: 50% (method 3)

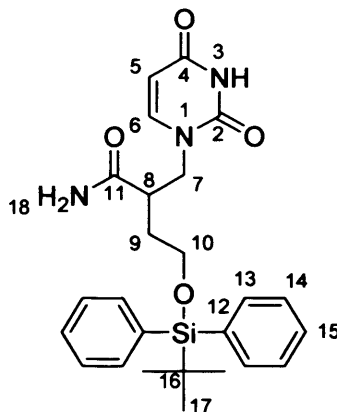
R_f: 0.4 in EtOAc/Hexane 9:1

¹H-NMR: (500 MHz; CDCl₃) δ 0.02 (6 H, s, 2 x C(12)H₃), 0.83 (9 H, s, 3 x C(14)H₃), 1.89 (2 H, q J=6.0, C(9)H₂), 2.90 (1 H, m, C(8)H), 3.69 (2 H, t J=6.0, C(10)H₂), 3.86 (2 H, m, C(7)H₂), 5.61 (1 H, d J=7.5, C(5)H), 7.35 (1 H, d J=7.5, C(6)H), 8.57 (1 H, s, C(11)H), 9.66 (1 H, s, N(3)H)

¹³C-NMR: (125 MHz; CDCl₃) δ -5.5 (2 x C-12), 18.2 (C-13), 25.8 (C-14), 30.8 (C-9), 47.7 (C-8), 49.0 (C-7), 60.1 (C-10), 101.8 (C-5), 145.9 (C-6), 150.9 (C-2), 165.8 (C-4), 202.2 (C-11)

LRMS (ES⁺): m/z= 327.2 [M+H]⁺

9.6 (61) 1-[2-(acetamide)-4-(*tert*-butyldiphenylsilyloxy)butyl]uracil



Compound **58** (300 mg, 0.64 mmol), NH_4Cl (42 mg, .77 mmol) and DhbtOH (121 mg, 0.74 mmol) were dissolved in DMF (5 mL) under argon at 0°C. NEt_3 (96 mg, 0.96 mmol) was added, followed by DCC (159 mg, 0.77 mmol) in DMF (2 mL). The reaction was stirred at 0°C for 1 h and then at RT overnight. A precipitate which was identified by ^1H NMR as DCU was filtered off. Following removal of solvent, further DCU side product was removed by precipitation from acetone. The crude was purified by flash chromatography (EtOAc/Hexane 0:100→50:50, $\text{CHCl}_3/\text{MeOH}$ 100:0→90:10) to yield the product as a yellow solid (240 mg).

Yield: 80%

R_f : 0.4 in $\text{CH}_2\text{Cl}_2/\text{MeOH}$ 90:10

Melting point: 90-93°C

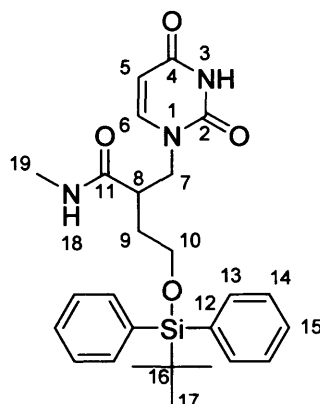
$^1\text{H-NMR}$: (500 MHz, $(\text{CD}_3)_2\text{CO}$) δ 1.01 (9 H, s, 3 x C(17) H_3), 1.61, 1.79 (2 H, m, C(9) H_2), 2.78 (1 H, m, C(8)H), 3.64, 3.85 (4 H, m, C(7) H_2 , C(10) H_2), 5.52 (1 H, d $J=7.7$ C(5)H), 6.34, 6.89 (2 H, 2 x s, N(18) H_2), 7.44-7.64 (11 H, m, 2 x C(15)H, 4 x C(14)H, 4 x C(13)H, C(6)H), 11.30 (1 H, s, N(3)H)

$^{13}\text{C-NMR}$: (125 MHz, $(\text{CD}_3)_2\text{CO}$) δ 19.7 (C-16), 27.5 (3 x C-17), 34.1 (C-9), 42.0 (C-8), 51.8 (C-7), 62.6 (C-10), 101.5 (C-5), 128.8 (2 x C-15), 130.6 (4 x C-14), 134.4 (4 x C-13), 136.2 (2 x C-12), 147.0 (C-6), 151.8 (C-2), 164.1 (C-4), 175.7 (C-11)

LRMS (ES^+): $m/z= 466.0$ $[\text{M}+\text{H}]^+$

HRMS (ES^+): Found: 488.1970 $[\text{M}+\text{Na}]^+$ $\text{C}_{25}\text{H}_{30}\text{O}_4\text{N}_3\text{SiNa}^+$ requires 488.1976

9.7 (62) 1-[2-(methylamido)-4-(*tert*-butyldiphenylsilyloxy)butyl]uracil



Compound **62** was synthesised according to general procedure C (Chapter 8) of EDC mediated amide coupling using **58** (200 mg, 0.43 mmol), methyl amine hydrochloride (24mg, 0.36 mmol) and EDC (89mg, 0.46mmol). The amine was neutralised by prestirring with Et₃N. The crude was purified by flash chromatography (EtOAc/Hexane 0:100→50:50, CHCl₃/MeOH 100:0→90:10) to yield the product as a clear wax (12 mg).

Yield: 7%

R_f: 0.4 in CH₂Cl₂/MeOH 95:5

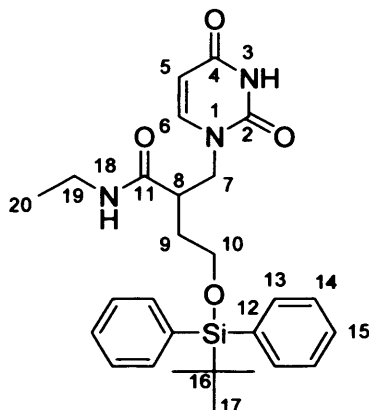
¹H-NMR: (500 MHz, CDCl₃) δ 1.00 (9 H, s, 3 x C(17)H₃), 1.66-1.70 (2 H, m, C(9)H₂), 2.55 (3 H, C(19)H₃), 2.91 (1 H, m, C(8)H), 3.55-3.95 (4 H, m, C(7)H₂, C(10)H₂), 5.50 (1 H, d *J*=7.8 C(5)H), 5.67 (1 H, s, N(18)H), 7.19-7.57 (11 H, m, 2 x C(15)H, 4 x C(14)H, 4 x C(13)H, C(6)H), 8.87 (1 H, s, N(3)H)

¹³C-NMR: (125 MHz, CDCl₃) δ 18.1 (C-16), 25.3 (C-19), 25.9 (3 x C-17), 32.0 (C-9), 41.4 (C-8), 50.5 (C-7), 60.2 (C-10), 100.3 (C-5), 126.8 (2 x C-15), 128.9 (4 x C-14), 132.2 (2 x C-12), 134.5 (4 x C-13), 145.1 (C-6), 149.7 (C-2), 162.7 (C-4), 172.0 (C-11)

LRMS (ES⁺): *m/z*= 480.1 [M+H]⁺

HRMS (ES⁺): Found: 502.2139 [M+Na]⁺ C₂₆H₃₂O₄N₃SiNa⁺ requires 502.2133

9.8 (64) 1-[2-(ethylamido)-4-(*tert*-butyldiphenylsilyloxy) butyl] uracil



The synthesis of **64** was carried out according to general procedure H using ethylamine hydrochloride (42 mg, 0.52 mmol), DhbtOH (81 mg, 0.49 mmol), **58** (200 mg, 0.43 mmol), Et₃N (65 mg, 0.64 mmol) and DCC (106 mg, 0.52 mmol). The crude was purified by flash chromatography (EtOAc/Hexane 0:100→50:50, CHCl₃/MeOH 100:0→90:10) to yield the desired product as a yellow wax (34 mg)

Yield: 16%

R_f: 0.6 in CH₂Cl₂/MeOH 90:10

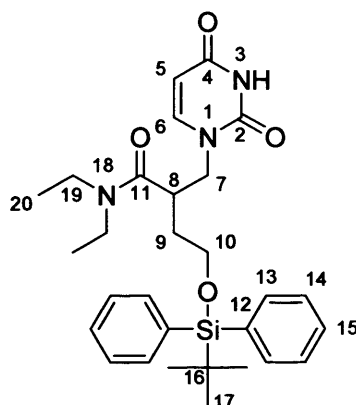
¹H-NMR: (500 MHz, (CD₃)₂CO) δ 0.86 (3 H, t *J*=7.3, C(20)H₃), 0.90 (9 H, s, 3 x C(17)H₃), 1.57- 1.80 (2 H, m, C(9)H₂), 2.80 (1 H, m, C(8)H), 2.94-3.08 (2 H, m, C(19)H₂), 3.51-3.90 (4H, m, C(7)H₂, C(10)H₂), 5.35 (1 H, d *J*=7.9, C(5)H), 7.21-7.58 (12 H, m, 2 x C(15)H, 4 x C(14)H, 4 x C(13)H, C(6)H, N(18)H), 9.90 (1 H, s, N(3)H)

¹³C-NMR: (125 MHz, (CD₃)₂CO) δ 15.2 (C-20), 19.4 (C-16), 27.1 (3 x C-17), 33.7 (C-9), 34.8 (C-19), 43.7 (C-8), 51.4 (C-7), 61.8 (C-10), 101.0 (C-5), 128.8 (2 x C-15), 130.7 (4 x C-14), 134.5 (2 x C-12), 136.3 (4 x C-13), 146.6 (C-6), 152.0 (C-2), 164.6 (C-4), 173.1 (C-11)

LRMS (ES⁺): *m/z*= 494.2 [M+H]⁺

HRMS (ES⁺): Found: 494.2482 [M+H]⁺ C₂₇H₃₂O₄N₃Si⁺ requires 494.2470

9.9 (65) 1-[2-(diethylamido)-4-(*tert*-butyldiphenylsilyloxy)butyl] uracil



The synthesis of **65** was carried out according to general procedure H using diethyl amine hydrochloride (56 mg, 0.52 mmol), DhbtOH (81 mg, 0.49 mmol), **58** (200 mg, 0.43 mmol), Et₃N (65 mg, 0.64 mmol) and DCC (106 mg, 0.52 mmol). The crude was purified by flash chromatography (EtOAc/Hexane 0:100→50:50, CHCl₃/MeOH 100:0→90:10) to yield the desired product as a yellow wax (85mg)

Yield: 38%

R_f: 0.5 in CH₂Cl₂/MeOH 95:5

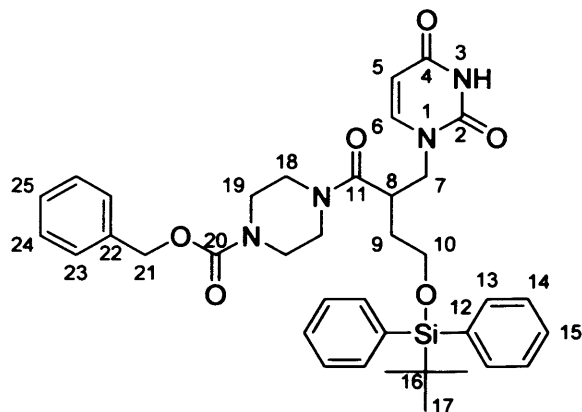
¹H-NMR: (500 MHz, CDCl₃) δ 0.94-1.00 (15 H, m, 2 x C(20)H₃, 3 x C(17)H₃), 1.60, 1.76 (2 H, m, C(9)H₂), 3.06 (1 H, m, C(8)H), 3.16-4.03 (8 H, m, 2 x C(19)H₃, C(7)H₂, C(10)H₂), 5.50 (1 H, d *J*=7.9, C(5)H), 7.19-7.61 (11 H, m, 2 x C(15)H, 4 x C(14)H, 4 x C(13)H, C(6)H), 9.06 (1 H, s, N(3)H)

¹³C-NMR: (125 MHz, CDCl₃) δ 13.3, 14.9 (2 x C-20), 19.2 (C-16), 26.9 (3 x C-17), 34.1 (C-9), 37.2 (C-8), 41.2, 42.3 (2 x C-19), 51.9 (C-7), 60.8 (C-10), 101.3 (C-5), 128.4 (2 x C-15), 130.3 (4 x C-14), 133.5 (2 x C-12), 135.9 (4 x C-13), 146.6 (C-6), 150.6 (C-2), 163.9 (C-4), 172.6 (C-11)

LRMS (ES⁺): *m/z*= 522.2 [M+H]⁺

HRMS (ES⁺): Found: 522.2795 [M+H]⁺ C₂₉H₄₀O₄N₃Si⁺ requires 522.2783

9.10 (67) 1-[2-(N-Z-piperazinamido)-4-(*tert*-butyldiphenyl silyloxy) butyl] uracil



The synthesis of **67** was carried out according to general procedure H using N-Cbz-piperazine (113 mg, 0.515 mmol), DhbtOH (81 mg, 0.494 mmol), **58** (200 mg, 0.429 mmol) and DCC (106 mg, 0.515 mmol). The crude was purified by flash chromatography (EtOAc/Hexane 0:100→50:50, CHCl₃/MeOH 100:0→90:10) to yield the desired product as a yellow wax (233 mg)

Yield: 81%

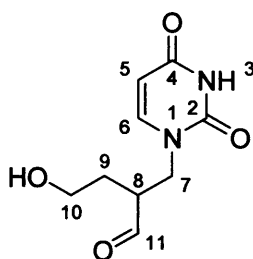
R_f: 0.2 in CH₂Cl₂/MeOH 95:5

¹H-NMR: (500 MHz, CDCl₃) δ 1.04 (9 H, s, 3 x C(17)H₃), 1.67, 1.85 (2 H, m, C(9)H₂), 3.25-3.77 (13 H, m, C(8)H, C(7)H₂, C(10)H₂, 2 x C(18)H₂, 2 x C(19)H₂), 5.16 (2 H, s, C(21)H₃), 5.60 (1 H, d *J*=7.7, C(5)H), 7.29-7.66 (16 H, m, 2 x C(15)H, 4 x C(14)H, 4 x C(13)H, C(6)H, 2 x C(23)H, 2 x C(24)H, C(25)H), 9.82 (1 H, s, N(3)H)

¹³C-NMR: (125 MHz, CDCl₃) δ 19.1 (C-16), 26.9 (3 x C-17), 33.4 (C-9), 36.6 (C-8), 41.8, (2 x C-18), 45.4 (2 x C-19), 51.8 (C-7), 61.5 (C-10), 68.1 (C-21), 101.3 (C-5), 127.8 (C-25), 128.1 (2 x C-15), 128.3 (2 x C-24), 130.3 (2 x C-23), 133.0 (2 x C-12), 135.5 (4 x C-13), 136.3 (C-22), 146.2 (C-6), 150.8 (C-2), 154.0 (C-20), 164.1 (C-4), 171.7 (C-11)

LRMS (ES⁺): *m/z* = 669.3 [M+H]⁺

HRMS (ES⁺): Found: 669.3128 [M+H]⁺ C₃₇H₄₅O₆N₄Si⁺ requires 669.3157

9.11 (70) 2-(1-methyluracil)-4-hydroxybutanal

1M TBAF solution in THF (0.61mL, 0.61mmol) was added to **48** (100mg, 0.307mmol). The yellow solution was left stirring at RT for 1h. The solvent was removed *in vacuo* and the crude was purified by flash chromatography (EtOAc/Hexane 1:4→4:1, then MeOH/CHCl₃ 0:100→5:95) to give the product as a clear oil (56 mg)

Yield: 72%

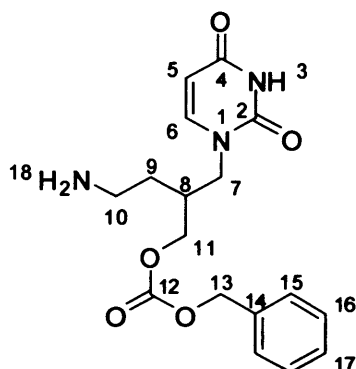
R_f: 0.00 in MeOH/CHCl₃ 1:4

¹H-NMR: (500 MHz; D₂O) δ 1.68, 2.05 (2 H, m, C(9)H₂), 2.51 (1 H, m, C(8)H), 3.76-4.07 (4 H, m, C(7)H₂, C(10)H₂), 5.69-5.77 (1 H, d J=7.7 C(5)H), 7.40-7.46 (1 H, m, C(6)H), 8.01-8.04 (1 H, br, N(3)H), 8.73 (1 H, s, C(11)H)

¹³C-NMR:(125 MHz; D₂O) δ 27.4 (C-9), 41.2 (C-7), 44.5 (C-8), 66.5 (C-10), 100.3 (C-5), 141.3 (C-6), 153.1 (C-2), 166.5 (C-4)

LRMS (ES⁺): m/z= 213.0 [M+H]⁺

9.12 (73) 1-[2-(carbobenzoxymethyl)-4-aminobutyl] uracil



Intermediate **72** (3 g, 8.04 mmol) supplied by Medivir was dissolved in pyridine (40 mL) under argon and triphenylphosphine (3.4 g, 12.87 mmol) was added. The solution was stirred at RT for 2.5 h after which time only starting material could be seen by TLC. NH_4OH conc. (117 mL) was added. The solution was stirred at 50° C for 2 d. the solvent was removed under reduced pressure and redissolved in CHCl_3 (30 mL). A precipitate formed which was identified by ^1H NMR as the phosphoimine intermediate. The filtrate was purified by flash chromatography on silica gel ($\text{NH}_3/\text{MeOH}/\text{CHCl}_3$ 0:0:100→1.2:6:94) to afford the product as a white solid (1.02 g).

Yield: 37%

R_f: 0.4 in $\text{CH}_2\text{Cl}_2/\text{MeOH}$ 90:10

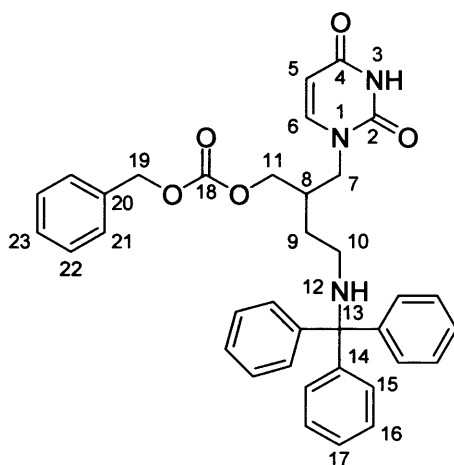
$^1\text{H-NMR}$: (500 MHz, pyridine) δ 1.73, 1.87 (2 H, m, C(9) H_2), 2.27 (1 H, m, C(8)H), 3.49, 3.56, 3.95 (6 H C(7) H_2 , C(10) H_2 , C(11) H_2), 5.24 (2 H, m, C(13) H_3), 5.70 (1 H, d $J=7.7$, C(5)H), 7.11-7.53 (6 H, m, 2 x C(15)H, 2 x C(16)H, C(17)H, C(6)H), 8.07, 13.28 (2 H, 2 x s, 2 x NH)

$^{13}\text{C-NMR}$: (125 MHz, pyridine) δ 30.4 (C-9), 39.0 (C-8), 39.7, (C-11), 49.9 (C-7), 61.5 (C-10), 66.6 (C-13), 102.0 (C-5), 128.6-129.4 (C-17, 2 x C-16, 2 x C-15), 138.7 (C-14), 146.6 (C-6), 153.1 (C-2), 157.6 (C-12), 165.3 (C-4)

LRMS (ES⁺): $m/z=$ 348.1 [M+H]⁺

HRMS (ES⁺): Found: 370.1357 [M+H]⁺ $\text{C}_{17}\text{H}_{21}\text{O}_5\text{N}_3\text{Na}^+$ requires 370.1373

9.13 (74) 1-[2-(carbobenzoxymethyl)-4-(triphenylmethyl)amino butyl] uracil



73 (1 g, 2.88 mmol) and trityl chloride (1.2 g, 4.32 mmol) were dissolved in pyridine (12 mL). The solution was divided into 3 equal batches in 5 mL reaction vials and DMAP (1mg, 0.3%w/w) was added to each batch. The solutions were exposed to MW radiation for 15min at 160°C twice after which time no starting material was observed by TLC. The crude was purified by flash chromatography on silica gel (EtOAc/Hexane 50:50→100:0, then MeOH/CHCl₃ 0:100→8:92) to yield the pure product as a sticky gum (1.69 g).

Yield: 100%

R_f: 0.5 in EtOAc/Hexane 50:50

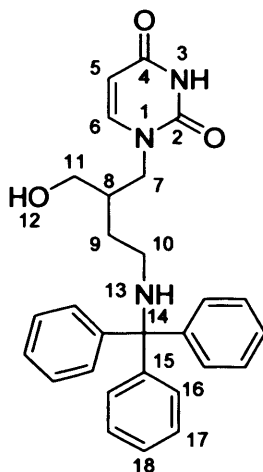
¹H-NMR: (500 MHz, CD₂Cl₂) δ 1.59, 1.71 (2 H, m, C(9)H₂), 2.06 (1 H, m, C(8)H), 3.11-3.27 (4 H, m, C(7)H₂, C(10)H₂), 3.72, 3.89 (2 H, m, C(11)H₂), 5.10 (2 H, m, C(19)H₃), 5.30 (1 H, d *J*=7.7 C(5)H), 6.75 (1 H, m, N(12)H), 7.32-7.44 (21 H, m, 6 x C(16)H, 6 x C(15)H, 3 x C(15)H, 2 x C(21)H, 2 x C(22)H, C(23)H, C(6)H), 9.47 (1 H, s, N(3)H)

¹³C-NMR: (125 MHz, CD₂Cl₂) δ 30.1 (C-9), 37.0 (C-8), 39.0, (C-11), 49.4 (C-7), 62.7 (C-10), 66.7 (C-19), 101.7 (C-5), 87.1 (C-13), 127.7-129.0 (3 x C-17, 6 x C-16, 6 x C-15, C-23, 2 x C-22, 2 x C-21), 137.5 (C-20), 144.0 (3 x C-14), 145.6 (C-6), 151.7 (C-2), 156.7 (C-18), 163.9 (C-4)

LRMS (ES⁺): *m/z*= 612.3 [M+H]⁺

HRMS (ES⁺): Found: 612.2475 [M+H]⁺ C₃₆H₃₅O₅N₃Na⁺ requires 612.2469

9.14 (75) 1-[2-(hydroxymethyl)-4-(triphenylmethyl)aminobutyl]uracil



75 was synthesised according to the general procedure H for the removal of the Cbz protecting group by hydrogenation using **74** (1.5 g, 2.55 mmol) and Pd/C (28 mg, 0.26 mmol) in MeOH:EtOH 1:1. The crude was purified by flash chromatography on silica gel (EtOAc/CHCl₃ 100:0→50:50, then MeOH/CHCl₃ 0:100→10:90) to give the product as a sticky gum (616 mg)

Yield: 53%

R_f: 0.4 in CH₂Cl₂/MeOH 95:5

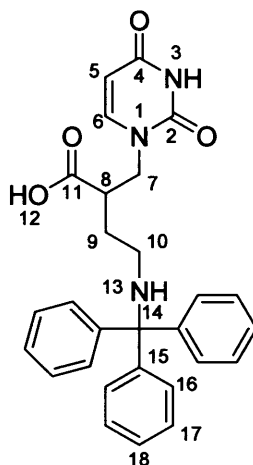
¹H-NMR: (500 MHz, DMSO) δ 1.57-1.67 (2 H, m, C(9)H₂), 2.14 (1 H, m, C(8)H), 2.94-3.02 (4 H, m, C(7)H₂, C(10)H₂), 3.69-3.76 (2 H, m, C(11)H₂), 5.42 (1 H, d *J*=7.8 C(5)H), 7.26-7.35 (18 H, m, 6 x C(16)H, 6 x C(17)H, 3 x C(18)H, C(6)H, 2 x NH)

¹³C-NMR: (125 MHz, DMSO) δ 30.1 (C-9), 36.4 (C-8), 47.7 (C-7), 62.4 (C-10), 78.6 (C-11), 85.9 (C-14), 100.8 (C-5), 128.2, 126.9, 127.8 (3 x C-18, 6 x C-17, 6 x C-16), 143.6 (3 x C-15), 145.8 (C-6), 150.9 (C-2), 163.4 (C-4)

LRMS (ES⁺): *m/z*= 456.2 [M+H]⁺

HRMS (ES⁺): Found: 456.2277 [M+H]⁺ C₂₈H₃₀O₃N₃⁺ requires 456.2282

9.15 (76) 1-[2-(carboxy)-4-(triphenylmethyl)aminobutyl] uracil



75 (600 mg, 1.30 mmol), BAIB (921 mg, 2.86 mmol) and TEMPO (41 mg, 0.26 mmol) were stirred in ACN:H₂O 50:50 overnight at RT. The crude was purified by flash chromatography on silica gel (MeOH/CHCl₃ 7:93) to yield the product as a white solid (350 mg)

Yield: 57%

Melting point: 71-75°C

R_f: 0.4 in CH₂Cl₂/MeOH 90:10

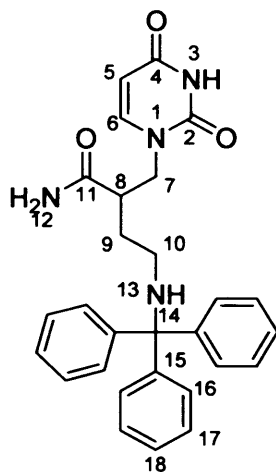
¹H-NMR: (500MHz, CDCl₃) δ 1.24 (2 H, m, C(9)H₂), 2.34 (1 H, m, C(8)H), 3.14-3.80 (4 H, m, C(7)H₂, C(10)H₂), 5.32 (1 H, d J=7.7 C(5)H), 6.65 (1 H, m, N(13)H), 7.14-7.31 (17 H, m, 6 x C(16)H, 6 x C(17)H, 3 x C(18)H, C(6)H, N(3)H), 9.39 (1 H, br, O(12)H)

¹³C-NMR: (125MHz, DMSO) δ 30.8 (C-9), 35.1 (C-8), 47.9 (C-7), 62.7 (C-10), 86.3 (C-14), 100.6 (C-5), 127.2-128.5 (3 x C-18, 6 x C-17, 6 x C-16), 143.8 (3 x C-15), 145.5 (C-6), 151.7 (C-2), 163.5 (C-4), 172.1 (C-11)

LRMS (ES⁻): m/z= 469.2 [M-H⁺], 227.0 [77-H]⁺

LRMS (ES⁺): m/z= 452.1 [78+H]⁺

9.16 (79) 1-[2-(acetamide)-4-(triphenylmethyl)aminobutyl] uracil



79 was synthesised according to general procedure H using ammonium hydrochloride (7 mg, 0.13 mmol), **76** (50 mg, 0.11 mmol), DhbtOH (20 mg, 0.12 mmol), NEt₃ (16 mg, 0.16 mmol) and DCC (26 mg, 0.13 mmol) in DMF (3 mL). The crude was purified by flash chromatography on silica gel (EtOAc/Hexane 50:50→100:0, EtOAc/CHCl₃ 100:0→0:100, MeOH/CHCl₃ 0:100→10:90) to yield the product as a white solid (5 mg).

Yield: 10%

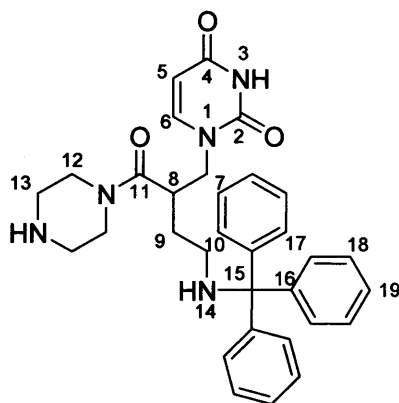
R_f: 0.8 in CH₂Cl₂/MeOH 90:10

¹H-NMR: (500 MHz, (CD₃)₂CO) δ 2.37, 2.43 (2 H, m, C(9)H₂), 2.61 (1 H, m, C(8)H), 3.14-3.87 (4 H, m, C(7)H₂, C(10)H₂), 5.37 (1 H, d J=7.7 C(5)H), 6.25, 6.89 (2 H, 2 x s, 2 x N(13)H), 7.24-7.46 (17 H, m, 6 x C(16)H, 6 x C(17)H, 3 x C(18)H, C(6)H, N(3)H)

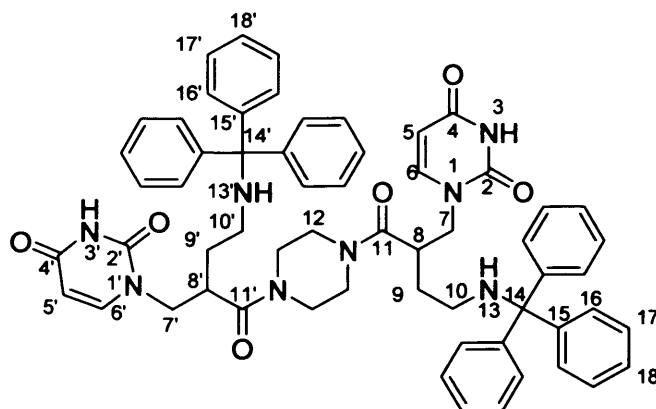
¹³C-NMR: (125 MHz, (CD₃)₂CO) δ 35.8 (C-9), 40.0 (C-8), 50.0 (C-7), 63.8 (C-10), 87.5 (C-14), 102.0 (C-5), 127.5-129.5 (3 x C-18, 6 x C-17, 6 x C-16), 144.8 (3 x C-15), 146.2 (C-6), 151.8 (C-2), 164.2 (C-4), 173.3 (C-11)

LRMS (ES⁺): m/z= 492.0 [M+H+Na]⁺

9.17 (81) Attempted synthesis of 1-[2-(piperazinamido)-4-(triphenylmethyl)aminobutyl] uracil



The synthesis of **80** was attempted according to general procedure H using piperazine (11 mg, 0.13 mmol), **76** (50 mg, 0.11 mmol), DhbtOH (20 mg, 0.122 mmol) and DCC (26 mg, 0.13 mmol) in DMF (3 mL). The crude was purified by flash chromatography on silica gel (EtOAc/Hexane 50:50→100:0, EtOAc/CHCl₃ 100:0→0:100, MeOH/CHCl₃ 0:100→10:90). Although the product was detected by mass spectrometry in one of the fractions, it was not pure and further purification on silica gel resulted in no product being isolated from the column. The dimer **84** was isolated from the column as a white solid (11 mg) and characterised by ¹H-NMR and ¹³C-NMR.



Yield: 10%

R_f: 0.7 in CH₂Cl₂/MeOH 95:5

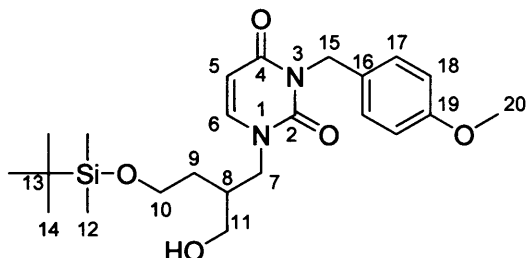
Melting point: 95-97°C

¹H-NMR: (500 MHz, (CD₃)₂CO) δ 1.59-1.75 (4 H, m, C(9)H₂, C(9')H₂), 2.33 (2 H, m, C(8)H, C(8')H), 3.07-3.80 (16 H, m, C(7)H₂, C(10)H₂, C(7')H₂, C(10')H₂, 4 x C(12)H₂, 5.35 (2 H, m, C(5)H, C(5')H), 7.09-7.33 (35 H, m, 12 x C(16)H, 12 x C(17)H, 6 x C(18)H, C(6)H, C(6')H, 2 x N(3)H, 2 x N(13)H)

¹³C-NMR: (125 MHz, (CD₃)₂CO) δ 35.8 (C-9), 40.0 (C-8), 50.0 (C-7), 63.8 (C-10), 87.5 (C-14), 102.0 (C-5), 127.5-129.5 (3 x C-18, 6 x C-17, 6 x C-16), 144.8 (3 x C-15), 146.2 (C-6), 151.8 (C-2), 164.2 (C-4), 173.3 (C-11)

LRMS (ES⁺): m/z= 990.2 [M+H]⁺

9.18 (85) 1-[2-(hydroxymethyl)-4-(*tert*-butyldimethylsilyloxy)butyl]-3-(*para*-methoxyphenyl) uracil



Previously supplied intermediate **57** (200 mg, 0.61 mmol) was dissolved in THF (5 mL) and cooled to 0°C under argon. NaH (22 mg, 0.92 mmol) was added. After 15min *tert*-butylammonium iodide (11 mg, 0.03 mmol) in THF (1 mL) was added, followed by 4-methoxybenzyl chloride (191 mg, 1.22 mmol) in THF (1 mL). The reaction was stirred overnight at RT. After 24 h starting material could still be detected by TLC. The reaction was heated to 40°C and left stirring for a further 18 h, after which time the solution turned milky and no starting material could be seen by TLC. The solvent was removed under reduced pressure. The crude was dissolved in EtOAc (10 mL), washed with brine (1 x 10 mL) and water (2 x 10 mL) and dried with MgSO₄. The organic fraction was concentrated to afford the product as a clear oil (270 mg).

Yield: 100%

R_f: 0.4 in EtOAc/Hexane 1:1

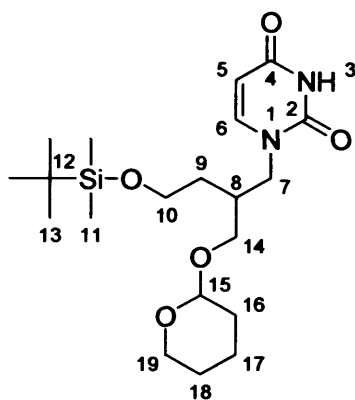
¹H-NMR: (500 MHz; CDCl₃) δ 0.02 (6 H, s, 2 x C(12)H₃), 0.84 (9 H, s, 3 x C(14)H₃), 1.53 (2 H, m, C(9)H₂), 1.96 (1 H, m, C(8)H), 3.39-3.45 (2 H, m, C(11)H₂), 3.68-3.73 (7 H, m, C(7)H₂, C(10)H₂, C(20)H₃), 4.97 (2 H, s, C(15)H₂), 5.65 (1 H, d *J*=7.8 C(5)H), 6.74-6.79 (2 H, m, C(17)H), 7.14-7.22 (2 H, m, C(16)H), 7.34 (1 H, d *J*=7.8 C(6)H)

¹³C-NMR: (125 MHz; CDCl₃) δ -3.6 (C-12), 18.0 (C-13), 25.9 (3 x C-14), 29.7 (C-9), 38.2 (C-8), 46.3 (C-15), 50.2 (C-7), 55.3 (C-19), 60.0 (C-11), 61.3 (C-10), 102.0 (C-5), 113.9 (2 x C-17), 128.7-130.3 (2 x C-16), 143.2 (C-6), 152.5 (C-2), 159.1-159.7 (C-18), 162.9 (C-4)

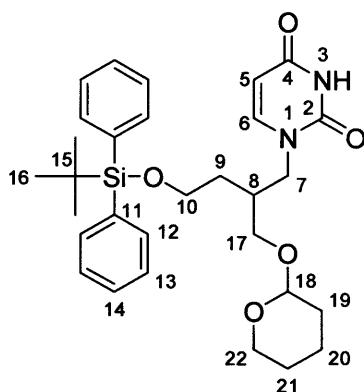
LRMS (ES⁺): *m/z* = 449.6 [M+H]⁺

9.19 (87) 1-[2-(dihydropyranyloxy)-4-(tert-butyldimethylsilyloxy)butyl] uracil and (88) 1-[2-(dihydropyranyloxy)-4-(tert-butyldiphenylsilyloxy)butyl] uracil

To a solution of previously supplied intermediate **57** (100 mg, 0.30 mmol for **87** and 1 g, 2.21 mmol for **88**) and dihydropyran (0.07 mL, 0.91 mmol for **87** and 0.6 mL, 6.63 mmol for **88**) in DCM (1.5 mL for **87** and 20 mL for **88**) was added *p*-toluene sulfonic acid hydrate (10% w/w) under argon. The solution was exposed to MW radiation at 100°C for 15 mins. Purification was carried out by flash chromatography in stepwise gradients (EtAc/Hexane 0:100→50:50) to yield the product as a clear oil (692 mg)

87**Yield:** 72%**R_f:** 0.2 in EtOAc/Hexane 1:1**¹H-NMR:** (500 MHz; CDCl₃) δ 0.00 (6 H, s, 2 x C(11)H₃), 0.85 (9 H, s, 3 x C(13)H₃), 1.40-1.59 (6 H, m, C(16)H₂, C(17)H₂, C(18)H₂), 1.65, 1.72 (2 H, m, C(9)H₂), 2.19 (1 H, m, C(8)H), 3.27, 3.41 (2 H, m, C(14)H₂), 3.60-3.87 (6 H, m, C(7)H₂, C(10)H₂, C(19)H₂), 4.45 (1 H, m, C(15)H), 5.60 (1 H, d *J*=7.8, C(5)H), 7.26 (1 H, d *J*=7.8, C(6)H), 9.22 (1 H, s N(3)H)**¹³C-NMR:** (125 MHz; CDCl₃) δ -5.4 (2 x C-11), 18.3 (C-12), 19.7, 20.0, 25.3, 25.4, 32.0, 32.1 (3 x C-12, C-16, C-17, C-18), 32.0, 32.1 (C-9), 35.4, 35.8 (C-8), 50.4, 50.5 (C-7), 60.8 (C-10), 62.7, 63.0 (C-14), 67.1, 67.7 (C-19), 99.1, 99.8 (C-15), 101.4, 101.5 (C-5), 145.6, 145.7 (C-6), 151.1, 151.2 (C-2), 163.9, 164.0 (C-4)**LRMS (ES⁺):** *m/z*= 435.2 [M+Na]⁺

88



Yield: 100%

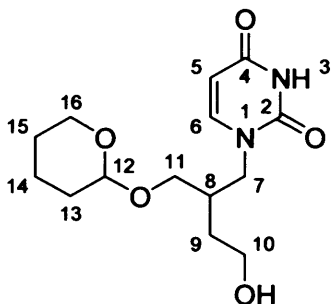
R_f: 0.5 in EtOAc/Hexane 1:1

¹H-NMR: (500 MHz; CDCl₃) δ 0.98 (9 H, s, 3 x C(16)H₃), 1.40-1.70 (8 H, m, C(9)H₂, C(19)H₂, C(20)H₂, C(21)H₂), 2.23 (1 H, m, C(8)H), 3.24-3.76 (8 H, m, C(7)H₂, C(10)H₂, C(17)H₂, C(22)H₂), 4.35, 4.42 (1 H, m, C(18)H), 5.56 (1 H, d *J*=7.8, C(5)H), 7.10-7.59 (11 H, C(6)H, 4 x C(12)H, 4 x C(13)H, 2 x C(14)H)

¹³C-NMR: (125 MHz; CDCl₃) δ 19.5 (C-15), 22.8 (3 x C-16), 25.3, 26.9, 30.7 (C-19, C-20, C-21), 31.8 (C-9), 35.2, 35.6 (C-8), 50.5, 50.6 (C-7), 61.4, 61.5 (C-10), 62.7, 63.0 (C-17), 67.1, 67.7 (C-22), 99.1, 99.9 (C-18), 101.4 (C-5), 127.7 (4 x C-13), 129.7 (2 x C-14), 133.6 (4 x C-12), 135.6 (2 x C-11), 145.6 (C-6), 150.8 (C-2), 163.3 (C-4)

LRMS (ES⁺): *m/z* = 537.2 [M+H]⁺

9.20 (89) 1-[2-(dihydropyran-2-yl)-4-hydroxybutyl] uracil



89 was synthesised according to general procedure G (Chapter 8) and the crude was purified by column chromatography on silica gel (MeOH/CHCl₃ 5:95) to isolate the pure product as a clear oil.

Yield: 93%

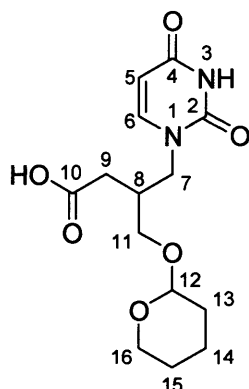
R_f: 0.2 in DCM/MeOH 95:5

¹H-NMR: (500 MHz; MeOD) δ 1.41-1.79 (8 H, m, C(9)H₂, C(13)H₂, C(14)H₂, C(15)H₂), 2.21 (1 H, m, C(8)H), 3.24-3.82 (8 H, m, C(7)H₂, C(10)H₂, C(11)H₂, C(16)H₂), 4.48 (1 H, dd *J*=7.8, 3.5 C(12)H), 5.59 (1 H, dd *J*=7.8, 3.5 C(5)H), 7.51 (1 H, d *J*=7.6 C(6)H)

¹³C-NMR: (125 MHz; MeOD) δ 26.6, 31.7, 31.9 (C-13, C-14, C-15), 33.1 (C-9), 36.3, 36.6 (C-8), 51.8, 52.1 (C-7), 60.5, 60.6 (C-10), 63.5, 63.7 (C-11), 68.5, 69.5 (C-16), 100.4, 100.9 (C-12), 101.7, 101.8 (C-5), 148.1, 148.2 (C-6), 153.1 (C-2), 166.9 (C-4)

LRMS (ES⁺): *m/z*= 299.1 [M+H]⁺

HRMS (ES⁺): Found: 321.1409 [M+Na]⁺ C₁₄H₂₂O₅N₂Na⁺ requires 321.1421

9.21 (90) 1-[2-(dihydropyrayloxy)-4-carboxybutyl] uracil

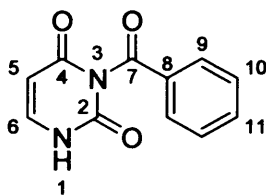
89 (300 mg, 1.0 mmol), BAIB (709 mg, 2.20 mmol) and TEMPO (31 mg, 0.20 mmol) were stirred in ACN:H₂O 1:1 (20 mL) for 5 h. The solvent was removed *in vacuo* and the desired product was triturated from diethyl ether as a sticky gum (310 mg).

Yield: 100%

R_f: 0.0 in DCM/MeOH 80:20

¹H-NMR: (500 MHz; CD₃CN) δ 1.44-1.67 (6 H, m, C(13)H₂, C(14)H₂, C(15)H₂), 2.11 (2 H, m, C(9)H₂), 2.41 (1 H, m, C(8)H), 3.20-3.68 (6 H, m, C(7)H₂, C(11)H₂, C(16)H₂), 4.45 (1 H, m, C(12)H), 5.46 (1 H, m, C(5)H), 7.26 (1 H, m, C(6)H)

¹³C-NMR: (125 MHz; CD₃CN) δ 24.9 (C-9), 29.6, 29.9, 30.2, 31.6, 32.8, 33.1 (C-13, C-14, C-15), 34.6, 35.0 (C-8), 49.8, 50.3 (C-7), 61.4, 61.6 (C-11), 66.6, 67.3 (C-16), 98.4, 98.8 (C-12), 101.1, 101.6 (C-5), 145.7 (C-6), 151.1 (C-2), 163.2 (C-4), 171.4 (C-10)

9.22 (92) 3-benzoyl uracil ¹³¹

Uracil (5.00 g, 44.64 mmol) was stirred in a mixture of acetonitrile (40 mL) and pyridine (16 mL) under argon. Benzoyl chloride (89.61 mmol, 10.4 mL) was added and the yellow solution was left stirring overnight during which time a precipitate formed. After a total of 24 h the solvent was evaporated off under reduced pressure and the residue was partitioned between DCM (200 mL) and water (200 mL). The organic layer was vacuumed down under reduced pressure and the mixture was taken up in dioxane (80 mL) and 0.5M K₂CO₃ in water (50 mL) and was stirred for 30 min. The pH of the solution was reduced to 5 and the solution concentrated and taken up in saturated NaHCO₃ (200 mL). The mixture was stirred at RT for 1 h and the precipitate which formed was filtered off and washed with cold water. The pure product was recrystallized from the precipitate in acetone/water 3:2 to yield a white solid (5.14 g)

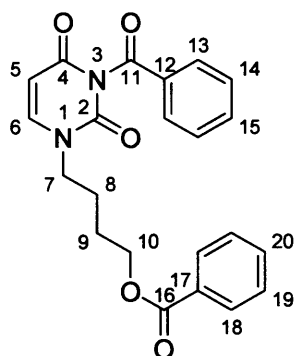
Yield: 53%

R_f: 0.1 in DCM/MeOH 80:20

¹H-NMR: (500 MHz; DMSO) δ 5.89 (1 H, d *J*=7.8, C(5)H), 7.65 (2 H, t *J*=8.1, 2 x C(10)H), 7.71 (1 H, d *J*=7.8, C(6)H), 7.81 (1 H, t *J*=6.3, C(11)H), 7.99 (2 H, d *J*=8.1, 2 x C(9)H), 11.65 (1 H, br, N(1)H)

¹³C-NMR: (125 MHz; CDCl₃;) δ 100.1 (C-5), 129.5 (2 x C-10), 130.2 (2 x C-9), 131.3 (C-11), 135.4 (C-8) 143.7 (C-6), 150.1 (C-2), 162.9 (C-4), 170.0 (C-7)

9.23 (94) 1-(4-benzoylbutyl)-3- benzoyl uracil



92 (300 mg, 1.39 mmol) and **93** (135 mg, 0.70 mmol) in THF (10 mL) were added to polymer bound Ph_3P (0.33 g/mmol) which had been swelled in THF for 15 min. DIAD (281 mg, 1.39 mmol) was then added and the mixture was left shaking overnight. The polymer was filtered off and washed with THF and MeOH and the crude product was purified by flash chromatography (Hexane:EtOAc 100:0→20:80) to afford the product as a colourless oil (211 mg).

Yield: 77%

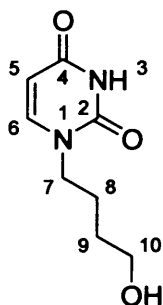
R_f: 0.2 in EtOAc/Hexane 2:3

¹H-NMR: (500 MHz; CDCl_3) δ 1.68-1.72 (4 H, m, C(8)H₂, C(9)H₂), 3.76 (2 H, t $J=6.9$, C(7)H), 4.25 (2 H, t $J=6.0$, C(10)H₂), 5.67 (1 H, d $J=7.9$, C(5)H), 7.29-7.95 (11 H, m, C(6)H, 2 x C(13)H, 2 x C(14)H, C(15)H, 2 x C(18)H, 2 x C(19)H, C(20)H)

¹³C-NMR: (125 MHz; CDCl_3) δ 25.7 (C-8), 31.3 (C-9), 48.6 (C-7), 63.9 (C-10), 102.0 (C-5), 128.4-129.5 (2 x C-13, 2 x C-14, 2 x C-18, 2 x C-19), 130.3, 131.4 (C-12, C-17), 133.2, 135.1 (C-15, C-20), 144.7 (C-6), 149.8 (C-2), 162.5 (C-4), 166.4, 169.0 (C-11, C-16)

LRMS (ES⁺): $m/z= 392.9$ [M+H]⁺

9.24 (95) 1-(4-hydroxybutyl) uracil



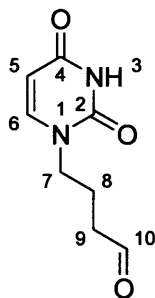
Compound **94** (211 mg, 0.54 mmol) was dissolved in 0.2 M NaOMe in MeOH (40 mL) and left stirring overnight at RT. Dowex H⁺ resin was added to the mixture to neutralise excess base. The resin was filtered off and the solvent removed under reduced pressure. The crude was purified by column chromatography (MeOH/CHCl₃ 1:9) to yield the product as a clear oil (35 mg).

Yield: 35%

R_f: 0.4 in MeOH/CHCl₃ 1:9

¹H-NMR: (500 MHz; MeOD) δ 1.48 (2 H, m, C(8)H₂), 1.57 (2 H, m, C(9)H₂), 3.51 (2 H, t $J=6.3$, C(7)H), 3.70 (2 H, t $J=7.3$, C(10)H), 5.55 (1 H, d $J=7.9$, C(5)H), 7.51 (1 H, d $J=7.9$, C(6)H)

LRMS (ES⁺): $m/z= 185.7$ [M+H]⁺

9.25 (96) 1-(4-butanal) uracil

Compound **95** (35 mg, 0.190 mmol) was dissolved in a mixture of ACN/DCM/DMF 2:2:1 (5 mL) and stirred with 4 Å molecular sieves under argon at RT. NMO (34 mg, 0.29 mmol) in dry DCM (1 mL) was added, followed by TPAP (3.5 mg, 1.01 mmol). The reaction was stirred at RT overnight. The mixture was filtered through celite and silica using MeOH/CHCl₃ as eluent. After filtration, the crude was pushed through a short silica plug in a PD-10 column containing a PTFE sieve. Although the product (yellow wax, 18 mg) was still contaminated with some tetrapropylammonium, it was carried on to the next step.

Yield: 51%

¹H-NMR: (500 MHz; MeOD) δ 1.34-1.62 (4 H, m, C(8)H₂, C(9)H₂), 3.70 (2 H, t *J*=7.3, C(7)H), 5.57 (1 H, d *J*=7.9 C(5)H), 7.49 (1 H, d *J*=7.9 C(6)H)

10 Experimental III

10.1 Docking of amino acid uracil conjugates

Compounds **98-160** were drawn and minimised using Sybyl 6.9. Minimisation was carried out using the TRIPOS force field in a dielectric constant of 80. The method used was conjugated gradient with a gradient of 0.05 kcal/mol and the number of iterations was set to 1000. Charges were not assigned as FlexX assigns formal charges to the ligand before docking calculations are carried out.

The pdb file of the protein was extracted and the water molecules removed. The active site was defined as being 6.5 Å around the reference ligand which had been co-crystallised with the protein and was part of the PDB file. In the case of the open form *T. cruzi* dUTPase, which had no co-crystallised ligand, the natural ligand dUDP was manually placed in the PDB file and the active site defined as 6.5 Å around it.

The compounds were then docked using FlexX. The uracil ring was manually defined as the base fragment. The calculations carried out by FlexX were not done on the whole proteins. Instead, to save time, the calculations were carried out 10 Å distance around the active site. The conformations generated were ranked by FlexX by decreasing FlexX total score (increasing ΔG) and visualised using Sybyl 6.9.

10.2 General solid phase synthesis

10.2.1 Loading of resin procedure

Wang resin (500mg) was weighed into each empty PD-10 column and allowed to swell in DMF for 30min. The appropriate amino acid (2 eq) and DIC (1 eq) were dissolved in DMF (6mL) and left for 1h at RT. The beads were dried by suction and the anhydride solutions and DMAP (0.05 eq) were added to the resin beads. The mixtures were left shaking overnight. The beads were dried by suction and washed with DMF using a peristaltic pump.

10.2.1.1 Measuring of resin loading

0.2-0.5 mg of washed derivatised resin was weighed into a quartz cuvette. 20% piperidine in DMF (3 mL) was added and the mixture agitated with a pipette. The UV absorbance was measured and the resin loading calculated according to the equation:

$$\text{Fmoc loading: mmole/g} = (\text{Abs}) / (1.65 \times \text{mg resin})$$

10.2.2 Fmoc deprotection procedure

20% piperidine in DMF (6 mL) was added to each column and the mixtures left shaking for 1 h. The derivatised beads were washed with 20% piperidine in DMF (approx. 20 mL/g) either with or without the use of the peristaltic pump. The beads were washed with DMF and dried by suction.

10.2.3 Ninhydrin test procedure

A small amount of resin beads were placed into a glass vial. EtOH/H₂O 2:1 (3 mL) was added. Ninhydrin reagent (0.5 mL) was added and the solution was heated to 100°C for 5 min. A positive result (blue beads) indicated the presence of a free amine and therefore the success of the deprotection procedure. If <60% of the beads were blue, the deprotection was repeated.

10.2.4 Coupling procedure

The appropriate amino acid or carboxyuracil (4 eq/mol loaded), TBTU (4 eq/mol loaded), HOBt (4 eq/mol loaded), and DIPEA (8 eq/mol loaded), were dissolved in DMF (3 mL). The solutions were added to the columns and the mixtures were left shaking overnight. The beads were dried by suction and washed with DMF with the aid of the peristaltic pump. The ninhydrin test was carried out and a negative result (colourless/pink beads) indicated absence of a free amine and therefore success of the coupling procedure.

10.2.5 Cleavage from the resin

10.2.5.1 Preparation procedure

The derivatised beads were washed with DMF (2 x 20 mL), DCM (2 x 20 mL) and MeOH (2 x 20 mL) to shrink the beads with or without the use of the peristaltic pump. The beads were dried by suction.

10.2.5.2 Cleavage procedure A

A solution of 95 % TFA, 2.5% TES and 2.5% DCM (7 mL) was added to each column. The mixtures were left shaking for 1 h. The solutions were collected via suction and the beads were washed with DCM which was also collected. The solvents were removed *in vacuo* and the samples dried using an ACTEvac chamber. The products were triturated from cold ether.

10.2.5.3 Cleavage procedure B

A solution of 95 % TFA, 2.5% TES and 2.5% DCM (7 mL) was added to each column. The mixtures were left shaking for 30min. The solutions were collected via suction and the beads were washed with DCM which was also collected. The solvents were removed *in vacuo* and the samples dried using an ACTEvac chamber. The products were triturated from cold ether.

10.2.5.4 Cleavage procedure C

A solution of 50 % TFA, 5% TES and 45% DCM (7 mL) was added to each column. The mixtures were left shaking for 1 h. The solutions were collected via suction and the beads were washed with DCM which was also collected. The solvents were removed *in vacuo* and the samples dried using an ACTEvac chamber. The products were triturated from cold ether.

10.2.5.5 Cleavage procedure D

A solution of 50% TFA, 2.5% TES and 47.5% DCM (7 mL) was added to each column. The mixtures were left shaking for 1 h. The solutions were collected via suction and the beads were washed with DCM which was also collected. The solvents were removed *in vacuo* and the samples dried using an ACTEvac chamber. The products were triturated from cold ether.

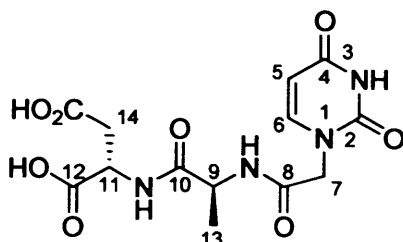
10.2.5.6 Cleavage procedure E

A solution of 50 % TFA, 2.5% TES and 47.5% DCM (7 ml) was added to each column. The mixtures were left shaking for 30 min. The solutions were collected via suction and the beads were washed with DCM which was also collected. The solvents were removed *in vacuo* and the samples dried using an ACTEvac chamber. The products were triturated from cold ether.

10.3 Results of amino acid uracil acetamide conjugate syntheses

Compounds were characterised by ¹H-NMR and LRMS and also by HRMS where possible. All NMR experiments were carried out in D₂O and mass spectrometry experiments were carried out in MeOH or MeOH/D₂O.

101

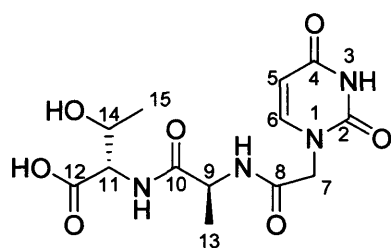


¹H-NMR: (300 MHz, D₂O) δ 1.28 (3 H, d *J*=7.1, C(13)H₃), 2.83 (2 H, m, C(14)H₂), 4.28 (1 H, q *J*=7.2, C(9)H), 4.45 (2 H, m, C(7)H₂), 4.63 (1 H, m, C(11)H), 5.75 (1 H, d *J*=7.9, C(5)H), 7.48 (1 H, d *J*=7.9, C(6)H)

LRMS (ES⁻): *m/z*= 297.1 [M-H]⁻

HRMS (ES⁻): Found: 297.0842 [M-H]⁻ C₁₁H₁₃O₆N₄⁻ requires 297.0835

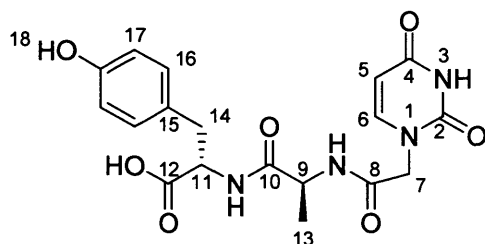
103



¹H-NMR: (300 MHz, D₂O) δ 1.08 (3 H, d $J=6.6$, C(15)H₃), 1.28 (3 H, d $J=7.3$, C(13)H₃), 4.38-4.40 (3 H, m, C(9)H, C(11)H), C(14)H), 4.48 (2 H, m, C(7)H₂), 5.71 (1 H, d $J=7.9$ C(5)H), 7.44 (1 H, d $J=7.9$ C(6)H)

LRMS (ES⁻): $m/z= 341.2$ [M-H]⁻

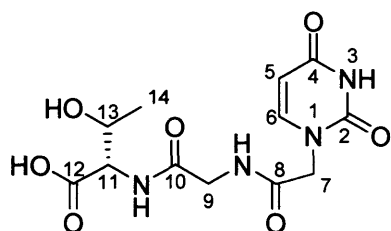
104



¹H-NMR: (300 MHz, D₂O) δ 1.15 (3 H, d $J=7.1$, C(13)H₃), 2.81, 3.05 (2 H, m, C(14)H₂), 4.18 (1 H, q $J=7.1$, C(9)H), 4.35 (2 H, m, C(7)H₂), 4.58 (1 H, m, C(11)H), 5.75 (1 H, d $J=7.8$ C(5)H), 6.65-6.95 (4 H, 2 x C(16)H, 2 x C(17)H), 7.39 (1 H, d $J=7.8$, C(6)H)

LRMS (ES⁻): $m/z= 403.1$ [M-H]⁻

124

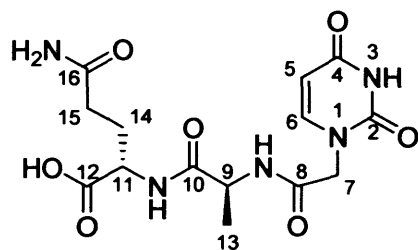


¹H-NMR: (300 MHz, D₂O) δ 1.11 (3 H, d $J=6.4$, C(14)H₃), 3.94 (2 H, s, C(9)H₂), 4.30-4.34 (2 H, m, C(11)H, C(13)H), 4.51 (2 H, s, C(7)H₂), 5.73 (1 H, d $J=7.9$ C(5)H), 7.52 (1 H, d $J=7.9$ C(6)H)

LRMS (ES⁺): $m/z= 351.1$ [M+Na]⁺

HRMS (ES⁺): Found: 351.0910 [M+H]⁺ C₁₂H₁₆O₇N₄Na⁺ requires 351.0917

161

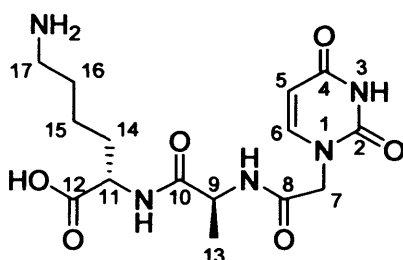


¹H-NMR: (300 MHz, D₂O) δ 1.31 (3 H, d $J=7.3$, C(13)H₃), 1.95, 2.15 (2 H, m, C(14)H₂), 2.69 (2 H, t $J=7.0$, C(15)H₂), 4.30 (1 H, m, C(9)H), 4.39 (1 H, m, C(11)H), 4.49 (2 H, s, C(7)H₂), 5.75 (1 H, d $J=7.9$, C(5)H), 7.51 (1 H, d $J=7.9$, C(6)H)

LRMS (ES⁻): $m/z= 368.1$ [M-H]⁻

HRMS (ES⁻): Found: 368.1202 [M-H]⁻ C₁₄H₁₈O₇N₅⁻ requires 368.1206

163

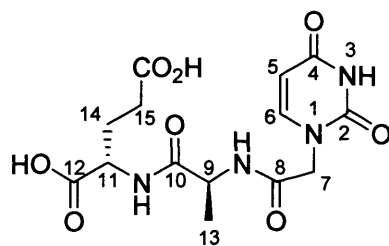


¹H-NMR: (300 MHz, D₂O) δ 1.30 (3 H, d $J=7.3$, C(13)H₃), 1.58, 1.69, 1.81 (6 H, m, C(14)H₂, C(15)H₂, C(16)H₂), 2.92 (2 H, t $J=7.7$, C(17)H₂), 4.25 (2 H, m, C(9)H, C(11)H), 4.42 (2 H, s, C(7)H₂), 5.73 (1 H, d $J=7.9$, C(5)H), 7.45 (1 H, d $J=7.9$, C(6)H)

LRMS (ES⁺): $m/z= 370.2$ [M+H]⁺

HRMS (ES⁺): Found: 370.1707 [M+H]⁺ C₁₅H₂₄O₆N₅⁺ requires 370.1721

164

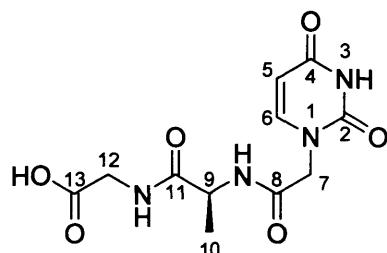


¹H-NMR: (300 MHz, D₂O) δ 1.32 (3 H, d $J=7.3$, C(13)H₃), 1.91-2.13 (2 H, m, C(14)H₂), 2.27 (2 H, t $J=7.5$, C(15)H₂), 4.31 (2 H, m, C(9)H, C(11)H), 4.49 (2 H, m, C(7)H₂), 5.78 (1 H, d $J=7.9$, C(5)H), 7.48 (1 H, d $J=7.9$, C(6)H)

LRMS (ES⁻): $m/z=$ 369.1 [M-H]⁻

HRMS (ES⁻): Found: 369.1055 [M-H]⁻ C₁₄H₁₇O₈N₄⁻ requires 369.1046

166

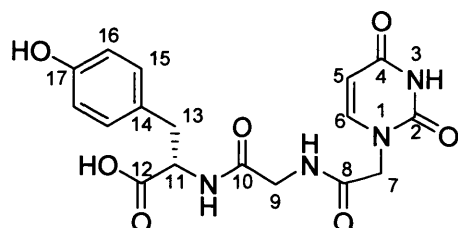


¹H-NMR: (300 MHz, D₂O) δ 1.45 (3 H, d $J=7.3$, C(13)H₃), 3.82 (2 H, s, C(12)H₂), 4.28 (1 H, m, C(9)H), 4.41 (2 H, s, C(7)H₂), 5.74 (1 H, d $J=7.9$, C(5)H), 7.47 (1 H, d $J=7.9$, C(6)H)

LRMS (ES⁻): $m/z=$ 297.1 [M-H]⁻

HRMS (ES⁻): Found: 297.0842 [M-H]⁻ C₁₁H₁₃O₆N₄⁻ requires 297.0835

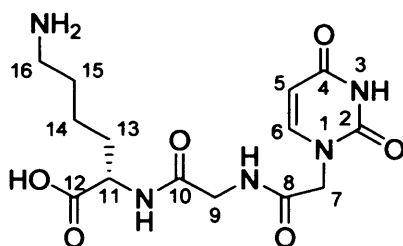
168



¹H-NMR: (300 MHz, D₂O) δ 2.91-3.15 (2 H, m, C(13)H₂), 3.89 (2 H, s, C(9)H₂), 4.40 (2 H, s, C(7)H₂), 4.67 (1 H, m, C(11)H), 5.79 (1 H, d $J=7.9$, C(5)H), 6.80 (2 H, m, 2 x C(15)H), 7.07 (2 H, m, 2 x C(16)H), 7.35 (1 H, d $J=7.9$, C(6)H)

LRMS (ES⁻): m/z= 389.2 [M-H]⁻

171

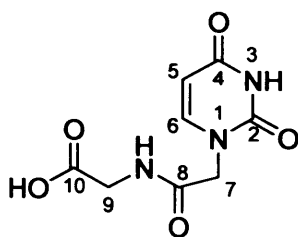


¹H-NMR: (300 MHz, D₂O) δ 1.32, 1.55, 1.69-1.80 (6 H, m, C(13)H₂, C(14)H₂, C(15)H₂), 2.82 (2 H, m, C(16)H₂), 3.88 (2 H, s, C(9)H₂), 4.25 (1 H, m, C(11)H), 4.48 (2 H, s, C(7)H₂), 5.72 (1 H, d *J*=7.9, C(5)H), 7.45 (1 H, d *J*=7.9, C(6)H)

LRMS (ES⁺): m/z= 356.2 [M+H]⁺

HRMS (ES⁺): Found: 356.1557 [M+H]⁺ C₁₄H₂₂O₆N₅⁺ requires 356.1565

172



¹H-NMR: (300 MHz, D₂O) δ 3.95 (2 H, s, C(9)H₂), 4.50 (2 H, s, C(7)H₂), 5.79 (1 H, d *J*=7.9, C(5)H), 7.52 (1 H, d *J*=7.9, C(6)H)

LRMS (ES⁻): m/z= 226.1 [M-H]⁻

HRMS (ES⁺): Found: 228.0622 [M+H]⁺ C₈H₁₀O₅N₃⁺ requires 228.0615

11 Appendix 1: Biological assays

11.1 Enzyme assays

All enzyme inhibition assays were carried out at Instituto de Parasitología y Biomedicina "Lopez-Neyra", Granada, Spain.

Nucleotide hydrolysis was monitored by mixing enzyme and substrate with a rapid kinetic accessory (Hi-Tech Scientific) attached to a Cary 50 (Varian) stopped-flow spectrophotometer connected to a computer for data acquisition and storage. Assays contained 30nM purified recombinant enzyme, 50µM dUTP, 5nM MgCl₂ and 2.5mM DTT, 1.25 mg/mL bovine serum albumin and 100mM KCl.

Changes in absorbance were directly proportional to the amount of product generated according to the equation:

$$[P]_t = \{(A_0 - A_t)/(A_0 - A_\infty)\}[S]_0$$

where: A₀, A_t, A_∞ denote the absorbance of the indicator at the start, time *t* and end of the reaction and [S]₀ the initial concentration of dUTP.

Kinetic parameters K_{mapp} and V_{max} were calculated using the Michaelis-Menten integrated rate equation:

$$[P]_t/t = K_{mapp}(2.3/t \log[S]_0/[S]) + V_{max}/(1 - K_m/K_i)$$

where: K_{mapp} = -K_m{(K_{ip} + [S]₀)/(K_{ip} - K_m)}

The different apparent K_m values attained were plotted against inhibitor concentration and K_i values were obtained according to the following equation:

$$K_{mapp} = -K_m[I]/K_i + K_m$$

11.2 *In vitro* assays

Compounds were screened against parasites for *in vitro* activity at The Swiss Tropical Institute, Basel, Switzerland.

11.2.1 *Trypanosoma brucei* (Sleeping sickness)

The bloodstream form trypomastigotes of the *Trypanosoma brucei rhodesiense* STIB 900 and *Trypanosoma brucei brucei* STIB 950 were maintained in MEM medium with Earle's salts supplemented with 25 mM HEPES, 1g/l additional glucose, 1% MEM non-essential amino acids (100x), 0.2 mM 2-mercaptoethanol, 2mM Na-pyruvate, 0.1mM hypoxanthine and 15% heat inactivated horse serum.

All cultures and assays were conducted at 37°C under an atmosphere of 5% CO₂ in air. Assays were performed in 96-well microtiter plates, each well containing 100 µL of culture medium with 8 x 10³ bloodstream forms with or without a serial drug dilution.

The highest concentration for the test compounds was 90 µg/mL. Seven 3-fold dilutions of compounds were used covering a range from 90 µg/L to 0.123 µg/mL. Each drug was tested in duplicate and each assay was repeated at least once.

After 72 hrs of incubation the plates were inspected under an inverted microscope to assure growth of the controls and sterile conditions. 10µL of Alamar Blue (12.5 mg resazurin dissolved in 100 mL distilled water) was added to each well and the plates incubated for another 2 hours. The plates were read with a Spectramax Gemini XS microplate fluorometer (Molecular Devices Cooperation, Sunnyvale, CA, USA) using an excitation wave length of 536 nm and an emission wave length of 588 nm.

Data was analysed using the microplate reader software Softmax Pro (Molecular Devices Cooperation, Sunnyvale, CA, USA).

The reference drug used was Melarsoprol with an IC₅₀ of 1.6 ng/mL.

11.2.2 *Trypanosoma cruzi* (Chagas' Disease)

The infective amastigote and trypomastigote stages were cultivated in L-6 cells (rat skeletal myoblast cell line) in RPMI 1640 supplemented with 2 mM L-glutamine and 10% heat-inactivated foetal bovine serum in 12.5 cm² tissue culture flasks. Intracellularly developed amastigote differentiated into trypomastigotes and left the host cell. The trypomastigotes infected new L-6 cells and were the stages used to initiate an infection in the assay. All cultures and assays are conducted at 37°C under an atmosphere of 5% CO₂ in air.

Assays were performed in sterile 96-well microtiter plates, each well containing 100 μ L medium with 2×10^3 L-6 cells. After 24 hours 50 μ L of a trypanosome suspension containing 5×10^3 trypomastigote bloodstream forms from culture were added to the wells. 48 hours later the medium was removed from the wells and replaced by 100 μ L fresh medium with or without a serial drug dilution.

Seven 3-fold dilutions of the compounds were used covering a range from 90 μ g/mL to 0.123 μ g/mL. Each drug was tested in duplicate. After 96 hours of incubation the plates were inspected under an inverted microscope to assure growth of the controls and sterility.

The substrate CPRG/ Nonidet (50 μ L) was added to all wells. A colour reaction became visible within 2-6 hours and was read photometrically at 540nm. Data was transferred into graphic programme (e.g. EXCEL), sigmoidal inhibition curves determined and IC_{50} values calculated.

Benznidazole was the reference drug used with an IC_{50} 0.34 μ g/mL

11.2.3 *Leishmania donovani* (Leishmaniasis)

The *Leishmania donovani* MHOM/ET/67/L82 strain was maintained in the hamster. Amastigotes were collected from the spleen of an infected hamster and adapted to axenic culture conditions at 37°C. The medium was a 1:1 mixture of SM medium and SDM-79 medium at pH 5.4 supplemented with 10% heat-inactivated FBS under an atmosphere of 5% CO_2 in air.

Assays were performed in 96-well microtiter plates, each well containing 100 μ L of culture medium with 10^5 amastigotes from axenic culture with or without a serial drug dilution. The highest concentration for the test compounds was 90 μ g/mL. Seven 3-fold dilutions were used covering a range from 30 μ g/mL to 0.041 μ g/mL. Each drug was tested in duplicate and each assay repeated at least once. After 72 hours of incubation the plates were inspected under an inverted microscope to assure growth of the controls and sterile conditions.

10 μ L of Alamar Blue (12.5 mg resazurin dissolved in 1L distilled water) was added to each well and the plates incubated for another 2 hours. The plates were read with a Spectramax Gemini XS microplate fluorometer (Molecular Devices Cooperation, Sunnyvale, CA, USA) using an excitation wave length of 536 nm and an emission wave length of 588 nm. Data was analysed using the microplate reader software Softmax Pro (Molecular Devices Cooperation, Sunnyvale, CA, USA).

Miltefosine was used as the reference drug with an IC_{50} value of 0.12 μ g/mL.

11.2.4 *Plasmodium falciparum* (Malaria)

The parasite strains were maintained in RPMI-1640 medium with 0.36 mM hypoxanthine supplemented with 25 mM HEPES, 25 mM NaHCO₃, neomycin (100 U/mL) and Albumax^R (lipid-rich bovine serum albumin) (GIBCO, Grand Island, NY) (5g/l), together with 5% washed human A+ erythrocytes. All cultures and assays were conducted at 37°C under an atmosphere of 4% CO₂, 3% O₂ and 93% N₂. Cultures were kept in incubation chambers filled with the gas mixture. Subcultures were diluted to a parasitaemia of 0.1-0.5% and the medium changed daily.

Assays were performed in sterile 96-well microtiter plates, each well containing 200 µL of parasite culture (0.15% parasitaemia, 2.5% hematocrit) with or without serial drug solutions. Seven 2-fold dilutions were used covering a range from 5 µg/mL to 0.078 µg/mL. For active compounds the highest concentration was lowered (e.g. to 100 ng/mL). Each drug was tested in duplicate and repeated once for active compounds showing an IC₅₀ below 0.5 µg/mL.

After 48 hours of incubation at 37°C, 0.5 µCi ³H-hypoxanthine was added to each well. Cultures were incubated for a further 24 h before they were harvested onto glass-fiber filters and washed with distilled water. The radioactivity was counted using a BetaplateTM liquid scintillation counter (Wallac, Zurich, Switzerland). The results were recorded as counts per minute (CPM) per well at each drug concentration and expressed as a percentage of the untreated controls. From the sigmoidal inhibition curves IC₅₀ values were calculated.

Cloroquine and artemesnin were the reference drugs used with respective IC₅₀ values 2.9ng/mL and 1.9 ng/mL against the NF54 strain and 48ng/mL and 0.8ng/mL against the K1 strains.

12 Appendix 2: Publications

McCarthy, O. K.; Schipani, A.; Musso Buendía, A.; Ruiz-Perez, L. M.; Kaiser, M.; Brun, R.; Gonzalez-Pacanowska, D.; Gilbert, I. H. Design, synthesis and evaluation of novel uracil amino acid conjugates for the inhibition of *Trypanosoma cruzi* dUTPase. *Bioorg. Med. Chem. Lett.* **2006**, *16*, 3809-3812.



Design, synthesis and evaluation of novel uracil amino acid conjugates for the inhibition of *Trypanosoma cruzi* dUTPase

Orla K. Mc Carthy,^{a,b} Alessandro Schipani,^{a,b} Alex Musso Buendía,^c Luis M. Ruiz-Perez,^c Marcel Kaiser,^d Reto Brun,^d Dolores González Pacanowska^c and Ian H. Gilbert^{a,b,*}

^aWelsh School of Pharmacy, Cardiff University, King Edward VII Avenue, Cardiff CF10 3XF, UK

^bSchool of Life Sciences, University of Dundee, MSIIWTB/CIR complex, Dow Street, Dundee DD1 5EH, UK

^cInstituto de Parasitología y Biomedicina "Lopez-Neyra", Consejo Superior de Investigaciones Científicas, Avda. del Conocimiento s/n Parque Tecnológico de Ciencias de la Salud, 18100-Armilla, Granada, Spain

^dSwiss Tropical Institute, Socinstrasse 57, CH-4002 Basel, Switzerland

Received 21 March 2006; revised 11 April 2006; accepted 11 April 2006

Available online 3 May 2006

Abstract—Potential inhibitors of the *Trypanosoma cruzi* dUTP nucleotidohydrolase were docked into the enzyme using the program FlexX. Compounds that docked selectively were then selected and synthesized using solid phase methodology, giving rise to a novel library of amino acid uracil acetamide compounds which were evaluated for enzyme inhibition and anti-parasitic activity.
© 2006 Elsevier Ltd. All rights reserved.

The protozoan parasite *Trypanosoma cruzi* is the causative agent of Chagas' disease, also called American trypanosomiasis. The parasite is transmitted by blood sucking triatomine insects and is one of three species of the genus *Trypanosoma* that are pathogenic to humans. Chagas' disease occurs mainly in South and Central America. It is estimated that 16–18 million people are infected with the disease, of which approximately 50,000 will die each year.¹ Although the number of incidences of the disease has declined over the past 20 years due to vector control initiatives,² there is still no satisfactory cure for American trypanosomiasis and current drug treatment is only effective against the early stages of the disease. The need for new drugs to treat this disease is therefore urgent.

Recently, deoxyuridine 5'-triphosphate nucleotidohydrolase (dUTPase) has been identified as a novel and valid target against trypanosomatidae.³ The enzyme is essential in both eukaryotes and prokaryotes, where investigated.^{4,5} dUTPase catalyses the hydrolysis of dUTP to dUMP in the presence of Mg²⁺ and plays a critical role in maintaining the level of dUTP in the cell 10⁻⁵ times lower than that of dTTP. In doing so, incor-

poration of uracil into DNA is minimized, excessive incorporation of which would normally lead to DNA fragmentation and cell death. dUTPases are known to exist in several oligomeric forms. Monomeric enzymes are encoded by herpes virus and Epstein–Barr virus, while the homotrimeric forms are present in mammals, various bacteria and viruses and also in the *Plasmodium falciparum* parasite, the causative agent for malaria. The homodimeric enzymes have been found in *Leishmania major*, *T. cruzi* and *Campylobacter jejuni*. The dimeric enzymes show no similarity in sequence or structure to the monomeric or trimeric forms and are thought to have reached their catalytic potential through a different evolutionary route. Crystal structures of seven trimeric (*Escherichia coli*,⁶ human,⁷ equine infectious anemia virus,⁸ feline immunodeficiency virus,⁹ *Methanococcus jannaschii*,¹⁰ *Mycobacterium tuberculosis*,¹¹ and *P. falciparum*¹²) and two dimeric (*T. cruzi*¹³ and *C. jejuni*¹⁴) dUTPases have been published to date.

It has been shown that relative to other eukaryotic dUTPase enzymes, α,β -imido-dUTP is a strong inhibitor of the dimeric enzymes. It has been proposed therefore that the triphosphate moiety is necessary for inhibition of the dimeric dUTPases.¹⁵ To emphasise the difference, tritylated nucleoside derivatives prepared by our group were good inhibitors of the trimeric enzymes¹² but are inactive against the dimeric parasitic

Keywords: dUTPase; Structure-based drug design.

* Corresponding author. Tel.: +44 0 1382 386 240; fax: +44 0 1382 386 373; e-mail: i.h.gilbert@dundee.ac.uk

dUTPases. In contrast to the trimeric dUTPases where a glycine-rich site for phosphate binding is common, the phosphates in the dimeric enzymes are held in place with hydrogen bonds to charged side chains.¹³ Taking advantage of the structural differences between these enzymes, it was thought that selective inhibitors for the dimeric *T. cruzi* dUTPase (TcdUTPase) could be designed and synthesized as lead compounds for the treatment of Chagas' disease.

Considering the hydrophilic nature of the TcdUTPase active site, compounds in which chains with good hydrogen bond donating or hydrogen bond accepting capability attached to N1 of the uracil ring were considered as potential inhibitors. Ease of synthesis of uracil acetamide derivatives, to which were attached one or two amino acids (Fig. 1), by the Fmoc solid phase strategy allowed for a wide range of structural diversity to be implemented and were therefore chosen for further study. Compounds such as those shown in Figure 1 were drawn, minimized and docked into the active site of TcdUTPase using the program FlexX. The ligand-free (native) TcdUTPase exists in an open form (pdb 1OGL). Binding of the substrate induces substantial structural changes so that the enzyme closes over the ligand (pdb 1OGK).¹³ Docking studies were carried out on the closed (complexed) form of the enzyme. The compounds which docked with the best superimposition over the endogenous dUDP ligand were synthesized using solid phase chemistry and tested for biological activity.

FlexX is a docking program that takes into account the flexibility of the ligand but not that of the receptor. The docking method it uses is based on an incremental construction algorithm which consists of three phases: (1) base selection, (2) base placement, and (3) complex construction.¹⁶ The interaction types and scoring functions in FlexX are based on work by Böhm and Klebe.¹⁷

Docking studies showed that: (1) the R side chain should be H or CH₃. Structures where the side chains, R, were bigger than those of Ala or Gly were too bulky to fit into the active site. (2) The optimum distance between the carbonyl marked with an * (Fig. 1) and the terminal atom was 2 or 3 but no more than 5 atoms. (3) The best scoring compounds were those where R' was a charged residue. A large degree of variation of the R' side chain without effecting the superimposition was, however, allowed. Compounds 1–11 (Table 1) were among those which docked best into the TcdUTPase active site (Fig. 2).

Compounds 1–11 were synthesized by solid phase Fmoc chemistry as shown in Scheme 1. Amino acids 12–19

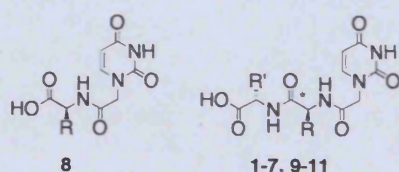


Figure 1. Structure of potential TcdUTPase inhibitors.

Table 1. Compounds docked into the TcdUTPase active site using FlexX and subsequently synthesized

Compound	R	R'	Colour
1	CH ₃		Orange
2	CH ₃		Red
3	CH ₃		Green
4	CH ₃	H	Blue
5	CH ₃		Purple
6	CH ₃		Magenta
7	CH ₃		Violet
8	H	—	Greenblue
9	H		Redorange
10	H		By atom type
11	H		White
dUDP			Yellow

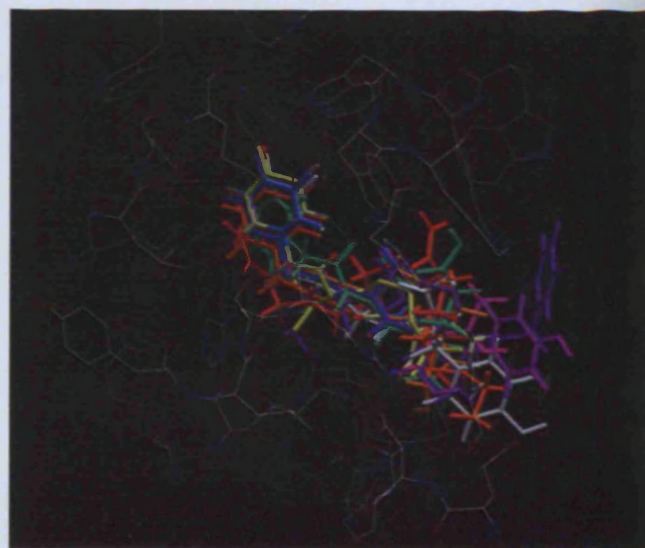
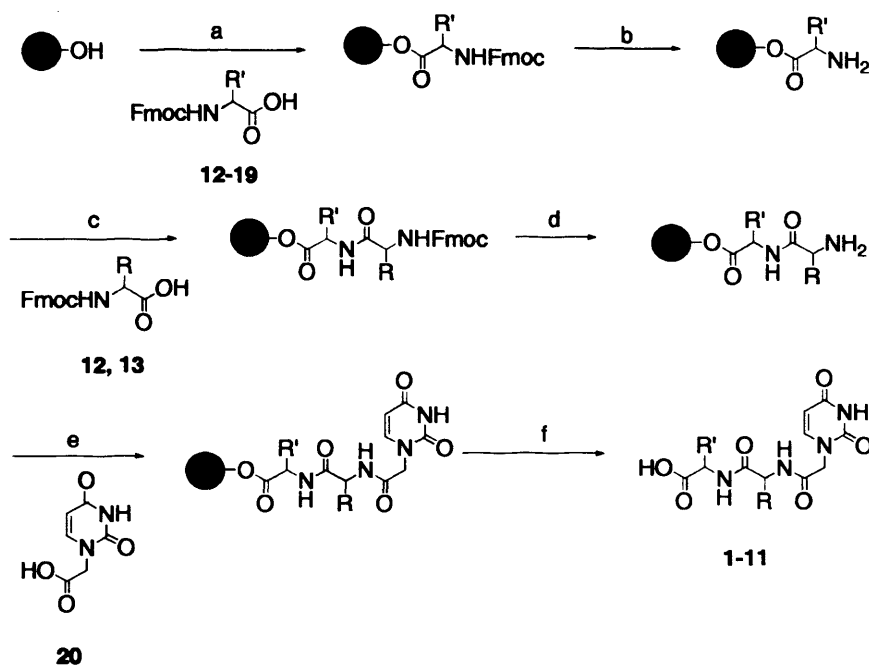


Figure 2. Docking of compounds 1–11 in TcdUTPase active site. Superimposition with dUDP.



Scheme 1. General synthesis of compounds 1–11: (a) DIC, 12–19, DMAP, DMF (12, Ala; 13, Gly; 14, Asp; 15, Gln; 16, Glu; 17, Lys; 18, Thr; 19, Tyr); (b) 20% piperidine, DMF; (c) TBTU, HOBt, 12–13, DIPEA, DMF; (d) 20% piperidine, DMF; (e) TBTU, HOBt, 20, DIPEA, DMF (f); 50% TFA, DCM, TES.

were first converted to the appropriate anhydrides using DIC. The anhydrides and DMAP were then added to Wang resin¹⁸ and the percentage loading was calculated by UV absorption.¹⁹ Subsequent deprotection of the Fmoc group with piperidine was then followed by coupling to the second amino acid using TBTU and HOBt.^{20,21} A final deprotection and coupling to 1-carboxymethyl uracil, 20,²² followed by cleavage from the resin beads using 50% TFA released the desired compounds 1–11. All final compounds were analysed and characterized by ¹H NMR and MS.

Compounds 1–11 were tested for both TcdUTPase enzyme inhibition²³ and in vitro effects on parasite growth.²⁴ As can be seen from Table 2, none of the com-

pounds inhibited the TcdUTPase enzyme at a concentration of 1 mM. Neither did the compounds inhibit parasite growth at the maximum concentrations shown.

Thus, the search so far for lead inhibitors of the dimeric dUTPase enzymes remains unsuccessful. There are a number of reasons why this design paradigm was not successful in this case. (i) Recently, the crystal structure of the dimeric *C. jejuni* dUTPase revealed the coordination of Mg²⁺ ions within the active site of the enzyme.¹⁴ These ions are absent in the TcdUTPase crystal structure. It is unclear if the Mg²⁺ ions are bound to the un-liganded enzyme, but it is possible that the presence of these ions must be taken into account when designing inhibitors in silico.

(ii) As previously mentioned, FlexX does not take into account the flexibility of the protein in question. Although this approximation reduces run time significantly, in this case where binding of the ligand induces a large conformational change in protein structure it is possible that a docking program in which protein flexibility is taken into account should be used.

(iii) There must be a mechanism by which the dUTPase undergoes the large conformational change on binding dUTP. Two mechanisms of binding could be envisaged. First, the uracil and deoxyribose moieties, which bind to motifs from the rigid domain of protein, would be recognized. The α , β , and subsequently γ phosphates, which are recognized by mobile domain motifs, would then bond to the Mg²⁺ ions and respective amino acid side chains sequentially and induce 'active site closure'. Alternatively, the phosphate moieties would be recognized by the mobile domain first and the protein would then undergo such a conformational change so as to

Table 2. Biological activity of compounds 1–11

Compound	Enzyme inhibition K_i	In vitro IC_{50} (μ M)	Cytotoxicity IC_{50}^a (μ M)
1	>1 mM	>84	>252
2	>1 mM	>81	>243
3	>1 mM	>81	210
4	>1 mM	>100	>301
5	>1 mM	>81	>243
6	>1 mM	>87	>262
7	>1 mM	>74	214
8	>1 mM	>132	>396
9	>1 mM	>84	>253
10	>1 mM	>91	>274
11	>1 mM	>76	>230
Standard	18.40 ^b μ M	1.04 ^c	0.15 ^d

^a Cytotoxicity tests were carried out on rat L6 cells.

^b dUMP.

^c Benznidazole.

^d Podophyllotoxin.

encapsulate the uracil and sugar moieties. In the latter case, the phosphate moieties would be more essential for ligand recognition and therefore replacement of them would be detrimental to ligand recognition. This would explain the lack of activity of compounds 1–11. In either case, the experimental biological data indicate that compounds 1–11 do not possess the required structure to bind to the open form of the enzyme sufficiently enough to induce the conformational change required for inhibition.

Although compounds 1–11 docked with good superimposition and favourable binding energies into the TcdUTPase active site with FlexX, it is apparent that other factors such as protein flexibility and the presence of Mg²⁺ ions should be taken into account when designing competitive inhibitors for these enzymes in silico.

Acknowledgments

The authors thank the European Union (QLRT-2001-00305), Cardiff University and the FIS Network RICET/C03 for funding of this project. The National EPSRC Mass Spectrometry service centre (Swansea) is acknowledged for accurate mass spectrometry.

Supplementary data

Supplementary data associated with this article can be found, in the online version, at doi:10.1016/j.bmcl.2006.04.027.

References and notes

1. <http://www.cdc.gov/ncidod/dpd/parasites/chagasdiseas>.
2. <http://www.who.int/ctd/chagas/>.
3. Hidalgo-Zarco, F.; González-Pacanowska, D. *Curr. Protein Pept. Sci.* **2001**, *2*, 389.
4. Gadsden, M. H.; McIntosh, E. M.; Game, J. C.; Wilson, P. J.; Haynes, R. H. *EMBO J.* **1993**, *12*, 4425.
5. El-Hajj, H. H.; Zhang, H.; Weiss, B. *J. Bacteriol.* **1988**, *170*, 1069.

6. Cedergren-Zeppezauer, E. S.; Larsson, G.; Nyman, P. O.; Dauter, Z.; Wilson, K. S. *Nature* **1992**, *355*, 740.
7. Mol, C. D.; Harris, J. M.; McIntosh, E. M.; Trainer, J. A. *Structure* **1996**, *4*, 1077.
8. Dauter, Z.; Persson, R.; Rosengren, A. M.; Nyman, P. O.; Wilson, K. S.; Cedergren-Zeppezauer, E. S. *J. Mol. Biol.* **1999**, *285*, 655.
9. Prasad, G. S.; Stura, E. A.; McRee, D. E.; Laco, G. S.; Hassekus-Light, C.; Elder, J. H.; Stout, C. D. *Protein Sci.* **1996**, *5*, 2429.
10. Huffman, J. L.; Li, H.; White, R. H.; Tainer, J. A. *J. Mol. Biol.* **2003**, *331*, 885.
11. Chan, S.; Segelke, B.; Legin, T.; Krupka, H.; Chō, U. S.; Kim, M.; So, M. Y.; Kim, C. Y.; Naranjo, C. M.; Rogers, Y. C.; Park, M. S.; Wald, G. S.; Pashkov, I.; Cascio, D.; Perry, J. L.; Sawaya, M. R. *J. Mol. Biol.* **2004**, *341*, 503.
12. Whittingham, J. L.; Leal, I.; Nguyen, C.; Kasinathan, G.; Bell, E.; Jones, A. F.; Berry, C.; Benito, A.; Turkenburg, J. P.; Dodson, E. J.; Perez, L. M. R.; Wilkinson, A. J.; Johansson, N. G.; Brun, R.; Gilbert, I. H.; Pacanowska, D. G.; Wilson, K. S. *Structure* **2005**, *13*, 329.
13. Harkiolaki, M.; Dodson, E. J.; Bernier-Villamor, V.; Turkenburg, J. P.; González-Pacanowska, D.; Wilson, K. S. *Structure* **2004**, *12*, 41.
14. Moroz, O. V.; Harkiolaki, M.; Galperin, M. Y.; Vagin, A. A.; Gonzalez-Pacanowska, D.; Wilson, K. S. *J. Mol. Biol.* **2004**, *342*, 1583.
15. Hidalgo-Zarco, F.; Camacho, A. G.; Bernier-Villamor, V.; Nord, J.; Ruiz-Perez, L. M.; Gonzalez-Pacanowska, D. *Protein Sci.* **2001**, *10*, 1426.
16. Rarey, M.; Kramer, B.; Lengauer, T.; Klebe, G. *J. Mol. Biol.* **1996**, *261*, 470.
17. Böhm, H.-J. *J. Comput. Aided Mol. Des.* **1994**, *8*, 243.
18. Wang, S.-S. *J. Org. Chem.* **1975**, *40*, 1235.
19. Merck Bioscience, (2002/2003); Novabiochem Catalog.
20. Knorr, R.; Trzeciak, A.; Bannwarth, W.; Gillissen, D. *Tetrahedron Lett.* **1989**, *30*, 1927.
21. Sarin, V. K.; Kent, S. B. H.; Tam, J. P.; Merrifield, R. B. *Anal. Biochem.* **1981**, *117*, 147.
22. Jacobsen, J. R.; Cochran, A. G.; Stephans, J. C.; King, D. S.; Schultz, P. G. *J. Am. Chem. Soc.* **1995**, *117*, 5453.
23. Bernier-Villamor, V.; Camacho, A.; Hidalgo-Zarco, F.; Perez, J.; Ruiz-Perez, L. M.; Gonzalez-Pacanowska, D. *FEBS Lett.* **2002**, *526*, 147.
24. Jones, S. M.; Urch, J. E.; Kaiser, M.; Brun, R.; Harwood, J. L.; Berry, C.; Gilbert, I. H. *J. Med. Chem.* **2005**, *48*, 5932.

